About the importance of mitochondrial complex I and associated gamma carbonic anhydrases for plant development, metabolism and the proteome

Von der Naturwissenschaftlichen Fakultät der

Gottfried Wilhelm Leibniz Universität Hannover

zur Erlangung des Grades

Doktorin der Naturwissenschaften

(Dr. rer. nat.)

genehmigte Dissertation

von

M. Sc. Steffanie Fromm

geboren am 02.07.1987 in Burgwedel

2016

Referent: Prof. Dr. Hans-Peter Braun

Koreferentin: Prof. Dr. Traud Winkelmann

Tag der Promotion: 27.04.2016

The following publications are part of this thesis:

1. **Fromm S**, Senkler J, Eubel H, Peterhänsel C, Braun HP (2016)

   Life without complex I: proteome analyses of an Arabidopsis mutant lacking the mitochondrial NADH dehydrogenase complex.

   Journal of Experimental Botany, **67**: 3079-3093.

2. **Fromm S,** Senkler J, Zabaleta E, Peterhänsel C, Braun HP (2016)

   The carbonic anhydrase domain of plant mitochondrial complex I.

   Physiologia Plantarum, in press, (doi: 10.1111/ppl.12424).

3. **Fromm S**, Braun HP, Peterhänsel C (2016)

   Mitochondrial gamma carbonic anhydrases are required for complex I assembly and plant reproductive development.

   New Phytologist, **211**: 194-207.

4. **Fromm S**, Göing J, Lorenz C, Peterhänsel C, Braun HP (2016)

   Depletion of the "gamma-type carbonic anhydrase-like" subunits of complex I affects central mitochondrial metabolism in *Arabidopsis thaliana*.

   Biochimica et Biophysica Acta **1857**: 60–71.

Zusammenfassung

In den meisten Eukaryoten stellt das mitochondriale System der "oxidativen Phosphorylierung" (OXPHOS) die Basis für die zelluläre Energieversorgung dar. Von besonderer Bedeutung für das OXPHOS System ist der mitochondriale NADH-Dehydrogenase Komplex (Komplex I). Dieser ist die Haupteintrittspforte für Elektronen in die mitochondriale Elektronentransportkette (mETC) und dadurch indirekt an der mitochondrialen ATP Synthese beteiligt. Der pflanzliche Komplex I ist insofern besonders, als dass er zusätzliche pflanzenspezifischen Untereinheiten, wie gamma-Typ Carboanhydrasen (γCA), beinhaltet. In der Modellpflanze *Arabidopsis thaliana* gibt es drei γCA und zwei gamma-Typ Carboanhydrase ähnliche (γCAL) Proteine: γCA1, γCA2, γCA3, γCAL1 und γCAL2. Drei dieser fünf Untereinheiten können gleichzeitig in der γCA Domäne, welche mit dem Membranarm des Komplex I assoziiert ist, enthalten sein. Die mögliche Untereinheitenzusammensetzungen der γCA Domäne, so wie sie sich aus den Ergebnissen dieser Arbeit und bereits zuvor erworbenen Erkenntnissen ableiten lassen, wurden in einem Übersichtsartikel zusammengefasst (**Kapitel 2.3**). Im Zentrum der vorliegenden Dissertation stand die Charakterisierung der Funktion der γCA/ γCAL Proteine und die damit verbundenen pflanzenspezifischen Funktionen des Komplex I. Um zwischen den direkten γCA/ γCAL und den indirekten, durch Komplex I hervorgerufenen, Funktionen unterscheiden zu können, wurden *ca1ca2* Doppelmutanten mit enzymatisch inaktiven CA2 Versionen hergestellt und mittels proteomischen und metabolomischen Methoden analysiert. Des Weiteren wurde besonderes Augenmerk auf die physiologische, molekulare und biochemische Charakterisierung der *ca1ca2* Doppelmutante gelegt. Die durchgeführten Studien deuteten darauf hin, dass die γCA/ γCAL Proteine für Komplex I strukturell essentiell sind. Die gleichzeitige Deletion der *CA1* und *CA2* Gene verursachte eine Komplex I Dysfunktion mit drastischen Auswirkungen auf die Samen- und Pflanzenentwicklung. Zudem kam es zu einer Reorganisation des OXPHOS Systems mit veränderten *in vitro* Aktivitäten der Komplexe II und IV, sowie einem erhöhten Fluss von Elektronen durch die mETC (**Kapitel 2.2**). Dieses konnte mit Hilfe von systematischen vergleichenden Proteomanalysen für die *ca1ca2* Mutante belegt werden (**Kapitel 2.4**). Zusätzlich wurde die *cal1cal2i* Mutante in dieser Dissertation hinsichtlich ihres mitochondrialen Proteoms und Metaboloms untersucht (**Kapitel 2.1**). Neue Erkenntnisse zur Diversität von Komplex I Mutanten und die unterschiedlichen daraus resultierenden Auswirkungen auf den pflanzlichen Phänotyp, die pflanzliche Entwicklung, das mitochondriale Proteom, sowie auf andere zelluläre Prozesse, wie die Photosynthese, wurden gewonnen. Diese Ergebnisse erlauben es, die pflanzenspezifischen Komplex I Funktionen besser zu definieren (**Kapitel 2.4**).

Schlagworte: *Arabidopsis thaliana*, Atmungskette, Carboanhydrase, Komplex I Dysfunktion, NADH Dehydrogenase Komplex

Abstract

The mitochondrial "oxidative phosphorylation" (OXPHOS) system is essential for the majority of energy dependent cellular processes in most species. Of particular importance for the OXPHOS system is the mitochondrial NADH dehydrogenase complex (complex I). It is the major electron entry site for the mitochondrial electron transport chain (mETC) and of outstanding importance for mitochondrial ATP generation. In comparison to other eukaryotes *Arabidopsis* complex I is composed of additional plant specific subunits including gamma-type carbonic anhydrase (γCA) proteins. In *Arabidopsis* three γCA and two gamma-type carbonic anhydrase like (γCAL) proteins are present, termed γCA1, γCA2, γCA3, γCAL1 and γCAL2. Three out of these five subunits are arranged in a γCA domain that is attached to the membrane arm of complex I. Results of this thesis and findings of priory analyzed *yca/ ycal* mutants were reviewed to propose a model for the subunit composition of the γCA domain (**Chapter 2.3**). The functions of γCA/ γCAL proteins and resulting functions for plant complex I were of particular interest for this thesis. To discriminate between direct functions of γCA/ γCAL proteins and indirect functions that are coupled to complex I, *ca1ca2* double mutants overexpressing enzymatically inactive CA2 versions were generated and analyzed by proteomic and metabolomic tools. Furthermore, special emphasis was placed on the physiological, molecular and biochemical characterization of *ca1ca2* double mutants. These studies highlighted that γCA proteins are structurally essential for complex I. The simultaneous mutation of *CA1* and *CA2* genes caused complex I dysfunction with drastic effects on seed and plant development. Increased *in vitro* activities of complexes II and especially IV as well as higher flux of electrons through the mETC were observed (**Chapter 2.2**). In addition, reorganization of the OXPHOS system in the double mutant was shown by systematic comparative proteome investigations using gel-based approaches as well as gel-free quantitative "shotgun" proteome approach for *ca1ca2* mutant plants and cell culture lines (**Chapter 2.4**). In addition, *cal1cal2i* mutants were analyzed with respect to the mitochondrial proteome and metabolism. Trace amounts of complex I levels and activity were remaining in the *cal1cal2i* mutant (**Chapter 2.1**). Novel insights into the diversity of complex I mutations and their differential effects on plant phenotype and development, the mitochondrial proteome as well as on photosynthesis were obtained. This allows to newly define complex I functions in plants (**Chapter 2.4**).

Keywords: *Arabidopsis thaliana*, carbonic anhydrase, complex I dysfunction, NADH dehydrogenase complex, respiratory chain

Table of contents

Chapter 2: Publications

Appendix

Abbreviations

1D	one-dimensional
2D	two-dimensional
ADP	adenine diphosphate
AOX	alternative oxidase
ATP	adenine trisphosphate
az	azygous
BCT	bicarbonate transporter
BN	Blue Native
C3	three carbon organic acids
C4	four carbon organic acids
CA	carbonic anhydrase
CAL	carbonic anhydrase like
CAM	gamma carbonic anhydrase of *Methanosarcina thermophila*
CCM	carbon dioxide concentrating mechanism
cDNA	complementary desoxyribonucleic acid
CMS	cytoplasmatic male sterility
complex I	NADH dehydrogenase complex
complex II	succinate dehydrogenase complex
complex III	cytochrome c reductase complex
complex IV	cytochrome c oxidase complex
complex V	ATP synthase complex
dap	days after pollination
DHODH	dihydroorotatedehydrogenase
DIC microscopy	differential interference contrast microscopy
DIGE	differential gel electrophorese
ETFQ-OR	flavoproteine: quinone oxidoreductase
FAD	flavin adenine dinucleotide; oxidized form
$FADH_2$	flavin adenine dinucleotide; reduced form
Fe/S cluster	iron-sulfur cluster
FMN	flavin mononucleotide
G3-P DH	glycerol-3-phosphate dehydrogenase
GLDH	L-galactone-1,4-lactone dehydrogenase
$I+III_2$	complex I with dimeric complex III
$I+III_2+IV_{1-4}$	monomeric complex I, dimeric complex III and one to four copies of complex IV
IEF	isoelectric focussing
III_2+IV_{1-2}	dimeric complex III with one or two copies of complex IV
IMM	inner mitochondrial membrane
IMS	inter membrane space

IPG	immobilized pH gradient
kDa	kilo Dalton
LβH	left-handed parallel β-helices
mETC	mitochondrial electron transport chain
mRNA	messenger ribonucleic acid
MS	mass spectrometry
NAD^+	nicotinamide adenine dinucleotide; oxidized form
NADH	nicotinamide adenine dinucleotide; reduced form
NADPH	nicotinamide adenine dinucleotide phosphate; reduced form
N-module	NADH oxidation module of complex I
OXPHOS	oxidative phosphorylation
PAGE	polyacrylamide gel electrophoresis
PCD	programmed cell death
PCR	polymerase chain reaction
P-module	proton translocation module of complex I
ProDH	proline dehydrogenase
Q-module	quinone reduction module of complex I
qPCR	quantitative polymerase chain reaction
ROS	reactive oxygen species
RuBisCO	ribulose-1,5-bisphosphate carboxylase/oxygenase
SDS	sodium dodecyl sulfate
TCA cycle	tricarboxylic acid cyle
TIM	translocases of the inner mitochondrial membrane
TOM	translocases of the outer mitochondrial membrane
V_2	dimeric complex V
wt	wildtype

Chapter 1: Introduction
Oxidative phosphorylation: Complex I and the gamma-type carbonic anhydrases

Chapter 1 provides the theoretical background of the thesis. It outlines general and plant specific features of the mitochondrial oxidative phosphorylation (OXPHOS) system. Special emphasis is placed on the NADH dehydrogenase complex and its plant specific γCA/ γCAL subunits.

1.1. Mitochondrial metabolism

1.1.1. Structural organization of mitochondria

Mitochondria are supposed to have an endosymbiotic origin. The endosymbiont hypothesis suggests that mitochondria were originally prokaryotic cells and became endosymbionts inside eukaryotic cells (Margulis, 1970). Most eukaryotic organisms contain mitochondria. However, mitochondria have not been detected in some unicellular eukaryotes of the protozoa kingdom (reviewed in Makiuchi and Nozaki, 2014).

The morphology of mitochondria is very dynamic. Their shape, size and number is controlled by fission and fusion (Logan, 2003). The general shape of mitochondria is spherical or rodlike, and their size range from 0.5 to 1.0 µm in diameter and 3 µm in length (Douce, 1985). The number of mitochondria per cell is variable and depends on the physiological and the developmental state of the cell as well as on the cell size. In plants, young leaves contain approximately 300 mitochondria per cell while older leaves have 450 mitochondria per cell (Preuten *et al.,* 2010).

Due to endosymbiosis mitochondria are organelles with a double membrane. The outer membrane completely surrounds the invaginated inner mitochondrial membrane (IMM). The invagination is called "cristae" and leads to a greatly enlarged surface area. The aqueous phase within the inner membrane is known as matrix and the region between the two membranes as intermembrane space. However, the inner and outer membranes can either get in close proximity via so called "contact sites" or be connected via bridge-like structures that provide the structural basis for membrane organization (Hackenbrock *et al.,* 1986; Senda and

Yoshinaga-Hirabayashi, 1998; Perkins *et al.,* 2001). These structures enable protein import and facilitate the passage of solutes and small molecules between cytosol and matrix (Senda and Yoshinaga-Hirabayashi, 1998; Logan, 2006). The IMM of plant mitochondria contains a diverse set of transporters that regulate the import and export of molecules like pyruvate, dicarboxylates, tricarboxylates, phosphate, ADP and ATP between the matrix and the cytosol (reviewed in Millar *et al.,* 2011). These transporters are important for exchanging substrates for the tricarboxylic acid (TCA) cycle that provides reduction equivalents for the oxidative phosphorylation (OXPHOS) system. The mitochondrial OXPHOS system consists of five different protein complexes that are embedded in the IMM and two mobile carriers. Four of the five complexes comprise are respiratory chain enzymes (complex I: NADH dehydrogenase complex; complex II: succinate dehydrogenase complex; complex III: cytochrome *c* reductase complex; complex IV: cytochrome *c* oxidase complex), the fifth complex is the ATP synthase complex (complex V). The two mobile electron transporters are ubiquinone and cytochrome *c*.

At present, two models of the arrangement of the OXPHOS complexes in the IMM have been proposed: The "fluid state model" and the "solid state model". The "fluid state model" assumes that the OXPHOS complexes are diffusing in the inner mitochondrial membrane. Here, electron transfer takes place by accidently collisions of the OXPHOS complexes. This is supported by the fact that all five OXPHOS complexes can be purified in a physiologically active form, and by the ability to use isolated mitochondrial membranes for liquid dilution experiments (Hackenbrock *et al.,* 1986; Boekema and Braun, 2007). In contrast, there also is evidence that supports the "solid state model" (Fowler and Richardson, 1963; Rich, 1984). This model assumes the OXPHOS complexes to be solid within in the membrane and thus, to interact with each other stably. The "solid state model" is generally supported by the occurrence of respiratory supercomplexes. Supercomplexes are associations of two or more OXPHOS complexes that can be found in organisms belonging to different kingdoms of eukaryotes (Chaban *et al.,* 2014). The association of OXPHOS complexes varies between different organisms (Chaban *et al.,* 2014). In *Arabidopsis thaliana* for example, supercomplexes of complex I associated with dimeric complex III ($I+III_2$) and dimeric complex V (V_2) exist (Dudkina *et al.,* 2010; Chaban *et al.,* 2014). In yeast and animals, these supercomplexes are stabilized by the lipid cardiolipin and stomatin-like proteins that bind cardiolipin and interact with prohibitins (Mileykovskaya *et al.,* 2012; Mitsopoulos *et al.,* 2015). Similar interactions are supposed for plants (Gehl and Sweetlove, 2014). These supercomplexes form even larger associations consisting of monomeric complex I, dimeric complex III and one to four copies of complex IV ($I+III_2+IV_{1-4}$) in some animals, yeast and plants such as *Solanum tuberosum* and

Spinacia oleracea (Chaban *et al.,* 2014). These large structures are named respirasomes and can autonomously carry out respiration in the presence of ubiquinone and cytochrome *c* (Schägger and Pfeiffer, 2000). Those associations result in shorter electron transport ways in the mETC and, thus, are advantageous for the OXPHOS system. Productions of reactive oxygen species (ROS) at complexes I and III are minimized by the rapid electron transfer due to shorter transfer paths for ubiquinone and cytochrome *c* (Chaban *et al.,* 2014). Furthermore, the supercomplexes determine the structure for the IMM and lead to increased protein insertion capacities (Boekema and Braun, 2007).

In conclusion, both models on their own cannot explain many experimental observations. The OXPHOS complexes are of dynamic nature and might switch between both states (Boekema and Braun, 2007).

1.1.2. General mechanism of the oxidative phosphorylation (OXPHOS) system

Plant mitochondria are involved in numerous metabolic processes including photorespiration, programmed cell death, cell signaling as well as the biosynthesis of amino acids, vitamin cofactors, fatty acids and iron sulfur-clusters (Mackenzie and McIntosh, 1999; Bowsher and Tobin, 2001; Logan and Knight, 2003; Youle and Karbowski, 2005; Peterhänsel *et al.,* 2010). Additionally, mitochondria are of particular importance for energy production of the cell and are also called "powerhouse of the cell". Respiration is the fundamental ATP generating process of most eukaryotes. However, plants and other photosynthetic organisms do not completely rely on mitochondria for energy production because the majority of ATP is generated by photosynthesis during daytime. Nevertheless, also plant mitochondria carry out the final steps of aerobic respiration and efficiently generate ATP through oxidative phosphorylation (OXPHOS) (reviewed in Millar *et al.,* 2011).

In general, the OXPHOS complexes catalyze the electron transfer from NADH or $FADH_2$ to molecular oxygen as the terminal electron acceptor (**Figure 1**). Glycolysis, the TCA cycle and photorespiratory processes in plant mitochondria generate NADH. The NADH dehydrogenase complex (complex I) oxidizes NADH to NAD^+ by its matrix exposed "peripheral arm". Two electrons are transferred in the mitochondrial electron transport chain (mETC).
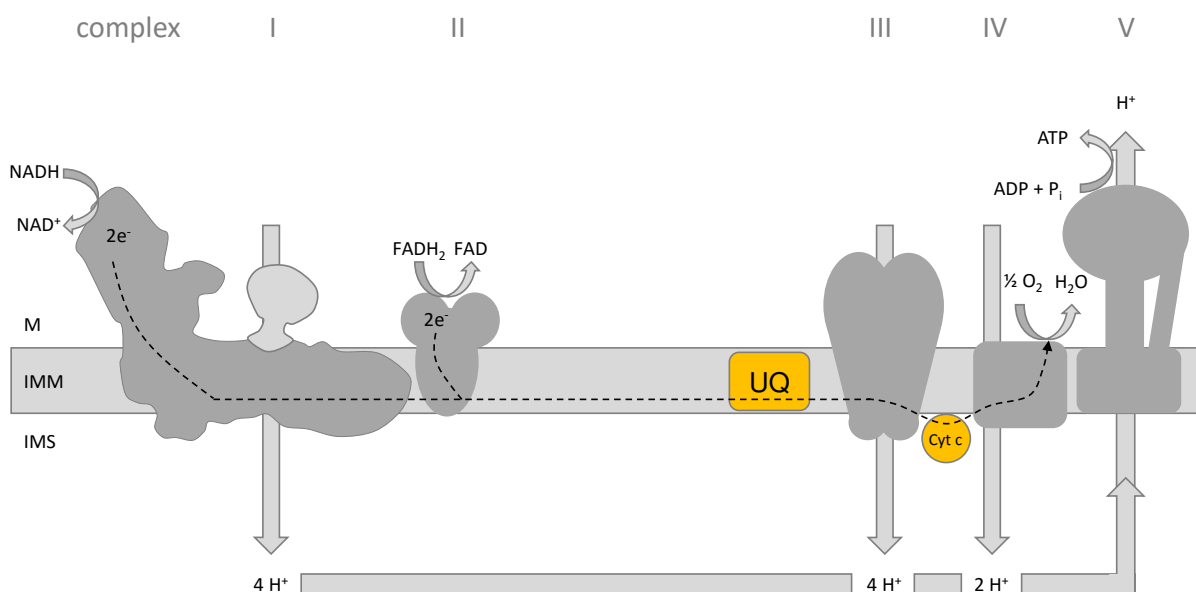
Figure 1: General oxidative phosphorylation system.

Electrons enter the mETC via complex I or complex II. These complexes are reduced by NADH respectively $FADH_2$. Electrons are transported via ubiquinone (UQ) to complex III and finally via Cytochrome c (Cyt c) to complex IV. Molecular oxygen (O_2) is reduced and water (H_2O) is produced. Coupled to electron transport is the proton (H^+) translocation across the IMM at complex I, III and IV. The proton gradient is used to drive the ATP synthesis at complex V in the mitochondrial matrix. M: mitochondrial matrix; IMM: inner mitochondrial membrane; IMS: inter membrane space; yellow proteins are mobile electron carrier.

Additionally, two electrons are inserted in the mETC by oxidation of $FADH_2$ at the succinate dehydrogenase complex (complex II). Complex II is a component of both the TCA cycle and the OXPHOS system. The inserted electrons are transferred to ubiqinone that is subsequently reduced to ubiquinol. This small lipid-soluble electron carrier can diffuse within the hydrophobic core of the membrane bilayer of the IMM. This characteristic enables the transport of electrons from complex I and II to the cytochrome c reductase complex (complex III) that is subsequently reduced. From here, electrons are transported via cytochrome c, a small protein loosely attached to the outer surface of the inner membrane, to the cytochrome c oxidase complex (complex IV).

Finally, complex IV, the terminal oxidase of the mETC, reduces one molecule of molecular oxygen by the consumption of four electrons (Siedow and Umbach, 1995). The reduced oxygen reacts with protons in the mitochondrial matrix to water. Peter Mitchell (1961) was the first who proposed that electron transport is coupled to the translocation of protons from the mitochondrial matrix into the intermembrane space at complexes I, III and IV. The translocation of protons results in a proton gradient across the inner mitochondrial membrane. The ATP synthase complex (complex V) can use this proton gradient to generate ATP. During ATP

synthesis protons are channeled back into the mitochondrial matrix decreasing the proton motive force. As already mentioned (see section **1.1.1**), the OXPHOS complexes can associate to supercomplexes to increase the flux of electrons and, thus, increase efficiency of ATP production. The produced ATP can be exported for energy requiring processes of the cell (reviewed in Millar *et al.,* 2011).

1.1.3. OXPHOS in plants: Alternative enzymes

Plants are sessile organisms and, therefore, the rapid adaptation to changing environmental conditions and the availability of minerals and nutrients is of fundamental importance. Rapidly changing environmental conditions (e.g. higher light conditions) can cause an overreduction of the mETC. Subsequently, reactive oxygen species (ROS) can be generated at complexes I, II and III (Møller and Sweetlove, 2010; Jardim-Messeder *et al.,* 2015). ROS are signaling molecules that regulate plant development and respond to stress. If ROS concentrations are elevated for a longer time period, decrease of the mitochondrial transmembrane potential and swelling of mitochondria is induced. This is followed by damage of cellular compartments and programmed cell death (PCD) (Li and Xing, 2010). In addition to classical OXPHOS complexes, plant mETC possess some alternative enzymes that can prevent the ROS formation and fulfill protective functions for mitochondria and the entire cell (**Figure 2**).

Plants, fungi, protists and some bacteria possess alternative NAD(P)H dehydrogenases that have not been reported for most animals (Rasmusson *et al.,* 2008). In *Arabidopsis*, seven alternative NAD(P)H dehydrogenases are present that are grouped in three families NDA, NDB and NDC (Michalecka *et al.,* 2003). NDA1, NDA2 and NDC are attached to the inner mitochondrial membrane at the matrix site. NDB1, NDB2, NDB3 and NDB4 are attached to the inner mitochondrial membrane in the intermembrane space. NDB1 (Ca^{2+} dependent) and NDC1 function as NADPH dehydrogenases, whereas NDB2 (Ca^{2+} stimulated), NDB3, NDB4, NDA1 and NDA2 oxidize NADH (Elhafez *et al.,* 2006; Geisler *et al.,* 2007).

The alternative NAD(P)H dehydrogenases are light regulated. An increase in photosynthetic metabolism subsequently leads to increased photorespiration with massive production of NADH in the mitochondrial matrix (Rasmusson and Escobar, 2007). If an excess of reduction equivalents is present in the mitochondrial matrix, the alternative NAD(P)H dehydrogenases can oxidize NADH or NADPH and reduce the ubiquinone pool by bypassing complex I

(Rasmusson *et al.,* 2004). In comparison to complex I, the alternative NAD(P)H dehydrogenases cannot translocate protons and have no impact on the proton motive force needed for ATP synthesis (Rasmusson and Wallström, 2010). However, alternative NAD(P)H dehydrogenases prevent the generation of ROS and fulfill protective functions for mitochondria and the entire cell (Rasmusson *et al.,* 2008).

In *Arabidopsis*, additional electron entry points are present. They further increase the complexity of the mETC and are shortly presented in the following. In addition to the alternative NAD(P)H dehydrogenases, the flavoproteins quinone oxidoreductase (ETFQ-OR), proline dehydrogenase (ProDH), dihydroorotatedehydrogenase (DHODH) and glycerol-3-phosphate dehydrogenase (G3-P DH) mediate electron insertion into the ubiquinone pool. A further electron entry point is the cytochrome *c* pool. L-galactone-1,4-lactone dehydrogenase (GLDH) and D-lactate dehydrogenase can transfer electrons to that mobile electron carrier and subsequently reduce complex IV (Rasmusson *et al.,* 2008; Schertl and Braun, 2014).
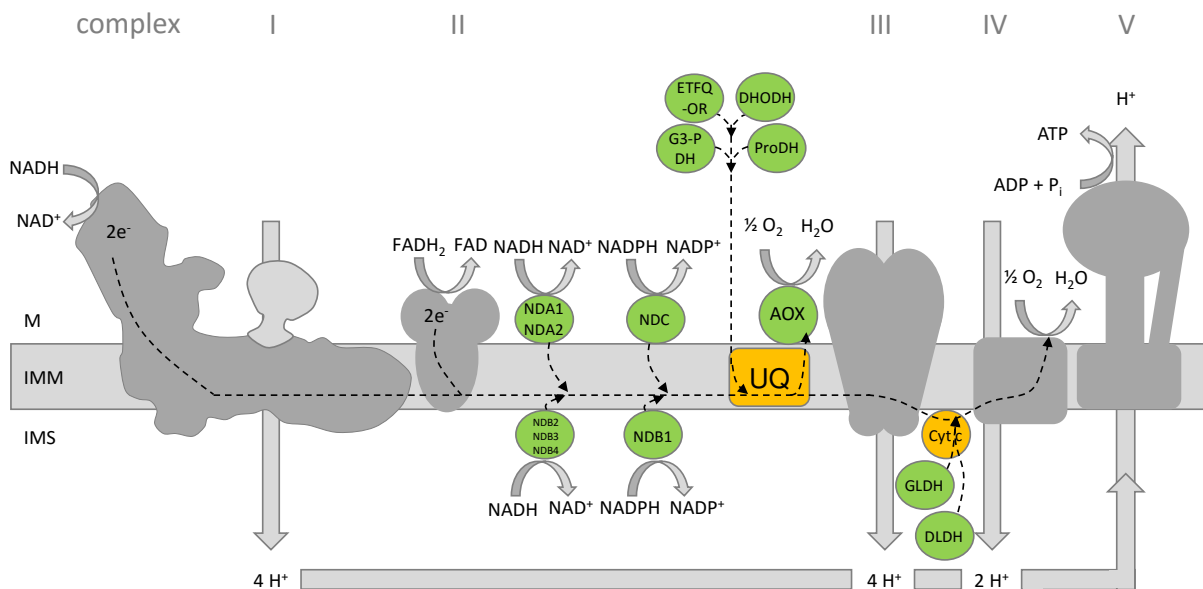
Figure 2: Alternative enzymes supporting the OXPHOS system.

Aside from the OXPHOS complexes I, II, III and IV and the ATP synthase complex (complex V), alternative enzymes that participate in mETC are present. Enzymes inserting electrons in the ubiquinone pool (UQ) are alternative NADH dehydrogenases (NDA, NDB and NDC), proline dehydrogenase (ProDH), flavoproteine: quinone oxidoreductase (ETFQ-OR), dihydroorotatedehydrogenase (DHODH) and glycerol-3-phosphate dehydrogenase (G3-P DH). Alternative oxidoreductase (AOX) can use electrons of the UQ pool to reduce molecular oxygen to water. L-galactone-1,4-lactone dehydrogenase (GLDH) and D-lactate dehydrogenase (DLDH) can reduce cytochrome *c* (Cyt c) by electron transfer. The alternative enzymes are not able to translocate protons. M: mitochondrial matrix; IMM: inner mitochondrial membrane; IMS: inter membrane space; yellow proteins are mobile electron carrier.

If the respiration rate exceeds the demand of the cell for ATP, an alternative oxidase (AOX) is activated by the elevated proton motive force. *Arabidopsis* possess five AOX genes, *AOX1a-AOX1d* and *AOX2*, that are facing the matrix site of the inner mitochondrial membrane (Thirkettle-Watts *et al.,* 2003). AOX is reduced by electrons out of the ubiquinol pool and can subsequently reduce molecular oxygen and, thereby, generate water. Thus, AOX bypasses the proton pumping complexes III and IV. The energy that would normally be used for ATP production is released as heat in this alternative pathway (Rogov and Zvyagilskaya, 2015). AOX can prevent an overreduction of complex III and complex VI when stress conditions lead to an inhibition of respiration. This can prevent the formation of ROS. Besides this, AOX is involved in defense mechanisms against a wide range of biotic or abiotic stresses e.g. light, temperature, osmotic stress, drought and pathogen attack (Rogov and Zvyagilskaya, 2015).

In addition, animal and plant mitochondria contain uncoupling proteins in the inner mitochondrial membrane. Uncoupling proteins allow proton flux from the intermembrane space into the mitochondrial matrix across the inner mitochondrial membrane. Thus, uncoupling proteins bypass the ATP synthase complex when an excess of protons is present in the intermembrane space (Vercesi *et al.,* 2006).

Finally, there is experimental evidence for an interaction between alternative enzymes that add electrons into the mETC and enzymes that use electrons out of the ubiquinol pool of mETC. An increased enzymatic capacity of alternative NAD(P)H dehydrogenases can directly increase the rate of either AOX or uncoupling proteins to establish a high flux of electrons through the mETC (Rasmusson and Wallström, 2010). These enzymes are protective for the entire cell. They can adjust the redox state of the cell and the mETC, if ATP generation has to be maintained and the generation of ROS needs to be prohibited.

1.1.4. Mitochondrial metabolism in developing seeds

Overall two distinct embryogenesis phases are defined: embryo morphogenesis and maturation of the embryo. Embryo morphogenesis is initiated by the double fertilization of the zygote that differentiates stepwise. Embryo morphogenesis comprises cell division and elongation of embryo and endosperm. The subsequent maturation stage is characterized by the accumulation of storage compounds and the acquisition of seed dormancy and desiccation tolerance (reviewed in Baud *et al.,* 2008). The embryo is a quickly developing tissue that can reach the

maturation stage within a few days after fertilization (reviewed in Baud *et al.,* 2008). To facilitate this rapid development about 17,500 distinct mRNAs are transcribed in *Arabidopsis* seeds to coordinate seed filling (Belmonte *et al.,* 2013). The differentiation of the embryo is enabled by rapid changes of seed metabolism. In addition to photosynthetic processes in green seeds, mitochondrial metabolism is of special importance for developing seeds.

Mitochondrial metabolite fluxes in green *Brassica napus* seeds were determined. Differences in mitochondrial metabolism between fully developed plants and developing seeds were estimated (Schwender *et al.,* 2006). The main organic compounds for metabolism in the mature embryo are sucrose, glucose, glutamate, glutamic acid and alanine that are used for replenishing the TCA cycle and protein biosynthesis. Especially, alanine and glutamine provide nitrogen for the transamination/deamination of other amino acids (Schwender *et al.,* 2006). However, cyclic flux around the TCA cycle is mainly absent which results in only minor fluxes through the OXPHOS system. 22 % of the ATP required for biosynthesis, cell division or cell expansion can be synthesized by the OXPHOS system. The majority of ATP is produced by photosynthetic light reactions and OXPHOS using cytosolic instead of mitochondrial NADH (Rolletschek *et al.,* 2003; Schwender *et al.,* 2006). However, a decrease in the contribution to ATP synthesis is reflected in a photosynthetic gradient from the outside to the inside of the embryo (Borisjuk *et al.,* 2013).

Instead of ATP production, the mitochondrial flux in green seeds is rather utilized to provide citrate as a precursor for cytosolic fatty acid elongation. Citrate is exported from mitochondria into the cytosol and used for the production of cytosolic acetyl-CoA by ATP citrate lysases. In the following, cytosolic oleic acid (C18:1) is elongated to C20:1 and C22:1 fatty acids (Fatland *et al.,* 2005). The by-product oxaloacetate is reimported into mitochondria where it either reacts with acetyl-CoA to restore citrate or is converted to malate. Malate can be transformed to pyruvate via malic enzyme. This is supported by the finding that 40 % of the mitochondrial pyruvate is produced by malic enzyme rather than being imported from the cytosol (Schwender *et al.,* 2006).

Along with fatty acid synthesis, a decarboxylation reaction takes place that leads to an elevated CO_2 concentration in seeds. Due to the enclosed environment by the silique, CO_2 concentrations are 600 to 2000 fold higher than in ambient air preventing photorespiration in seeds (Rolletschek *et al.,* 2003; Goffman *et al.,* 2004). Additionally, oxygen concentrations tend to be very low and limit respiration. Especially, young, undifferentiated, heterotrophic embryos are mainly dependent on respiration but suffer from hypoxic conditions because molecular

oxygen cannot pass the silique from the outside. During differentiation, the embryo becomes green and is able to produce molecular oxygen by photosynthesis. The molecular oxygen can be used for respiratory processes (Rolletschek *et al.,* 2003).

In summary, young undifferentiated embryos are dependent on respiration. However, after greening of the seed, photosynthesis provides the majority of ATP and mitochondrial metabolism mainly contributes to the synthesis of seed storage compounds like fatty acids to allow the production of viable seeds. After seed dormancy, seeds need these accumulated seed storage compounds for energy supply during germination.

1.1.5. Germination: Biogenesis of mitochondria and establishment of respiration

Seed dormancy is a seed characteristic that avoids seed germination under unfavorable conditions for subsequent seedling establishment and reproductive growth. The phytohormones abscisic acid (low levels) and gibberellins (high levels) that are environmentally influenced can break seed dormancy (Finch-Savage and Leubner-Metzger, 2006). The transition from the dormant stage to a metabolic active seedling requires energy for cell division and expansion.

Energy for germination can originate from degradation of seed storage compounds like accumulated fatty acids. These are degraded by beta-oxidation to produce carbon skeletons for sucrose synthesis. Sucrose is an energy source for respiration. The marginal functional mitochondria that even lack cristae structures have to be converted to metabolic active organelles during imbibition, before respiratory processes can generate energy for germination (Howell e*t al.,* 2006; Howell *et al.,* 2007; Carrie *et al.,* 2013). For establishing metabolic active mitochondria an ordered assembly of mitochondrial components is required. First, the mitochondrial import apparatus is established, then the TCA cycle and the OXPHOS system components are either imported or synthesized in mitochondria (Carrie *et al.,* 2013). An accumulation of ATP synthase and cytochrome *c* oxidase transcripts six hours after imbibition was shown in maize (Ehrenshaft and Brambl, 1990). During this time, the TCA cycle and the OXPHOS system are not fully functional. The mitochondria are mainly powered by alternative NADH dehydrogenases (Logan *et al.,* 2001). Mitochondria of typical size and shape were established after 12 hours of imbibition under continuous light conditions (Law *et al.,* 2012).

Once mitochondria are functional, embryonic cells start to divide rapidly and expand for breaking the seed coat and establishment of a seedling.

1.2. Complex I

1.2.1. Structure and subunit composition

As already mentioned (see section **1.1.2**), the NADH dehydrogenase complex (complex I; EC 1.6.5.3) is important for the OXPHOS system. This is why the majority of mitochondria containing organisms have a functional complex I. Exceptions are *Saccharomyces cerevisiae*, a facultative anaerobic yeast, and organisms belonging to the *Plasmodium* genus. The structure of complex I has been elucidated for complex I containing organisms like *Escherichia coli*, *Thermus thermophilus*, *Bos taurus*, *Yarrowia lipolytica* and *Arabidopsis thaliana* (Sunderhaus *et al.,* 2006; Morgan and Sazanov, 2008; Baradaran *et al.,* 2013; Vinothkumar *et al.,* 2014; Zickermann *et al.,* 2015). The L-like structure that originates from two orthogonal arranged arms is well conserved in these organisms. One arm is hydrophobic and embedded in the inner mitochondrial membrane and termed "membrane arm". The second, "peripheral arm", is hydrophilic, attached to the membrane arm end to end and protrudes into the mitochondrial matrix.

In contrast to the conserved structure, organisms differ in complex I size and number of complex I subunits. Prokaryotic organisms contain a minimalistic complex I that has 14-17 subunits and is ~550 kDa in mass (Dupuis *et al.,* 1998; Friedrich, 1998; Yip *et al.,* 2011; Berrisford *et al.,* 2016). In contrast, complex I in eukaryotes is nearly twice as large. With its molecular mass of 1000 kDa it is the largest of the OXPHOS complexes (Friedrich and Böttcher, 2004). Beside the conserved prokaryotic core subunits, eukaryotes possess a large number of accessory complex I subunits (Friedrich, 2001). However, due to lineage specific additions of subunits, the number of complex I subunits is variable among different eukaryotes (*Yarrowia lipolytica*: 42; *Chlamydomonas reinhardtii*: 42; *Bos taurus*: 45; *Arabidopsis thaliana*: 49) (Cardol *et al.,* 2004; Carroll *et al.,* 2006; Angerer *et al.,* 2011; Peters *et al.,* 2013).

Because of the conserved complex I core subunits, the functional mechanism of complex I and of OXPHOS system explored in prokaryotes can also be applied to eukaryotes. However, taking into consideration that eukaryotes contain a large number of accessory subunits, mechanistic

insights generated by analyses in prokaryotes might not provide full information (Lazarou *et al.,* 2009).

1.2.2. Functional mechanism of complex I

Within the last years, the functional mechanism of complex I was elucidated by the analysis of complex I' crystal structures of *Escherichia coli*, *Thermus thermophilus* and the obligate aerobic yeast *Yarrowia lipolytica* (Efremov e*t al.,* 2010; Efremov and Sazanov, 2011; Sazanov *et al.,* 2013; Zickermann *et al.,* 2015). Complex I can be subdivided into three major modules (Efremov and Sazanov, 2012): the N-module (NADH oxidation module), the Q-module (quinone reduction module) and the P-module (proton translocation module) (**Figure 3**).

The N-module binds and oxidizes NADH by a non-covalently bound flavin mononucleotide (FMN) that is attached to the 51-kDa subunit of the "peripheral arm". Electrons are transferred through a series of seven iron-sulfur cluster (Fe/S) (N3, N1b, N5, N4, N6a, N6b, N2) from the N- to the Q-module that binds and transfers electrons to the final acceptor ubiquinone (Sazanov, 2014). An eighth Fe/S cluster (N1a) is located above the N3 cluster and does not belong to the main redox chain. It probably functions as a temporary electron storage reducing electron leakage and preventing the formation of ROS (Sazanov and Hinchliffe, 2006). For every pair of transferred electrons from NADH to ubiquinone, proton translocation from the mitochondrial matrix into the intermembrane space takes place. This involves the P-module that is embedded in the inner mitochondrial membrane and represents the membrane arm. From the distal tip to the peripheral arm it contains the following subunits: ND5, ND4, ND2, ND4L, ND6, ND3 and ND1. The last subunit might connect peripheral and membrane arm and is of special importance (Sazanov, 2014).

By resolving the crystal structure of the membrane arm of *Thermus thermophilus* and *Escherichia coli* a special structural arrangement was discovered (Efremov *et al.,* 2010; Efremov and Sazanov, 2011). The subunits ND5, ND4 and ND2 contain 14 transmembrane helices and an imbedded discontinuous helix. This discontinuous helix were also found to be present in other channels and transporters with the highest homology to Na^+/H^+ antiporters (Sazanov, 2014). Two anti-symmetrical half-channels are supposed to interact during proton translocation at these three proton translocation sites.
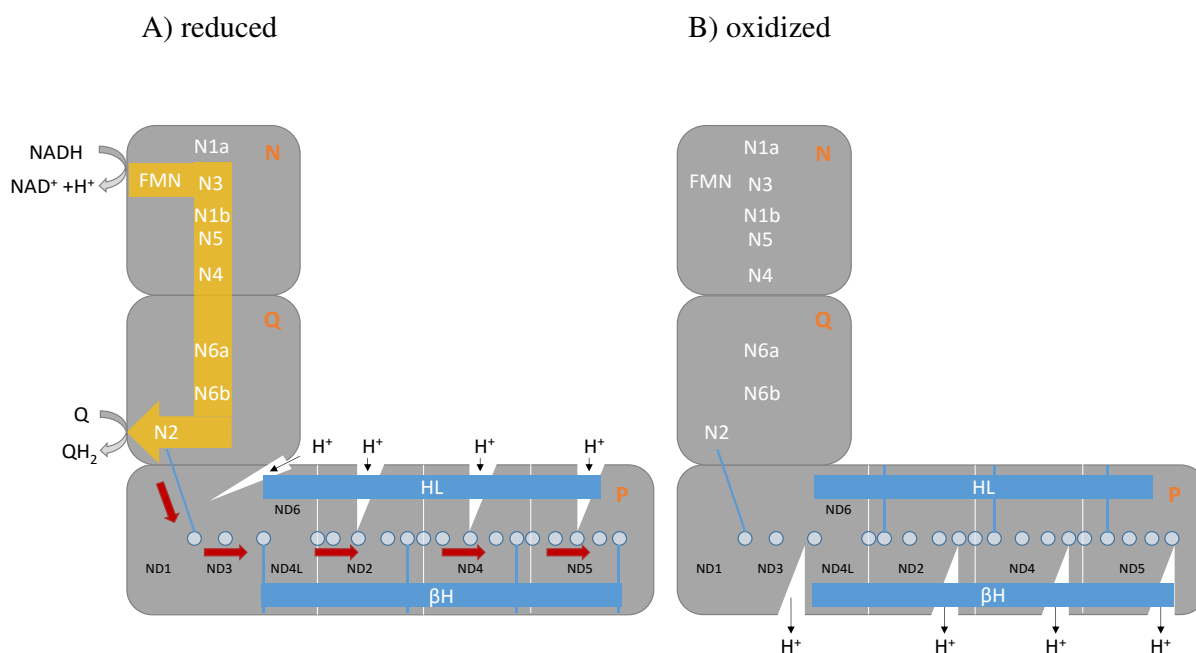
Figure 3: Electron transfer and proton translocation mechanism at complex I (adapted from Sazanov et al., 2013)**.**

Complex I is composed of three functional modules: N-, Q- and P-module. The N- and Q-module contain eight Fe/S cluster that can transfer electrons from NADH to Ubiquinone. The Fe/S cluster N1a does not belong to the main redox chain functions and is supposed to be an electron storage. A) If complex I is reduced by NADH the electrons are transferred to ubiquinone via Fe/S cluster. The Fe/S cluster N2 is linked to the proton translocation site containing (ND1, ND6 and ND4L) and initiates a cascade of conformational changes in the complex through the four proton translocation sites by two helices (HL and βH) that span the entire membrane arm. These are linked to a polar axis of charged residues in the middle of the membrane arm (light blue dots). Anti-symmetrical half channels are opening in the membrane arm of complex I at the matrix site. One proton per channel enters the membrane arm. B) In the oxidized state the membrane arm of complex I releases four protons by action of HL opening the corresponding half channels on the inter membrane space site of complex I.

The fourth proton translocation site is proposed to involve the subunits ND1, ND6 and ND4L that are located at the interface between peripheral arm and membrane arm (Sazanov, 2014). The extended quinone headgroup binds to the Fe/S cluster N2 that is linked to the fourth proton translocation site (ND1, ND6 and ND4L) (Berrisford and Sazanov, 2009).

The reductive energy of NADH is commonly used for the reduction of quinone but can also be released to cluster N2 near the quinone headgroup (Efremov and Sazanov, 2012). This initiates a cascade of conformational changes that disperse from the fourth proton translocation site to the other three proton translocation sites through a polar axis of charged and polar residues in the transmembrane helices in the middle of the membrane (Efremov *et al.,* 2010). An amphipathic helix (HL) and a β-H element are linked to this polar axis and are orientated in parallel to the membrane surface and span the entire length of the membrane arm. These elements are in contact with the discontinuous helices and facilitate conformational changes

resulting in opening and closing the anti-symmetrical half channels for proton translocation (Efremov and Sazanov, 2011; Steimle *et al.,* 2012). This is a two-step mechanism (**Figure 3**). In the oxidized state of complex I the discontinuous proton translocation channels are open to the periplasm and can release four protons. If complex I is reduced, the HL and β-H elements are supposed to move the discontinuous helices of the antiporter. Now, the channels are opened for proton uptake from the cytosol (Sazanov *et al.,* 2013).

1.2.3. Complex I in plants – γCA domain

In 2005, the structure of *Arabidopsis* complex I was resolved by single particle electron microscopy (EM) (Dudkina *et al.,* 2005). The L-like shape is similar to all other organisms analyzed so far. Surprisingly, an additional spherical domain was detected that has not been found before in animals, fungi or prokaryotes (Morgan and Sazanov, 2008; Baradaran *et al.,* 2013; Vinothkumar *et al.,* 2014; Zickermann *et al.,* 2015). This domain is attached to the membrane arm and protrudes into the mitochondrial matrix (Dudkina *et al.,* 2005). Biochemical analysis of the membrane arm of complex I in *Arabidopsis* showed that proteins with homology to carbonic anhydrases are localized within this domain (Sunderhaus *et al.,* 2006). Phylogenetic analysis identified them as gamma-type carbonic anhydrases (γCA) (Parisi *et al.,* 2004; for detailed information see section **1.3.2**).

γCA have also been described to be part of complex I in other organisms like *Chlamydomonas reinhardtii*, *Polytomella sp.*, *Oryza sativum*, *Zea mays* and *Solanum tuberosum* (**Table 1**) but not in Opisthokonta (Morgan and Sazanov, 2008; Baradaran *et al.,* 2013; Vinothkumar *et al.,* 2014; Zickermann *et al.,* 2015). In the Amoebozoa *Acanthamoeba castellanii* γCA proteins are present in complex I, but there are no crystal or EM structures available that show that complex I possess the γCA domain (Gawryluk and Gray, 2010).

In *Arabidopsis*, the γCA domain consists of three γCA proteins (γCA1, γCA2, γCA3) and two gamma-type carbonic anhydrase like proteins (γCAL; γCAL1 and γCAL2) (Perales *et al.,* 2004; Klodmann *et al.,* 2010) (**Figure 4**). Whereas, the sequence identities between γCA and γCAL proteins are only ~ 30 %, the sequence identity is 65 to 70 % between the γCA1, γCA2 and γCA3 proteins and even ~ 90 % between γCAL1 and γCAL2 (Klodmann and Braun, 2011; Wang *et al.,* 2012).

Table 1: Occurrence of γCA homologs and their association with complex I in different organisms.

| supergroup	organism	γCA homolog	association with complex I	reference
Euryarchaeota	*Methanosarcina thermophila*	yes	no	Ferry, 2010
	Pyrococcus horikoshii	yes	no	Ferry, 2010
Cyanobacteria	*Synechococcus* sp.	yes	no	Pena *et al.,* 2010
	Nostoc sp.	yes	no	Araujo *et al.,* 2014
Amoebozoa	*Acanthamoeba castellanii*	yes	(yes)	Gawryluk, and Gray, 2010
Chlorophyta	*Chlamydomonas reinhardtii*	yes	yes	Cardol *et al.,* 2004
	Polytomella sp.	yes	yes	Sunderhaus *et al.,* 2006
Plantae	*Arabidopsis thaliana*	yes	yes	Sunderhaus *et al.,* 2006
	Oryza sativa	yes	yes	Heazlewood *et al.,* 2003
	Zea mays	yes	yes	Peters *et al.,* 2008
	Solanum tuberosum	yes	yes	Bultema *et al.,* 2009
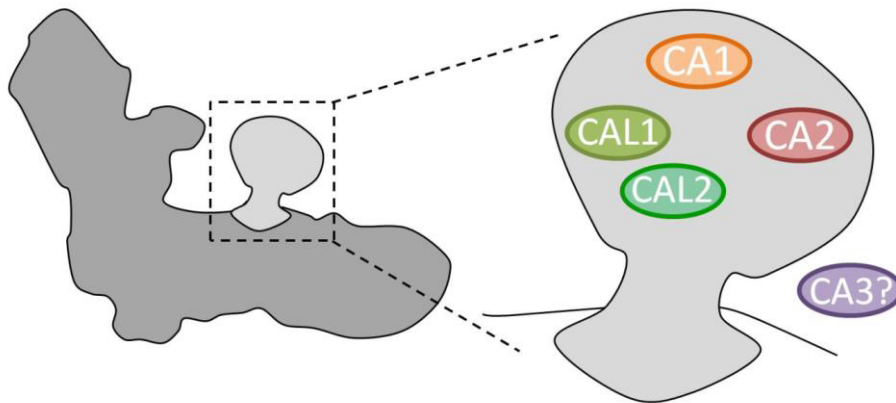
Figure 4: γCA domain is associated with complex I (Fromm et al., 2016c).

Three γCA (CA1, CA2, CA3) and two γCAL (CAL1, CAL2) proteins were identified. CA1, CA2, CAL1 and CAL2 are localized in the domain. The CA3 protein could not be found in association with the other γCA/ γCAL proteins. Three of the four γCA/ γCAL proteins can be localized in the 85 kDa domain at the same time.

All γCA/ γCAL proteins are nuclear encoded and have to be imported into mitochondria. Interestingly, γCA proteins have a molecular mass of ~ 30 kDa but no cleavable presequence. Contrary to this, the γCAL proteins have cleavable presequences and are therefore slightly smaller (~ 25 kDa) as mature proteins (Huang *et al.,* 2009; Klodmann *et al.,* 2010). The γCA domain itself has a mass of 85 kDa (Klodmann *et al.,* 2010). Consequently, only three out of the five γCA/ γCAL proteins can be localized in the γCA domain at the same time. Interactions of two γCA2 proteins with either γCAL1 or γCAL2 were identified in a yeast-two hybrid screen (Perales *et al.,* 2004).

In addition, the trimer can also consist of either two γCA1 and one γCAL protein or of two different γCA proteins and one γCAL protein (e.g. γCA1 + γCA2+ γCAL1 or γCAL2) (Klodmann *et al.,* 2010). The role of γCA3 is different because it was not found to be localized in the γCA domain. Furthermore, an interaction of γCA3 with other γCA/ γCAL proteins has not been detected within the yeast-two hybrid screen (Perales *et al.,* 2004; Klodmann *et al.,* 2010). Six γCA domain compositions have been suggested (**Chapter 2.3**).

The γCA/ γCAL proteins make plant complex I more complex than its eukaryotic counterparts and might add specific functions of complex I in the plant system.

1.3. Gamma-type carbonic anhydrases

1.3.1. General overview – families and CA functions

Carbonic anhydrases (CA; EC 4.2.1.1) are zinc (Zn)-containing metalloenzymes that have first been characterized in human erythrocytes in 1933 (Meldrum and Roughton, 1933). Since 1933, the CAs were detected in several organisms of all three domains of life (Hewett-Emmett and Tashian, 1996). However, sequence analysis revealed that the CA sequences of different organisms share no significant sequence homologies (Hewett-Emmett and Tashian, 1996). Therefore, the CAs were subdivided in six CA gene families that are called α, β, γ, δ, ε and ζ (So *et al.,* 2004; reviewed in Ferry, 2010). Due to some sequence similarities to other CA families the classification of δ, ε and ζ is still discussed controversially (Sawaya *et al.,* 2006; Park *et al.,* 2007).

Although the CA families are very different in their sequence, they have the same catalytic activity (Hewett-Emmett and Tashian, 1996). Depending on the pH of the surrounding media, CAs catalyze the reversible hydration of one carbon dioxide molecule to one bicarbonate molecule and one proton (pH 8.0) (**Equation 1**). CO_2 reacts with a Zn-OH intermediate at the active site of the enzyme. In the reverse dehydration reaction, HCO_3^- reacts with $Zn-H_2O$ to CO_2 (pH 6.4). CAs can convert up to 10^6 carbon dioxide molecules per second (Khalifah, 1971; Moroney *et al.,* 2011).

$$CO_2 + H_2O \leftrightarrow HCO_3^- + H^+$$

$$\xrightarrow{\quad 6.4 \qquad\qquad 8.0 \quad}$$
$$pH$$
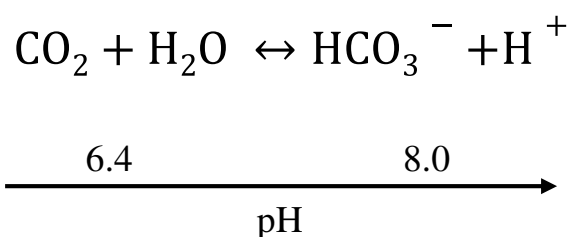
Equation 1: The catalytic equilibrium catalyzed by carbonic anhydrases is pH dependent (adapted from Khalifah, 1971)**.**

Regarding their catalytic activity, carbonic anhydrases play an important role in carbon concentrating mechanisms (CCM). Photosynthetic organisms like cyanobacteria, algae and higher plants have evolved different forms of CCM. In general, CAs provide CO_2 for refixation by ribulose-1,5-bisphosphate carboxylase/oxygenase (RuBisCO) (Badger, 2003). One of the best investigated CCMs is the single-cell CCM in cyanobacteria. The HCO_3^- is enriched in the

cytosol of the cell by active transport of HCO_3^- and CO_2 from the outside. CO_2 uptake is facilitate by NDH-1 complex that subsequently, converts CO_2 to HCO_3^- in the cytosol (Rae *et al.,* 2013). HCO_3^- diffuses and accumulates in the central compartment of the CCM, the carboxysome. The carboxysome encapsulates RuBisCO and a carboxysomal CA. The carboxysomal CA catalyzes the conversion of HCO_3^- to CO_2. The efflux of CO_2 is prevented by the protein shell of the carboxysome and leads to an enrichment of CO_2 in the carboxysome. Finally, RuBisCO can fix CO_2 molecules for the carboxylation reaction (Rae *et al.*, 2013).

However, the single-cell CCM of cyanobacteria contrasts the multicellular CCM of C4 plants. Mesophyll and bundle sheath cells exchange metabolites for carbon fixation by RuBisCO that is located in bundle sheath cells. In the cytosol of mesophyll cells incoming CO_2 is hydrated by a βCA to HCO_3^-. Phosphoenolpyruvate carboxylase converts HCO_3^- and phosphoenolpyruvate to oxaloacetate. Oxaloacetate can be metabolized either to malate (chloroplast of mesophyll cell) or aspartate (cytosol of the mesophyll cell). The C4-acid intermediates diffuse into the bundle sheath cells where they are decarboxylated again. The released CO_2 can be fixed to ribulose-1,5-bisphosphate by RuBisCO (Badger, 2003). This multicellular anatomical differentiation and metabolic co-ordination within the leaf minimizes the oxygenation reaction of RuBisCO. C3 plants do not possess such a mechanism. Hence, carbon dioxide and molecular oxygen compete for the binding site at RuBisCO. The oxygenation reaction of RuBisCO results in photorespiration (reviewed in Peterhänsel *et al.,* 2010). Nevertheless, several chloroplastidic CAs were identified in C3 plants. They are very abundant and can make up 2 % of the total leaf protein (Peltier *et al.,* 2006). The function of these CAs is mainly unknown but it is assumed that their impact on CO_2 refixation is rather low in comparison to C4 plants (Ignatova *et al.,* 2011; Ludwig, 2012).

Our current understanding of CA biochemistry and biological functions is largely based on α and βCAs. Beside αCAs and βCAs, higher plants possess a third CA family, the γCAs (Moroney *et al.,* 2011). Great efforts were made to characterize the gamma-type carbonic anhydrases of plants more in detail within the last decade.

1.3.2. Gamma-type carbonic anhydrases in *A. thaliana* – Phylogeny and activity

In 2000, the genome of *Arabidopsis thaliana* was sequenced (Arabidopsis Genome Initiative, 2000). Among others, five new genes were identified. They were annotated as homologues of the gamma-type carbonic anhydrase family because sequence analysis yielded in a high consensus sequence with the prototype γCA (CAM) of *Methanosarcina thermophila* (Kisker *et al.,* 1996; Moroney *et al.,* 2001; Parisi *et al.,* 2004). High homology between CAM and γCA of *Arabidopsis* was obtained for an amino acid sequence (50 – 220 AS) of CAM annotated as PaaY motif (carbonic anhydrase/ acetyltransferase, isoleucine patch family) (Parisi *et al.,* 2004). This motif contains hexapeptide repeats that are very important for a catalytic active conformation of CAM - the first described biochemical active γCA protein (Alber and Ferry, 1994). Due to the conservation of the PaaY motif, the γCA proteins of *Arabidopsis* are also supposed to catalyze the hydration/dehydration reaction of CO_2/HCO_3^- (**Equation 1**). However, only marginal evidences for this catalytic activity of *Arabidopsis* γCA proteins exist. It was demonstrated that the *Arabidopsis* γCA2 protein can bind inorganic carbon (Martin *et al.,* 2009). Nevertheless, the entire catalytic reaction has not been shown for plant γCAs so far. However, catalytic activity of *Arabidopsis* γCA proteins cannot be excluded. In the following homologies of catalytic important amino acids, conservations in folding and structure between active CAM and γCA of *Arabidopsis* are summarized.

Zinc atoms are essential for the active site constitution of CAM to enable CA activity (reviewed in Ferry, 2010). The positions of the three metal ligands - histidines - that coordinate the zinc atoms are mostly conserved between CAM and γCA of *Arabidopsis*. Three out of the five gamma-type carbonic anhydrases are homologous for all three histidine residues of CAM (CAM: histidine 81 (His81), histidine 117 (His117) and histidine 122 (His122)). However, two proteins lack two out of three histidine residues. Therefore, these are termed gamma-type carbonic anhydrase like (γCAL) proteins (Parisi *et al.,* 2004). In addition to the zinc atom, some amino acids were found to be important for catalysis. Most important residues for catalysis are conserved between CAM, γCA and γCAL proteins (CAM: arginine 59 (Arg59), aspartic acid 61 (Asp61), glutamine 75 (Gln75), glutamine 73 (Gln73) and aspartic acid 76 (Asp76)). Notably, CAM residues glutamic acid 62 (Glu62), glutamic acid 84 (Glu84), and asparagine 202 (Asn202) are absent in γCA and γCAL proteins of *Arabidopsis* (Parisi *et al.,* 2004;

reviewed in Ferry, 2010). Glu84 is essential for acidic loop formation and together with Glu62 involved in proton transport during catalysis by CAM (Iverson *et al.,* 2000).

Phylogenetic analysis estimated that γCA proteins of other organisms manly lack Glu62, Glu84 and Asn202 similar to γCA and γCAL proteins of *Arabidopsis*. It seems that the γCA family is dominated by a subclass missing the acidic loop and the proton shuttle residues (reviewed in Ferry, 2010). Nevertheless, it is supposed that alternative amino acids might fulfill the functions of the missing residues (Parisi *et al.,* 2004).

Aside from the conservation of most catalytic important residues, the folding and the structure of plant γCA proteins are also relevant for catalytic activity. The CAM protein contains the PaaY motif with hexapetide repeats that fold into left-handed parallel β-helices (LβH) (Raetz and Roderick, 1995). Folding into LβH was also investigated for γCA proteins of *Arabidopsis* by structural modeling (Parisi *et al.,* 2004). Furthermore, the trimeric conformation is common to CAM and γCA/ γCAL proteins associated in a γCA domain of complex I. It also seems likely that the γCA domain has to be attached to mitochondrial complex I to be catalytically active (Parisi *et al.,* 2004) (see section **1.2.3**). For this reason the investigation of catalytic activity of *Arabidopsis* γCA/ γCAL proteins that were overexpressed in bacteria might have failed.

1.3.3. Functions of plant complex I and associated gamma-type carbonic anhydrases

As already outlined in this thesis, complex I is of fundamental importance for maintaining the redox homeostasis of the cell and inserting electrons in the mitochondrial electron transport chain. The mETC is coupled to proton translocation by electrostatic chain reactions in the membrane arm (Sazanov, 2014). Complex I generates 40 % of the proton motive force contributing to ATP synthesis by proton translocation (Hunte *et al.,* 2010). For the generation of one molecule ATP, three out of the four translocated protons at complex I have to pass through the ATP synthase complex (Rich, 2003).

Furthermore, complex I is also a major source for ROS that are harmful for the mitochondria and the entire cell (Møller and Sweetlove, 2010).

Additional functions of plant complex I were investigated with mutants that have gene defects in core and accessory subunits, assembly or splicing factors. Plants are attractive experimental

systems for studying complex I because plants are still viable even though complex I is lost completely. In contrast, in animal or human complex I mutations leading to the absence of the protein complex are generally lethal, presumably because alternative mETC enzymes like alternative NAD(P)H dehydrogenase are not present (Fassone and Rahman, 2012).

Some complex I mutants were described in *Nicotiana sylvestris*, *Zea mays* and *Arabidopsis thaliana*.

The cytoplasmatic male sterile II (*cmsII*) mutant of *Nicotiana sylvestris* lacks a functional complex I due to a deletion in the mitochondrial *NAD7* gene (Pla *et al.,* 1995). The *cmsII* mutant is delayed in seed germination and development. It is also characterized by a light-dependent male sterile phenotype. Loss of complex I results in a decreased efficiency of photosynthetic electron transfer (Sabar *et al.,* 2000; Dutilleul *et al.,* 2003). In addition, photosynthetic processes are influenced in other complex I mutants with complex I absence or deletion (Sabar *et al.,* 2000; Meyer *et al.,* 2009; Juszczuk *et al.,* 2012).

In *Zea mays*, the non-chromosomal stripe II (*ncsII*) mutant is also deficient in complex I, but complex I assembly intermediates were detected. This mutation is caused by a deletion at the 3' end of the mitochondrial *NAD4* gene (Marienfeld and Newton, 1994). Plants show an abnormal leaf development and a defect in kernel development. The mutant leaves have pale green stripes implying an influence of complex I in chloroplast function (Newton and Coe, 1986). The ultrastructure of chloroplasts was abnormal. Additionally, a decrease in the CO_2 fixation rate and defects in photosystem I have been detected (Roussell *et al.,* 1991). This underlines the importance of complex I and mitochondria for photosynthetic performance of the plant cell. This finding is supported by a higher complex I abundance in green compared to non-green tissues (Peters *et al.,* 2012). The abnormal chloroplast ultrastructure was also shown for mutants of other OXPHOS complexes like complex IV. Consequently, these defects are not limited to complex I dysfunction but rather to a total mitochondrial impairment causing pleiotropic effects (Newton *et al.,* 2004).

In *Arabidopsis*, analyzed complex I mutants that lack complex I are not male sterile (Remacle *et al.,* 2012). However, they also show a curly leaf phenotype and are delayed in vegetative and reproductive development (de Longevialle *et al.,* 2007; Meyer *et al.,* 2009; Wang *et al.,* 2012; Hsu *et al.,* 2014; Kühn *et al.,* 2015). The strength of the developmental delay and the curly leaf phenotype correlate with the amount of complex I that is efficiently assembled. This is underlined by a comparative analysis of *ndufv1* (absence of complex I) and *ndufs4* (depletion of complex I) mutants (Kühn *et al.,* 2015). Additionally, flux through glycolysis and the TCA

cycle were investigated for both mutants. The complete absence of complex I causes a metabolic switch that leads to increased fluxes through both pathways that were not observed for wildtype and *ndufs4* mutant. This indicates that complex I is a negative regulator of both glycolysis and the TCA cycle (Kühn *et al.,* 2015).

As described before (see section **1.2.3**), *Arabidopsis* complex I is even more complex than its prokaryotic or even eukaryotic counterparts. For the majority of accessory complex I subunits no function has been assigned yet. Generally it is assumed that the accessory subunits fulfill functions in stabilization, regulation and assembly of complex I (Heazlewood *et al.,* 2003; Marques *et al.,* 2005; Meyer *et al.,* 2011; Vinothkumar *et al.,* 2014; Letts and Sazanov, 2015). The assembly of complex I subunits is a multistep process that proceeds via defined assembly intermediates and is supported by a number of assembly factors (Klodmann *et al.,* 2010; Meyer *et al.,* 2011; Subrahmanian *et al.,* 2016). For example, the accessory NUMM subunit (orthologue to NUDFS6) of *Yarrowia lipolytica* contains a functional zinc site. The subunit is important for stable insertions of the Fe/S cluster N4 in the N module and for proper assembly of complex I (Kmita *et al.,* 2015).

The γCA/ γCAL proteins are unique accessory subunits of plant complex I. For functional investigation of γCA/ γCAL proteins, single and double mutants (*ca1ca3, cal1cal2i, ca2cal1, ca2cal2* and *ca1ca2*) were analyzed (Perales *et al.,* 2005; Wang *et al.,* 2012; Soto *et al.,* 2015; Córdoba *et al.,* 2016; **Chapter 2.1, 2.2** and **2.4**).

In *Arabidopsis*, single knockout mutant plants for *CA1*, *CA2*, *CA3*, *CAL1* and *CAL2* genes showed no developmental or growth defects in comparison to wildtype plants (Wang *et al.,* 2012; **Chapter 2.2**). However, the cell culture line of the *ca2* mutant has reduced growth rates, decreased respiration rates and reduced complex I levels (~ 20 % complex I are left) and activity (Perales *et al.,* 2005). Immunoblot analyses of seven complex I mutants - including the *ca2* single mutant - that lack different complex I subunits, were carried out (Meyer *et al.,* 2011). Based on this analysis and ^{15}N-labeling experiments, γCA2 was found to be present from the beginning of the early assembly process of complex I. This indicates an essential role for γCA2 during early complex I assembly (Li *et al.,* 2013). The assembly of complex I is a stepwise process during which assembly intermediates are associated by assembly factors to form the holocomplex. The assembly process in plants shows unique characteristics. It is assumed that the γCA domain has to be assembled, before complex I holocomplex can be assembled (Perales *et al.,* 2004; Subrahmanian *et al.,* 2016). Therefore, γCA2 and the other γCA/ γCAL proteins are of fundamental importance for the complex assembly process. However, γCA2 and the other

γCA/ γCAL proteins cannot be viewed solely as assembly factors because they are also part of the mature complex I. In general, assembly factors help to assemble the complex I intermediates but are not part of the holocomplex. Assembly factors identified in plants are L-galactone-1,4-lactone dehydrogenase (GLDH) and iron-sulfur protein required for NADH dehydrogenase (INDH) (Pineau *et al.,* 2008; Wydro *et al.,* 2013).

Single particle electron microscopy showed that complex I particles from *ca2* mutant cell lines have normal shape and include the γCA domain (Sunderhaus *et al.,* 2006). This implies that γCA/ γCAL subunits can substitute for each other in the γCA domain. Hence, *γCA/ γCAL* double mutants were generated to study the γCA function in more detail.

The *ca1ca3* double mutant shows no alterations in growth as well as vegetative and reproductive development compared to wildtype plants (Wang *et al.,* 2012). As mentioned before (see section **1.2.3**), the role of CA3 in the γCA domain is not completely understood. Therefore, this mutant might be an exception. Simultaneous mutation of two other *γCA/ γCAL* genes causes more drastic effects.

The *ca2cal1*, *ca2cal2*, *cal1cal2i* and *ca1ca2* double mutants show retarded growth with the typical curly leaf phenotype for complex I mutants (Wang *et al.,* 2012; Soto *et al.,* 2015; **Chapter 2.1** and **2.2**). In the *ca2cal1*, *ca2cal2* and *cal1cal2i* mutants trace amounts of complex I are left. These mutants can complete embryogenesis and maturation of the seeds, germinate and establish growing seedlings. The plants have a smaller rosette diameter and are slightly delayed in establishing flowers (Wang *et al.,* 2012; Soto *et al.,* 2015; **Chapter 2.1**). Besides this, *cal1ca2i* lines were hypersensitive to light independent of the wave length. Furthermore, they showed a higher accumulation of anthocyanin compared to the wildtype suggesting a functional association of γCA/ γCAL with photomorphogenesis (Wang *et al.,* 2012).

In contrast, simultaneous mutation of *γCAL1* and *γCAL2* (*cal1cal2*) or *γCA1* and *γCA2* (*ca1ca2*) leads to complex I dysfunction that causes defects in the embryogenesis of *Arabidopsis* seeds ending up in embryo lethality (Wang *et al.,* 2012; Córdoba *et al.,* 2016; **Chapter 2.2**). The *cal1cal2* embryo is delayed in embryo development, had problems to synthesize chlorophyll pigments and in the end the seeds were not able to germinate (Wang *et al.,* 2012). Further analysis of *ca1ca2* mutant embryos indicated that the mutant contains less active mitochondria, accumulates ROS and has fewer but larger oil bodies (Córdoba *et al.,* 2016). Plants and cell suspension culture lines show a reorganized respiration with increased respiration rates (**Chapter 2.2** and **2.4**).

However, the strength of the retardation correlates to the residual complex I level and activity as described before for *ndufv1* and *ndufs4* (Kühn *et al.,* 2015).

RuBisCO is the key enzyme of photosynthesis and is a bifunctional enzyme that binds carbon dioxide as well as molecular oxygen (Bowes *et al.,* 1971; Bowes and Ogren, 1972). If RuBisCO is carboxylated, 3-phosphoglycerate molecules are converted to polysaccharides by the Calvin cycle. The resulting sugars can be catabolized and supply the cell with ATP and reduction equivalents. If RuBisCO binds oxygen, photorespiratory processes are initiated which compromises reactions in chloroplast, peroxisome and mitochondrion. Toxic 2-phosphoglycolate is produced that has to be converted back to 3-phosphoglycerate for synthesis of polysaccharides by the Calvin cycle. This is a complex, energy and reduction equivalent consuming process which releases prior fixed CO_2 into mitochondria (Peterhänsel *et al.,* 2010). For prevention of oxygenation of RuBisCO, many photosynthetic organisms evolved different types of CCMs such as C4 photosynthesis in some plants or single-cell CCM in cyanobacteria to increase the carboxylation of RuBisCO by spatial segregation and action of CA enzymes (see section **1.3.1**). In C3 plants RuBisCO is not spatial segregated and photorespiration occurs. However, the γCA/ γCAL proteins were supposed to be involved in conversion and transport of released CO_2 for refixation by RuBisCO in C3 plants (Braun and Zabaleta, 2007; Zabaleta *et al.,* 2012).

Photorespiration leads to an increasing CO_2 production in mitochondria by the conversion of two glycine molecules to one serine molecule (Peterhänsel *et al.,* 2010). If the passive transport by diffusion of CO_2 across the mitochondrial membranes is too slow, an unequal CO_2 balance between the chloroplast and the mitochondrion might be the consequence. This might be readjusted by an active transport mechanism, which potentially involves mitochondrial respiratory complex I and the associated γCA domain. The hypothesis assumes that γCA proteins are catalytically active and can convert carbon dioxide to bicarbonate (Braun and Zabaleta, 2007; Zabaleta *et al.,* 2012) (**Figure 5**). As already mentioned (see section **1.3.1**), the equilibrium is dependent on the pH. Thus, a pH around 8 is required for an excessive hydration of CO_2 to bicarbonate. The required pH predominates in the mitochondrial matrix where CO_2 is released during the conversion of glycine to serine. Additionally, proton translocation across complex I could lead to alkaline pockets at the matrix side of complex I and, thereby, facilitate the conversion of CO_2 to bicarbonate in the mitochondrial matrix (Braun and Zabaleta, 2007).
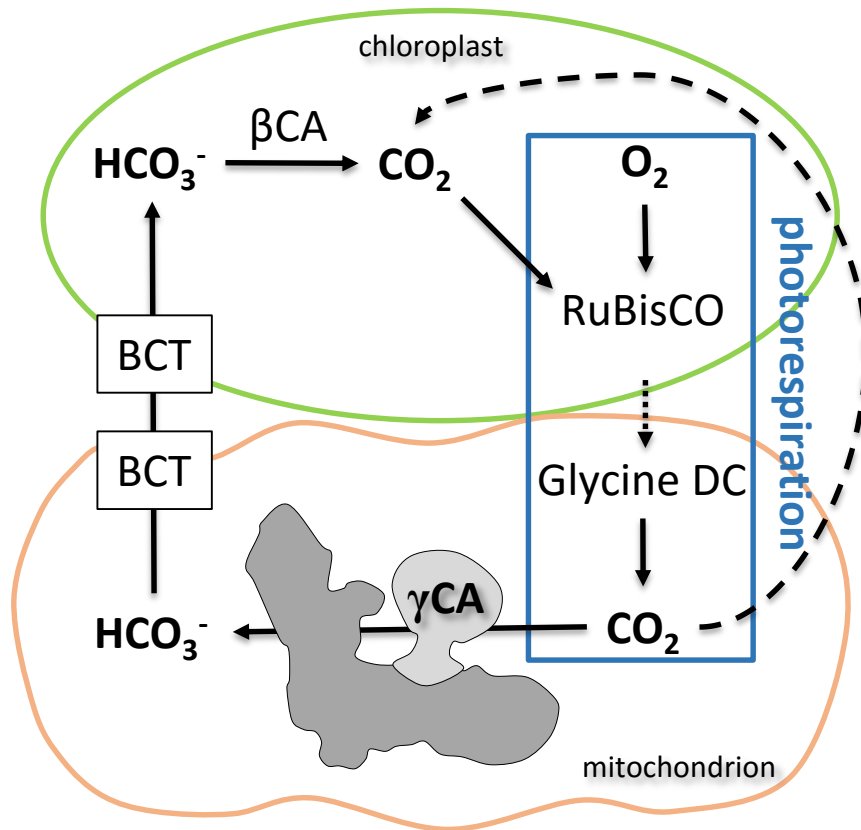
Figure 5: Refixation of mitochondrial released CO_2 by RuBisCO via γCA associated with complex I (adapted from Braun and Zabaleta, 2007)**.**

Photorespiration occurs by oxygenation of RuBisCO and previously fixed CO_2 is released by glycine decarboxylase complex (GDC) during the conversion of Glycine to serine in mitochondria. The released CO_2 might diffuse across the multi membraned organelles to RuBisCO. Another possibility is the conversion of CO_2 to bicarbonate (HCO_3^-) by γCA domain of complex I. HCO_3^- might be transported across mitochondrial and chloroplastidic membranes by bicarbonate transporter (BCT). In the chloroplast HCO_3^- can be reconverted by a βCA to CO_2 to be fixed by RuBisCO for synthesis of polysaccharides in the Calvin cycle.

The bicarbonate could be transported out of mitochondria by a putative bicarbonate transporter (BCT). Alternatively, the γCA domain might transport bicarbonate itself by a porous structure near the domain (Zabaleta *et al.,* 2012).

Bicarbonate could get into the intermembrane space surrounded by the permeable outer mitochondrial membrane. Having reached the cytosol, it could be imported into the stroma of the chloroplast by another putative BCT. For subsequent reconversion of bicarbonate to CO_2 either a shifted equilibrium to CO_2 by RuBisCO' CO_2 consumption, or an acidic pH is required. According to insights in CCM of *Chlamydomas reinhardtii*, bicarbonate might be transported into the acidic thylakoid lumen of the chloroplast and converted to CO_2 (Moroney *et al.,* 2011). Finally, CO_2 could diffuse across the thylakoid membrane into the stroma of the chloroplast for refixation by RuBisCO.

Some findings support the hypothesized CO_2 conversion and transport mechanism that involves the complex I associated γCA domain in C3 plants:

(i)   The complex I associated γCA domain is present in plants but absent in non-photosynthetic organisms like animals and fungi (Sunderhaus *et al.,* 2006; Vinothkumar *et al.,* 2014; Zickermann *et al.,* 2015).

(ii)   A sequence similarity of γCA/ γCAL proteins to the M-subunit of the cyanobacterial carbon concentrating mechanism machinery has been shown (Parisi *et al.,* 2004).

(iii)   In cyanobacteria, the conversion of CO_2/HCO_3^- is also coupled to a complex I like enzyme (NDH-I) (Rae *et al.,* 2013).

(iv)   The γCA2 protein can bind inorganic carbon (Ci) (Martin *et al.,* 2009). This supports the performance of CA catalysis by γCA proteins.

(v)   Transcription of γ*CA2* and γ*CA3* is downregulated at elevated CO_2 concentrations (restricting photorespiration) (Perales *et al.,* 2005).

(vi)   When comparing the photosynthetic rates between protoplasts and isolated chloroplasts, protoplasts perform better at low CO_2 concentrations. It was suggested that an internal CO_2 source was available in protoplasts but not in chloroplasts (Riazunnisa *et al.,* 2006).

(vii)   The complex I mutant *cmsII* has a 20 to 30 % reduced photosynthesis under atmospheric CO_2 concentrations. This reduction was diminished when mutants were cultivated under high CO_2 or low O_2 concentrations (restricting photorespiration) (Dutilleul *et al.,* 2003).

(viii) *ca2cal1* and *ca2cal2* mutants show reduced growth rates under atmospheric but not under elevated CO_2 concentrations compared to the wildtype and single mutants (Soto *et al.,* 2015).

In summary, complex I is not only an oxidoreductase but a multifunctional protein complex with versatile functions. The plant specific accessory subunits might also imply special complex I function in plant mitochondria with probable impact on the whole plant metabolism (Braun *et al.,* 2014). The γCA/ γCAL proteins are important for complex I assembly and might fulfill additional functions that are not completely characterized. In most cases, the mutations of γ*CA*/ γ*CAL* genes have also an impact on complex I level and activity. Therefore, the discrimination between direct and indirect γCA/ γCAL functions remains challenging.

1.4.   Objectives of this thesis

The overall aim of this thesis is to increase the knowledge of the γCA and γCAL proteins that are associated in a γCA domain with mitochondrial complex I in *Arabidopsis thaliana*. Here, special focus is placed on the functional characterization of γCA/ γCAL proteins. In this thesis, generated and provided γCA/ γCAL double mutants are analyzed with versatile set of genomic, metabolomic and proteomic tools.

(i)   The main focus lies on a characterization of the *ca1ca2* double mutant. I planned to generate the *ca1ca2* mutant and analyze the filial generations with genetic tools to investigate the inheritance and the occurrence of *ca1ca2* double mutant. Furthermore, analyses according to development and physiology of *ca1ca2* plants should be performed (**Chapter 2.2**). The influence of the simultaneous mutation of *CA1* and *CA2* genes on the OXPHOS complexes has to be monitored by proteomic approaches (**Chapter 2.2**). In addition, gel-based and gel-free comparative proteomic investigations are planned to elucidate the effects of simultaneous *CA1* and *CA2* mutation and the subsequent absence of complex I on the mitochondrial and the whole cellular proteome (**Chapter 2.4**). As already mentioned, it is challenging to discriminate between direct functions of γCA/ γCAL proteins and indirect functions that are coupled to complex I depletion until the catalytic activity of γCA/ γCAL enzymes remains to be elusive. For better distinction *ca1ca2* mutants overexpressing enzymatically inactive CA2 versions shall be generated. Amino acids that are supposed to be important for carbonic anhydrase activity shall be exchanged against structural similar amino acids (**Chapter 2.2**). These complemented *ca1ca2::CA2* lines should also be used to investigate the carbon refixation hypothesis.

(ii)   The *cal1cal2i* double mutant was generated by Wang *et al.* (2012). They already pointed to some particular functions of the γCAL proteins. However, the impact of the mutation on complex I level and activity as well as on the mitochondrial proteome has to be figured out. In addition, the *cal1cal2i* mutant also should be investigated according to the carbon refixation hypothesis. Different carbon dioxide concentrations should be applied to *cal1cal2i* mutants and wildtype plants to monitor the growth rates. Furthermore, metabolites should be analyzed for these plants and glycine/serine ratios, an indicator for photorespiration, are planned to be evaluated (**Chapter 2.1**).

(iii) Finally, a model for the γCA domain composition shall be supposed by summarizing experimental investigations on *γca*/ *γcal* mutants (**Chapter 2.3**).

1.5. References

Alber BE, Ferry JG (1994) A carbonic anhydrase from the archaeon *Methanosarcina thermophila. Proceedings of the National Academy of Sciences of the United States of America* **91:** 6909–6913.

Angerer H, Zwicker K, Wumaier Z, Sokolova L, Heide H, Steger M, Kaiser S, Nubel E, Brutschy B, Radermacher M, Brandt U, Zickermann V (2011) A scaffold of accessory subunits links the peripheral arm and the distal proton-pumping module of mitochondrial complex I. *The Biochemical Journal* **437:** 279–288.

Arabidopsis Genome Initiative (2000) Analysis of the genome sequence of the flowering plant *Arabidopsis thaliana. Nature* **408:** 796–815.

Araujo C de, Arefeen D, Tadesse Y, Long BM, Price GD, Rowlett RS, Kimber MS, Espie GS (2014) Identification and characterization of a carboxysomal gamma-carbonic anhydrase from the *cyanobacterium Nostoc sp.* PCC 7120. *Photosynthesis Research* **121:** 135–150.

Badger M (2003) The roles of carbonic anhydrases in photosynthetic CO_2 concentrating mechanisms. *Photosynthesis Research* **77:** 83–94.

Baradaran R, Berrisford JM, Minhas GS, Sazanov LA (2013) Crystal structure of the entire respiratory complex I. *Nature* **494:** 443–448.

Baud S, Dubreucq B, Miquel M, Rochat C, Lepiniec L (2008) Storage reserve accumulation in *Arabidopsis*: metabolic and developmental control of seed filling. *The Arabidopsis book / American Society of Plant Biologists* **6:** e0113.

Belmonte MF, Kirkbride RC, Stone SL, Pelletier JM, Bui AQ, Yeung EC, Hashimoto M, Fei J, Harada CM, Munoz MD, Le BH, Drews GN, Brady SM, Goldberg RB, Harada JJ (2013) Comprehensive developmental profiles of gene activity in regions and subregions of the *Arabidopsis* seed. *Proceedings of the National Academy of Sciences of the United States of America* **110:** 435-444.

Berrisford JM, Sazanov LA (2009) Structural basis for the mechanism of respiratory complex I. *The Journal of biological chemistry* **284:** 29773–29783.

Berrisford JM, Baradaran R, Sazanov LA (2016) Structure of bacterial respiratory complex I. *Biochimica et Biophysica Acta*, *in press*: doi**:** 10.1016/j.bbabio.2016.01.012.

Boekema EJ, Braun HP (2007) Supramolecular structure of the mitochondrial oxidative phosphorylation system. *The Journal of Biological Chemistry* **282:** 1–4.

Borisjuk L, Neuberger T, Schwender J, Heinzel N, Sunderhaus S, Fuchs J, Hay JO, Tschiersch H, Braun HP, Denolf P, Lambert B, Jakob PM, Rolletschek H (2013) Seed architecture shapes embryo metabolism in oilseed rape. *The Plant Cell* **25:** 1625–1640.

Bowes G, Ogren WL, Hageman RH (1971) Phosphoglycolate production catalyzed by ribulose diphosphate carboxylase. *Biochemical and Biophysical Research Communications* **45:** 716–722.

Bowes G, Ogren WL (1972) Oxygen inhibition and other properties of soybean ribulose 1,5-diphosphate carboxylase. *The Journal of Biological Chemistry* **247:** 2171–2176.

Bowsher CG, Tobin AK (2001) Compartmentation of metabolism within mitochondria and plastids. *Journal of Experimental Botany* **52:** 513–527.

Braun HP, Binder S, Brennicke A, Eubel H, Fernie AR, Finkemeier I, Klodmann J, König A, Kühn K, Meyer E, Obata T, Schwarzländer M, Takenaka M, Zehrmann A (2014) The life of plant mitochondrial complex I. *Mitochondrion* **19:** 295–313.

Braun HP, Zabaleta E (2007) Carbonic anhydrase subunits of the mitochondrial NADH dehydrogenase complex (complex I) in plants. *Physiologia Plantarum* **129:** 114–122.

Bultema JB, Braun HP, Boekema EJ, Kouril R (2009) Megacomplex organization of the oxidative phosphorylation system by structural analysis of respiratory supercomplexes from potato. *Biochimica et Biophysica Acta* **1787:** 60–67.

Cardol P, Vanrobaeys F, Devreese B, van Beeumen J, Matagne RF, Remacle C (2004) Higher plant-like subunit composition of mitochondrial complex I from *Chlamydomonas reinhardtii*: 31 conserved components among eukaryotes. *Biochimica et Biophysica Acta* **1658:** 212–224.

Carrie C, Murcha MW, Giraud E, Ng S, Zhang MF, Narsai R, Whelan J (2013) How do plants make mitochondria? *Planta* **237:** 429–439.

Carroll J, Fearnley IM, Skehel JM, Shannon RJ, Hirst J, Walker JE (2006) Bovine complex I is a complex of 45 different subunits. *The Journal of Biological Chemistry* **281:** 32724–32727.

Chaban Y, Boekema EJ, Dudkina NV (2014) Structures of mitochondrial oxidative phosphorylation supercomplexes and mechanisms for their stabilisation. *Biochimica et Biophysica Acta* **1837:** 418–426.

Córdoba JP, Marchetti F, Soto D, Martin MV, Pagnussat GC, Zabaleta E (2016) The CA domain of the respiratory complex I is required for normal embryogenesis in *Arabidopsis thaliana*. *Journal of Experimental Botany*, in press: doi**:** 10.1093/jxb/erv556.

de Longevialle, Andeol Falcon, Meyer EH, Andres C, Taylor NL, Lurin C, Millar AH, Small ID (2007) The pentatricopeptide repeat gene *OTP43* is required for trans-splicing of the mitochondrial nad1 Intron 1 in *Arabidopsis thaliana*. *The Plant Cell* **19:** 3256–3265.

Douce R (1985) Mitochondria in higher plants: Structure, function, and biogenesis. Academic Press, Orlando, FL.

Dudkina NV, Eubel H, Keegstra W, Boekema EJ, Braun HP (2005) Structure of a mitochondrial supercomplex formed by respiratory-chain complexes I and III. *Proceedings of the National Academy of Sciences of the United States of America* **102:** 3225–3229.

Dudkina NV, Kouril R, Peters K, Braun HP, Boekema EJ (2010) Structure and function of mitochondrial supercomplexes. *Biochimica et Biophysica Acta* **1797:** 664–670.

Dupuis A, Chevallet M, Darrouzet E, Duborjal H, Lunardi J, Issartel JP (1998) The complex I from *Rhodobacter capsulatus*. *Biochimica et Biophysica Acta* **1364:** 147–165.

Dutilleul C, Driscoll S, Cornic G, Paepe R de, Foyer CH, Noctor G (2003) Functional mitochondrial complex I is required by tobacco leaves for optimal photosynthetic performance in photorespiratory conditions and during transients. *Plant Physiology* **131:** 264–275.

Efremov RG, Baradaran R, Sazanov LA (2010) The architecture of respiratory complex I. *Nature* **465:** 441–445.

Efremov RG, Sazanov LA (2011) Structure of the membrane domain of respiratory complex I. *Nature* **476:** 414–420.

Efremov RG, Sazanov LA (2012) The coupling mechanism of respiratory complex I - a structural and evolutionary perspective. *Biochimica et Biophysica Acta* **1817:** 1785–1795.

Ehrenshaft M, Brambl R (1990) Respiration and mitochondrial biogenesis in germinating embryos of maize. *Plant Physiology* **93:** 295–304.

Elhafez D, Murcha MW, Clifton R, Soole KL, Day DA, Whelan J (2006) Characterization of mitochondrial alternative NAD(P)H dehydrogenases in *Arabidopsis*: intraorganelle location and expression. *Plant and Cell Physiology* **47:** 43–54.

Fassone E, Rahman S (2012) Complex I deficiency: clinical features, biochemistry and molecular genetics. *Journal of Medical Genetics* **49:** 578–590.

Fatland BL, Nikolau BJ, Wurtele ES (2005) Reverse genetic characterization of cytosolic acetyl-CoA generation by ATP-citrate lyase in *Arabidopsis*. *The Plant Cell* **17:** 182–203.

Ferry JG (2010) The gamma class of carbonic anhydrases. *Biochimica et Biophysica Acta* **1804:** 374–381.

Finch-Savage WE, Leubner-Metzger G (2006) Seed dormancy and the control of germination. *The New Phytologist* **171:** 501–523.

Fowler LR, Richardson SH (1963) Studies on the electron transfer system. On the mechanism of reconstitution of the mitochondrial electron transfer system. *The Journal of Biological Chemistry* **238:** 456–463.

Friedrich T (1998) The NADH:ubiquinone oxidoreductase (complex I) from *Escherichia coli*. *Biochimica et Biophysica Acta* **1364:** 134–146.

Friedrich T (2001) Complex I: a chimaera of a redox and conformation-driven proton pump? *Journal of Bioenergetics and Biomembranes* **33:** 169–177.

Friedrich T, Böttcher B (2004) The gross structure of the respiratory complex I: a lego system. *Biochimica et Biophysica Acta* **1608:** 1–9.

Gawryluk, Ryan M R, Gray MW (2010) Evidence for an early evolutionary emergence of gamma-type carbonic anhydrases as components of mitochondrial respiratory complex I. *BMC Evolutionary Biology* **10:** 176.

Gehl B and Sweetlove LJ (2014) Mitochondrial band-7 family proteins: scaffolds for respiratory chain assembly? *Frontiers in Plant Science* **5:** 141.

Geisler DA, Broselid C, Hederstedt L, Rasmusson AG (2007) Ca^{2+}-binding and Ca^{2+}-independent respiratory NADH and NADPH dehydrogenases of *Arabidopsis thaliana*. *The Journal of Biological Chemistry* **282:** 28455–28464.

Goffman FD, Ruckle M, Ohlrogge J, Shachar-Hill Y (2004) Carbon dioxide concentrations are very high in developing oilseeds. *Plant Physiology and Biochemistry* **42:** 703–708.

Hackenbrock CR, Chazotte B, Gupte SS (1986) The random collision model and a critical assessment of diffusion and collision in mitochondrial electron transport. *Journal of Bioenergetics and Biomembranes* **18:** 331–368.

Heazlewood JL, Howell KA, Millar AH (2003) Mitochondrial complex I from *Arabidopsis* and rice: orthologs of mammalian and fungal components coupled with plant-specific subunits. *Biochimica et Biophysica Acta-Bioenergetics* **1604:** 159–169.

Hewett-Emmett D, Tashian RE (1996) Functional diversity, conservation, and convergence in the evolution of the alpha-, beta-, and gamma-carbonic anhydrase gene families. *Molecular Phylogenetics and Evolution* **5:** 50–77.

Howell KA, Millar AH, Whelan J (2006) Ordered assembly of mitochondria during rice germination begins with pro-mitochondrial structures rich in components of the protein import apparatus. *Plant Molecular Biology* **60:** 201–223.

Howell KA, Millar AH, Whelan J (2007) Building the powerhouse: What are the signals involved in plant mitochondrial biogenesis? *Plant Signaling and Behavior* **2:** 428–430.

Hsu Y, Wang H, Hsieh M, Hsieh H, Jauh G, Buratti E (2014) *Arabidopsis* mTERF15 is required for mitochondrial *nad2* Intron 3 splicing and functional complex I activity. *PLoS ONE* **9:** e112360.

Huang S, Taylor NL, Whelan J, Millar AH (2009) Refining the definition of plant mitochondrial presequences through analysis of sorting signals, N-terminal modifications, and cleavage motifs. *Plant Physiology* **150:** 1272–1285.

Hunte C, Zickermann V, Brandt U (2010) Functional modules and structural basis of conformational coupling in mitochondrial complex I. *Science* **329:** 448–451.

Ignatova LK, Rudenko NN, Mudrik VA, Fedorchuk TP, Ivanov BN (2011) Carbonic anhydrase activity in *Arabidopsis thaliana* thylakoid membrane and fragments enriched with PSI or PSII. *Photosynthesis Research* **110:** 89–98.

Iverson TM, Alber BE, Kisker C, Ferry JG, Rees DC (2000) A closer look at the active site of gamma-class carbonic anhydrases: high-resolution crystallographic studies of the carbonic anhydrase from *Methanosarcina thermophila*. *Biochemistry* **39:** 9222–9231.

Jardim-Messeder D, Caverzan A, Rauber R, de Souza Ferreira, Eduardo, Margis-Pinheiro M, Galina A (2015) Succinate dehydrogenase (mitochondrial complex II) is a source of reactive oxygen species in plants and regulates development and stress responses. *The New Phytologist* **208:** 776–789.

Juszczuk IM, Szal B, Rychter AM (2012) Oxidation-reduction and reactive oxygen species homeostasis in mutant plants with respiratory chain complex I dysfunction. *Plant, Cell and Environment* **35:** 296–307.

Khalifah RG (1971) The carbon dioxide hydration activity of carbonic anhydrase. I. Stop-flow kinetic studies on the native human isoenzymes B and C. *The Journal of Biological Chemistry* **246:** 2561–2573.

Kisker C, Schindelin H, Alber BE, Ferry JG, Rees DC (1996) A left-hand beta-helix revealed by the crystal structure of a carbonic anhydrase from the archaeon *Methanosarcina thermophila*. *The EMBO Journal* **15:** 2323–2330.

Klodmann J, Sunderhaus S, Nimtz M, Jänsch L, Braun HP (2010) Internal architecture of mitochondrial complex I from *Arabidopsis thaliana*. *The Plant Cell* **22:** 797–810.

Klodmann J, Braun HP (2011) Proteomic approach to characterize mitochondrial complex I from plants. *Plant Proteomics* **72:** 1071–1080.

Kmita K, Wirth C, Warnau J, Guerrero-Castillo S, Hunte C, Hummer G, Kaila, Ville R I, Zwicker K, Brandt U, Zickermann V (2015) Accessory NUMM (NDUFS6) subunit harbors a Zn-binding site and is essential for biogenesis of mitochondrial complex I. *Proceedings of the National Academy of Sciences of the United States of America* **112:** 5685–5690.

Kühn K, Obata T, Feher K, Bock R, Fernie AR, Meyer EH (2015) Complete mitochondrial complex I deficiency induces an upregulation of respiratory fluxes that is abolished by traces of functional complex I. *Plant Physiology* **168:** 1537-1549.

Law SR, Narsai R, Taylor NL, Delannoy E, Carrie C, Giraud E, Millar AH, Small I, Whelan J (2012) Nucleotide and RNA metabolism prime translational initiation in the earliest events of mitochondrial biogenesis during *Arabidopsis* germination. *Plant Physiology* **158:** 1610–1627.

Lazarou M, Thorburn DR, Ryan MT, McKenzie M (2009) Assembly of mitochondrial complex I and defects in disease. *Biochimica et Biophysica Acta* **1793:** 78–88.

Letts JA, Sazanov LA (2015) Gaining mass: the structure of respiratory complex I-from bacterial towards mitochondrial versions. *Current Opinion in Structural Biology* **33:** 135–145.

Li L, Nelson CJ, Carrie C, Gawryluk, Ryan M R, Solheim C, Gray MW, Whelan J, Millar AH (2013) Subcomplexes of ancestral respiratory complex I subunits rapidly turn over *in vivo* as productive assembly intermediates in *Arabidopsis*. *The Journal of Biological Chemistry* **288:** 5707–5717.

Li Z, Xing D (2010) Mitochondrial pathway leading to programmed cell death induced by aluminum phytotoxicity in *Arabidopsis*. *Plant Signaling and Behavior* **5:** 1660–1662.

Logan DC, Millar AH, Sweetlove LJ, Hill SA, Leaver CJ (2001) Mitochondrial biogenesis during germination in maize embryos. *Plant Physiology* **125:** 662–672.

Logan DC (2003) Mitochondrial dynamics. *The New Phytologist* **160:** 463–478.

Logan DC, Knight MR (2003) Mitochondrial and cytosolic calcium dynamics are differentially regulated in plants. *Plant Physiology* **133:** 21–24.

Logan DC (2006) The mitochondrial compartment. *Journal of Experimental Botany* **57:** 1225–1243.

Ludwig M (2012) Carbonic anhydrase and the molecular evolution of C4 photosynthesis. *Plant, Cell and Environment* **35:** 22–37.

Mackenzie, McIntosh (1999) Higher plant mitochondria. *The Plant Cell* **11:** 571–586.

Makiuchi T, Nozaki T (2014) Highly divergent mitochondrion-related organelles in anaerobic parasitic protozoa. *Biochimie* **100:** 3–17.

Marienfeld JR, Newton KJ (1994) The maize NCS2 abnormal growth mutant has a chimeric nad4-nad7 mitochondrial gene and is associated with reduced complex I function. *Genetics* **138:** 855–863.

Margulis L (1970) Origin of eukaryotic cells. Yale University Press, New Haven, CT.

Marques I, Duarte M, Assuncao J, Ushakova AV, Videira A (2005) Composition of complex I from *Neurospora crassa* and disruption of two "accessory" subunits. *Biochimica et Biophysica Acta* **1707:** 211–220.

Martin V, Villarreal F, Miras I, Navaza A, Haouz A, Gonzalez-Lebrero RM, Kaufman SB, Zabaleta E (2009) Recombinant plant gamma carbonic anhydrase homotrimers bind inorganic carbon. *FEBS Letters* **583:** 3425–3430.

Meldrum NU, Roughton FJ (1933) The state of carbon dioxide in blood. *The Journal of Physiology* **80:** 143–170.

Meyer EH, Tomaz T, Carroll AJ, Estavillo G, Delannoy E, Tanz SK, Small ID, Pogson BJ, Millar AH (2009) Remodeled respiration in *ndufs4* with low phosphorylation efficiency suppresses *Arabidopsis* germination and growth and alters control of metabolism at night. *Plant Physiology* **151:** 603–619.

Meyer EH, Solheim C, Tanz SK, Bonnard G, Millar AH (2011) Insights into the composition and assembly of the membrane arm of plant complex I through analysis of subcomplexes in *Arabidopsis* mutant lines. *The Journal of Biological Chemistry* **286:** 26081–26092.

Michalecka AM, Svensson AS, Johansson FI, Agius SC, Johanson U, Brennicke A, Binder S, Rasmusson AG (2003) *Arabidopsis* genes encoding mitochondrial type II NAD(P)H dehydrogenases have different evolutionary origin and show distinct responses to light. *Plant Physiology* **133:** 642–652.

Mileykovskaya E, Penczek PA, Fang J, Mallampalli, Venkata K P S, Sparagna GC, Dowhan W (2012) Arrangement of the respiratory chain complexes in *Saccharomyces cerevisiae* supercomplex III_2IV_2 revealed by single particle cryo-electron microscopy. *The Journal of Biological Chemistry* **287:** 23095–23103.

Millar AH, Whelan J, Soole KL, Day DA (2011) Organization and regulation of mitochondrial respiration in plants. *Annual Review of Plant Biology* **62:** 79–104.

Mitchell P (1961) Coupling of phosphorylation to electron and hydrogen transfer by a chemi-osmotic type of mechanism. *Nature* **191:** 144–148.

Mitsopoulos P, Chang Y, Wai T, Konig T, Dunn SD, Langer T, Madrenas J (2015) Stomatin-like protein 2 is required for *in vivo* mitochondrial respiratory chain supercomplex formation and optimal cell function. *Molecular and Cellular Biology* **35:** 1838–1847.

Møller IM, Sweetlove LJ (2010) ROS signalling-specificity is required. *Trends in Plant Science* **15:** 370–374.

Morgan DJ, Sazanov LA (2008) Three-dimensional structure of respiratory complex I from *Escherichia coli* in ice in the presence of nucleotides. *Biochimica et Biophysica Acta* **1777:** 711–718.

Moroney JV, Bartlett SG, Samuelsson G (2001) Carbonic anhydrases in plants and algae. *Plant Cell and Environment* **24:** 141–153.

Moroney JV, Ma Y, Frey WD, Fusilier KA, Pham TT, Simms TA, DiMario RJ, Yang J, Mukherjee B (2011) The carbonic anhydrase isoforms of *Chlamydomonas reinhardtii*: intracellular location, expression, and physiological roles. *Photosynthesis Research* **109:** 133–149.

Newton KJ, Coe EH (1986) Mitochondrial DNA changes in abnormal growth (nonchromosomal stripe) mutants of maize. *Proceedings of the National Academy of Sciences of the United States of America* **83:** 7363–7366.

Newton KJ, Gabay-Laughnan S, Paepe de R (2004) Mitochondrial mutations in plants, in: D. Day, A.H.Millar, J.Whelan (Eds.), Plant Mitochondria: From Genome to Function, Springer Netherlands, pp. 121–141.

Parisi G, Perales M, Fornasari MS, Colaneri A, Gonzalez-Schain N, Gomez-Casati D, Zimmermann S, Brennicke A, Araya A, Ferry JG, Echave J, Zabaleta E (2004) Gamma carbonic anhydrases in plant mitochondria. *Plant Molecular Biology* **55:** 193–207.

Park H, Song B, Morel, Francois MM (2007) Diversity of the cadmium-containing carbonic anhydrase in marine diatoms and natural waters. *Environmental Microbiology* **9:** 403–413.

Peltier J, Cai Y, Sun Q, Zabrouskov V, Giacomelli L, Rudella A, Ytterberg AJ, Rutschow H, van Wijk, Klaas J (2006) The oligomeric stromal proteome of *Arabidopsis thaliana* chloroplasts. *Molecular and Cellular Proteomics* **5:** 114–133.

Pena KL, Castel SE, Araujo C de, Espie GS, Kimber MS (2010) Structural basis of the oxidative activation of the carboxysomal gamma-carbonic anhydrase, CcmM. *Proceedings of the National Academy of Sciences of the United States of America* **107:** 2455–2460.

Perales M, Parisi G, Fornasari MS, Colaneri A, Villarreal F, Gonzalez-Schain N, Echave J, Gomez-Casati D, Braun HP, Araya A, Zabaleta E (2004) Gamma carbonic anhydrase like complex interact with plant mitochondrial complex I. *Plant Molecular Biology* **56:** 947–957.

Perales M, Eubel H, Heinemeyer J, Colaneri A, Zabaleta E, Braun HP (2005) Disruption of a nuclear gene encoding a mitochondrial gamma carbonic anhydrase reduces complex I and supercomplex I+III$_2$ levels and alters mitochondrial physiology in *Arabidopsis*. *Journal of Molecular Biology* **350:** 263–277.

Perkins GA, Renken CW, van der Klei, I J, Ellisman MH, Neupert W, Frey TG (2001) Electron tomography of mitochondria after the arrest of protein import associated with Tom19 depletion. *European Journal of Cell Biology* **80:** 139–150.

Peterhänsel C, Horst I, Niessen M, Blume C, Kebeish R, Kürkcuoglu S, Kreuzaler F (2010) Photorespiration. *The Arabidopsis book / American Society of Plant Biologists* **8:** e0130.

Peters K, Dudkina NV, Jaensch L, Braun HP, Boekema EJ (2008) A structural investigation of complex I and I+III$_2$ supercomplex from *Zea mays* at 11-13 angstrom resolution: Assignment of the carbonic anhydrase domain and evidence for structural heterogeneity within complex I. *Biochimica et Biophysica Acta* **1777:** 84–93.

Peters K, Niessen M, Peterhansel C, Spath B, Holzle A, Binder S, Marchfelder A, Braun HP (2012) Complex I-complex II ratio strongly differs in various organs of *Arabidopsis thaliana*. *Plant Molecular Biology* **79:** 273–284.

Peters K, Belt K, Braun HP (2013) 3D gel map of *Arabidopsis* Complex I. *Frontiers in plant science* **4:** 153.

Pineau B, Layoune O, Danon A, Paepe R de (2008) L-galactono-1,4-lactone dehydrogenase is required for the accumulation of plant respiratory complex I. *The Journal of Biological Chemistry* **283:** 32500–32505.

Pla M, Mathieu C, Paepe R de, Chetrit P, Vedel F (1995) Deletion of the last two exons of the mitochondrial nad7 gene results in lack of the NAD7 polypeptide in a *Nicotiana sylvestris* CMS mutant. *Molecular and General Genetics* **248:** 79–88.

Preuten T, Cincu E, Fuchs J, Zoschke R, Liere K, Borner T (2010) Fewer genes than organelles: extremely low and variable gene copy numbers in mitochondria of somatic plant cells. *The Plant Journal* **64:** 948–959.

Rae BD, Long BM, Whitehead LF, Förster B, Badger MR, Price GD (2013) Cyanobacterial carboxysomes: microcompartments that facilitate CO$_2$ fixation. *Journal of Molecular Microbiology and Biotechnology* **23:** 300–307.

Raetz CR, Roderick SL (1995) A left-handed parallel beta helix in the structure of UDP-N-acetylglucosamine acyltransferase. *Science* **270:** 997–1000.

Rasmusson AG, Soole KL, Elthon TE (2004) Alternative NAD(P)H dehydrogenases of plant mitochondria. *Annual Review of Plant Biology* **55:** 23–39.

Rasmusson AG, Escobar MA (2007) Light and diurnal regulation of plant respiratory gene expression. *Physiologia Plantarum* **129:** 57–67.

Rasmusson AG, Geisler DA, Møller IM (2008) The multiplicity of dehydrogenases in the electron transport chain of plant mitochondria. *Mitochondrion* **8:** 47–60.

Rasmusson AG, Wallström SV (2010) Involvement of mitochondria in the control of plant cell NAD(P)H reduction levels. *Biochemical Society Transactions* **38:** 661–666.

Remacle C, Hamel P, Larosa V, Subrahmanian N (2012), Complexes I in the green lineage, first ed. Springer, New York.

Riazunnisa K, Padmavathi L, Bauwe H, Raghavendra AS (2006) Markedly low requirement of added CO_2 for photosynthesis by mesophyll protoplasts of pea (*Pisum sativum*): possible roles of photorespiratory CO_2 and carbonic anhydrase. *Physiologia Plantarum* **128:** 763–772.

Rich P (1984) Electron and proton transfers through quinones and cytochrome bc complexes. *Biochimica et Biophysica Acta* **768:** 53–79.

Rich P (2003) Chemiosmotic coupling: The cost of living. *Nature* **421:** 583.

Rogov AG, Zvyagilskaya RA (2015) Physiological role of alternative oxidase (from yeasts to plants). *Biochemistry* **80:** 400–407.

Rolletschek H, Weber H, Borisjuk L (2003) Energy status and its control on embryogenesis of legumes. embryo photosynthesis contributes to oxygen supply and is coupled to biosynthetic fluxes. *Plant Physiology* **132:** 1196–1206.

Roussell DL, Thompson DL, Pallardy SG, Miles D, Newton KJ (1991) Chloroplast structure and function is Altered in the NCS2 Maize Mitochondrial Mutant. *Plant Physiology* **96:** 232–238.

Sabar M, Paepe R de, Kouchkovsky Y de (2000) Complex I impairment, respiratory compensations, and photosynthetic decrease in nuclear and mitochondrial male sterile mutants of *Nicotiana sylvestris*. *Plant Physiology* **124:** 1239–1250.

Sawaya MR, Cannon GC, Heinhorst S, Tanaka S, Williams EB, Yeates TO, Kerfeld CA (2006) The structure of beta-carbonic anhydrase from the carboxysomal shell reveals a distinct subclass with one active site for the price of two. *The Journal of Biological Chemistry* **281:** 7546–7555.

Sazanov LA, Hinchliffe P (2006) Structure of the hydrophilic domain of respiratory complex I from *Thermus thermophilus*. *Science* **311:** 1430–1436.

Sazanov LA, Baradaran R, Efremov RG, Berrisford JM, Minhas G (2013) A long road towards the structure of respiratory complex I, a giant molecular proton pump. *Biochemical Society Transactions* **41:** 1265–1271.

Sazanov LA (2014) The mechanism of coupling between electron transfer and proton translocation in respiratory complex I. *Journal of Bioenergetics and Biomembranes* **46:** 247–253.

Schägger H, Pfeiffer K (2000) Supercomplexes in the respiratory chains of yeast and mammalian mitochondria. *The EMBO Journal* **19:** 1777–1783.

Schertl P, Braun HP (2014) Respiratory electron transfer pathways in plant mitochondria. *Frontiers in Plant Science* **5:** 163.

Schwender J, Shachar-Hill Y, Ohlrogge JB (2006) Mitochondrial metabolism in developing embryos of *Brassica napus*. *The Journal of Biological Chemistry* **281:** 34040–34047.

Senda T, Yoshinaga-Hirabayashi T (1998) Intermembrane bridges within membrane organelles revealed by quick-freeze deep-etch electron microscopy. *The Anatomical Record* **251:** 339–345.

Siedow JN, Umbach AL (1995) Plant mitochondrial electron transfer and molecular biology. *The Plant Cell* **7:** 821–831.

So AK, Espie GS, Williams EB, Shively JM, Heinhorst S, Cannon GC (2004) A novel evolutionary lineage of carbonic anhydrase (epsilon class) is a component of the carboxysome shell. *Journal of Bacteriology* **186:** 623–630.

Soto D, Cordoba JP, Villarreal F, Bartoli C, Schmitz J, Maurino VG, Braun HP, Pagnussat GC, Zabaleta E (2015) Functional characterization of mutants affected in the carbonic anhydrase domain of the respiratory complex I in *Arabidopsis thaliana*. *The Plant Journal* **83**: 831-844.

Steimle S, Willistein M, Hegger P, Janoschke M, Erhardt H, Friedrich T (2012) Asp563 of the horizontal helix of subunit NuoL is involved in proton translocation by the respiratory complex I. *FEBS Letters* **586:** 699–704.

Subrahmanian N, Remacle C, Hamel PP (2016) Plant mitochondrial complex I composition and assembly: A review. *Biochimica et Biophysica Acta*. doi**:** 10.1016/j.bbabio.2016.01.009

Sunderhaus S, Dudkina NV, Jansch L, Klodmann J, Heinemeyer J, Perales M, Zabaleta E, Boekema EJ, Braun HP (2006) Carbonic anhydrase subunits form a matrix-exposed domain attached to the membrane arm of mitochondrial complex I in plants. *The Journal of Biological Chemistry* **281:** 6482–6488.

Thirkettle-Watts D, McCabe TC, Clifton R, Moore C, Finnegan PM, Day DA, Whelan J (2003) Analysis of the alternative oxidase promoters from soybean. *Plant Physiology* **133:** 1158–1169.

Vercesi AE, Borecky J, Maia, Ivan de Godoy, Arruda P, Cuccovia IM, Chaimovich H (2006) Plant uncoupling mitochondrial proteins. *Annual review of Plant Biology* **57:** 383–404.

Vinothkumar KR, Zhu J, Hirst J (2014) Architecture of mammalian respiratory complex I. *Nature* **515:** 80–84.

Wang Q, Fristedt R, Yu X, Chen Z, Liu H, Lee Y, Guo H, Merchant SS, Lin C (2012) The gamma-carbonic anhydrase subcomplex of mitochondrial complex I is essential for development and important for photomorphogenesis of *Arabidopsis*. *Plant Physiology* **160:** 1373–1383.

Wydro MM, Sharma P, Foster JM, Bych K, Meyer EH, Balk J (2013) The evolutionarily conserved iron-sulfur protein INDH is required for complex I Assembly and mitochondrial translation in *Arabidopsis*. *The Plant Cell* **25:** 4014–4027.

Yip C, Harbour ME, Jayawardena K, Fearnley IM, Sazanov LA (2011) Evolution of respiratory complex I: "supernumerary" subunits are present in the alpha-proteobacterial enzyme. *The Journal of Biological Chemistry* **286:** 5023–5033.

Youle RJ, Karbowski M (2005) Mitochondrial fission in apoptosis. *Nature reviews. Molecular Cell Biology* **6:** 657–663.

Zabaleta E, Martin MV, Braun HP (2012) A basal carbon concentrating mechanism in plants? *Plant Science* **187:** 97–104.

Zickermann V, Wirth C, Nasiri H, Siegmund K, Schwalbe H, Hunte C, Brandt U (2015) Structural biology. Mechanistic insight from the crystal structure of mitochondrial complex I. *Science* **347:** 44–49.

Chapter 2: Publications

Publication 1

2.1. Depletion of "gamma-type carbonic anhydrase-like" subunits of complex I affects central mitochondrial metabolism in *Arabidopsis thaliana*

Steffanie Fromm[1,2], Jennifer Göing[2], Christin Lorenz[1], Christoph Peterhänsel[2], Hans-Peter Braun[1]

[1] Institut für Pflanzengenetik, Leibniz Universität Hannover, Herrenhäuser Str. 2, 30419 Hannover, Germany
[2] Institut für Botanik, Leibniz Universität Hannover, Herrenhäuser Str. 2, 30419 Hannover, Germany

Type of authorship:	First author
Type of article:	Research article
Share of the work:	80 %
Contribution to the publication:	planned and performed all experiments, analyzed data, prepared all figures and wrote parts of the paper
Journal:	Biochimica et Biophysica Acta - Bioenergetics
5-year impact factor:	5.132
Date of publication:	January 31th, 2016
Number of citations (google scholar on May. 24th, 2016):	7
DOI:	10.1016/j.bbabio.2015.10.006
PubMed-ID:	26482706

CrossMark

Depletion of the "gamma-type carbonic anhydrase-like" subunits of complex I affects central mitochondrial metabolism in Arabidopsis thaliana

Steffanie Fromm [a,b], Jennifer Göing [b], Christin Lorenz [a], Christoph Peterhänsel [b], Hans-Peter Braun [a,*]

[a] Institut für Pflanzengenetik, Leibniz Universität Hannover, Herrenhäuser Str. 2, 30419 Hannover, Germany
[b] Institut für Botanik, Leibniz Universität Hannover, Herrenhäuser Str. 2, 30419 Hannover, Germany

ARTICLE INFO

ABSTRACT

"Gamma-type carbonic anhydrase-like" (CAL) proteins form part of complex I in plants. Together with "gamma carbonic anhydrase" (CA) proteins they form an extra domain which is attached to the membrane arm of complex I on its matrix exposed side. In Arabidopsis two CAL and three CA proteins are present, termed CAL1, CAL2, CA1, CA2 and CA3. It has been proposed that the carbonic anhydrase domain of complex I is involved in a process mediating efficient recycling of mitochondrial CO_2 for photosynthetic carbon fixation which is especially important during growth conditions causing increased photorespiration. Depletion of CAL proteins has been shown to significantly affect plant development and photomorphogenesis. To better understand CAL function in plants we here investigated effects of CAL depletion on the mitochondrial compartment. In mutant lines and cell cultures complex I amount was reduced by 90–95% but levels of complexes III and V were unchanged. At the same time, some of the CA transcripts were less abundant. Proteome analysis of CAL depleted cells revealed significant reduction of complex I subunits as well as proteins associated with photorespiration, but increased amounts of proteins participating in amino acid catabolism and stress response reactions. Developmental delay of the mutants was slightly alleviated if plants were cultivated at high CO_2. Profiling of selected metabolites revealed defined changes in intermediates of the citric acid cycle and amino acid catabolism. It is concluded that CAL proteins are essential for complex I assembly and that CAL depletion specifically affects central mitochondrial metabolism.

© 2015 Elsevier B.V. All rights reserved.

1. Introduction

The mitochondrial NADH dehydrogenase complex (complex I) is the largest enzyme complex of the respiratory chain. It transfers electrons from NADH to ubiquinone and at the same time translocates protons across the inner mitochondrial membrane [1]. Complex I is composed of two large and longish domains called "arms": the "membrane arm", which is mostly embedded into the inner mitochondrial membrane, and the "peripheral arm", which protrudes into the mitochondrial matrix. Both arms are connected end-by-end forming an L-like particle. NADH oxidation takes place at the tip of the peripheral arm. Electrons are transferred to the 'ubiquinone-binding pocket'. Reduction of

ubiquinone finally drives protein translocation across the membrane arm. Until recently, the coupling between electron transfer and protein translocation at complex I was not understood. Meanwhile, the crystal structure of bacterial complex I has been resolved [2]. Furthermore, structural data were reported for yeast and mammalian complex I [3,4,5]. Interpretation of these structures indicates that far-ranging conformational changes take place within complex I during its catalytic cycle [2,6,5,7].

Mitochondrial complex I of higher eukaryotes includes more than 40 subunits (44 in bovine and about 49 in Arabidopsis mitochondria; [8,9,10,11]). In plants complex I comprises an extra spherical domain which is attached to the membrane arm on its matrix exposed side [12]. It includes subunits resembling γ-type carbonic anhydrases which are absent in complex I particles from fungi and animals [13,14]. The Arabidopsis genome encodes five distinct γ-type carbonic anhydrases, all of which form part of mitochondrial complex I: three subunits which contain a completely conserved active site, termed carbonic anhydrase 1, 2 and 3 (CA1, CA2 and CA3), and two more derived subunits which lack some of the active site amino acid, termed "carbonic anhydrase-like" proteins 1 and 2 (CAL1 and CAL2). Not all five CA/CAL proteins are simultaneously present in individual

complex I particles because the extra spherical domain most likely is a trimer [15,16,11]. The CAL1 and CAL2 proteins of Arabidopsis exhibit 91% sequence identity and possibly represent isoforms. Carbonic anhydrase activity so far has not been demonstrated for any of the CA/CAL proteins but it was shown that CA2 homotrimers bind CO_2/HCO_3^- [17].

The physiological role of the CA/CAL subunits of complex I in plants has been investigated by the use of Arabidopsis knock out lines [18,15, 19,20]. Deletion of the genes encoding CA2 or CA3 did not cause a visible phenotype under the conditions tested. However, an Arabidopsis cell culture lacking CA2 had a reduced growth rate and reduced respiration. Interestingly, amounts of complex I are very low in $\Delta ca2$ mutants, indicating an essential role of CA2 for assembly of this protein complex [18]. Electrophoretic analyses of the remaining complex I revealed that absence of CA2 does not alter subunit composition of complex I to a significant extent. Similarly, analyses by single particle electron microscopy revealed that the carbonic anhydrase domain of complex I has a normal shape in plants lacking CA2. It has been concluded that CA2 is replaceable by other CA subunits [15]. CA2 forms part of small assembly intermediates of complex I which accumulate in some complex I mutants [19]. Additionally, labeling experiments using ^{15}N and in vitro assembly studies revealed that the CA/CAL domain represents a key factor for early steps in complex I assembly in plants [21]. Single mutants of all five CA/CAL proteins were phenotypically analyzed by Wang et al. [20]. All mutants did not exhibit altered phenotypes compared to wild-type plants at the conditions tested. Therefore, plants lines defective in more than one gene encoding CA/CAL subunits of complex I have to be generated to further investigate the physiological role of this protein family.

So far, four different Arabidopsis double mutants with respect to the complex I integrated carbonic anhydrases have been analyzed, $\Delta cal1/\Delta cal2$, $\Delta ca1/\Delta ca3$ and two lines lacking CA2 and additionally either CAL1 or CAL2 [20,22]. While plants defective in CA1 and CA3 do not have an altered phenotype, the $\Delta ca2/\Delta cal1$ and $\Delta ca2/\Delta cal2$ lines show growth retardation which is reverted by cultivating plants in a high carbon dioxide atmosphere [22]. In contrast, plants lacking CAL1 and CAL2 suffer from embryonic defects [20]. Seeds homozygous for CAL1 and CAL2 deletions initially have a colorless and later a deep-brown phenotype. To obtain viable plants the CAL2 gene was down-regulated by RNAi in the background of a homozygous CAL1 knockout. $\Delta cal1/cal2i$ plants showed delayed germination and significantly postponed development. In the light, $\Delta cal1/cal2i$ plants developed a short hypocotyl phenotype. The gene encoding chalcone synthase, a key enzyme of anthocyanin synthesis, was induced in the mutant lines. It is concluded that CAL1 and CAL2 play important roles in light-dependent growth and development in Arabidopsis [20].

To better understand the physiological role of CAL proteins in plants, we here report a characterization of $\Delta cal1/cal2i$ lines with respect to the mitochondrial compartment. Complex I level in the mutant is reduced by 90%–95%. Also, oxygen consumption of isolated mitochondria is much diminished. Comparative proteome analyses reveal several changes in the mutant, which not only refer to complex I subunits, but also point to specific alterations of central mitochondrial metabolism. This finding was confirmed by the profiling of selected mitochondrial metabolites. Conclusions on the physiological role of the complex I-integrated CAL proteins are discussed.

2. Material and methods

2.1. Plant material and growth conditions

Arabidopsis (Arabidopsis thaliana) lines used for this study were of the Columbia ecotype. RNAi lines were obtained from Qin Wang, Hunan University, China (for details see [20]).Plants were grown on 1/2 MS medium in climate chambers under the following

conditions: 12 h of light (120 μmol s^{-1} m^{-2}) / 12 h of dark, 22 °C, 65% humidity, and either 400 ppm or 2000 ppm CO_2. After four weeks plants were transferred to soil and cultivation was continued at the same conditions.

Cell cultures of Arabidopsis lines were established as described by May and Leaver [23]. Callus was maintained as suspension culture according to Sunderhaus et al. [15]. Growth rates of cell cultures were determined using 1.5 g starting material. Weight increase was determined after three, five and seven days. This time period was chosen because growth of cell culture lines is linear up to seven days [24].

2.2. Transcript analysis

RNA preparation with TRIzol and cDNA synthesis were performed according to Heimann et al. [25]. The concentration of RNA was measured photometrically and controlled by agarose gel electrophoresis. Quantitative PCR was carried out using sequence specific oligonucleotides. The following primer combinations were used:

*CA*1.
    5′-GTTCGAGAAGGTTCTACGCAAGA-3′ and. 5′-GAGGTTAAGCTC
TGGTGGAGTT-3′,
*CA*2.
    5′-GATAGTATACATCTCACAGTCAGC-3′ and. 5′-CTTCTTCCTAAG
CGCTCTCTCAA-3′,
*CA*3.
    5′-GTTCGGCTGTGGAGTACTCCAA-3′ and. 5′-CTGAATCATATTCT
GTATCGCGAGC-3′,
*CAL*1.
    5′-TAGCCATCAACCACTTAAGCG-3′ and. 5′-GCGATCCCAAGGGA
CTTCTT-3′,
*CAL*2.
    5′-CAAACATTGATCGATAGGTACGTGA-3′ and. 5′-TGCCAGGTGG
TAAAACAGAACCA-3′,
GAPDH.
    5′-GGAATCTGAAGGCAAAATGAAGG-3′ and. 5′-TGTTGTCACCAA
CAAAGTCGG-3′.

SYBR Green mediated fluorescence was measured using an ABI PRISM 7300 camera (Life Technologies). Amplification started with an initial denaturation (2 min, 95 °C) and was followed by 40 alternating cycles of 15 s at 95 °C/1 min at 60 °C. Afterwards, a melting curve was recorded. Transcript quantities were standardized for abundance of the housekeeping transcript glyceraldehyde-3-phosphat-dehydrogenase (*GAPDH*, At1g13440).

2.3. Isolation of mitochondria

Mitochondria from cell culture were purified by differential centrifugation and Percoll density gradient centrifugation as described by Werhahn et al. [26]. Isolation of mitochondria from green leaves was performed according to the protocol of Keech et al. [27] (method A).

2.4. Protein gel electrophoresis procedures

One-dimensional Blue native PAGE (1D BN PAGE) was performed according to Wittig et al. [28]. Mitochondrial membranes were solubilized by digitonin at a concentration of 5 g/g mitochondrial protein [29].

Two-dimensional IEF/SDS-PAGE was carried out as described by Mihr and Braun [30]. For the IEF gel dimension, Immobiline DryStrip gels (24 cm, nonlinear gradient pH 3–11) were used. Focusing took place for 24 h at 30 to 8000 V using the Ettan IPGphor 3 system (GE Healthcare).

For the second gel dimension, IPG stripes were equilibrated for 15 min with DTT (0.4 g/40 ml) and afterwards 15 min with iodoacetamide. SDS PAGE was carried out using the High Performance Electrophoresis (HPE) FlatTop Tower-System (Serva Electrophoresis) using precast Tris–Glycine gels (12.5% polyacrylamide, 24 × 20 cm).

Polyacrylamide gels were stained with Coomassie Brilliant Blue G250 according to the protocol of Neuhoff et al. [31,32]. However, methanol in the fixing and staining solutions was substituted by ethanol (p.A.). Comparative proteome analyses were based on gel triplicates and data evaluation using the Delta 2D software 4.3 (Decodon, Greifswald, Germany) according to Berth et al. [33] and Lorenz et al. [34].

2.5. Protein identification by mass spectrometry

Tryptic digestion of proteins and identification of proteins by MS using the EASY-nLC System (Proxeon, Thermo Scientific, Bremen, Germany) and coupled MS analyses using the MicrOTOF-Q II mass spectrometer (Bruker Bremen, Germany) were performed as described by Klodmann et al. [16].

MS primary data were evaluated using the Proteinscape software (version 2.1, Bruker, Bremen, Germany), the Mascot Search Engine (Matrix Science, London, UK), the Arabidopsis protein database (www.arabidopsis.org; release TAIR 10), and an updated version of a complex I database [16], that represents a subset of the Arabidopis protein database. The threshold Mascot Score was set to 80 for proteins and 20 for peptides.

2.6. Enzyme activity assays

In-gel NADH dehydrogenase activity staining for complex I was carried out according to Jung et al. [35]. Stripes of one-dimensional gels were washed twice for 10 min in ddH$_2$O. Afterwards, gel stripes were incubated in staining solution (100 mM Tris–HCl, pH 7.4, 0.14 mM NADH, 1 mg/ml NBT) until the purple staining of the bands representing the I + III$_2$ of supercomplex and monomeric complex I become visible. The reaction was stopped in a solution containing 15% (v/v) ethanol (p.A.) and 10% (v/v) acetic acid. All steps were carried out at room temperature.

Photometric NADH dehydrogenase activity was measured using 2 μg mitochondrial proteins at 420 nm in an Epoch Microplate Spectrophotometer (Biotek, Winooski, VT, USA) at room temperature in the presence of 50 mM Tris–HCl, pH 7.4, 500 μM K$_3$Fe(CN)$_6$ and 200 μM deamino NADH [36,37].

2.7. Oxygen consumption measurements

Oxygen consumption of isolated mitochondria was measured using a Clark-type oxygen electrode (Hansatech Instrument, Norfolk, UK) according to Meyer et al. [38]. Reaction buffer included 100 μg mitochondrial protein in 3 ml respiration buffer (300 mM sucrose, 5 mM KH$_2$PO$_4$, 10 mM TES, 10 mM NaCl, 2 mM MgSO4, 0.1% (w/v) BSA, pH 6.8) in the presence 120 μM CoA, 200 μM TPP, 2 mM NAD$^+$, 10 mM glutamate and 10 mM malate. At stable oxygen consumption, 200 μM ADP was added for measuring ADP dependent respiration.

2.8. Metabolite analysis

For metabolite extraction, Arabidopsis plants were grown at 400 ppm CO$_2$ and 2000 ppm CO$_2$ with a day night rhythm of 12 h/12 h at 120 μE. Whole plants were harvested at the age of 4 weeks. Material of five to six plants of the same genotype was pooled. Plant material was subsequently ground in reaction tubes. One ml of prechilled extraction buffer (1 vol. of H$_2$O, 1 vol. of ChCl$_3$, and 2.5 vols. of methanol) containing 5 μl ^{12}C-ribitol of a 2 mg/ml stock solution was added to 20 to 50 mg of sample material for polar phase preparation. The samples were mixed for 5 min at 4 °C. After centrifugation (2 min, 16.000 ×g), 500 μl of the supernatant were mixed with 250 μl of ultra pure H$_2$O and centrifuged again (2 min, 16.000 ×g). 250 μl of the top layer (polar phase) were dried in a speed-vac concentrator. Derivatization, addition of standards, and sample injection were performed as described in Lisec et al. [39]. Chromatograms and mass spectra were analyzed and evaluated using ChromaTOF® (LECO Corporation, St. Joseph, Mi, USA) software. A standard curve of pure metabolites was used for calculating the amount of metabolites in the samples per g fresh weight.

3. Results

3.1. Arabidopsis Δcal1/cal2i lines and cell cultures grow slower

To verify developmental properties previously described for Δcal1/cal2i lines [20], wild-type and mutant plants were cultivated in soil at standard growth conditions (Fig. 1). Three independent mutant lines, termed Δcal1/cal2i-1, Δcal1/cal2i-5 and Δcal1/cal2i-20, were analyzed. At seven weeks rosettes of the mutants were clearly smaller (rosette diameter: 7 versus 14 cm; number of rosette leaves: 16 versus 38). Furthermore, flowering was significantly delayed in all mutant lines (Fig. 1). These results are in line with observations published before [20]. To facilitate biochemical investigations, suspension cell cultures were established for Δcal1/cal2i and wild-type plants. Growth rates of mutant cell cultures were reduced by about 50% relative to the wild-type culture (Fig. 2). Expression analyses of the five CA/CAL genes in Δcal1/cal2i plants revealed that CAL1 expression was reduced by about 90% and CAL2 expression by about 50%. (Fig. 3). These values correspond exactly to previously published data ([20], Fig. 5A). Residual detection of CAL1 transcripts probably occurs due to the insertion site of the T-DNA within an intron of the gene (the T-DNA might become partially excised by splicing). Interestingly, expression of the CA1, CA2 and CA3 genes also was slightly reduced in some of the RNAi lines.
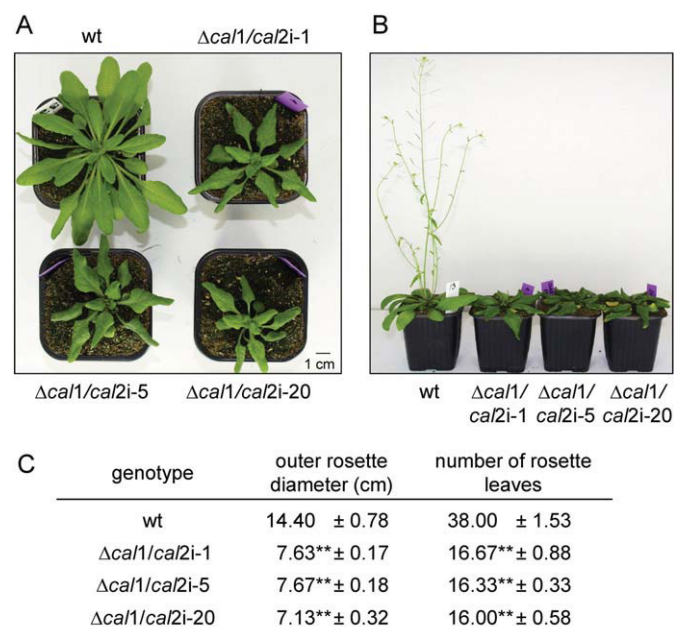
Fig. 1. Comparison of phenotypes of Arabidopsis wt and Δcal1/cal2i lines. A: rosette of four weeks old plants, B: six weeks old plant, C: outer rosette diameter and number of rosette leaves of wt and Δcal1/cal2i lines. n = 6 (biological), mean ± SE, **p ≤ 0.01 (student's t-test).

genotype	outer rosette diameter (cm)	number of rosette leaves
wt	14.40 ± 0.78	38.00 ± 1.53
Δcal1/cal2i-1	7.63**± 0.17	16.67**± 0.88
Δcal1/cal2i-5	7.67**± 0.18	16.33**± 0.33
Δcal1/cal2i-20	7.13**± 0.32	16.00**± 0.58

63

Fig. 2. Fresh weight increase of Arabidopsis wt and Δcal1/cal2i-5 cell cultures. Starting material (day 0) for wt (black bars) and Δcal1/cal2i-5 (white bars) was 1.5 g, respectively. Fresh weight (g) was recorded after three, five and seven days. n = 9 (biological), mean ± SE, **p ≤ 0.01 (student's t-test).

Fig. 4. Oxygen consumption of Arabidopsis wt and Δcal1/cal2i-5 lines. Oxygen consumption of isolated mitochondria was measured at state III using a Clark-type oxygen electrode. n = 5 (technical), mean ± SE, **p ≤ 0.01 (student's t-test).

3.2. Isolated mitochondria of Δcal1/cal2i lines have reduced oxygen consumption rates and drastically reduced amounts of complex I

Mitochondria were isolated from Δcal1/cal2i-5 and wild-type cell lines in order to monitor consequences of the induced genetic alterations on mitochondrial metabolism. Using malate and glutamate as substrates, state III respiration was reduced by 30% in mitochondria isolated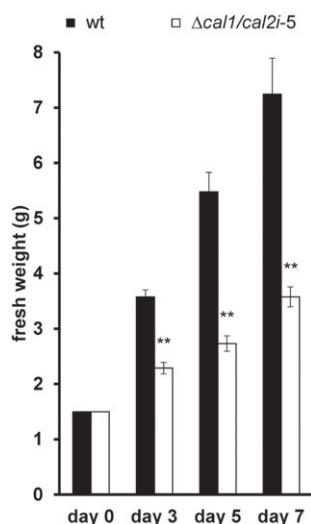 from the mutant cell lines (Fig. 4). Blue native (BN) polyacrylamide gel electrophoresis (PAGE) was carried out to investigate the protein
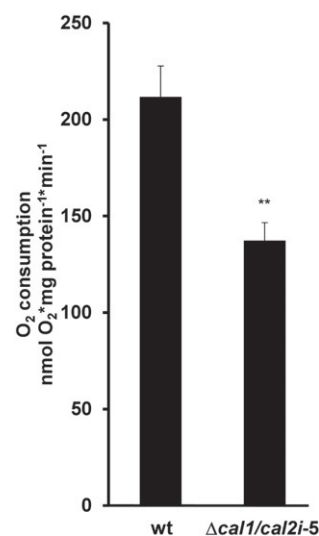
complexes of the mitochondrial oxidative phosphorylation (OXPHOS) system in mutant and wild-type lines. Bands representing the I + III$_2$ supercomplex and monomeric complex I were drastically reduced by 90–95% in organelles from mutant lines (Fig. 5A). In contrast, the complexes III$_2$ and V of the OXPHOS system were present at unchanged abundances. Bands representing complex II and IV in general are diffuse upon BN-PAGE of mitochondrial fractions from Arabidopsis and are not clearly detectable. However, no differences were visible in the respective gel regions in wt and mutant cell lines. We therefore conclude that complexes II and IV most probably also are of unchanged abundance in the mutant lines. Residual complex I and I + III$_2$ supercomplex have NADH:NBT oxidoreductase activity as revealed by an in gel activity assay (Fig. 5B). BN PAGE analysis was repeated for organelles isolated from leaves of wild-type and Δcal1/cal2i plants (Fig. 5C and D). As found for organelles isolated from cell cultures, complex I and I + III$_2$ levels were drastically reduced. Finally, a photometric NADH dehydrogenase assay was performed for mutant and wild-type cells. Deamino NADH was used for this assay because it can be used by complex I but not as well by the alternative NADH dehydrogenases for substrate [40]. Reduction of activity in the mutant was in the range of 70%. In summary, complex I and I + III$_2$ supercomplex levels in Δcal1/cal2i lines are strongly reduced, causing a substantial drop in complex I activity. However, residual complex I activity is still detectable in the mutant lines.

3.3. Δcal1/cal2i mutants do not accumulate complex I assembly intermediates

Complex I assembly proceeds via assembly intermediates of about 200, 420, 470, 650 and 850 kDa which were described previously [19,41,21]. Their abundances are comparatively low but they can be visualized by BN PAGE in combination with immunoblotting using antibodies directed against complex I subunits. Using this experimental approach, several assembly intermediates were detectable in wild-type plants, which all included CA as well as CAL proteins (Fig. 6A). In a strict sense, this experiment does not allow discriminating between assembly intermediates of complex I and break-down products. However, the masses of the observed subcomplexes nicely match to those previously identified representing assembly products of complex I [19]. In Δcal1/cal2i lines complex I and supercomplex I + III$_2$ levels were much reduced (only became visible upon prolonged immune

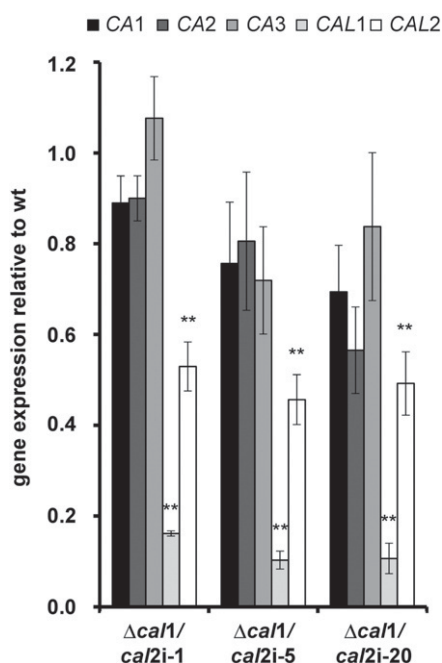**Fig. 3.** Expression of CA and CAL genes in Arabidopsis Δcal1/cal2i-1, Δcal1/cal2i-5 and Δcal1/cal2i-20 lines relative to wt. n = 5 (biological), mean ± SE, **p ≤ 0.01 (student's t-test).
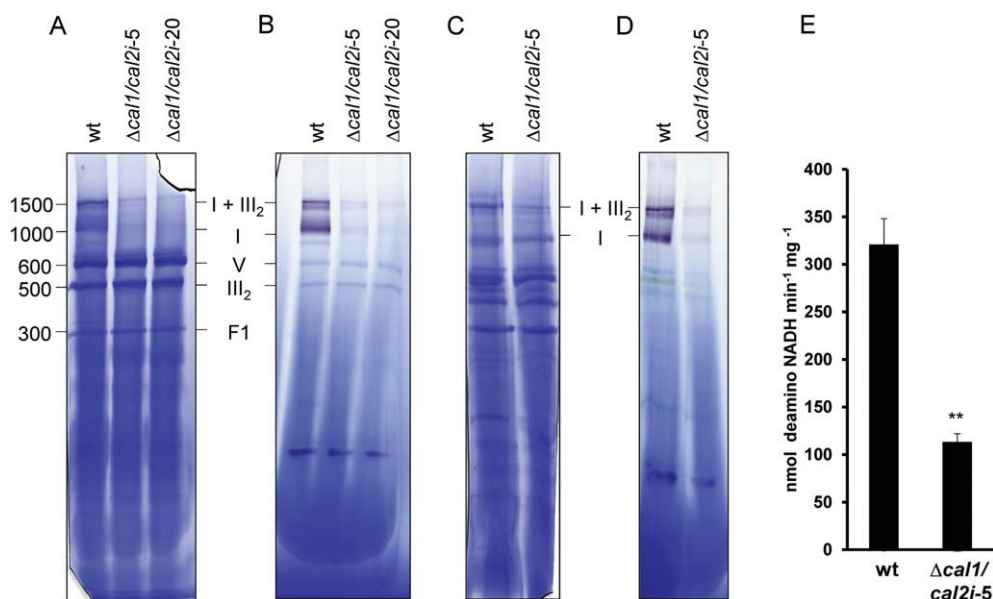
Fig. 5. NADH oxidation activity of complex I in mitochondrial fractions of Arabidopsis wt and Δ*cal*1/*cal*2i-5 and 20 lines. Protein complexes of mitochondria isolated from cell culture (A and B) and plant leaves (C and D) were resolved by Blue native PAGE. Gels were stained with colloidal Coomassie (A and C). Corresponding gels (B and D) were used for in gel activity assays using NBT as artificial electron acceptor. Molecular masses of the resolved protein complexes are given to the left of the figure. Identity of selected mitochondrial protein complexes are given in between the gels (I: complex I; V: complex V; III$_2$: dimeric complex III; I + III$_2$: supercomplex formed of complex I and dimeric complex III; F1: F1 part of complex V). E: Photometric NADH dehydrogenase activity assay of mitochondria isolated from cell culture using deamino NADH. n = 3 (biological), mean ± SE, **p ≤ 0.01 (student's t-test). Note: Deamino NADH is well suited to monitor complex I activity specifically. However, residual activity of other NADH dehydrogenases cannot be totally excluded.

staining) and the assembly intermediates were hardly visible (Fig. 6B). Results could not be evaluated quantitatively, but clearly indicate that assembly intermediates did not accumulate in mutant lines. We conclude that the entire complex I assembly process is strongly compromised in mutant lines.
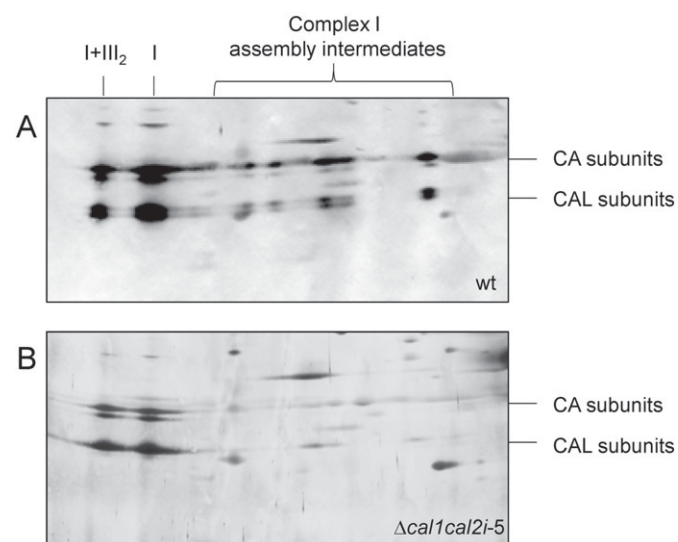

Fig. 6. Complex I assembly intermediates in Arabidopsis wt (A) and Δ*cal*1/*cal*2i-5 (B) lines. Total mitochondrial proteins were separated by 2D BN-SDS PAGE. Gels were immunoblotted and stained with an antibody directed against CA/CAL proteins. Note: since immune signals were hardly visible in the mitochondrial fraction of the mutant the immune development was prolonged (part B of the figure). The positions of CA and CAL proteins are indicated to the right of the blots. I + III$_2$: supercomplex formed by one copy of complex I and dimeric complex III (I + III$_2$); I: complex I.

3.4. Comparative proteome analysis of wild-type and Δcal1/cal2i lines

Reduced complex I assembly may cause accumulation of monomeric complex I subunits. Furthermore, reduction of CA/CAL proteins might induce further changes within the mitochondrial proteome. To systematically compare abundances of mitochondrial proteins in wild-type and Δ*cal*1/*cal*2i lines, total protein of isolated mitochondria was separated by 2D IEF-SDS PAGE. About 1200 protein spots were detected on the resulting 2D gels upon Coomassie staining (Supp. Fig. S1A). Data evaluation was carried out using the Delta 2D software package (Decodon, Greifswald) (Supp. Fig. S1B).

Volumes of 123 protein spots were significantly changed between wild-type and mutant lines (change >1.5 fold). Of these, 81 protein spots were of reduced volume in the Δcal1/cal2i line, whereas 42 protein spots were of increased volume in the mutant (Fig. 7). All 123 spots were analyzed by mass spectrometry (spots of decreased volume in the mutant were cut out from the wild-type 2D gel, spots of increased volume in the mutant from the 2D gel of the mutant). Overall, 283 proteins were identified. Total number of different proteins was 150 (some proteins were identified in more than one spot). At the same time, more than one protein was identified for several spots. Changes in volume were only assigned to a specific protein, if a spot only included one main protein. This further reduced the number of unambiguously changed proteins to 85. 56 of these proteins were of decreased abundance in the mutant and 29 of increased abundance (Table 1).

Evaluation of the set of 84 reveals specific differences between the mitochondrial proteomes of mutant and wild-type cells (Fig. 8): (i) Overall, 23 complex I subunits were identified. All of them are less abundant in the mutant except for one subunit. The average reduction with respect to wild-type cells is 3 fold (the highest reduction is 8 fold). (ii) The L subunit of the glycine decarboxylase complex (GDC) and serine hydroxymethyl transferase (SHMT), both involved in photorespiratory metabolism, were reduced about 2.3 fold in average. However, the SHMT2 isoform identified here is not involved in photorespiration in leaf mesophyll cells [42]. (iii) Likewise, subunits of
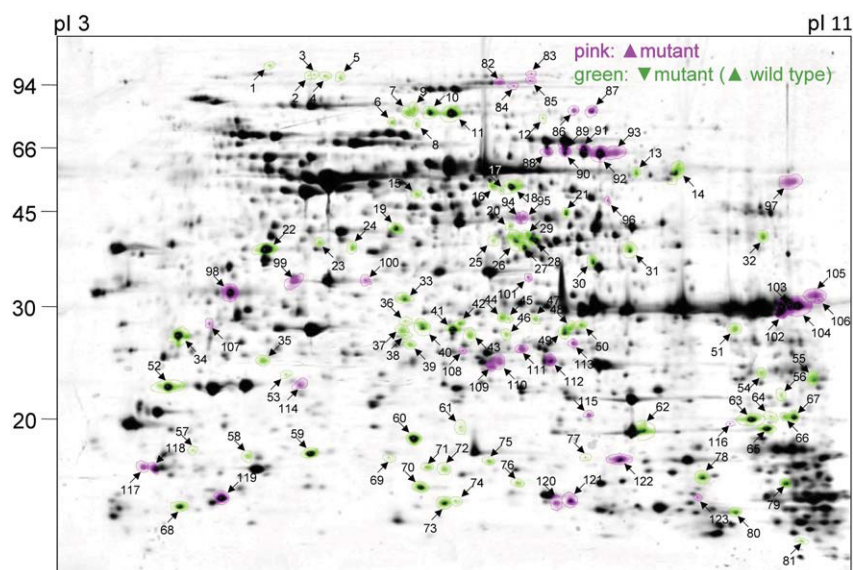
Fig. 7. Comparative analysis of the mitochondrial proteomes of Arabidopsis wt and Δ*cal*1/*cal*2i-5 lines. Mitochondria were isolated as described in Materials and Methods. Total mitochondrial protein was separated by 2D IEF–SDS PAGE and proteins were stained by Coomassie blue. Three replicates were produced per fraction and used for the calculation of master gels (Delta 2D software package, Decodon, Germany). The molecular masses of standard proteins are given to the left of the 2D gel (in kDa). Isoelectric focusing range is form pH 3 (left) to pH 11 (right). Proteins indicated in pink are more abundant in the mutant (>1.5 fold increase); proteins indicated in green are less abundant in the mutant. Spots indicated by numbers were identified by mass spectrometry (for results see Table 1).

pyruvate dehydrogenase were reduced 2 fold in average. (iv) Glutamate dehydrogenase and oxoglutarate dehydrogenase were both induced in the mutant (1.7 to 3.5 fold). The latter enzyme catalyzes a step of the TCA cycle. In contrast, no other enzymes of the TCA cycle were found to be of changed abundance in the mutant. (v) Prohibitins and several stress related proteins were much induced in the mutant (1.5 to 7 fold). (vi) Several further proteins were of changed abundance and are potentially involved in metabolic adaptations necessary to compensate for reduced CAL levels.

We conclude that non-assembled complex I subunits did not accumulate in Δ*cal*1/*cal*2i lines, but subunits were either synthesized at lower rates or specifically degraded or both. Reduction of the L subunit of the GDC might cause a reduced capacity for glycine — serine conversion during photorespiration. In contrast, glutamate and pyruvate break down might be increased in the mutant. Finally, biosynthesis of several stress-related proteins was clearly induced in the mutant.

3.5. Growth properties of wild-type and Δcal1/cal2i lines at low and high CO₂

Reduced abundance of the L-protein of GDC might affect photorespiration. To test for a photorespiratory phenotype, wild-type and mutant plants were cultivated in parallel at 400 and 2000 ppm CO_2. Rosette diameters of plants were determined after six weeks of cultivation. In accordance with our previous investigations (Fig. 1), rosette diameter of mutant plants was reduced by about 50% compared to wt plants at 400 ppm CO_2 (Fig. 9). Cultivation at high CO_2 did not revert the mutant phenotype: rosette diameters for wt and mutant plants were slightly increased, but the rosette diameter of the mutant plants was still significantly smaller. Increase in the rosette diameter at high CO_2 was +19% for wt plants and +22–34% for mutant plants. We conclude that the increase in rosette diameter of mutant plants with respect to wt plants was slightly larger. However, high CO_2 did not revert the phenotype of the mutant which was reported for several other mutants of genes directly involved in photorespiration [43].

3.6. Central mitochondrial metabolism is modified in Δcal1/cal2i lines

Changes in protein levels related to photorespiration and pyruvate and glutamate metabolism indicated alterations of the central

mitochondrial metabolism in Δ*cal*1/*cal*2i lines. Therefore, selected metabolites related to mitochondrial metabolism were quantified by GC–MS (Fig. 10). As reported previously [44], glycine was high at 'end of the day' (EoD) in wt plants but much lower at 'end of the night' (EoN). Two out of three mutant lines showed a reduction in glycine accumulation EoD. At 2000 ppm CO_2, glycine accumulation during the day was diminished for all genotypes. However, levels were here higher in the mutants compared to the wt. Differences in serine concentrations were less pronounced in mutants and wt. This resulted in an overall reduced glycine/serine (gly/ser) ratio in the mutants at 400 ppm CO_2, but not 2000 ppm CO_2. Gly/ser ratios are often used as a proxy for photorespiratory flux. Levels of most TCA cycle intermediates and glutamate were increased in the mutants with the exception of succinate that was decreased (Fig. 10). These data suggest that mitochondrial respiratory and photorespiratory metabolism is changed in the mutants.

4. Discussion

Δ*cal*1/*cal*2i plants have been previously characterized with respect to development, photomorphogenesis and photosynthesis [20]. To investigate the role of CAL proteins in metabolism, mutants here were characterized with respect to the mitochondrial compartment. Five different types of CA/CAL proteins, CA1, CA2, CA3, CAL1 and CAL2, were previously shown to form part of respiratory complex I [14,16]. All proteins were found exclusively as constituents of complex I or its assembly intermediates but not as free proteins [16]. So far, carbonic anhydrase activity could not be monitored for any of the CA/CAL proteins [45,20]. However, *Escherichia coli* lysates overexpressing CA2 were shown to efficiently bind CO_2/HCO_3^- [17]. What could be the physiological role of the CA/CAL proteins?

4.1. The function of the CA/CAL proteins

It has been proposed that complex I-integrated CA/CAL proteins are involved in a CO_2 recycling mechanism by promoting efficient transfer of CO_2 from mitochondria to chloroplasts [46,47]. The mechanism involves CO_2-bicarbonate conversion in mitochondria, transport of

bicarbonate from mitochondria to chloroplasts, re-conversion of CO_2 from bicarbonate by chloroplast-localized carbonic anhydrases and finally re-fixation of CO_2 by RubisCO. It should be of special importance at high photorespiration, so low CO_2 concentrations. The proposed process resembles the well-studied carbon concentration mechanism (CCM) of cyanobacteria, which also requires presence of (cyanobacterial) complex I [48,49]. Some experimental results were interpreted to support presence of the proposed CO_2 transfer mechanism from mitochondria to chloroplasts: (i) When photosynthetic rates were compared between protoplasts and isolated chloroplasts, the protoplasts performed better at low CO_2 suggesting that an internal CO_2 source was available in protoplasts but not in isolated chloroplasts [50]. Increase of photosynthesis rates in protoplasts was repressed in the presence of inhibitors of carbonic anhydrases. (ii) Transcription of genes encoding the CA/CAL proteins is reduced if plants are cultivated at high CO_2 [18,22]. (iii) The tobacco ΔcmsII mutant which has drastically reduced amounts of complex I exhibits diminished steady-state photosynthesis. Inhibition of photosynthesis was reduced if plants are cultivated at high CO_2 [51]. This was very recently also described for an Arabidopsis mutant lacking CA2 and additionally, either the CAL1 or the CAL2 protein [22]. Under photorespiratory conditions carbon assimilation is diminished and glycine accumulates in double mutant plants. However, plants were cultivated at comparatively low light and it remains to be established if the Δca2/Δcal2 phenotype is completely rescued by high CO_2 in the presence of increased light intensities [22]. In summary, the specific role of the CA/CAL proteins during photosynthesis is still not fully understood and has to be further investigated.

The CA/CAL proteins belong to an acetyltransferase superfamily [45,20]. Indeed, overexpressed CAL2 has been shown to have a low but measurable in vitro histone acetyltransfrase activity [20]. However, mitochondrial substrates could not be identified. In conclusion, the biochemical role of the CA/CAL proteins still is far from clear.

In this study, we provide additional insights into the metabolic context of CA/CAL function. Protein analyses revealed down-regulation of the L-subunit of the GDC complex (Table 1 and Fig. 8) and reduced gly/ser ratios in the mutants (Fig. 10). These results might indicate lower photorespiratory flux in the mutants. At first glance, these data are not supporting the inner-cellular CO_2 transfer hypothesis, because higher rates of photorespiration would be expected if the CO_2 pump would be inactive in the mutants. Consequences of the mutation on photorespiration might not only affect the CO_2 recycling but also the NAD^+/NADH ratio. However, reduced growth of the mutants at normal conditions (Fig. 1) suggests that also photosynthetic rates were reduced in the mutants and that reduced photorespiration was simply a consequence of reduced photosynthesis. This is also in line with the slightly more positive growth response of the mutants when atmospheric CO_2 concentrations were increased (Fig. 9) and the higher concentration of stress-related proteins (Table 1 and Fig. 8). Data on photosynthetic rates of the mutants at different CO_2 concentrations would be helpful to better understand these results but we were not able to generate these data as mutant leaves were too small for reproducible gas exchange measurements. It can be concluded that CA/CAL function is relevant in the context of photorespiration but evidence that this group of proteins is specifically involved in the proposed CO_2 transfer mechanism is still not conclusive.

4.2. Proteome analyses for investigating CAL function in plants

Proteome analyses have been carried out to systematically investigate consequences of CAL depletion in mitochondria of plants. More than 80 proteins were identified which were specifically changed in abundance. In general, complex I subunits were much reduced. This was shown for 23 different subunits of this protein complex. Overall, complex I comprises about 49 subunits in plants [10,11]. It can be assumed that complex I subunits not identified by our study also are of

reduced abundance in Δcal1/cal2i lines but were not detected due to hydrophobicity (hydrophobic proteins are poorly resolved by IEF) or spot overlappings on the 2D gels. Interestingly, enzymes of defined metabolic pathways were of increased abundance in the mutants, like enzymes involved in pyruvate and glutamate catabolism. Indeed, accumulation of glutamate was observed for Δcal1/cal2i lines by metabolite analysis. Finally, stress-related proteins clearly are induced in the mutant. Some of the stress-related proteins were previously assigned to other cellular compartments, like the cytoplasm and the ER. It remains to be established whether these proteins are imported into mitochondria upon stress or rather attached to the surface of the organelles. A comparative whole-plant proteome experiment would be desirable for not only monitoring protein changes in the mitochondrial compartment but the entire cell.

4.3. Complex I mutants in plants

Some other complex I deficient mutants were characterized previously [52,51,18,38,53]. Complex I mutants exhibit rather heterogeneous phenotypic properties [11]. In general, growth of mutant plants is reduced, development is delayed and leaves are curled. The extend of growth reduction depends on the level of residual complex I [53]. Mutants with a complete loss of complex I are also impaired in seed development and germination [54,53]. Also the Δcal1/cal2i lines have a delayed development (Fig. 1) curled leaves and reduced germination rates (Fig. 9A). For the tobacco ΔcmsII mutant it has been shown that complex I deficiency has an impact on photosynthetic efficiency [51]. In contrast, the Δcal1/cal2i lines showed no differences in photosynthetic efficiency [20]. This was confirmed in the frame of our study (data not shown). For the $\Delta ndufs$4 and $\Delta ndufv$1 mutants, which largely or completely lack complex I, increased levels of TCA cycle intermediates have been reported [53]. Increased levels of TCA metabolites also were found for Δcal1/cal2i lines with the exception of succinate. However, day times of harvesting plant material differ between the two studies, thereby limiting the comparability of the data sets. Overall, both studies indicate that complex I represents a negative regulator of the TCA cycle. In summary, effects caused by CAL depletion basically resemble those obtained for other complex I mutants and therefore, do not allow drawing conclusions on specific CAL function.

4.4. Regulation of nuclear gene expression with respect to mitochondrial proteins

Most complex I subunits are encoded by nuclear genes, synthesized in the cytosol and posttranslationally transported into the organelle [11]. In Δcal1/cal2i mutant lines complex I levels were much reduced (Fig. 5). At the same time, accumulation of assembly intermediates or singular complex I subunits did not occur (Fig. 6). This either could be caused by specific degradation of excess subunits or by the down-regulation of the genes encoding complex I subunits in the nucleus and in the mitochondrial compartment. Indeed, transcription of CA genes localized in the nucleus is slightly reduced in some of the CAL-depleted plants (Fig. 3). We cannot exclude off-target effects of the CAL2-directed RNAi construct but alternatively conclude that down-regulation of complex I genes in the mutant lines and the ER might be caused by specific signaling processes. The chemical nature of the signals for adapting nuclear gene expression to the requirements of the mitochondrial compartment is currently unknown. Signals can be assumed to be highly specific because levels of other OXPHOS complexes were not changed in CAL-deficient plants (Fig. 5).

5. Conclusion

In conclusion, new molecular adaptations to depletion of the complex I-integrated CA/CAL proteins have been identified, but more insights into the physiological role of this group of proteins, besides

Table 1
Proteins of changed abundance between wt and Δcal1/cal2i 5 lines. Numbers of analyzed spots refer to Fig. 7.
Spot volumes indicated with − are of >1.5 fold increased abundance in wt and spot volumes indicated with + are of >1.5 fold increased abundance in the mutant.

Identity in Arabidopsis

spot[a]	Accession[b]	Name[c]	Functional context	Localization[d]	Mass [kDa][e]	Mascot score[f]	Peptides[g]	Unique peptides[h]	Coverage [%][i]	Ratio of mean normalized volume 'mutant'/mean normalized volume 'wt' Delta 2D[j]	p-Value of ratio of mean normalized volume 'mutant'/mean normalized volume 'wt' Delta 2D[k]
78	AT3G62790	Complex I, 15 kDa-1 subunit	Respiratory chain	M	9.89	196	25	4	37.35	−2.37	0.00326
65	AT5G67590	Complex I, 18 kDa subunit	Respiratory chain	M	17.12	348	51	8	37.66	−5.11	0.00512
36	AT4G02580	Complex I, 24 kDa subunit	Respiratory chain	M	28.37	262	18	7	26.27	−2.19	0.00877
41	AT4G02580	Complex I, 24 kDa subunit	Respiratory chain	M	28.37	649	93	12	34.12	−4.32	0.00028
31	AT2G20360	Complex I, 39 kDa subunit	Respiratory chain	M	43.91	876	89	22	37.06	−2.13	0.00286
13	AT5G08530	Complex I, 51 kDa subunit	Respiratory chain	M	53.42	994	76	22	42.18	−2.14	0.00372
14	AT5G08530	Complex I, 51 kDa subunit	Respiratory chain	M	53.42	1245	118	29	53.50	−2.96	0.00313
20	AT5G08530	Complex I, 51 kDa subunit	Respiratory chain	M	53.42	682	45	14	23.87	−3.92	0.00471
7	AT5G37510	Complex I, 75 kDa subunit	Respiratory chain	M	81.13	1322	90	26	38.26	−3.62	0.00062
11	AT5G37510	Complex I, 75 kDa subunit	Respiratory chain	M	81.13	2437	200	49	54.90	−3.12	0.00207
74	ATMG00510	Complex I, ND7	Respiratory chain	M	44.93	97	14	3	8.12	−2.39	0.00104
52	AT5G52840	Complex I, B13	Respiratory chain	M	19.17	1042	92	19	75.74	−2.01	0.00074
69	AT5G52840	Complex I, B14	Respiratory chain	M	19.17	149	9	4	27.81	−1.85	0.00910
61	AT2G42210	Complex I, B14.7	Respiratory chain	M	16.99	178	23	5	22.64	−1.76	0.00802
62	AT2G42210	Complex I, B14.7	Respiratory chain	M	16.99	286	56	10	26.42	−2.00	0.00337
64	AT3G03100	Complex I, B17.2	Respiratory chain	M	18.31	349	31	7	46.54	−3.89	0.00453
67	AT3G03100	Complex I, B17.2	Respiratory chain	M	18.31	566	60	12	62.26	−2.60	0.00502
71	AT4G34700	Complex I, B22	Respiratory chain	M	13.61	448	42	8	63.25	−2.73	0.00028
75	AT4G34700	Complex I, B22	Respiratory chain	M	13.61	414	37	9	48.72	−5.10	0.00309
43	AT1G19580	Complex I, CA1	Respiratory chain	M	29.95	345	28	10	35.27	−2.97	0.00135
50	AT1G19580	Complex I, CA1	Respiratory chain	M	29.95	428	37	8	40.36	−1.93	0.00833
47	AT1G47260	Complex I, CA2	Respiratory chain	M	30.05	665	52	15	55.40	−4.83	0.00092
50	AT1G47260	Complex I, CA2	Respiratory chain	M	30.05	474	36	10	36.69	−1.93	0.00833
40	AT5G66510	Complex I, CA3	Respiratory chain	M	27.82	488	38	9	42.25	−1.79	0.00065
49	AT3G48680	Complex I, CAL2	Respiratory chain	M	27.94	678	64	11	42.58	−4.28	0.00744
34	AT1G79010	Complex I, TYKY-1	Respiratory chain	M	25549	669	109	18	57.21	−2.70	0.00009
34	AT1G16700	Complex I, TYKY-2	Respiratory chain	M	25.36	568	106	6	52.70	−2.70	0.00009
55	AT5G11770	Complex I, PSST	Respiratory chain	M	24.03	456	73	12	36.70	−1.97	0.00975
68	AT5G47570	Complex I, ASHI	Respiratory chain	M	13.20	126	32	3	19.20	−3.50	0.00111
58	AT1G67350	Complex I, plant specific subunit	Respiratory chain	M	11.78	308	40	7	61.22	−2.99	0.00002
59	AT1G67350	Complex I, plant specific subunit	Respiratory chain	M	11.78	376	75	12	56.12	−4.97	0.00000
69	AT1G67350	Complex I, plant specific subunit	Respiratory chain	M	11.78	138	9	3	28.57	−1.85	0.00910
70	AT2G42310	Complex I, plant specific subunit	Respiratory chain	M	12.62	146	28	4	33.33	−3.20	0.00002
76	AT2G42310	Complex I, plant specific subunit	Respiratory chain	M	12.62	120	15	3	33.33	−2.12	0.00458
80	AT4G20150	Complex I, plant specific subunit	Respiratory chain	M	9.20	263	47	8	29.63	−7.69	0.00296
122	AT2G27730	Complex I, plant specific subunit	Respiratory chain	M	11.94	404	35	6	51.33	+3.85	0.00091
40	AT1G17350	Complex I interm. Assoc. protein 30	Respiratory chain	M	25.23	594	67	13	40.09	−1.79	0.00065
102	AT5G40650	Complex II, SDH2-2	Respiratory chain	M	31.12	813	92	20	53.93	+1.70	0.00764
38	AT3G02090	Complex III, MPPbeta	Respiratory chain	M	59.12	481	39	10	18.64	−3.34	0.00132
33	AT1G19140	Ubiquinone biosynthesis protein COQ	Respiratory chain	M	34.32	745	107	21	41.48	−1.97	0.00042
122	AT1G66590	Complex IV, COX19-1	Respiratory chain	M	10.93	310	27	7	70.41	+3.85	0.00091
16	AT1G48030	Glycine decarboxylase L-1 (GDC-L-1)	Photorespiration	M	53.95	1254	127	26	53.85	−1.80	0.00479
17	AT1G48030	Glycine decarboxylase L-1 (GDC-L-1)	Photorespiration	M	53.95	794	62	18	38.66	−2.96	0.00741
18	AT1G48030	Glycine decarboxylase L-1 (GDC-L-1)	Photorespiration	M	53.95	1557	170	29	53.85	−1.58	0.00037
19	AT1G48030	Glycine decarboxylase L-1 (GDC-L-1)	Photorespiration	M	53.95	1394	120	24	50.49	−1.99	0.00216
35	AT5G26780	Serine hydroxymethyltransferase 2 (SHMT 2)	Photorespiration	M	57.31	509	65	12	22.24	−2.09	0.00278
39	AT5G26780	Serine hydroxymethyltransferase 2 (SHMT 2)	Photorespiration	M	57.31	683	63	13	32.11	−3.04	0.00553
44	AT5G26780	Serine hydroxymethyltransferase 2 (SHMT 2)	Photorespiration	M	57.31	489	29	9	18.57	−2.43	0.00084
46	AT5G26780	Serine hydroxymethyltransferase 2 (SHMT 2)	Photorespiration	M	57.31	505	54	10	17.79	−2.33	0.00294
25	AT1G59900	Pyruvate dehydrogenase E1 alpha-1 (PDC)	Pyruvate catabolism	M	43.03	512	45	15	34.45	−2.45	0.00867
28	AT1G59900	Pyruvate dehydrogenase E1 alpha-1 (PDC)	Pyruvate catabolism	M	43.03	1502	176	35	57.07	−1.74	0.00155
29	AT1G24180	Pyruvate dehydrogenase E1 alpha-2 (PDC)	Pyruvate catabolism	M	43.33	1082	98	29	53.18	−1.85	0.00728
22	AT5G50850	Pyruvate dehydrogenase E1 beta (PDC)	Pyruvate catabolism	M	39.15	970	100	18	43.80	−1.89	0.00181
82	AT3G55410	Oxoglutarate dehydrogenase E1-2	Glutamate catabolism	M	115.09	907	60	18	23.89	+2.78	0.00257
85	AT5G65750	Oxoglutarate dehydrogenase E1-1	Glutamate catabolism	M	116.33	224	14	7	9.07	+3.50	0.00305
94	AT5G18170	Glutamate dehydrogenase 1 (GDH1)	Glutamate catabolism	M	44.50	660	64	14	32.36	+1.67	0.00722

Table 1 (continued)

Identity in Arabidopsis

| spot[a]	Accession[b]	Name[c]	Functional context	Localization[d]	Mass [kDa][e]	Mascot score[f]	Peptides[g]	Unique peptides[h]	Coverage [%][i]	Ratio of mean normalized volume 'mutant'/mean normalized volume 'wt' Delta 2D[j]	p-Value of ratio of mean normalized volume 'mutant'/mean normalized volume 'wt' Delta 2D[k]
95	AT5G18170	Glutamate dehydrogenase 1 (GDH1)	Glutamate catabolism	M	44.50	763	68	18	36.25	+1.83	0.00847
95	AT5G07440	Glutamate dehydrogenase 2 (GDH2)	Glutamate catabolism	M	44.67	569	46	7	30.90	+1.83	0.00847
4	AT1G06950	Tic110	Transport	P	112.05	642	25	14	16.24	−1.78	0.00100
5	AT1G06950	Tic110	Transport	P	112.05	841	42	17	23.43	−1.84	0.00921
6	AT4G01660	ABC1	Transport	M	68.58	1408	87	27	47.03	−1.69	0.00673
79	AT5G14040	Mt phosphate transporter	Transport	M	40.06	414	60	9	16.00	−2.12	0.00102
106	AT5G19760	Dicarboxylate/tricarboxylate carrier (DTC)	Transport	M	31.89	624	59	13	46.64	+4.67	0.00269
114	AT5G40930	TOM20-4	Transport	M	20.96	481	56	11	42.78	+2.12	0.00606
119	AT3G46560	TIM9	Transport	M	10.71	567	131	19	79.57	+1.66	0.00519
9	AT2G45030	Elongation factor 2 (EFG/EF2)	Protein biosynthesis	M	83.06	761	61	19	26.66	−2.44	0.00273
94	AT4G02930	Elongation factor Tu	Protein biosynthesis	M	49.38	502	40	13	34.58	+1.67	0.00722
97	AT1G07920	Elongation factor 1-alpha	Protein biosynthesis	C	49.47	497	38	11	28.95	+2.14	0.00243
103	AT4G28510	Prohibitin-1	Protein folding & processing	M	31.69	756	53	14	43.75	+1.59	0.00804
103	AT5G03860	Prohibitin-2	Protein folding & processing	M	31.79	649	54	6	39.16	+1.59	0.00804
104	AT1G03860	Prohibitin-2	Protein folding & processing	M	31.79	672	71	12	48.60	+2.13	0.00081
105	AT2G20530	Prohibitin-6	Protein folding & processing	M	31.62	779	78	17	52.80	+5.22	0.00004
15	AT4G35850	Pentatricopeptide repeat3 (PPR3)	Processing of nucleic acids	M	50.42	507	45	14	36.04	−1.89	0.00307
54	AT3G20390	Endoribonuclease L-PSP family protein	Processing of nucleic acids	P	19.80	547	26	9	58.82	−1.92	0.00135
62	AT4G11010	Nucleoside diphosphate kinase 3 (NDPK3)	Processing of nucleic acids	M	25.72	346	27	8	29.83	−2.00	0.00337
86	AT5G04130	DNA gyrase B2 (GYRB2)	Processing of nucleic acids	M	81.00	577	63	12	17.49	+2.61	0.00244
87	AT5G04130	DNA gyrase B2 (GYRB2)	Processing of nucleic acids	M	81.00	681	78	15	19.54	+3.30	0.00246
101	AT5G51080	RNase H family protein	Processing of nucleic acids	M	35.38	601	52	12	36.34	+8.65	0.00444
107	AT4G30930	Ribosomal RPL21M protein	Processing of nucleic acids	M	30.89	281	14	5	22.22	+1.86	0.00372
113	AT1G14620	DECOY	Processing of nucleic acids	M	27.12	644	69	14	39.91	+1.60	0.00783
112	AT3G06790	Multiple organelle RNA edit. Factor 3 (MORF3)	Processing of nucleic acids	M	27.54	321	24	6	30.33	+1.50	0.00882
21	AT1G48850	Embryo defective 1144 (EMB1144)	Amino acid metabolism	P	47.29	743	72	18	36.93	−2.72	0.00227
29	AT4G35630	Phosphoserine aminotransferase (PSAT)	Amino acid metabolism	P	47.33	1003	105	24	46.28	−1.85	0.00728
17	AT3G10050	L-O-methylthreonine resistant 1 (OMR1)	Amino acid metabolism	P	64.59	644	44	15	28.89	−2.96	0.00741
72	AT5G10860	Cystathionine beta-synthase (CBS) family protein	Amino acid metabolism	M	22.71	351	45	9	30.58	−1.88	0.00749
109	AT5G65720	Nitrogen fixation S-like 1 (NFS1)	Amino acid metabolism	M	36.10	414	44	17	24.62	+1.77	0.00875
27	AT3G09260	Beta-glucosidase 23 (BGLU23 or PYK 10)	Stress response	ER	59.68	527	44	11	25.57	−1.51	0.00119
89	AT1G66270	Beta-glucosidase 21 (BGLU21)	Stress response	ER	59.63	1011	126	23	40.84	+2.73	0.00033
91	AT1G66270	Beta-glucosidase 21 (BGLU21)	Stress response	ER	59.63	1056	109	23	39.12	+3.31	0.00060
115	AT1G66270	Beta-glucosidase 21 (BGLU21)	Stress response	ER	59.63	306	28	6	10.50	+7.09	0.00031
88	AT1G66280	Beta-glucosidase 22 (BGLU22)	Stress response	ER	59.74	625	51	13	29.96	+2.46	0.00515
90	AT1G66280	Beta-glucosidase 22 (BGLU22)	Stress response	ER	59.74	924	81	20	36.83	+2.31	0.00485
92	AT1G66280	Beta-glucosidase 22 (BGLU22)	Stress response	ER	59.74	1350	146	28	40.84	+1.82	0.00307
93	AT1G66280	Beta-glucosidase 22 (BGLU22)	Stress response	ER	59.74	745	67	16	37.21	+3.01	0.00449
96	AT1G66280	Beta-glucosidase 22 (BGLU22)	Stress response	ER	59.74	389	32	8	20.04	+3.32	0.00082
98	AT3G16450	Jacalin-related lectin 33 (JAL33)	Stress response	ER	32.00	1002	92	18	52.67	+1.59	0.00378
99	AT3G16420	PYK 10 binding protein (PBP1)	Stress response	C	32.14	625	70	11	36.91	+2.25	0.00091
100	AT3G16420	PYK 10 binding protein (PBP1)	Stress response	C	32.14	459	41	9	27.18	+4.24	0.00864
1	AT1G29900	Carbamoyl phosphate synthetase B (CARB)	Other metabolic pathways	P	129.87	236	9	5	7.41	−2.95	0.00860
12	AT5G27600	Long chain acyl-CoA synthetase 7 (LACS7)	Other metabolic pathways	PX	77.30	130	8	3	5.86	−1.72	0.00929
23	AT4G29130	Hexokinase 1 (HXK1)	Other metabolic pathways	M	53.67	627	57	11	26.61	−1.59	0.00458
26	AT2G01140	Fructose-bisphosphate aldolase	Other metabolic pathways	P	42.30	985	74	20	46.29	−1.52	0.00428
30	AT4G05390	Root-type ferredoxin:NADP'(H) oxidor. (RFNR1)	Other metabolic pathways	P	42.37	1230	150	35	60.85	−2.98	0.00214
32	AT4G08770	Peroxidase 37 (Prx37)	Other metabolic pathways	EX	38.18	511	63	13	28.61	−3.48	0.00348
42	AT4G16800	Enoyl-CoA hydratase	Other metabolic pathways	M	32.77	958	95	22	63.79	−1.98	0.00259
51	AT4G05530	Indole-3-butyric acid response (IBR1)	Other metabolic pathways	PX	26.75	640	73	12	43.70	−1.57	0.00909
60	AT3G07480	2Fe-2S ferredoxin-like superfamily protein	Other metabolic pathways	M	17.59	407	41	6	32.70	−7.81	0.000002
111	AT1G02920	Glutathione S-transferase 7 (ATGSTF7)	Other metabolic pathways	C	23.58	593	55	12	55.98	+2.98	0.00252
24	AT1G43800	Plant stearoyl-acyl-carrier-protein desaturase family	Not known	P	44.13	818	93	21	34.78	−2.89	0.00235
63	AT5G08060	not described	Not known	M	15.03	547	134	16	83.21	−3.27	0.00005
73	AT3G03070	NADH-ubiquinone oxidoreductase-related	Not known	M	12.23	195	33	5	16.36	−4.37	0.00031
81	AT2G46540	Not described	Not known	M	6.80	180	28	2	36.92	−7.09	0.00229
83	AT5G09840	Not described	Not known	M	102.30	121	4	2	2.27	+2.61	0.00258
110	AT2G45060	Not described	Not known	N	30.32	556	44	10	36.76	+1.71	0.00317
117	AT1G80230	Rubredoxin-like superfamily protein	Not known	M	18.57	413	64	10	43.86	+2.69	0.00756
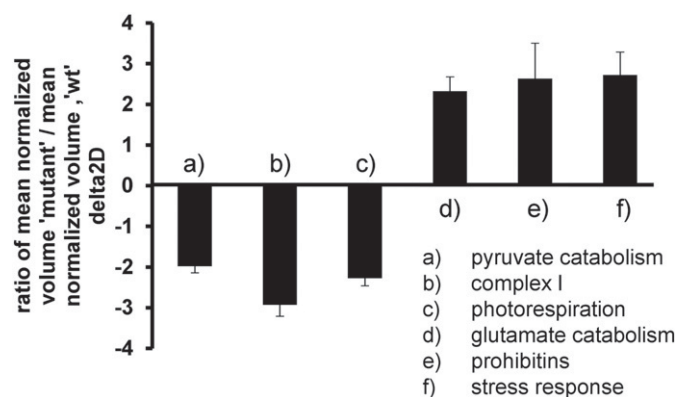
Fig. 8. Protein categories changed in Δcal1/cal2i plants relative to wt plants. a) pyruvate catabolism (3 proteins), b) complex I subunits (23 proteins), c) photorespiration (2 proteins), d) glutamate catabolism (4 proteins), e) prohibitins (3 proteins), f) proteins involved in stress response (5 proteins).

their requirement for complex I assembly, are still required. Analysis of further double and eventually triple and quadruple mutants will be necessary in future research, as well as transformation of CA/CAL deficient plants with constructs encoding altered versions of CA and CAL proteins. This eventually will allow discriminating between the biochemical functions of the CA/CAL proteins and their role in complex I assembly.

Supplementary data to this article can be found online at http://dx.doi.org/10.1016/j.bbabio.2015.10.006.

Transparency document

The Transparency document associated with this article can be found, in the online version.

Acknowledgments & author contributions

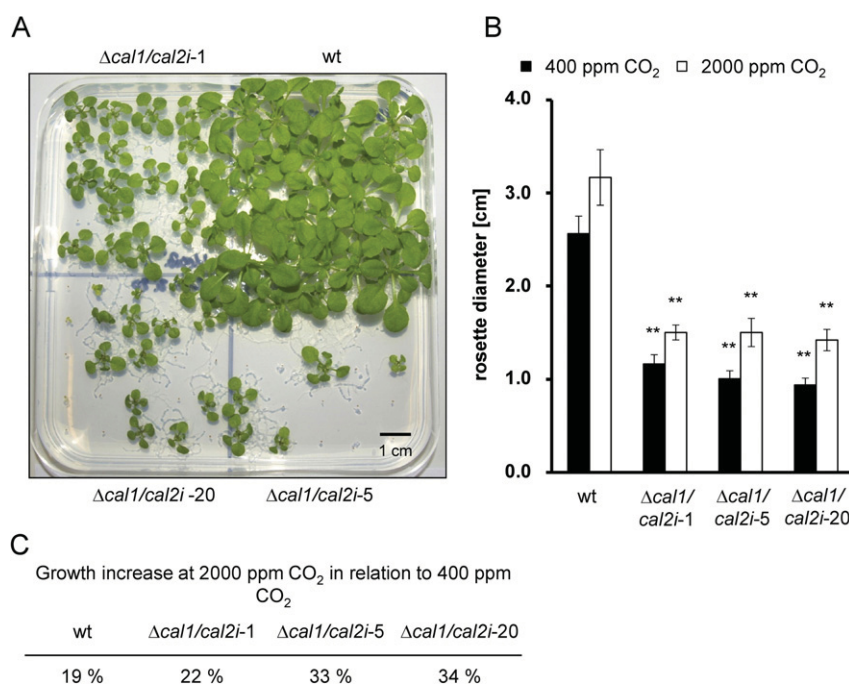**Fig. 9.** Phenotype of Arabidopsis wt and Δcal1/cal2i lines at 400 ppm and 2000 ppm CO_2. Rosette diameters of wt, Δcal1/cal2i-1, Δcal1/cal2i-5 and Δcal1/cal2i-20 plants were measured after cultivation for four weeks at 400 ppm CO_2 (A, B: black bars) and 2000 ppm CO_2 (B: white bars) (n = 11 to 15). The growth increase at 2000 ppm CO_2 in relation to 400 ppm CO_2 was calculated for each genotype (C). n = 6 to 15 (biological), mean ± SE, ** p ≤ 0.01 (student's t-test).

Notes to Table 1:
- [a] Spot number in accordance with Fig. 7. Note: some spots include more than one protein.
- [b] Accession numbers as given by TAIR (http://www.arabidopsis.org/).
- [c] Proteins are named according to the corresponding genes annotated at TAIR (www.arabidopsis.org).
- [d] Subcellular localization according to SUBAcon (http://suba3.plantenergy.uwa.edu.au/, [55]): mitochondrion (M), plastid (P), peroxisome (PX), endoplasmatic reticulum (ER), cytosol (C), nucleus (N), extracellular (EX).
- [e] Calculated molecular mass of the identified protein as deduced from the corresponding gene. Note that in some cases mitochondrial targeting peptides (2–5 kDa) are removed from the proteins after import into mitochondria.
- [f] Probability score for the protein identification based on mass spectrometry analysis and MASCOT search.
- [g] Number of matching peptides.
- [h] Unique peptides out of the number of matching peptides.
- [i] Sequence coverage of a protein by identified peptides in %.
- [j] Ratio of spot volume of mutant to ratio of spot volume to wt. Spot volumes were calculated on the basis of the master gels shown in Fig. 7 using the Delta 2D software (Decodon, Germany). −: decreased spot volume in mutant; +: increased spot volume in mutant.
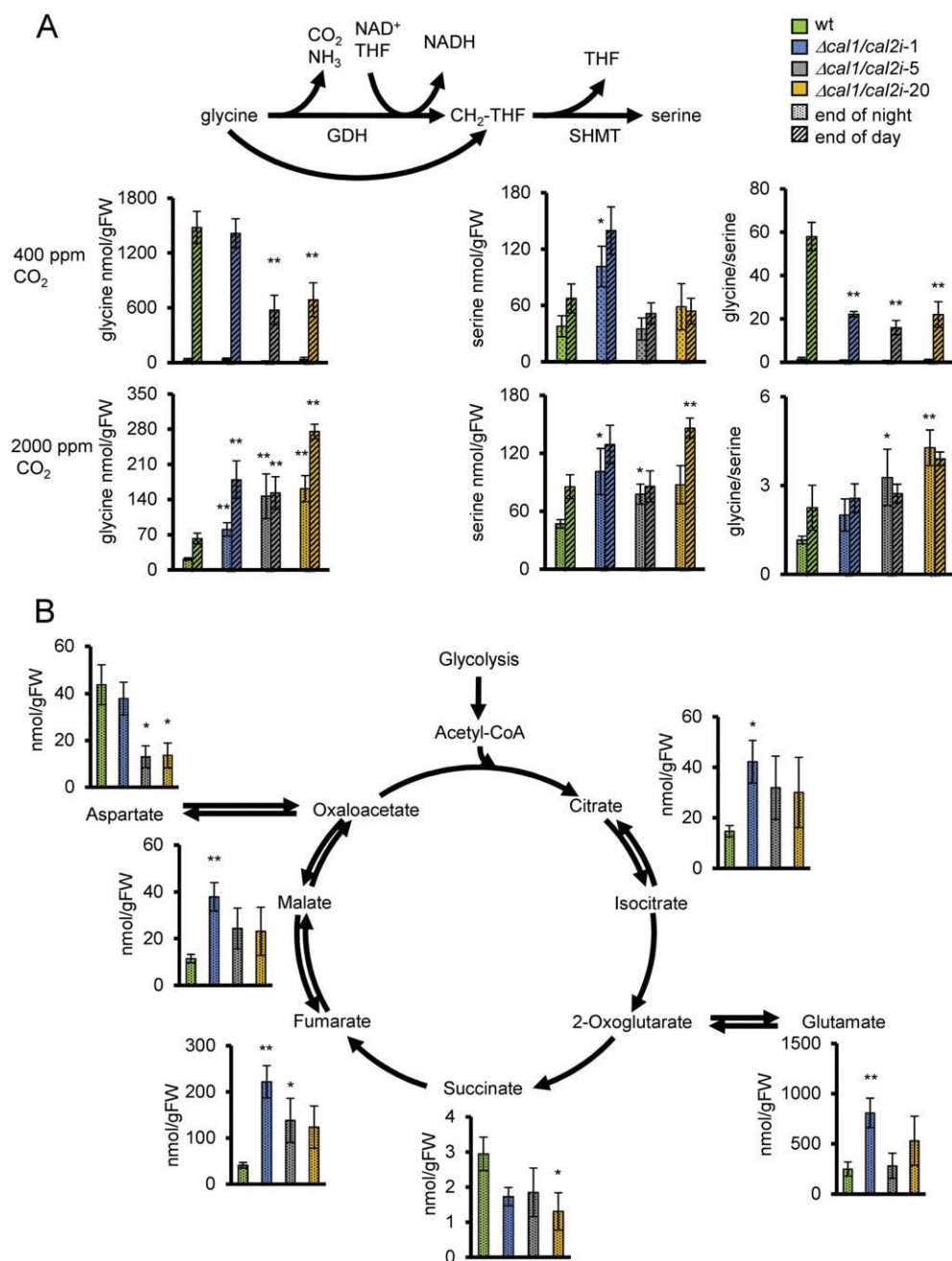- [k] p-values of ratio of spot volume of mutant to ratio of spot volume to wt.

Fig. 10. Quantification of metabolites of Arabidopsis wt and Δcal1/cal2i lines. Glycine and serine contents at 400 ppm CO_2 and 2000 ppm CO_2 at the end of night (dotted bars) and end of day (dashed bars) were analyzed (A). The glycine serine ratio was calculated from the contents. Metabolites of the citric acid cycle were measured at 400 ppm at the end of the night (B). For each sample, three to four plants were pooled and extracts were analyzed by GC–MS. n = 6 (biological), mean ± SE, *p ≤ 0.05 or **p ≤ 0.01 (student's t-test).

References

[1] J. Hirst, Mitochondrial complex I, Annu. Rev. Biochem. 82 (2013) 551–575.

[2] R. Baradaran, J.M. Berrisford, G.S. Minhas, L.A. Sazanov, Crystal structure of the entire respiratory complex I, Nature 494 (2013) 443–448.

[3] C. Hunte, V. Zickermann, U. Brandt, Functional modules and structural basis of conformational coupling in mitochondrial complex I, Science 329 (2010) 448–451.

[4] K.R. Vinothkumar, J. Zhu, J. Hirst, Architecture of mammalian respiratory complex I, Nature 515 (2014) 80–84.

[5] V. Zickermann, C. Wirth, H. Nasiri, K. Siegmund, H. Schwalbe, C. Hunte, U. Brandt, Structural biology. Mechanistic insight from the crystal structure of mitochondrial complex I, Science 347 (2015) 44–49.

[6] T. Friedrich, On the mechanism of respiratory complex I, J. Bioenerg. Biomembr. 46 (2014) 255–268.

[7] L.A. Sazanov, A giant molecular proton pump: structure and mechanism of respiratory complex I, Nat. Rev. Mol. Cell Biol. 16 (2015) 375–388.

[8] J. Carroll, I.M. Fearnley, J.M. Skehel, R.J. Shannon, J. Hirst, J.E. Walker, Bovine complex I is a complex of 45 different subunits, J. Biol. Chem. 281 (2006) 32724–32727.

[9] E. Balsa, R. Marco, E. Perales-Clemente, R. Szklarczyk, E. Calvo, M.O. Landázuri, J.A. Enríquez, NDUFA4 is a subunit of complex IV of the mammalian electron transport chain, Cell Metab. 16 (2012) 378–386.

[10] K. Peters, K. Belt, H.P. Braun, 3D gel map of Arabidopsis complex I, Front. Plant Sci. 4 (2013) 153.

[11] H.P. Braun, S. Binder, A. Brennicke, H. Eubel, A.R. Fernie, I. Finkemeier, J. Klodmann, A.C. König, K. Kühn, E. Meyer, T. Obata, M. Schwarzländer, M. Takenaka, A. Zehrmann, The life of plant mitochondrial complex I, Mitochondrion 19 (Pt B) (2014) 295–313.

[12] N.V. Dudkina, H. Eubel, W. Keegstra, E.J. Boekema, H.P. Braun, Structure of a mitochondrial supercomplex formed by respiratory-chain complexes I and III, Proc. Natl. Acad. Sci. U. S. A. 102 (2005) 3225–3229.

[13] J.L. Heazlewood, K.A. Howell, A.H. Millar, Mitochondrial complex I from Arabidopsis and rice: orthologs of mammalian and fungal components coupled with plant-specific subunits, Biochim. Biophys. Acta 1604 (2003) 159–169.

[14] M. Perales, G. Parisi, M.S. Fornasari, A. Colaneri, F. Villarreal, N. Gonzalez-Schain, J. Echave, D. Gomez-Casati, H.P. Braun, A. Araya, E. Zabaleta, Gamma carbonic anhydrase like complex interact with plant mitochondrial complex I, Plant Mol. Biol. 56 (2004) 947–957.

[15] S. Sunderhaus, N. Dudkina, L. Jänsch, J. Klodmann, J. Heinemeyer, M. Perales, E. Zabaleta, E. Boekema, H.P. Braun, Carbonic anhydrase subunits form a matrix-exposed domain attached to the membrane arm of mitochondrial complex I in plants, J. Biol. Chem. 281 (2006) 6482–6488.

[16] J. Klodmann, S. Sunderhaus, M. Nimtz, L. Jänsch, H.P. Braun, Internal architecture of mitochondrial complex I from Arabidopsis thaliana, Plant Cell 22 (2010) 797–810.

[17] V. Martin, F. Villarreal, I. Miras, A. Navaza, A. Haouz, R.M. González-Lebrero, S.B. Kaufman, E. Zabaleta, Recombinant plant gamma carbonic anhydrase homotrimers bind inorganic carbon, FEBS Lett. 583 (2009) 3425–3430.

[18] M. Perales, H. Eubel, J. Heinemeyer, A. Colaneri, E. Zabaleta, H.P. Braun, Disruption of a nuclear gene encoding a mitochondrial gamma carbonic anhydrase reduces complex I and supercomplex I + III$_2$ levels and alters mitochondrial physiology in Arabidopsis, J. Mol. Biol. 350 (2005) 263–277.

[19] E.H. Meyer, C. Solheim, S.K. Tanz, G. Bonnard, A.H. Millar, Insights into the composition and assembly of the membrane arm of plant complex I through analysis of subcomplexes in Arabidopsis mutant lines, J. Biol. Chem. 286 (2011) 26081–26092.

[20] Q. Wang, R. Fristedt, X. Yu, Z. Chen, H. Liu, Y. Lee, H. Guo, S.S. Merchant, C. Lin, The γ-carbonic anhydrase subcomplex of mitochondrial complex I is essential for development and important for photomorphogenesis of Arabidopsis, Plant Physiol. 160 (2012) 1373–1383.

[21] L. Li, C.J. Nelson, C. Carrie, R.M. Gawryluk, C. Solheim, M.W. Gray, J. Whelan, A.H. Millar, Subcomplexes of ancestral respiratory complex I subunits rapidly turn over in vivo as productive assembly intermediates in Arabidopsis, J. Biol. Chem. 288 (2013) 5707–5717.

[22] D. Soto, J.P. Córdoba, F. Villarreal, C. Bartoli, J. Schmitz, V. Maurino, H.P. Braun, G.C. Pagnussat, E. Zabaleta, Functional characterization of mutants affected in the carbonic anhydrase domain of the respiratory complex I in Arabidopsis thaliana, Plant J. (2015)http://dx.doi.org/10.1111/tpj.12930.

[23] M.J. May, C.J. Leaver, Oxidative stimulation of glutathione synthesis in Arabidopsis thaliana suspension cultures, Plant Physiol. 103 (1993) 621–627.

[24] J.D. de Virville, I. Aaron, M.F. Alin, F. Moreau, Isolation and properties of mitochondria from Arabidopsis thaliana cell suspension cultures, Plant Physiol. Biochem. 32 (1994) 159–166.

[25] L. Heimann, I. Horst, R. Perduns, B. Dreesen, S. Offermann, C. Peterhansel, A common histone modification code on C4 genes in maize and its conservation in Sorghum and Setaria 23 talic, Plant Physiol. 162 (2013) 456–469.

[26] W. Werhahn, A. Niemeyer, L. Jänsch, V. Kruft, U.K. Schmitz, H. Braun, Purification and characterization of the preprotein translocase of the outer mitochondrial membrane from Arabidopsis. Identification of multiple forms of TOM20, Plant Physiol. 125 (2001) 943–954.

[27] O. Keech, P. Dizengremel, P. Gardeström, Preparation of leaf mitochondria from Arabidopsis thaliana, Physiol. Plant. 124 (2005) 403–409.

[28] I. Wittig, R. Carrozzo, F.M. Santorelli, H. Schägger, Supercomplexes and subcomplexes of mitochondrial oxidative phosphorylation, Biochim. Biophys. Acta 1757 (2006) 1066–1072.

[29] H. Eubel, L. Jänsch, H.P. Braun, New insights into the respiratory chain of plant mitochondria. Supercomplexes and a unique composition of complex II, Plant Physiol. 133 (2003) 274–286.

[30] C. Mihr, H.P. Braun, Proteomics in plant biology, in: P. Michael (Ed.), Handbook of Proteomics Methods, Humana, Totowa 2003, pp. 409–416.

[31] V. Neuhoff, R. Stamm, H. Eibl, Clear background and highly sensitive protein staining with Coomassie blue dyes in polyacrylamide gels: a systematic analysis, Electrophoresis 11 (1985) 427–448.

[32] V. Neuhoff, R. Stamm, I. Pardowitz, N. Arold, W. Ehrhardt, D. Taube, Essential problems in quantification of proteins following colloidal staining with Coomassie brilliant blue dyes in polyacrylamide gels, and their solution, Electrophoresis 11 (1990) 101–117.

[33] M. Berth, F. Moser, M. Kolbe, J. Bernhardt, The state of the art in the analysis of two-dimensional gel electrophoresis images, Appl. Microbiol. Biotechnol. 76 (2007) 1223–1243.

[34] C. Lorenz, H. Rolletschek, S. Sunderhaus, H.P. Braun, Brassica napus seed endosperm — metabolism and signaling in a dead end tissue, J. Proteome 108 (2014) 382–426.

[35] C. Jung, C.M.J. Higgins, Z. Xu, Measuring the quantity and activity of mitochondrial electron transport chain complexes in tissues of central nervous system using blue native polyacrylamide gel electrophoresis, Anal. Biochem. 286 (2000) 214–223.

[36] T.P. Singer, Determination of the activity of succinate, NADH, choline, and alpha-glycerophosphate dehydrogenases, Methods Biochem. Anal. 22 (1974) 123–175.

[37] G. Zhou, W. Jiang, Y. Zhao, G. Ma, W. Xin, J. Yin, B. Zhao, Sodium tanshinone II a sulfonate mediates electron transfer reaction in rat heart mitochondria, Biochem. Pharmacol. 65 (2003) 51–57.

[38] E.H. Meyer, T. Tomaz, A.J. Carroll, G. Estavillo, E. Delannoy, S.K. Tanz, I.D. Small, B.J. Pogson, A.H. Millar, Remodeled respiration in ndufs4 with low phosphorylation efficiency suppresses Arabidopsis germination and growth and alters control of metabolism at night, Plant Physiol. 151 (2009) 603–619.

[39] J. Lisec, N. Schauer, J. Kopka, L. Willmitzer, A.R. Fernie, Gas chromatography mass spectrometry-based metabolite profiling in plants, Nat. Protoc. 1 (2006) 387–396.

[40] A. Rasmusson, I. Moller, NAD(P)H dehydrogenases on the inner surface of the inner mitochondrial membrane studied using inside-out submitochondrial particles, Physiol. Plant. 83 (1991) 357–365.

[41] P. Schertl, S. Sunderhaus, J. Klodmann, G.E. Grozeff, C.G. Bartoli, H.P. Braun, L-galactono-1,4-lactone dehydrogenase (GLDH) forms part of three subcomplexes of mitochondrial complex I in Arabidopsis thaliana, J. Biol. Chem. 287 (2012) 14412–14419.

[42] L.M. Voll, A. Jamai, P. Renné, H. Voll, C.R. McClung, A.P. Weber, The photorespiratory Arabidopsis shm1 mutant is deficient in SHM1, Plant Physiol. 140 (2006) 59–66.

[43] C. Peterhänsel, I. Horst, M. Niessen, C. Blume, R. Kebeish, S. Kürkcüoglu, F. Kreuzaler, Photorespiration, The Arabidopsis Book, American Society of Plant Biologists, Rockville, MD, 2010http://dx.doi.org/10.1199/tab.0130.

[44] S. Timm, A. Florian, M. Wittmiss, K. Jahnke, M. Hagemann, A.R. Fernie, H. Bauwe, Serine acts as a metabolic signal for the transcriptional control of photorespiration-related genes in Arabidopsis, Plant Physiol. 162 (2013) 379–389.

[45] G. Parisi, M. Perales, M.S. Fornasari, A. Colaneri, N. Gonzalez-Schain, D. Gomez-Casati, S. Zimmermann, A. Brennicke, A. Araya, J.G. Ferry, J. Echave, E. Zabaleta, Gamma carbonic anhydrases in plant mitochondria, Plant Mol. Biol. 55 (2004) 193–207.

[46] H.P. Braun, E. Zabaleta, Carbonic anhydrase subunits of the mitochondrial NADH dehydrogenase complex (complex I) in plants, Physiol. Plant. 129 (2007) 114–122.

[47] E. Zabaleta, M.V. Martin, H.P. Braun, A basal carbon concentrating mechanism in plants? Plant Sci. 187 (2012) 97–104.

[48] M.R. Badger, G.D. Price, CO$_2$ concentrating mechanisms in cyanobacteria: molecular components, their diversity and evolution, J. Exp. Bot. 54 (2003) 609–622.

[49] B.D. Rae, B.M. Long, L.F. Whitehead, B. Förster, M.R. Badger, G.D. Price, Cyanobacterial carboxysomes: microcompartments that facilitate CO$_2$fixation, J. Mol. Microbiol. Biotechnol. 23 (2013) 300–307.

[50] K. Riazunnisa, L. Padmavathi, H. Bauwe, A.S. Raghavendra, Markedly low requirement of added CO$_2$ for photosynthesis by mesophyll protoplasts of pea (Pisum sativum): possible roles of photorespiratory CO$_2$ and carbonic anhydrase, Physiol. Plant. 128 (2006) 763–772.

[51] C. Dutilleul, S. Driscoll, G. Cornic, R. De Paepe, C.H. Foyer, G. Noctor, Functional mitochondrial complex I is required by tobacco leaves for optimal photosynthetic performance in photorespiratory conditions and during transients, Plant Physiol. 131 (2003) 264–275.

[52] J.R. Marienfeld, K.J. Newton, The maize NCS2 abnormal growth mutant has a chimeric nad4-nad7 mitochondrial gene and is associated with reduced complex I function, Genetics 138 (1994) 855–863.

[53] K. Kühn, T. Obata, K. Feher, R. Bock, A.R. Fernie, E.H. Meyer, Complete mitochondrial complex I deficiency induces an up-regulation of respiratory fluxes that is abolished by traces of functional complex I, Plant Physiol. 168 (2015) 1537–1549.

[54] A.F. De Longevialle, E.H. Meyer, C. Andrés, N.L. Taylor, C. Lurin, A.H. Millar, I.D. Small, The pentatricopeptide repeat gene OTP43 is required for trans-splicing of the mitochondrial nad1 intron 1 in Arabidopsis thaliana, Plant Cell 19 (2007) 3256–3265.

[55] S.K. Tanz, I. Castleden, C.M. Hooper, M. Vacher, I.D. Small, H.A. Millar, SUBA3: a database for integrating experimentation and prediction to define the SUBcellular location of proteins in Arabidopsis, Nucleic Acids Res. 41 (2013) D1185–D1191.
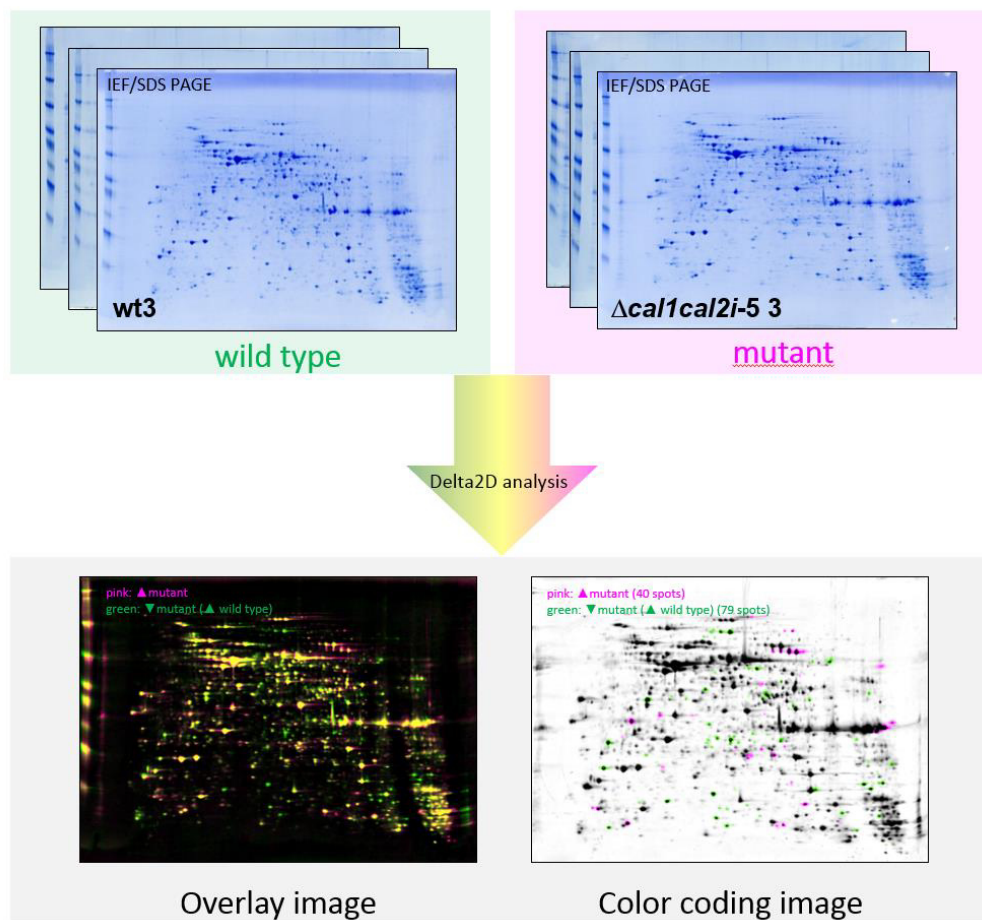
SUPPLEMENTARY FIGURE

Supplementary figure 1

A
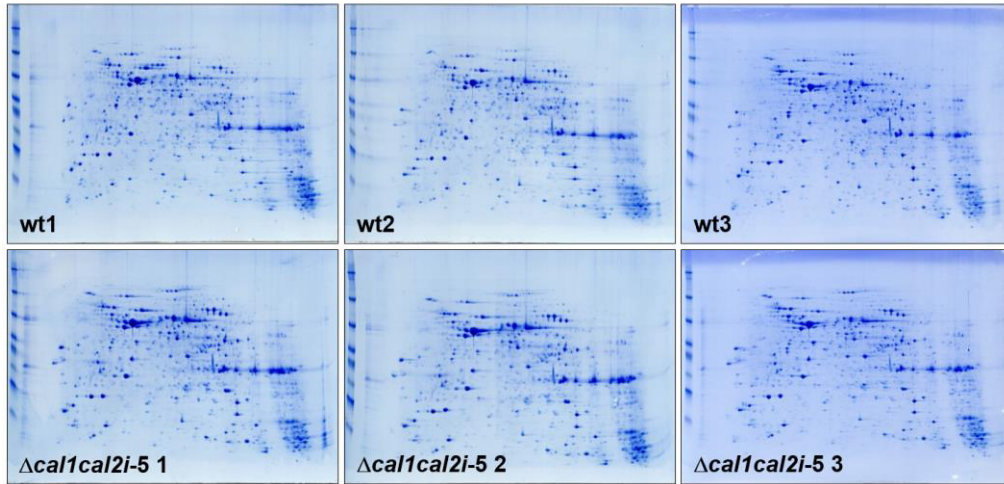
B

SUPPLEMENTARY FIGURE 1: 2D IEF/SDS PAGE of mitochondrial proteins of wt and Δ*cal*1*cal*2*i*-5 lines (A). A set of three gels per genotype were used for calculation of the master gels using the Delta 2D software package (Decodon, Freiburg, Germany) (B).

CORRIGENDUM

Corrigendum to "Depletion of the "gamma-type carbonic anhydrase-like" subunits of complex I affects central mitochondrial metabolism in Arabidopsis thaliana"

[Biochimica et Biophysica Acta 1857 [2016] 60–71]

Steffanie Fromm[a,b], Jennifer Göing[b], Christin Lorenz[a], Christoph Peterhänsel[b], Hans-Peter Braun[a]

[a] Institut für Pflanzengenetik, Leibniz Universität Hannover, Herrenhäuser Str. 2, 30419 Hannover, Germany
[b] Institut für Botanik, Leibniz Universität Hannover, Herrenhäuser Str. 2, 30419 Hannover, Germany

————————————————————————

The authors regret to inform the readers of our article that the results presented in Figure 10 were not correctly calculated. The corrected figure is presented below.
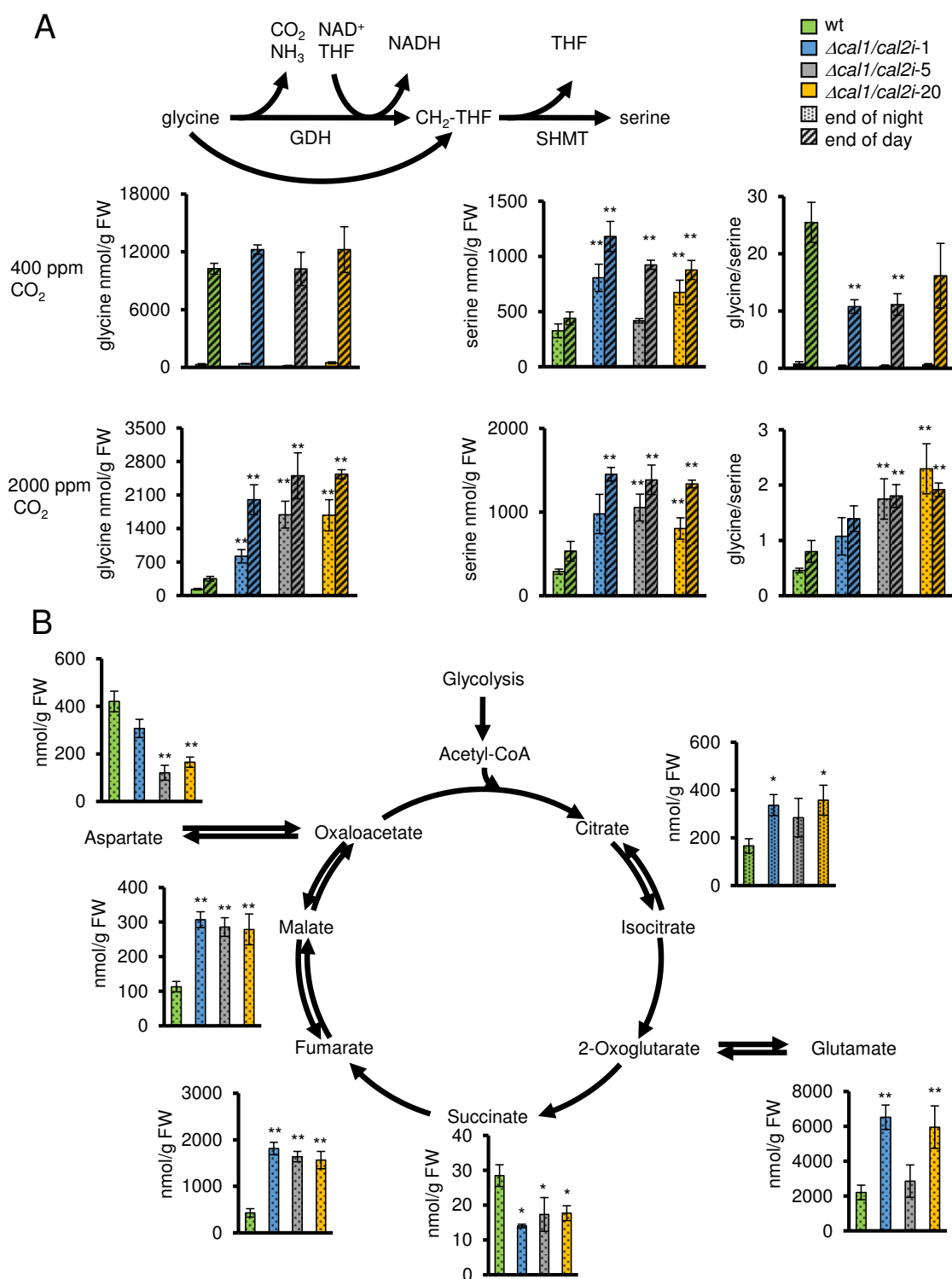
Cor. Figure 10: Quantification of metabolites of Arabidopsis wt and Δ*cal*1/*cal2i* lines. Glycine and serine contents at 400 ppm CO₂ and 2000 ppm CO₂ at the end of night (dotted bars) and end of day (dashed bars) were analyzed (A). The glycine serine ratio was calculated from the contents. Metabolites of the citric acid cycle were measured at 400 ppm at the end of the night (B). For each sample, three to four plants were pooled and extracts were analyzed by GC-MS. n = 6 (biological), mean ± SE, * p ≤ 0.05 or ** p ≤ 0.01 (student's t-test).

Due to the changes in Figure 10, three sentences in the text paragraph related to this Figure have to be corrected (Page 65, results section, 2nd column, lines 5-13)

Published version (sentences to be changed are given in colors)

Two out of three mutant lines showed a reduction in glycine accumulation EoD. At 2000 ppm CO_2, glycine accumulation during the day was diminished for all genotypes. However, levels were here higher in the mutants compared to the wt. Differences in serine concentrations were less pronounced in mutants and wt. This resulted in an overall reduced glycine/serine (gly/ser) ratio in the mutants at 400 ppm CO_2, but not 2000 ppm CO_2. Gly/ser ratios are often used as a proxy for photorespiratory flux. Levels of most TCA cycle intermediates and glutamate were increased in the mutants with the exception of succinate that was decreased (Fig. 10).

Has to be corrected into (corrected sentences are given in colors)

Wt plants and mutant lines have the same glycine content at 400 ppm (EoD). At 2000 ppm CO_2, glycine accumulation during the day was diminished for all genotypes. However, levels were here higher in the mutants compared to the wt. All mutant lines accumulated serine at 400 ppm and 2000 ppm EoD. At EoN serine content increased in two out of three mutant lines at 400 ppm and 2000 ppm. This resulted in an overall reduced glycine/serine (gly/ser) ratio in the mutants at 400 ppm CO_2, but not 2000 ppm CO_2. Gly/ser ratios are often used as a proxy for photorespiratory flux. Levels of most TCA cycle intermediates and glutamate were increased in the mutants with the exceptions of succinate and aspartate (Fig. 10).

The authors would like to apologise for any inconvenience caused.

Corresponding author:

Hans-Peter Braun,
mail: braun@genetik.uni-hannover.de

Publication 2

2.2. Mitochondrial gamma carbonic anhydrases are required for complex I assembly and plant reproductive development

Steffanie Fromm[1,2], Hans-Peter Braun[1], Christoph Peterhänsel[2]

[1] Leibniz Universität Hannover, Institute of Plant Genetics, 30419 Hannover, Germany
[2] Leibniz Universität Hannover, Institute of Botany, 30419 Hannover, Germany

Type of authorship:	First author
Type of article:	Research article
Share of the work:	85 %
Contribution to the publication:	planned and performed all experiments, analyzed data, prepared all figures and wrote parts of the paper
Journal:	New Phytologist
5-year impact factor:	7.84
Date of publication:	(in press)
Number of citations (google scholar on May. 24th, 2016):	1
DOI:	10.1111/nph.13886
PubMed-ID:	26889912

New
Phytologist

Mitochondrial gamma carbonic anhydrases are required for complex I assembly and plant reproductive development

Steffanie Fromm[1,2], Hans-Peter Braun[1] and Christoph Peterhansel[2]

[1]Institute of Plant Genetics, Leibniz Universität Hannover, 30419 Hannover, Germany; [2]Institute of Botany, Leibniz Universität Hannover, 30419 Hannover, Germany

Author for correspondence:
Christoph Peterhansel
Tel: +49 511 7622632
Email: cp@botanik.uni-hannover.de

Summary

- Complex I of the mitochondrial electron transport chain (mETC) in plants contains an extra domain that is made up from proteins homologous to prokaryotic gamma-carbonic anhydrases (γCA). This domain has been suggested to participate in complex I assembly or to support transport of mitochondrial CO_2 to the chloroplast.
- Here, we generated mutants lacking CA1 and CA2 – two out of three CA proteins in *Arabidopsis thaliana*. Double mutants were characterized at the developmental and physiological levels. Furthermore, the composition and activity of the mETC were determined, and mutated CA versions were used for complementation assays.
- Embryo development of double mutants was strongly delayed and seed development stopped before maturation. Mutant plants could only be rescued on sucrose media, showed severe stress symptoms and never produced viable seeds. By contrast, callus cultures were only slightly affected in growth. Complex I was undetectable in the double mutants, but complex II and complex IV were upregulated concomitant with increased oxygen consumption in mitochondrial respiration. Ectopic expression of inactive CA variants was sufficient to complement the mutant phenotype.
- Data indicate that CA proteins are structurally required for complex I assembly and that reproductive development is dependent on the presence of complex I.

Introduction

The mitochondrial electron transport chain (mETC) comprises four multiprotein complexes. These complexes transfer electrons from NADH or organic acids via multiple carriers ultimately to oxygen as the terminal electron acceptor, resulting in the formation of water. During this process, protons are translocated across the inner mitochondrial membrane, forming an electrochemical gradient that can be used by ATP synthase for formation of ATP from ADP. ATP derived from this reaction is the major energy source for metabolic reactions in mitochondria and the cytosol (Millar *et al.*, 2011).

Complex I is the major NADH dehydrogenase of the mETC. It transfers electrons from NADH to ubiquinone and translocates protons during this process (Baradaran *et al.*, 2013; Brandt, 2013). The complex has an L-like shape with a membrane arm embedded in the inner mitochondrial membrane and a peripheral arm protruding into the mitochondrial matrix (Hunte *et al.*, 2010; Hirst, 2013; Vinothkumar *et al.*, 2014; Letts & Sazanov, 2015; Zickermann *et al.*, 2015). This structure is conserved between prokaryotes and eukaryotes. However, prokaryotic complex I is composed of 14 core subunits and eukaryotic complex I of > 40 subunits; for example, plant complex I is composed of 49 subunits (Baradaran *et al.*, 2013; Peters *et al.*, 2013; Braun *et al.*, 2014). In plants, in contrast to animal and fungi, an additional

spherical domain directly attached to the membrane arm has been identified (Heazlewood *et al.*, 2003; Perales *et al.*, 2004; Dudkina *et al.*, 2005; Sunderhaus *et al.*, 2006; Klodmann *et al.*, 2010). This domain is made up exclusively by proteins with homology to gamma-carbonic anhydrases (γCA) from bacteria and archaea (Parisi *et al.*, 2004; Sunderhaus *et al.*, 2006; Klodmann *et al.*, 2010). Complex I from the protist *Acanthamoeba* also contains γCA proteins, but it is unknown whether they form a separate domain (Gawryluk & Gray, 2010). The Arabidopsis genome encodes five γCA proteins: Three proteins have a highly conserved catalytic domain and are termed carbonic anhydrase 1–3 (CA1, CA2, CA3). Two additional proteins that show less homology to their prokaryotic homologues especially in the catalytic domain are termed γCA-like proteins (CAL1 and CAL2) (Perales *et al.*, 2004). CO_2 hydration activity has never been validated experimentally for plant γCA enzymes. However, a truncated version of CA2 has been shown to form a homotrimer that can bind CO_2/bicarbonate (Martin *et al.*, 2009). By contrast, residues required for catalytic activity of CAM, the γCA from the archaeon *Methanosarcina thermophila*, have been characterized in great detail. Replacement of an arginine residue (R59) by alanine at the N-terminus has been shown to affect CA activity by destabilizing the homotrimer (Tripp *et al.*, 2002), whereas a glutamine (Q75) was important for catalytic activity. Furthermore, three histidines (H81, H117, H122) were shown to be essential for

New
Phytologist

activity, most probably because they are involved in Zn^{2+} binding (Kisker *et al.*, 1996). Based on structural modeling, all of these sequence elements are highly conserved in plant γCA (Parisi *et al.*, 2004).

The function of complex I-associated γCA in plant mitochondria is not well defined. Based on the presence of CA2 in early assembly intermediates of complex I, it was suggested that γCA might act as subunits required for assembly of the multiprotein complex (Meyer *et al.*, 2011; Li *et al.*, 2013). This was consistent with the clear decrease of complex I amounts and activity in *ca2* mutants (Perales *et al.*, 2005). However, no experimental evidence is currently available that γCA is absolutely required for complex I assembly. An alternative hypothesis suggested that γCA might help to translocate CO_2 released in photorespiration from mitochondria to chloroplasts in order to increase the probability of refixation (Braun & Zabaleta, 2007; Zabaleta *et al.*, 2012). Experimental support for this hypothesis was recently obtained by the description of double mutants in *ca2 ca1* and *ca2 ca2*, respectively. These mutants showed reduced growth at normal CO_2 concentrations, but not at elevated CO_2 (Soto *et al.*, 2015).

Beside the γCA domain of complex I, the presence of alternative electron donors and acceptors in plants is another difference between the mETC of plants and animals (Millar *et al.*, 2011). On the one hand, alternative NADH and NADPH dehydrogenases, located both at the matrix side and the inter-membrane side of the inner mitochondrial membrane, can transfer electrons from reduced adenylates to ubiquinone (Rasmusson *et al.*, 2008). These reactions are not linked to proton translocation across the membrane and, thus, not to ATP synthesis (Rasmusson *et al.*, 2004). Probably because of the presence of these alternative enzymes, most complex I mutants in plants can survive under normal growth conditions (e.g. Gutierres *et al.*, 1999; Karpova *et al.*, 2002; Meyer *et al.*, 2009; Juszczuk *et al.*, 2012), whereas complex I mutations in animals are mostly lethal (Fassone & Rahman, 2012). On the other hand, alternative oxidases transfer electrons from ubiquinol to molecular oxygen without proton translocation (Moore *et al.*, 2013). These oxidases are not restricted to plants (Rogov & Zvyagilskaya, 2015). The activity of both alternative NAD(P)H dehydrogenases and oxidases has been mostly associated with stress situations where production and demand of NAD(P)H or ATP were out of balance (Giraud *et al.*, 2008; Rasmusson *et al.*, 2008; Wallström *et al.*, 2014; Dahal *et al.*, 2015).

In this study, we show that *ca1 ca2* double mutants completely lacked complex I. This resulted in strongly retarded embryo development that could only be rescued at high external sugar supply. Overexpression of enzymatically inactive CA2 was sufficient for complementation. These data provide new insights into the function of γCA and the role of complex I in plant development.

Materials and Methods

Plant material and growth conditions

Arabidopsis thaliana (L.) Heynh. lines SALK_109391 (At1 g19580, *ca1/ca1*) and SALK_010194 (At1 g47260, *ca2/ca2*)

were obtained from NASC. Mutants were crossed to generate *ca1 ca2* double mutants. Plants were grown on $0.5\times$ MS medium in climate chambers at 8–12 h light (see figure legends), 120 μmol $m^{-2}\,s^{-1}$, 22°C, 65% humidity and atmospheric CO_2 concentrations. After 4 wk, plants were transferred to soil. Plantlets with fully opened cotyledons of homozygous *ca1 ca2* mutants were rescued on $0.5\times$ MS medium containing 3% (w/v) sucrose.

Cell cultures were established from sterile 10-d-old Arabidopsis plants. Leaf or hypocotyl tissue was cut and transferred to Gamborg B5 solid medium (0.316% (w/v) B5 medium, 3% (w/v) sucrose, 1% (w/v) plant agar, 0.0001% (w/v) 2,4 dichlorphenoxyacetic acid, 0.00001% (w/v) kinetin, pH 5.8). Emerging calli were cultivated for 3 wk in darkness and maintained as suspension cultures. Growth rates of cell cultures were determined using 1.5 g starting material. Weight increase was determined after 3, 5 and 7 d.

Generation of CA2 variants

The coding sequence of *CA2* was amplified from cDNA (5′-CACCATGGGAACCCTAGGA-3′ and 5′-TTAGAAGTAC TGAGTAGACGG-3′) and inserted in pENTR™/D-TOPO® vector (Invitrogen). Site-directed mutagenesis was performed using the QuikChange® Kit (Stratagene, La Jolla, CA, USA). Oligonucleotide combinations were 5′-TGGTATGGCTGTGT TCTT**GC**AGGTGATGTGAATAACATCAGTGTTG-3′ and 5′-CAACACTGATGTTATTCACATCACCTGCAAGAACA AGCCATACCA-3′ for *CA2* R86A and 5′-TGTAACAGT AGGT**A**ACAGTGCTGTCATT**A**ATGGGTGTACTGTTG-A-3′ and 5′-TCAACAGTACACCCAT**T**AATGACAGCAC TG**TT**ACCTACTGTTACA-3′ for *CA2* H130N H135N. Mutant *CA2* sequences were transferred to pEarleyGate 100 (Earley *et al.*, 2006) by recombination (Gateway® LR Clonase™ Enzyme Mix; Invitrogen). Floral dip transformation of *CA1/ca1 ca2/ca2* mutants or *ca2/ca2* mutants was carried out according to Clough & Bent (1998).

Genotyping of mutants

For DNA extraction, leaves or calli were homogenized, 500 μl extraction buffer (50 mM Tris-HCl (pH 7.6), 0.5% (w/v) SDS) and 500 μl water-saturated phenol were added, and the suspension was mixed for 10 min. Phases were separated by centrifugation (16 000 ***g***, 10 min, 22°C). 400 μl supernatant was added to 40 μl 3 M sodium acetate (pH 5.2) and 800 μl 96% (v/v) ethanol, samples were mixed and centrifuged (16 000 ***g***, 20 min, 4°C). The pellet was washed with 70% (v/v) ethanol and dissolved in water.

PCR reactions were performed at standard conditions (95°C 5 min, 35 cycles of 95°C 30 s, 58°C 30 s and 72°C 90 s, 72°C 5 min) with *c.* 30 ng genomic DNA template. Oligonucleotide sequences for genotyping were derived from http://signal.salk.edu/: SALK_109391: LP: 5-TAGCGATTCTGGA TTCGAATG-3′, RP: 5′-CATCCCATGCTTTTCAACAAC-3′. SALK_010194: LP: 5′-ACGGAAACAAAGGTGGTTCTC-3′,

RP: 5′-TGATGTTCAGATCGGAAAAGG-3′, T-DNA: 5′-AT TTTGCCGATTTCGGAAC-3. *ACTIN2* (At3 g18780) RP: 5′-GGTAACATTGTGCTCAGTGGTGG-3′, LP: 5′-GGTGCAA CGACCTTAATCTTCAT-3′.

Transcript analysis

RNA was isolated using the TRIZOL method (Chomczynski, 1993). 100 ng RNA were used for cDNA synthesis. DNA contaminations were digested (1 U DNase (Thermo Scientific), 37°C, 30 min) and DNase was inactivated at 70°C for 15 min. 50 pmol of random nonamer oligonucleotide were added and annealed at 70°C for 5 min. Reverse transcription (1 mM dNTPs, 200 U MMLV-RT, Promega) was carried out at 37°C for 60 min and inactivated at 70°C for 10 min. Quantitative RT-PCR was performed on an ABI PRISM 7300 (Applied Biosystems, Darmstadt, Germany) using SYBR Green fluorescence (Platinum SYBR Green qPCR Mix; Life Technologies, Carlsbad, CA, USA) for detection.

Primer combinations were 5′-GTTCGAGAAGGTTCTACG CAAGA-3′ and 5′-GAGGTTAAGCTCTGGTGGAGTT-3′ for *CA1*, 5′-GATAGTATACATCTCACAGTCAGC-3′ and 5′-CT TCTTCCTAAGCGCTCTCTCAA-3′ for *CA2*, 5′-GTTCGGC TGTGGAGTACTCCAA-3′ and 5′-CTGAATCATATTCTGT ATCGCGAGC-3′ for *CA3*, 5′-TAGCCATCAACCACTTAA GCG-3′ and 5′-GCGATCCCAAGGGACTTCTT-3′ for *CAL1*, 5′-CAAACATTGATCGATAGGTACGTGA-3′ and 5′-TGCC AGGTGGTAAAACAGAACCA-3′ for *CAL2*. *UBIQUITIN 10* (At4 g05320) expression was used as an internal standard (5′-GGCCTTGTATAATCCCTGATGAATAAG-3′ and 5′-AA AGAGATAACAGGAACGGAAACATAGT-3′).

Analysis of embryo development

Recently opened flowers were marked with colored threads over a time series of 15 d. Siliques were harvested and dissected, and seeds were transferred to an object slide covered with Hoyer's solution (15 ml distilled water, 3.75 g gum arabic, 3 mM glycerin, 50 g chloral hydrate). Seeds were incubated overnight at 4°C in Hoyer's solution for clearing. Developmental stages were analyzed by differential inference contrast (DIC) microscopy (Axioskop 2 mot plus; Zeiss, Oberkochen, Germany) with Nomarski objectives. Pictures were taken with an Axio cam MRc5 camera (Zeiss).

Embryo rescue

Seeds 7, 10 and 14 d after pollination (dap) were transferred to 0.5× MS medium containing 3% (w/v) sucrose and cultured at 8 h light (120 μmol m^{-2} s^{-1}, 22°C, 65% humidity), and atmospheric CO_2 concentrations for several weeks.

Pollen tube germination assay

Pollen grains were transferred on to objective slides with pollen tube germination medium (1 mM calcium chloride, 1 mM calcium nitrate, 1 mM magnesium sulfate, 1.6 mM boric acid, 18% (w/v) sucrose, 0.5% (w/v) agar) by dabbing recently opened flowers on the slides. Samples were incubated up to 24 h at 100% humidity.

Superoxide detection

Superoxide was detected by formazan staining for 5 h in 0.1 mg ml^{-1} nitro blue tetrazolium chloride (NBT) and 25 mM HEPES, pH 7.6. After incubation, chlorophyll was removed from leaves with 80% ethanol for 2 h at 70°C. Superoxide anions were visualized as a dark precipitate (Welchen *et al.*, 2012). Note that this assay might also indicate complex II activity (Boerjan *et al.*, 1991).

Metabolite analysis

Plants were grown for 4 wk in short day conditions. Afterwards, half of the plants were shifted to 100 ppm CO_2 for 2 d. Plants were harvested at 4 h light. Metabolites were extracted and quantified as described in Fromm *et al.* (2016).

Isolation of mitochondria

Mitochondria from cell culture were isolated as described by Werhahn *et al.* (2001). For total protein extracts, 5 g leaf material were homogenized in 10 ml disruption buffer (300 mM mannitol, 50 mM Tris-HCl (pH 7.4), 1 mM EDTA, 1% (v/v) Triton X-100, 0.2 mM PMSF) with a mortar and sea sand, filtered through gauze, and centrifuged (10 min, 18 300 *g*, 4°C). The supernatant was transferred to a new reaction tube. All steps were carried out at 4°C or on ice.

Protein gel electrophoresis

One-dimensional Blue Native polyacrylamide gel electrophoresis (1D BN-PAGE) and two-dimensional BN-sodium dodecyl sulfate (SDS)-PAGE were performed according to Schägger (2001). A gradient gel (4.5–16% acrylamide) with a 4% stacking gel was used. Mitochondrial membranes were solubilized by digitonin according to Eubel *et al.* (2003).Gels were fixed for 2 h in 15% (v/v) ethanol, 10% (v/v) acetic acid and stained with Coomassie Brilliant Blue G-250 (Neuhoff *et al.*, 1985, 1990).

Mass spectrometry

Tryptic digestion of proteins and identification of proteins using the EASY-nLC System (Proxeon; Thermo Scientific, Bremen, Germany) and coupled MS analyses (MicrOTOF-Q II mass spectrometer; Bruker, Bremen, Germany) were performed as described by Klodmann *et al.* (2010). Mass spectrometry primary data were evaluated using the PROTEINSCAPE v.2.1 software (Bruker, Bremen, Germany), the Mascot Search Engine (Matrix Science, London, UK), the Arabidopis protein database (release TAIR 10) and an updated version of a complex I database (Klodmann *et al.*, 2010), which represents a subset of the Arabidopis

New
Phytologist

protein database. The threshold Mascot Score was set to 30 for proteins and 20 for peptides.

Enzyme activity assays

In-gel staining for complexes I, II and IV was carried out according to Jung *et al.* (2000) with modifications. Gels were washed twice for 10 min in H_2O. For NADH : NBT oxidoreductase activity staining, BN gel strips were incubated in staining solution (100 mM Tris-HCl, pH 7.4, 0.14 mM NADH, 1 mg ml^{-1} NBT) until the purple staining of the bands became visible. Complex II activity staining was carried out in 50 mM KH_2PO_4 buffer (pH 7.4), 84 mM succinate, 0.2 mM PMS and 2 mg ml^{-1} NBT. For complex IV activity staining, gels were incubated in 10 mM KH_2PO_4 buffer (pH 7.4), 1 mg ml^{-1} DAB and three tips of a spatula of cytochrome c. Complex V activity staining was carried out in 35 mM Tris-HCl (pH 7.4), 270 mM glycine, 14 mM $MgSO_4$, 0.2% (w/v) $Pb(NO_3)_2$ and 8 mM ATP overnight (Cox *et al.*, 1978). Reactions were stopped in fixing solution containing 15% (v/v) ethanol and 10% (v/v) acetic acid. All steps were carried out at room temperature. Densitometric analyses were carried out using IMAGEJ. In addition, photometric activity measurements for complexes I, II and IV were done with the Epoch Microplate Spectrophotometer (Biotek, Winooski, VT, USA). Complex I activity was measured at 420 nm using 2 µg mitochondrial protein, 50 mM Tris-HCl, pH 7.4, 500 mM $K_3Fe(CN)_6$ and 200 mM NADH (Singer, 1974; Zhou *et al.*, 2003). For complex II activity, 15 µg mitochondrial protein was incubated for 5 min in 25 mM KH_2PO_4 buffer (pH 7.4), 5 mM $MgCl_2$, 20 mM succinate, 0.3 mM ATP. Afterwards, 500 µM SHAM, 100 µM ubiquinone (oxidized) and 2 mM KCN were added. Reactions were started with 50 µM DCPIP and activity was measured at 600 nm (Birch-Machin *et al.*, 1994). Complex IV activity was measured at 550 nm using 1 µg mitochondrial protein, 25 mM KH_2PO_4 buffer (pH 7.4), 15 µM reduced cytochrome c, and 300 mM dodecylmaltoside (Birch-Machin *et al.*, 1994).

Oxygen consumption

Oxygen consumption of isolated mitochondria was measured using a Clark-type oxygen electrode (Hansatech Instruments, Norfolk, UK) according to Meyer *et al.* (2009). Reaction buffer included 100 µg mitochondrial protein in 3 ml respiration buffer (300 mM sucrose, 5 mM KH_2PO_4, 10 mM TES, 10 mM NaCl, 2 mM $MgSO_4$, 0.1% (w/v) BSA, pH 6.8) supplied with 120 µM CoA, 200 µM TPP, 2 mM NAD^+, 10 mM glutamate and 10 mM malate. At stable oxygen consumption, 200 µM ADP was added for measuring ADP-dependent respiration.

Results

In order to elucidate the function of mitochondrial CA proteins, we generated mutants with mutations in more than one *CA* gene. We started with genetic crossings of *ca1* and *ca2* mutants. The possible role of *CA3* is evaluated below in the Discussion.

T-DNA integration sites are shown schematically in Fig. 1(a). The *ca1* and *ca2* mutants did not show an obvious growth phenotype compared with wild-type (WT) (Fig. 1b). However, amounts of *CA1* and *CA2* mRNAs, respectively, were highly decreased in the mutants. Expression of other *CA* and *CAL* genes remained unaffected (Fig. 1c). Strongly decreased transcription also reduced protein levels beyond detection levels (Fig. 1d). This was evidenced by separation of complex I and supercomplex I+III$_2$ on 2D-BN-SDS gels and protein identification by mass spectrometry (bold: identified by unique peptides, other: ambigious peptides that correspond to more than one CA/CAL protein). For the WT, unique peptides corresponding to all CA and CAL proteins were detected, whereas the *ca1* mutant did not contain CA1-specific peptides. In the *ca2* mutant, unique peptides were identified for CA1, CAL1 and CAL2, but only ambiguous peptides derived from either CA2 or CA3. Also, it had been demonstrated previously for the *ca2* mutant that CA2 was absent not only in complex I, but also from complex I subcomplexes, and that no CA2 monomers had been detected (Perales *et al.*, 2005). Together, these results provided strong evidence that the CA1 protein was absent in the *ca1* mutant and the CA2 protein was absent in the *ca2* mutant without much affecting the abundance of other subunits.

We also isolated mitochondria from leaves of mutants and determined the NADH : NBT oxidoreductase activity for complex I (Supporting Information Fig. S1). We observed a slight decrease of complex I activity for the *ca1* mutant (89% residual activity with *in gel* activity measurement and no decrease in photometrical assay), but for the *ca2* mutant a decrease by *c.* 75% for the *in gel* activity measurement and 50% in the photometrical assay. Together, growth was unaffected and complex I abundance partially decreased in *ca1* and *ca2* mutants.

We performed reciprocal crosses of *ca1* and *ca2* mutants where *ca1* and *ca2* mutants were used as male or female parent, respectively. In these crosses, we were able to recover all predicted genotypes with the exception of the *ca1 ca2* double mutant genotype. We therefore isolated individual F$_2$ plants that were homozygous for one T-DNA integration, but hemizygous for the other T-DNA integration (*ca1/ca1 CA2/ca2* or *CA1/ca1 ca2/ca2* derived from reciprocal crosses) and again analyzed genotypes in the next generation after selfing (F$_3$ progeny; Table 1). Independent of the parental genotype, we again did not recover *ca1 ca2* double mutants. Segregation ratios significantly deviated from the expected 3 : 1 segregation according to the χ^2 test. This was not due to differences in germination rates of the tested F$_3$ families that were all between 78 and 88% (data not shown).

When analyzing maturing siliques from individual plants that were homozygous for the T-DNA integration in one *CA* locus, but hemizygous for the T-DNA integration in the other (*ca1/ca1 CA2/ca2* or *CA1/ca1 ca2/ca2* derived from reciprocal crosses), we observed green and pale developing seeds (Fig. 2a). However, siliques of the single mutants grown in parallel almost exclusively contained green developing seeds. When quantifying the number of pale seeds, we found *c.* 2% for the single mutants, but 21–24% for the segregating genotypes (Table 2). Abundance of pale seeds was in accordance with a 3 : 1 segregation according to the χ^2 test.
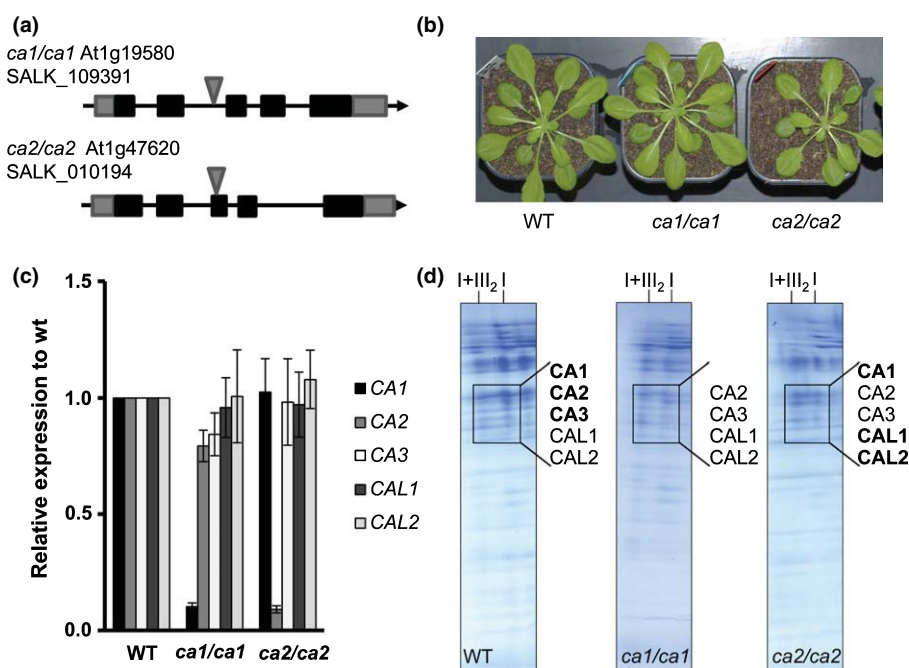
Fig. 1 Characterization of *Arabidopsis thaliana ca1* and *ca2* single mutants. (a) *CA1* and *CA2* gene structure with T-DNA insertion (grey triangles) for the SALK lines used in this study. Black boxes indicate exons, grey boxes the 5′ and 3′ UTRs, and lines introns. (b) Phenotype of wild-type (WT), *ca1* mutants and *ca2* mutants that were grown for 7 wk under short day (8 h : 16 h, light : dark) conditions. (c) *CA* and *CAL* transcript abundance relative to WT levels analyzed by RT-qPCR ($n = 5$–7, mean $\pm$ SE). (d) Detection of CA and CAL proteins in complex I and supercomplex I + III$_2$. Protein complexes were isolated from leaf mitochondria and separated by Blue Native sodium dodecyl sulfate polyacrylamide gel electrophoresis. Identity of CA and CAL proteins was determined by LC-MS. Proteins indicated in bold were identified by unique peptides, other proteins had no unique peptides and could not be unambiguously identified.

Table 1 Analysis of F$_3$ progeny genotypes of reciprocal crossings between *Arabidopsis thaliana ca1* and *ca2* mutants

Crossing	*F$_2$* individual	*F$_3$* progeny	Expectation (%) (1 : 2 : 1)	Observation (%)	χ^2 (3 : 1)	*P*-value
ca1/ca1 $\times$ *ca2/ca2*	*ca1/ca1 CA2/ca2*	*ca1/ca1 CA2/CA2*	25	36 $\pm$ 1	228	< 0.001
		ca1/ca1 CA2/ca2	50	64 $\pm$ 1		
		ca1/ca1 ca2/ca2	25	0 $\pm$ 0		
	CA1/ca1 ca2/ca2	*CA1/CA1 ca2/ca2*	25	35 $\pm$ 1	127	< 0.001
		CA1/ca1 ca2/ca2	50	65 $\pm$ 1		
		ca1/ca1 ca2/ca2	25	0 $\pm$ 0		
ca2/ca2 $\times$ *ca1/ca1*	*ca2/ca2 CA1/ca1*	*ca2/ca2 CA1/CA1*	25	44 $\pm$ 3	80	< 0.001
		ca2/ca2 CA1/ca1	50	56 $\pm$ 3		
		ca2/ca2 ca1/ca1	25	0 $\pm$ 0		
	CA2/ca2 ca1/ca1	*CA2/CA2 ca1/ca1*	25	40 $\pm$ 3	69	< 0.001
		CA2/ca2 ca1/ca1	50	60 $\pm$ 3		
		ca2/ca2 ca1/ca1	25	0 $\pm$ 0		

Observed segregation ratios were derived from the F$_3$ progeny ($n = 5$–10 independent F$_2$ individuals, mean $\pm$ SE). χ^2 values were calculated based on absolute numbers of segregants with 1 df.

We sought to genotype embryos in pale developing seeds. In order to generate sufficient material for genotyping, embryos were isolated and callus cultures were established (Fig. S2a). DNA from these cultures was then used for genotyping. DNAs from leaves of azygous (az), hemizygous and homozygous single mutants were used as controls (Fig. S2b–d). Azygous plants are derived from the same mother plant, but have lost the transgene by segregation. Ten out of 10 pale seeds were homozygous for both the *ca1* and the *ca2* T-DNA insertions indicating that embryos in pale seeds were *ca1 ca2* double mutants. Reciprocal crosses with WT plants suggested that this effect was not due to paternal or maternal sterility (Table S1).

We then recorded by microscopy embryo development in siliques of azygous plants, *ca1* and *ca2* single mutants, and *CA1/ca1 ca2/ca2* mutants. For *CA1/ca1 ca2/ca2*, the embryo development in pale (double mutant) and green seeds from individual siliques was recorded separately. Table 3 shows days after pollination at which embryos reached a particular developmental stage. Embryos of azygous plants and *ca1* or *ca2* single mutants developed similarly between 4 and 12 dap from transition stage to green mature stage. Green seeds of *CA1/ca1 ca2/ca2* plants already showed a delay in some embryo developmental stages. The transition stage was reached at 6.4 dap compared with 4.0 dap for the azygous lines. This delay remained almost constant throughout development and the mature stage was reached 1.5 d later compared with azygous embryos. Embryos in pale seeds from this genotype reached the transition stage and the heart stage at similar time points compared with green seeds from the same mother plant, but were then drastically delayed in further development. Late torpedo stage was reached 5.8 d after
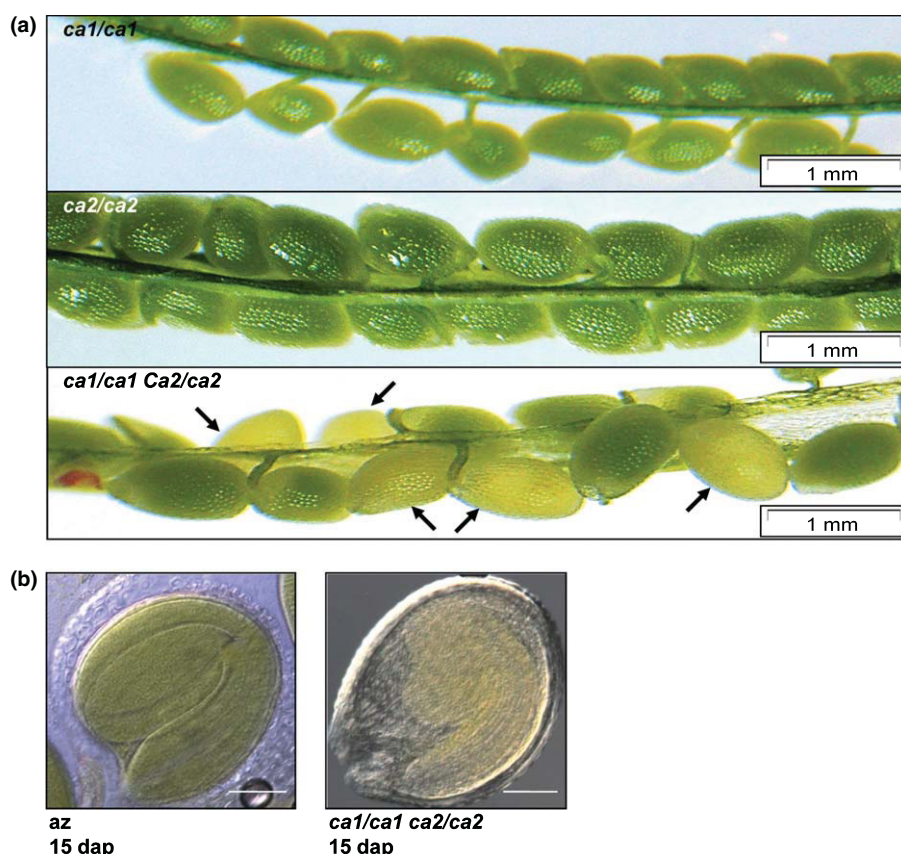
65

Fig. 2 Defect seed and embryo development of *Arabidopsis thaliana ca1 ca2* double mutants. (a) Seeds in the siliques of *ca1* or *ca2* single mutants and the *ca1/ca1 CA2/ca2* genotype. Pictures were taken at 12 d after pollination (dap). Pale seeds are indicated by arrows. (b) Typical embryo developmental stages at 15 dap of azygous and *ca1 ca2* double mutant seeds. Azygous (az) embryo is in the green mature stage and *ca1 ca2* double mutant embryo in the late torpedo stage. Bar, 100 μm.

Table 2 Ratios of green and pale developing seeds in siliques of *Arabidopsis thaliana* azygous plants, *ca1* and *ca2* single mutants and segregating lines derived from reciprocal crosses of these mutants

♂ ♀	Azygous	ca1/ca1 CA2/CA2	CA1/CA1 ca2/ca2	ca1/ca1 CA2/ca2	CA1/ca1 ca2/ca2	ca2/ca2 CA1/ca1	CA2/ca2 ca1/ca1
Green ovules	99% ± 0	98% ± 0	98% ± 0	79% ± 5	76% ± 3	77% ± 1	77% ± 1
Pale ovules	1% ± 0	2% ± 0	2% ± 0	21% ± 5	24% ± 3	23% ± 1	23% ± 1
χ^2 (3 : 1)	–	–	–	1.6	3.5	1.4	2.5
P-value	–	–	–	<0.25	<0.10	<0.25	<0.25

Genotypes are indicated in the table. Ten independent plants per genotype were analyzed (*n* > 800 seeds, mean ± SE). χ^2 values were calculated based on absolute numbers of segregants with 1 df.

Table 3 Embryo development of *Arabidopsis thaliana* azygous (az) plants, *ca1* and *ca2* mutants and segregating *CA1/ca1 ca2/ca2* plants derived from reciprocal crosses of these mutants

Parental genotype	Seed colour	Embryo stage					
		Transition	Heart	Early torpedo	Torpedo	Late torpedo	Mature
az		4.0 ± 0.1	5.4 ± 0.5	6.6 ± 0.3	7.5 ± 0.3	8.0 ± 0.6	11.8 ± 0.4
ca1/ca1		4.3 ± 0.6	6.0 ± 1.2	6.8 ± 0.3	7.5 ± 0.1	8.3 ± 0.1	12.4 ± 0.2
ca2/ca2		4.7 ± 0.2	5.6 ± 0.4	7.2 ± 0.1	7.9 ± 0.3	10.2* ± 0.1	11.9 ± 0.6
CA1/ca1 ca2/ca2	Green	6.4** ± 0.2	7.7 ± 0.8	7.6 ± 0.3	9.0* ± 0.2	10.4* ± 0.3	13.3* ± 0.1
	Pale	7.2** ± 0.1	7.7** ± 0.2	10.7** ± 0.2	12.5** ± 0.3	13.8** ± 0.1	–

Embryo development was analyzed in three biological replicates from 4 d after pollination (dap) to 15 dap by differential inference contrast microscopy. For segregating lines, green and pale ovules were separately analyzed (*n* > 500 seeds, mean dap ± SE). *, $P \leq 0.05$; **, $P \leq 0.01$ according to Student's *t*-test mutants compared with wild-type.

azygous embryos. We did not observe mature embryos in pale seeds during the investigated time period (Fig. 2b). Thus, simultaneous mutation of *CA1* and *CA2* resulted in a strong delay in embryo development. Very similar delays were also obtained for other parental genotype combinations (*ca1/ca1 CA2/ca2* and reciprocal father/mother combinations; Table S2). However, seed development was WT-like for the *ndufs4* mutant (Table S2), although complex I levels are strongly decreased in this mutant (Meyer *et al.*, 2009; Kühn *et al.*, 2015).

Our data suggested that *ca1 ca2* double mutant seeds aborted embryo development. However, in exceptional cases (< 1%), double mutant seeds matured and germinated. Seedlings derived from these seeds did not turn green and died after few days. However, when these seedlings were transferred to sucrose medium (3% w/v), some of these plants survived, formed green rosette leaves and eventually flowered. These plants were much smaller than controls and their development was strongly retarded (Fig. 3a–c) which was often associated with anthocyanin accumulation. We determined superoxide anion levels by NBT staining as a representative for reactive oxygen species (Fig. 3d). The *ca1 ca2* double mutants showed clearly enhanced staining compared with corresponding azygous segregants. However, note that this assay might also indicate complex II activity (Boerjan *et al.*, 1991). Siliques of these plants developed only few seeds. All remaining seeds were pale up to 12 dap. In older seeds (> 15 dap), we always observed endosperm degeneration and seed abortion (Fig. S3). Seeds derived from *ca1 ca2* double mutants never germinated even on high sucrose media. Defects in pollen development as assayed by *in vitro* pollen germination assays were not detected (Fig. S4).

In addition to growth of young double mutant seedlings on sucrose medium shown here, we were also able to recover double mutants by the embryo rescue technique. These plants showed a similar phenotype and are shown in Fig. S5.

γCA proteins are part of complex I of the mitochondrial electron transport chain (mETC; see the Introduction section). We therefore wanted to analyze the activity of mETC complexes in double mutants. Analyses of mitochondria from leaf samples were hampered by the low availability of leaf material from the few rescued double mutant plants. We therefore generated callus cultures from *ca1 ca2* embryos (see earlier) and analyzed mETC complexes in mitochondria derived from this source. *ca2* single mutants and WT were used as controls (Fig. 4a). *ca1 ca2* double mutant cultures grew slightly slower than WT cultures, but comparable to the *ca2* single mutant (Fig. S6). Complex I protein and NADH : NBT oxidoreductase activity of complex I were lower in the *ca2* mutant (20%), but absent (1% or less of WT) in the double mutant. We confirmed the absence of complex I by mass spectrometry. Proteins were extracted from BN-PAGE gels at the expected position of complex I. Most complex I subunits could be identified in protein from WT mitochondria. However, we could not detect any complex I subunit in the corresponding double mutant samples (Fig. S7). The remaining NADH : NBT oxidoreductase activity in the lower part of the gel was previously assigned to alternative NADH dehydrogenases or to the activity of dehydrolipoamide dehydrogenase (Meyer *et al.*, 2009).

Complex II activity was also less (44%) in the *ca2* mutant, but slightly increased in the double mutant (Fig. 4a). However, complex IV activity was clearly increased (261%) in the double mutant compared with both controls. Complex V activity remained largely unaffected (73%). Together, these data indicated that mitochondria from the *ca1 ca2* double mutant did not contain any intact complex I. This coincided with an upregulation of complex II and complex IV activity.
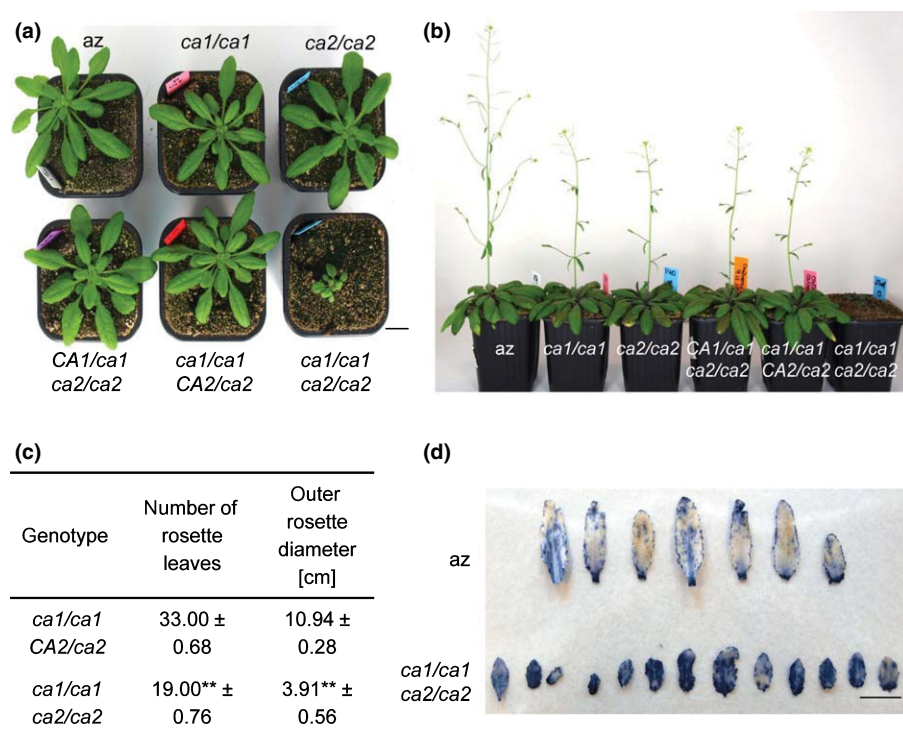
(a)

Genotype	Number of rosette leaves	Outer rosette diameter [cm]
ca1/ca1 *CA2/ca2*	33.00 ± 0.68	10.94 ± 0.28
ca1/ca1 *ca2/ca2*	19.00** ± 0.76	3.91** ± 0.56

Fig. 3 Phenotype of *Arabidopsis thaliana* *ca1 ca2* double mutants in comparison to azygous (az) plants, *ca1* and *ca2* single mutants and hemizygous individuals. (a) Rosettes of 10-wk-old plants grown under short-day (10 h : 14 h, light : dark) conditions. Scale bar is 2 cm. (b) 12-week-old plants (12 h : 12 h, light : dark) with flowers. (c) Number of rosette leaves and outer rosette diameter of 10-wk-old double mutant plants and a control line (*n* = 8, mean ± SE). **, $P \leq 0.01$ according to Student's *t*-test *ca1/ca1 ca2/ca2* mutant compared with *ca1/ca1 CA2/ca2*. (d) Superoxide detection in azygous and *ca1 ca2* leaves as determined by NBT staining. Bar, 1 cm.

67

New
Phytologist

Fig. 4 Activity of respiratory protein complexes in *Arabidopsis thaliana* wild-type (WT), *ca2*, and *ca1 ca2* mutants. (a) Protein complexes of mitochondria isolated from cell culture were resolved by Blue Native polyacrylamide gel electrophoresis. Gels were stained with colloidal Coomassie. Corresponding gels were used for *in gel* activity assays of complex I, II, IV and V (for details see the Material and Methods section). Identities of selected mitochondrial protein complexes are indicated beside the gels (I, complex I; II, complex II; III$_2$, dimeric complex III; I + III$_2$, supercomplex formed of complex I and dimeric complex III; IV, complex IV; V, complex V; F$_1$, F1 part of complex V). Relative density was estimated with IMAGEJ. Closed triangle, faint NADH : NBT oxidoreductase activity stain. Photometrical activity assays of mitochondria isolated from cell culture were carried out for: (b) complex I, (c) complex II and (d) complex IV ($n = 5$, mean ± SE). **, $P \leq 0.01$ according to Student's *t*-test mutants compared with WT. (e) Protein complexes of mitochondria isolated from leaves were resolved by BN-PAGE. Gels were stained with colloidal Coomassie. Corresponding gel was used for *in gel* activity assay of complex I.
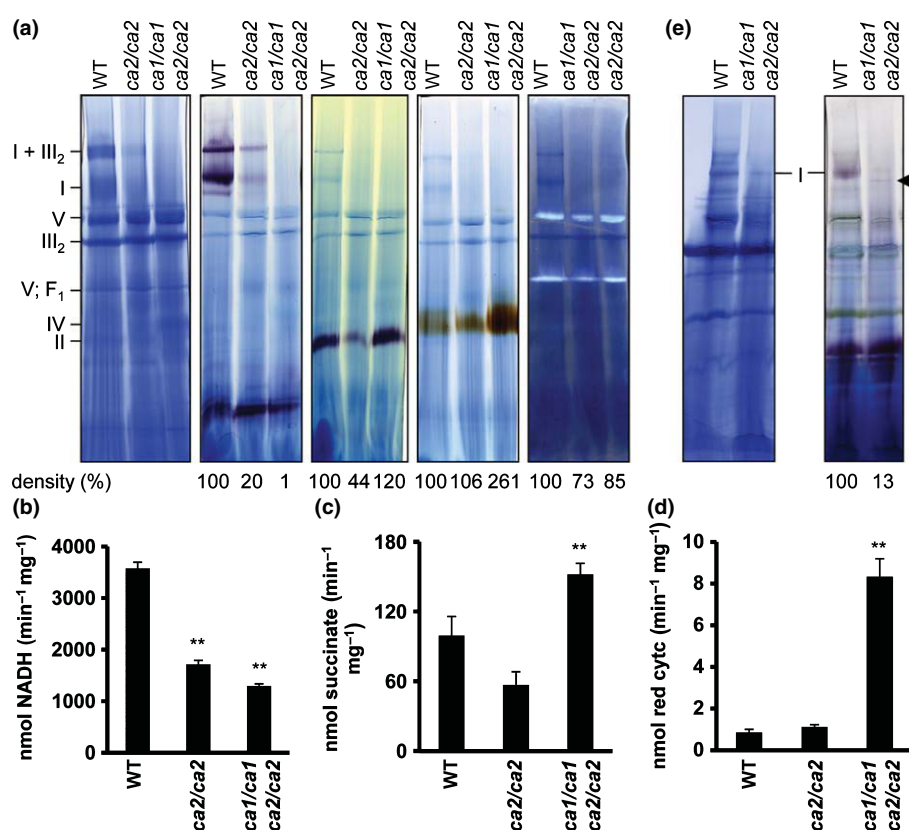
We further performed photometrical activity assays with protein isolated from mitochondria (Fig. 4b–d). NADH : ferricyanide oxidoreductase activity decreased by more than two-fold in the *ca2* mutant compared with the WT and a further decrease was observed in the double mutant. This assay cannot discriminate complex I activity from other alternative mitochondrial dehydrogenases that might be responsible for the remaining activity in the double mutant. Complex II activity was slightly lower for *ca2* mutants, but significantly higher for the double mutant, compared with the WT. Most significantly, complex IV activity was strongly increased by more than eight-fold in the double mutant. This is greater than observed in *in gel* assays and might be caused by different dynamic ranges of the different assays. Together, these data supported the observations from *in gel* assays indicating that absence of complex I was partially compensated for by upregulation of other mETC complexes.

In an effort to verify the absence of complex I in leaf samples from double mutants, we prepared mitochondria from the limited number of available leaves. These preparations were inevitably contaminated with chloroplast proteins (Fig. 4e). We observed a strong band of the expected size in the complex I activity stain from WT samples, but not from double mutant samples. A very faint activity stain was visible below the size of the expected complex I band (indicated by a closed triangle). We therefore again confirmed the absence of complex I by mass spectrometry as described earlier for material from callus cultures (Fig. S7). We could not detect any complex I subunit in double mutant samples.

We determined the capacity of the complete mETC in intact mitochondria from double mutants and control lines by oxygen consumption measurements (Fig. 5). In the WT, background oxygen consumption in the absence of external ADP was increased by 67% after ADP addition resulting in an ADP-dependent oxygen consumption of *c.* 86 nmol mg^{-1} min^{-1}. This was almost identical for the *ca2* mutant. However, oxygen consumption was significantly increased in the double mutant controls, both before and after ADP addition. ADP-dependent activity was 106 nmol mg^{-1} min^{-1}. This indicated increased activity of the mETC in spite of the absence of complex I.

The *ca1 ca2* double mutants lacked assembled complex I (Fig. 4). We wanted to understand whether structure or enzymatic function of CA proteins was important for complex I assembly. We failed to detect CA activity of recombinant proteins overexpressed in *E. coli* despite significant efforts (data not shown) and therefore created versions of CA2 with mutations that would very probably disrupt the activity of the enzyme (see Introduction and Fig. 6a). In version H130N/H135N, two histidines important for Zn^{2+} ligation (Kisker *et al.*, 1996; Parisi *et al.*, 2004) were replaced by aspartic acid. In version R86A, an asparagine residue was replaced by an alanine. The homologous substitution had been shown to disrupt activity of the γCA from *Methanosarcina thermophila* (Tripp *et al.*, 2002). Constructs encoding the modified CA2 versions were transformed into plants homozygous for the *ca2* mutation and heterozygous for the *ca1* mutation (*CA1/ca1 ca2/ca2*). T$_1$ plants were selected on MS medium containing Glufosinate and selfed. Individual T$_2$
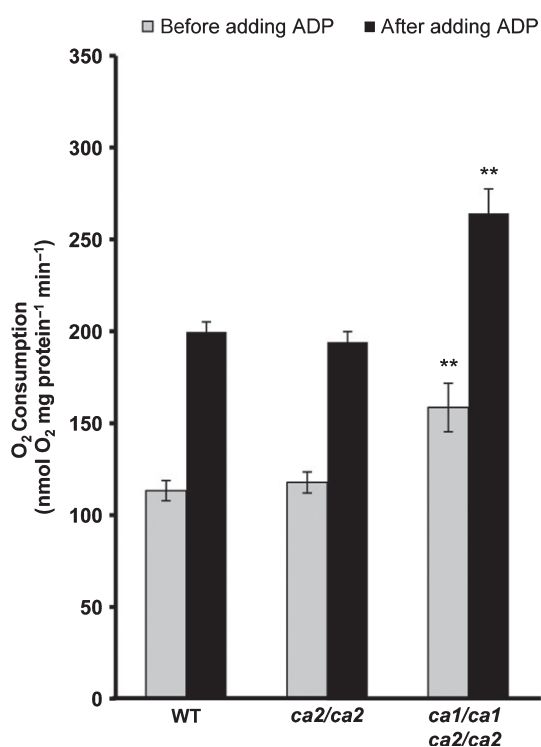
Fig. 5 Oxygen consumption of mitochondria derived from *Arabidopsis thaliana* wild-type (WT), *ca2* mutant and *ca1 ca2* double mutant lines. Oxygen consumption of isolated mitochondria was measured before (grey bars) and after adding ADP (black bars) using a Clark-type oxygen electrode as described in the Materials and Methods section ($n = 5$, mean $\pm$ SE). **, $P \leq 0.01$ according to Student's t-test mutants compared with WT.

segregants were genotyped for T-DNA integrations at the *CA1* and the *CA2*. We expected to detect *ca1 ca2* double mutants in the T_2 only if the modified CA2 versions could complement the severely impaired embryo development of the double mutant. *ca1 ca2* double mutants were detected both among plants transformed with the H130N/H135N (three plants) and R86A (one plant) constructs. T_3 plants that grew on MS supplemented with Glufosinate were again genotyped (Fig. S8). Phenotypically, we could not discriminate between complemented lines from WT plants (Fig. 6b) and seed development was normal in these lines. Moreover, complemented double mutant lines again showed WT-like complex I NADH : NBT oxidoreductase activity on BN-PAGE gels (Fig. 6c). This was comparable to complex I NADH : NBT oxidoreductase activity in plants that were complemented with the nonmutated *CA2* sequence (Fig. S9). To further support this observation, we also transformed the constructs encoding the modified CA2 versions into *ca2* single mutants (*CA1/CA1 ca2/ca2*). As shown earlier (Figs 1, 3), these mutants were not impaired in growth, but had decreased complex I levels. This decrease was confirmed in this experiment, but lines overexpressing the H130N/H135N or R86A constructs showed WT-like levels of complex I (Fig. 6c). Together, these data suggest that γCA enzymatic activity is dispensable for complex I assembly and seed development.

We additionally tested a possible function of γCA enzymatic activity in CO_2 transfer from mitochondria to chloroplasts (see

Introduction). Our hypothesis was that CO_2 transfer would reduce oxygenation of RuBP by Rubisco and – by this – photorespiration. Inactive γCA versions could not support CO_2 transfer and this would result in higher rates of photorespiration. We used glycine : serine (gly : ser) ratios as an estimate for photorespiratory flux (Novitskaya *et al.*, 2002) and determined this parameter at normal (400 ppm) and enhanced (100 ppm) photorespiratory conditions (Fig. 6d). As expected, gly : ser ratios increased at 100 ppm compared with 400 ppm for all genotypes. When comparing the different genotypes, both complemented lines with inactive γCA versions showed slightly lower gly : ser ratios than WT plants, indicating similar or lower rates of photorespiration. These data do not support a role for γCA enzymatic activity in CO_2 transfer.

Discussion

Whereas mutation of the *CA1* or *CA2* genes, respectively, had little influence on the plant phenotype (Fig. 1), *ca1 ca2* double mutants were characterized by delayed embryo development and an inability to form viable seeds under normal growth conditions (Table 3; Fig. S3). Moreover, rescued seedlings showed strong defects in vegetative growth (Fig. 3). These observations could be either assigned to the function of carbonic anhydrase (CA) proteins as essential subunits for the assembly of plant complex I (Meyer *et al.*, 2011; Li *et al.*, 2013) or to the enzymatic activity of these proteins (Parisi *et al.*, 2004; Martin *et al.*, 2009). We were now able to discriminate between these two possibilities by complementation analyses with inactive versions of the plant γCA2. Admittedly, we and others were unable to determine the activity of the overexpressed protein, but – given that the protein would possess CA activity – the introduced mutations would very probably eliminate this activity. Still, these inactive versions fully complemented the growth phenotype and this was associated with reconstitution of a wild-type (WT)-like amounts of assembled complex I (Fig. 6). Furthermore, rates of photorespiration as estimated by gly/ser ratios did not support a role in CO_2 transfer. Thus, function as a complex I assembly factor is probably more important for plant viability than the predicted enzymatic function. Our data do not exclude a function in the equilibration of subcellular CO_2 concentrations in the leaf (Braun & Zabaleta, 2007; Zabaleta *et al.*, 2012; Soto *et al.*, 2015) under specific growth conditions that we did not test.

Beside functions in primary metabolism, complex I has also been associated with ascorbate biosynthesis. This was based on the physical interaction of complex I and L-galactono-1,4-lactone dehydrogenase (GLDH) (Heazlewood *et al.*, 2003), the last enzyme of the ascorbate biosynthetic pathway in plants (Wheeler *et al.*, 1998). Thus, the growth phenotype of *ca1 ca2* double mutants might be caused by a disruption of ascorbate biosynthesis. This is consistent with higher superoxide levels in the mutants (Fig. 3). However, GLDH is only transiently associated with complex I assembly intermediates and absent from mature complex I (Schimmeyer *et al.*, 2015). Most GLDH in mitochondria is actually not complexed, but exists as a free monomer according to Gelmap (Klodmann *et al.*, 2011). Leaves of the tobacco

Fig. 6 Complementation of *Arabidopsis thaliana ca1 ca2* double mutants with inactive versions of CA2. (a) In the CA2 protein sequence, the amino acid arginine 86 (R86) was replaced by alanine and histidine 130 and histidine 135 (H130 H135) were replaced by asparagine. (b) Phenotype of 9-wk-old azygous plants, *ca1 ca2* double mutants and complemented plants (8 h : 16 h, light : dark). Bar, 2 cm. Image sections are assembled from different parts of a gel photo. (c) Reconstitution of complex I in complementation lines. Protein complexes of protein extracts were separated in a BN-PAGE and used for in gel complex I activity staining (I, complex I). Image sections are assembled from different parts of a gel that have been reorganized. Relative density was estimated with IMAGEJ. (d) Ratio of glycine and serine contents in complemented lines at 400 ppm and 100 ppm CO_2 ($n = 4$, mean ± SE). *, $P \leq 0.05$ according to Student's *t*-test mutants compared with azygous plants.

CMSII mutant that lacked complex I contained normal ascorbate concentrations (Dutilleul *et al.*, 2003). Moreover, growth of *ca1 ca2* double mutants in heterotrophic cell cultures was only slightly slower compared with WT (Fig. S6) even though the growth medium did not contain ascorbate. We conclude that ascorbate deficiency is probably not the reason for the severe growth phenotype of *ca1 ca2* double mutants.

Our results indicate that presence of either CA1 or CA2 is an absolute requirement for complex I assembly (Fig. 4). CA2 is the dominant isoform in WT leaves. As complex I amounts clearly decreased in *ca2* single mutants (Perales *et al.*, 2005; Meyer *et al.*, 2011; this study), but only slightly affected in *ca1* mutants (Fig. S1), CA2 is seemingly more important for complex I assembly than CA1. The remaining CA3 protein obviously cannot compensate for the absence of the other two γCAs. This is consistent with the observation that *ca1 ca3* double mutants showed a WT-like phenotype (Wang *et al.*, 2012). In addition, CA3 was

the only γCA that was not detected in the extra CA domain of complex I but, rather, was associated with the core membrane arm of the complex I (Klodmann *et al.*, 2010), and the amounts of *CA3* transcripts in developing seeds are low compared with *CA1* and *CA2* transcripts (Fig. S10). Thus, the currently available data do not provide evidence for a function of *CA3* in complex I assembly. Beside CA proteins, CAL proteins are seemingly also important for seed development and plant growth because *cal1 cal2* double mutants were characterized by an embryo-lethal phenotype (Wang *et al.*, 2012; Fromm *et al.*, 2016). One CAL protein was sufficient for normal growth. In addition, combinations of *ca* mutants and *cal* mutants were investigated (Soto *et al.*, 2015). Both *ca2 cal1* and *ca2 cal2* double mutants were slightly retarded in growth, but plants did not show stress symptoms and were capable of completing their life cycle. We conclude that at least one CA isoform and one CAL isoform are required for complex I assembly and reproductive development.

Homozygous *ca1 ca2* double mutant seeds were strongly affected in development (Table 3; Fig. 2) and the few rescued double mutant plants did not produce any viable seeds (Fig. S3). This is consistent with the phenotype of other Arabidopsis complex I mutants such as *otp43* (de Longevialle *et al.*, 2007), *ndufv1* (Kühn *et al.*, 2015) and *indh* (Wydro *et al.*, 2013): whereas *otp43* plants do not properly splice a mitochondrial pre-mRNA encoding a complex I subunit, the *ndufv1* mutant lacks the catalytic subunit of complex I, and the *indh* mutant an iron-sulfur protein required for complex I assembly. None of the mutants presented detectable amounts of complex I and were also characterized by retarded growth and low viability of seeds. However, other mutants with decreased, but not completely abolished complex I levels, mostly showed normal reproductive development (Gutierres *et al.*, 1999; Perales *et al.*, 2005; Meyer *et al.*, 2009, 2011; Kühn *et al.*, 2015). Thus, only low amounts of complex I are required for embryo and seed development. There is conflicting information about the importance of mitochondrial respiration during embryo and seed development. On the one hand, based on flux labeling of metabolites, it has been suggested that developing seeds of *Brassica napus* lack a complete TCA cycle and probably mainly use the light reactions of photosynthesis and the plastidal oxidative pentose phosphate pathway for NADPH and ATP production (Schwender *et al.*, 2006; Baud *et al.*, 2008). On the other, efficient oxygen supply (as terminal electron acceptor of mitochondrial respiration) is important for seed development (Borisjuk *et al.*, 2003; Geigenberger, 2003; Rolletschek *et al.*, 2003) and mutants deficient in complex IV (Dahan *et al.*, 2014) or the biosynthesis of ubiquinone (Okada *et al.*, 2004), both components of mitochondrial respiration, were arrested very early in embryo development. We also observed delayed embryo development from early stages in embryo maturation for the *ca1 ca2* double mutant (heart stage; Table 3). We therefore suggest that complex I activity and, thus, efficient ATP synthesis by the mitochondrial electron transport chain (Wikstrom, 1984; Heazlewood *et al.*, 2003; Galkin *et al.*, 2006) is of special importance during early embryo development where embryo photosynthesis cannot provide sufficient energy equivalents to sustain cellular metabolism. Other observations such as absence of embryo greening or shrinking of seeds might be secondary effects that are common to many mutants in embryo development (e.g. Eastmond *et al.*, 2002; van Dijken *et al.*, 2004; Gómez *et al.*, 2006; Hsu *et al.*, 2014) and that might be due to active maternal abortion of the development of unhealthy seeds in order to save sugars and other nutrients (Sun *et al.*, 2004).

Even when seeds of *ca1 ca2* double mutants were rescued on high sugar media, the resulting plants showed strongly retarded growth and stress symptoms such as anthocyanin and reactive oxygen species (ROS) accumulation (Fig. 3). This is reminiscent of plants with an imbalance in redox homeostasis (Winkel-Shirley, 2002; Juszczuk *et al.*, 2012; Baxter *et al.*, 2014). Heterotrophic callus cultures of *ca1 ca2* mutants also grew slower than wt cultures, but these effects were less pronounced than for plants (Fig. S6). At the molecular level, we observed increases in complex II and particularly complex IV activity that were associated with higher oxygen consumption in respiration (Fig. 5).

This argues for an upregulation of electron transport through the mitochondrial electron transport chain (mETC) in order to compensate for the decreased proton translocation caused by the absence of complex I. Electron transfer into the mETC could be catalyzed by alternative NADH dehydrogenases, but also multiple organic acid dehydrogenases in the mitochondrial matrix (Schertl & Braun, 2014), and additional electron donors could be provided by an upregulation of glycolysis or the tricarboxylic acid (TCA) cycle. This kind of compensatory upregulation of upstream processes has recently been determined for the *ndufv1* mutant (Kühn *et al.*, 2015). Interestingly, *ndufv1* mutants also showed increased respiratory oxygen consumption, but this was mainly assigned to higher activities of alternative oxidases (AOX) and not to increases in complex IV activity as for *ca1 ca2* double mutants. However, we also observed higher ADP-independent respiration in our mutants (Fig. 5). This might indicate higher AOX activity, because AOX do not contribute to formation of the proton gradient and are therefore not linked to ATP synthesis (Rogov & Zvyagilskaya, 2015). A direct comparison of both mutants under identical growth conditions is probably required to resolve these differences at the molecular level. However, both datasets indicate that a complete loss of complex I results in compensatory adaptations that might cause an imbalance between NADH production and consumption in leaves.

In conclusion, simultaneous deletion of *ca1* and *ca2* caused strong growth defects most probably because of the absence of detectable amounts of complex I in these plants. We observed a drastic rearrangement of the mETC in response to this deficiency. This also provides additional evidence about an important function of the enigmatic γCA domain in complex I assembly.

Acknowledgements

Author contributions

S.F. performed all experiments and analyzed the data. H-P.B. and C.P. jointly designed and supervised the work. The manuscript was written jointly by all authors.

References

Baradaran R, Berrisford JM, Minhas GS, Sazanov LA. 2013. Crystal structure of the entire respiratory complex I. *Nature* **494**: 443–448.
Baud S, Dubreucq B, Miquel M, Rochat C, Lepiniec L. 2008. Storage reserve accumulation in Arabidopsis: metabolic and developmental control of seed filling. *The Arabidopsis book/American Society of Plant Biologists* **6**: e0113.
Baxter A, Mittler R, Suzuki N. 2014. ROS as key players in plant stress signalling. *Journal of Experimental Botany* **65**: 1229–1240.
Birch-Machin MA, Briggs HL, Saborido AA, Bindoff LA, Turnbull DM. 1994. An evaluation of the measurement of the activities of complexes I–IV in the

respiratory chain of human skeletal muscle mitochondria. *Biochemical Medicine and Metabolic Biology* **51**: 35–42.

Boerjan ML, Baarends WM, Ruven HJ. 1991. A cytochemical staining procedure for succinate dehydrogenase activity in pre-ovulatory mouse oocytes embedded in low gelling temperature agarose. *The Journal of Histochemistry and Cytochemistry* **39**: 135–138.

Borisjuk L, Rolletschek H, Walenta S, Panitz R, Wobus U, Weber H. 2003. Energy status and its control on embryogenesis of legumes: ATP distribution within *Vicia faba* embryos is developmentally regulated and correlated with photosynthetic capacity. *The Plant Journal* **36**: 318–329.

Brandt U. 2013. Inside view of a giant proton pump. *Angewandte Chemie International Edition* **52**: 7358–7360.

Braun HP, Binder S, Brennicke A, Eubel H, Fernie AR, Finkemeier I, Klodmann J, König AC, Kühn K, Meyer E *et al.* 2014. The life of plant mitochondrial complex I. *Mitochondrion* **19**: 295–313.

Braun HP, Zabaleta E. 2007. Carbonic anhydrase subunits of the mitochondrial NADH dehydrogenase complex (complex I) in plants. *Physiologia Plantarum* **129**: 114–122.

Chomczynski P. 1993. A reagent for the single-step simultaneous isolation of RNA, DNA and proteins from cell and tissue samples. *BioTechniques* **15**: 536–537.

Clough SJ, Bent AF. 1998. Floral dip: a simplified method for *Agrobacterium*-mediated transformation of *Arabidopsis thaliana*. *The Plant Journal* **16**: 735–743.

Cox GB, Downie JA, Fayle DR, Gibson F, Radik J. 1978. Inhibition, by a protease inhibitor, of the solubilization of the F_1-portion of the Mg^{2+}-stimulated adenosine triphosphatase of *Escherichia coli*. *Journal of Bacteriology* **133**: 287–292.

Dahal K, Martyn GD, Vanlerberghe GC. 2015. Improved photosynthetic performance during severe drought in *Nicotiana tabacum* overexpressing a nonenergy conserving respiratory electron sink. *New Phytologist* **208**: 382–395.

Dahan J, Tcherkez G, Macherel D, Benamar A, Belcram K, Quadrado M, Arnal N, Mireau H. 2014. Disruption of the *CYTOCHROME C OXIDASE DEFICIENT1* gene leads to cytochrome c oxidase depletion and reorchestrated respiratory metabolism in Arabidopsis. *Plant Physiology* **166**: 1788–1802.

van Dijken AJ, Schluepmann H, Smeekens SC. 2004. Arabidopsis trehalose-6-phosphate synthase 1 is essential for normal vegetative growth and transition to flowering. *Plant Physiology* **135**: 969–977.

Dudkina NV, Eubel H, Keegstra W, Boekema EJ, Braun HP. 2005. Structure of a mitochondrial supercomplex formed by respiratory-chain complexes I and III. *Proceedings of the National Academy of Sciences, USA* **102**: 3225–3229.

Dutilleul C, Garmier M, Noctor G, Mathieu C, Chetrit P, Foyer CH, de Paepe R. 2003. Leaf mitochondria modulate whole cell redox homeostasis, set antioxidant capacity, and determine stress resistance through altered signaling and diurnal regulation. *The Plant Cell* **15**: 1212–1226.

Earley KW, Haag JR, Pontes O, Opper K, Juehne T, Song K, Pikaard CS. 2006. Gateway-compatible vectors for plant functional genomics and proteomics. *The Plant Journal* **45**: 616–629.

Eastmond PJ, van Dijken AJ, Spielman M, Kerr A, Tissier AF, Dickinson HG, Jones JD, Smeekens SC, Graham IA. 2002. Trehalose-6-phosphate synthase 1, which catalyses the first step in trehalose synthesis, is essential for Arabidopsis embryo maturation. *The Plant Journal* **29**: 225–235.

Eubel H, Jänsch L, Braun HP. 2003. New insights into the respiratory chain of plant mitochondria. Supercomplexes and a unique composition of complex II. *Plant Physiology* **133**: 274–286.

Fassone E, Rahman S. 2012. Complex I deficiency: clinical features, biochemistry and molecular genetics. *Journal of Medical Genetics* **49**: 578–590.

Fromm S, Göing J, Lorenz C, Peterhänsel C, Braun HP. 2016. Depletion of the "gamma-type carbonic anhydrase-like" subunits of complex I affects central mitochondrial metabolism in *Arabidopsis thaliana*. *Biochimica et Biophysica Acta* **1857**: 60–71.

Galkin A, Dröse S, Brandt U. 2006. The proton pumping stoichiometry of purified mitochondrial complex I reconstituted into proteoliposomes. *Biochimica et Biophysica Acta* **1757**: 1575–1581.

Gawryluk RMR, Gray MW. 2010. Evidence for an early evolutionary emergence of gamma-type carbonic anhydrases as components of mitochondrial respiratory complex I. *BMC Evolutionary Biology* **10**: 176.

Geigenberger P. 2003. Response of plant metabolism to too little oxygen. *Current Opinion in Plant Biology* **6**: 247–256.

Giraud E, Ho LH, Clifton R, Carroll A, Estavillo G, Tan Y, Howell KA, Ivanova A, Pogson BJ, Millar AH *et al.* 2008. The Absence of ALTERNATIVE OXIDASE1a in Arabidopsis results in acute sensitivity to combined light and drought stress. *Plant Physiology* **147**: 595–610.

Gómez LD, Baud S, Gilday A, Li Y, Graham IA. 2006. Delayed embryo development in the *ARABIDOPSIS TREHALOSE-6-PHOSPHATE SYNTHASE 1* mutant is associated with altered cell wall structure, decreased cell division and starch accumulation. *The Plant Journal* **46**: 69–84.

Gutierres S, Combettes B, de Paepe R, Mirande M, Lelandais C, Vedel F, Chétrit P. 1999. In the *Nicotiana sylvestris* CMSII mutant, a recombination-mediated change 5′ to the first exon of the mitochondrial nad1 gene is associated with lack of the NADH:ubiquinone oxidoreductase (complex I) NAD1 subunit. *European Journal of Biochemistry* **261**: 361–370.

Heazlewood JL, Howell KA, Millar AH. 2003. Mitochondrial complex I from Arabidopsis and rice: orthologs of mammalian and fungal components coupled with plant-specific subunits. *Biochimica et Biophysica Acta* **1604**: 159–169.

Hirst J. 2013. Mitochondrial complex I. *Annual Review of Biochemistry* **82**: 551–575.

Hsu YW, Wang HJ, Hsieh MH, Hsieh HL, Jauh GY. 2014. Arabidopsis mTERF15 is required for mitochondrial nad2 intron 3 splicing and functional complex I activity. *PLoS ONE* **9**: e112360.

Hunte C, Zickermann V, Brandt U. 2010. Functional modules and structural basis of conformational coupling in mitochondrial complex I. *Science* **329**: 448–451.

Jung C, Higgins CM, Xu Z. 2000. Measuring the quantity and activity of mitochondrial electron transport chain complexes in tissues of central nervous system using blue native polyacrylamide gel electrophoresis. *Analytical Biochemistry* **286**: 214–223.

Juszczuk IM, Szal B, Rychter AM. 2012. Oxidation-reduction and reactive oxygen species homeostasis in mutant plants with respiratory chain complex I dysfunction. *Plant, Cell & Environment* **35**: 296–307.

Karpova OV, Kuzmin EV, Elthon TE, Newton KJ. 2002. Differential expression of alternative oxidase genes in maize mitochondrial mutants. *The Plant Cell* **14**: 3271–3284.

Kisker C, Schindelin H, Alber BE, Ferry JG, Rees DC. 1996. A left-hand beta-helix revealed by the crystal structure of a carbonic anhydrase from the archaeon *Methanosarcina thermophila*. *The EMBO Journal* **15**: 2323–2330.

Klodmann J, Senkler M, Rode C, Braun HP. 2011. Defining the protein complex proteome of plant mitochondria. *Plant Physiology* **157**: 587–598.

Klodmann J, Sunderhaus S, Nimtz M, Jänsch L, Braun HP. 2010. Internal architecture of mitochondrial complex I from *Arabidopsis thaliana*. *The Plant Cell* **22**: 797–810.

Kühn K, Obata T, Feher K, Bock R, Fernie AR, Meyer EH. 2015. Complete mitochondrial complex I deficiency induces an upregulation of respiratory fluxes that is abolished by traces of functional complex I. *Plant Physiology* **168**: 1537–1549.

Letts JA, Sazanov LA. 2015. Gaining mass: the structure of respiratory complex I-from bacterial towards mitochondrial versions. *Current Opinion in Structural Biology* **33**: 135–145.

Li L, Nelson CJ, Carrie C, Gawryluk RM, Solheim C, Gray MW, Whelan J, Millar AH. 2013. Subcomplexes of ancestral respiratory complex I subunits rapidly turn over *in vivo* as productive assembly intermediates in Arabidopsis. *Journal of Biological Chemistry* **288**: 5707–5717.

de Longevialle AF, Meyer EH, Andrés C, Taylor NL, Lurin C, Millar AH, Small ID. 2007. The pentatricopeptide repeat gene OTP43 is required for trans-splicing of the mitochondrial nad1 Intron 1 in *Arabidopsis thaliana*. *The Plant Cell* **19**: 3256–3265.

Martin V, Villarreal F, Miras I, Navaza A, Haouz A, Gonzalez-Lebrero RM, Kaufman SB, Zabaleta E. 2009. Recombinant plant gamma carbonic anhydrase homotrimers bind inorganic carbon. *FEBS Letters* **583**: 3425–3430.

Meyer EH, Solheim C, Tanz SK, Bonnard G, Millar AH. 2011. Insights into the composition and assembly of the membrane arm of plant complex I through analysis of subcomplexes in Arabidopsis mutant lines. *Journal of Biological Chemistry* **286**: 26 081–26 092.

Meyer EH, Tomaz T, Carroll AJ, Estavillo G, Delannoy E, Tanz SK, Small ID, Pogson BJ, Millar AH. 2009. Remodeled respiration in ndufs4 with low phosphorylation efficiency suppresses Arabidopsis germination and growth and alters control of metabolism at night. *Plant Physiology* 151: 603–619.

Millar AH, Whelan J, Soole KL, Day DA. 2011. Organization and regulation of mitochondrial respiration in plants. *Annual Review of Plant Biology* 62: 79–104.

Moore AL, Shiba T, Young L, Harada S, Kita K, Ito K. 2013. Unraveling the heater: new insights into the structure of the alternative oxidase. *Annual Review of Plant Biology* 64: 637–663.

Neuhoff V, Stamm R, Eibl H. 1985. Clear background and highly sensitive protein staining with coomassie blue dyes in polyacrylamide gels: a systematic analysis. *Electrophoresis* 6: 427–448.

Neuhoff V, Stamm R, Pardowitz I, Arold N, Ehrhardt W, Taube D. 1990. Essential problems in quantification of proteins following colloidal staining with coomassie brilliant blue dyes in polyacrylamide gels, and their solution. *Electrophoresis* 11: 101–117.

Novitskaya L, Trevanion SJ, Driscoll S, Foyer CH, Noctor G. 2002. How does photorespiration modulate leaf amino acid contents? A dual approach through modelling and metabolite analysis. *Plant, Cell & Environment* 25: 821–835.

Okada K, Ohara K, Yazaki K, Nozaki K, Uchida N, Kawamukai M, Nojiri H, Yamane H. 2004. The AtPPT1 gene encoding 4-hydroxybenzoate polyprenyl diphosphate transferase in ubiquinone biosynthesis is required for embryo development in *Arabidopsis thaliana*. *Plant Molecular Biology* 55: 567–577.

Parisi G, Perales M, Fornasari MS, Colaneri A, González-Schain N, Gómez-Casati D, Zimmermann S, Brennicke A, Araya A, Ferry JG *et al.* 2004. Gamma carbonic anhydrases in plant mitochondria. *Plant Molecular Biology* 55: 193–207.

Perales M, Eubel H, Heinemeyer J, Colaneri A, Zabaleta E, Braun HP. 2005. Disruption of a nuclear gene encoding a mitochondrial gamma carbonic anhydrase reduces complex I and supercomplex I+III2 levels and alters mitochondrial physiology in Arabidopsis. *Journal of Molecular Biology* 350: 263–277.

Perales M, Parisi G, Fornasari MS, Colaneri A, Villarreal F, González-Schain N, Echave J, Gómez-Casati D, Braun HP, Araya A *et al.* 2004. Gamma carbonic anhydrase like complex interact with plant mitochondrial complex I. *Plant Molecular Biology* 56: 947–957.

Peters K, Belt K, Braun HP. 2013. 3D gel map of Arabidopsis complex I. *Frontiers in Plant Science* 4: 153.

Rasmusson AG, Geisler DA, Møller IM. 2008. The multiplicity of dehydrogenases in the electron transport chain of plant mitochondria. *Mitochondrion* 8: 47–60.

Rasmusson AG, Soole KL, Elthon TE. 2004. Alternative NAD(P)H dehydrogenases of plant mitochondria. *Annual Review of Plant Biology* 55: 23–39.

Rogov AG, Zvyagilskaya RA. 2015. Physiological role of alternative oxidase (from yeasts to plants). *Biochemistry (Moscow)* 80: 400–407.

Rolletschek H, Weber H, Borisjuk L. 2003. Energy status and its control on embryogenesis of legumes. Embryo photosynthesis contributes to oxygen supply and is coupled to biosynthetic fluxes. *Plant Physiology* 132: 1196–1206.

Schägger H. 2001. Blue-native gels to isolate protein complexes from mitochondria. *Methods in Cell Biology* 65: 231–244.

Schertl P, Braun HP. 2014. Respiratory electron transfer pathways in plant mitochondria. *Frontiers in Plant Science* 5: 163.

Schimmeyer J, Bock R, Meyer EH. 2015. L-Galactono-1,4-lactone dehydrogenase is an assembly factor of the membrane arm of mitochondrial complex I in Arabidopsis. *Plant Molecular Biology.* 90: 117–126.

Schwender J, Shachar-Hill Y, Ohlrogge JB. 2006. Mitochondrial metabolism in developing embryos of *Brassica napus*. *The Journal of Biological Chemistry* 281: 34040–34047.

Singer TP. 1974. Determination of the activity of succinate, NADH, choline, and alpha-glycerophosphate dehydrogenases. *Methods of Biochemical Analysis* 22: 123–175.

Soto D, Córdoba JP, Villarreal F, Bartoli C, Schmitz J, Maurino VG, Braun HP, Pagnussat GC, Zabaleta E. 2015. Functional characterization of mutants affected in the carbonic anhydrase domain of the respiratory complex I in *Arabidopsis thaliana*. *The Plant Journal* 85: 831–844.

Sun K, Hunt K, Hauser BA. 2004. Ovule abortion in Arabidopsis triggered by stress. *Plant Physiology* 135: 2358–2367.

Sunderhaus S, Dudkina NV, Jänsch L, Klodmann J, Heinemeyer J, Perales M, Zabaleta E, Boekema EJ, Braun HP. 2006. Carbonic anhydrase subunits form a matrix-exposed domain attached to the membrane arm of mitochondrial complex I in plants. *The Journal of Biological Chemistry* 281: 6482–6488.

Tripp BC, Tu C, Ferry JG. 2002. Role of arginine 59 in the γ-class carbonic anhydrases. *Biochemistry* 41: 669–678.

Vinothkumar KR, Zhu J, Hirst J. 2014. Architecture of mammalian respiratory complex I. *Nature* 515: 80–84.

Wallström SV, Florez-Sarasa I, Araújo WL, Aidemark M, Fernández-Fernández M, Fernie AR, Ribas-Carbó M, Rasmusson AG. 2014. Suppression of the external mitochondrial NADPH dehydrogenase, NDB1, in *Arabidopsis thaliana* affects central metabolism and vegetative growth. *Molecular Plant* 7: 356–368.

Wang Q, Fristedt R, Yu X, Chen Z, Liu H, Lee Y, Guo H, Merchant SS, Lin C. 2012. The gamma-carbonic anhydrase subcomplex of mitochondrial complex I is essential for development and important for photomorphogenesis of Arabidopsis. *Plant Physiology* 160: 1373–1383.

Welchen E, Hildebrandt TM, Lewejohann D, Gonzalez DH, Braun HP. 2012. Lack of cytochrome c in Arabidopsis decreases stability of Complex IV and modifies redox metabolism without affecting Complexes I and III. *Biochimica et Biophysica Acta* 1817: 990–1001.

Werhahn W, Niemeyer A, Jänsch L, Kruft V, Schmitz UK, Braun H. 2001. Purification and characterization of the preprotein translocase of the outer mitochondrial membrane from Arabidopsis. Identification of multiple forms of TOM20. *Plant Physiology* 125: 943–954.

Wheeler GL, Jones MA, Smirnoff N. 1998. The biosynthetic pathway of vitamin C in higher plants. *Nature* 393: 365–369.

Wikstrom M. 1984. Two protons are pumped from the mitochondrial matrix per electron transferred between NADH and ubiquinone. *FEBS Letters* 169: 300–304.

Winkel-Shirley B. 2002. Biosynthesis of flavonoids and effects of stress. *Current Opinion in Plant Biology* 5: 218–223.

Wydro MM, Sharma P, Foster JM, Bych K, Meyer EH, Balk J. 2013. The evolutionarily conserved iron-sulfur protein INDH is required for complex I assembly and mitochondrial translation in Arabidopsis. *The Plant Cell* 25: 4014–4027.

Zabaleta E, Martin MV, Braun HP. 2012. A basal carbon concentrating mechanism in plants? *Plant Science* 187: 97–104.

Zhou G, Jiang W, Zhao Y, Ma G, Xin W, Yin J, Zhao B. 2003. Sodium tanshinone IIA sulfonate mediates electron transfer reaction in rat heart mitochondria. *Biochemical Pharmacology* 65: 51–57.

Zickermann V, Wirth C, Nasiri H, Siegmund K, Schwalbe H, Hunte C, Brandt U. 2015. Structural biology. Mechanistic insight from the crystal structure of mitochondrial complex I. *Science* 347: 44–49.

Supporting Information

Additional supporting information may be found in the online version of this article.

Fig. S1 Complex I activity in Arabidopsis WT and *ca1* and *ca2* single mutants.

Fig. S2 Genotyping of pale developing seeds.

Fig. S3 *ca1 ca2* double mutant seeds were aborted in the silique.

Fig. S4 Analysis of male sterility of azygous, *ca1* and *ca2* single mutants and *ca1 ca2* double mutants.

Fig. S5 Embryo rescue of azygous and *ca1 ca2* lines.

New
Phytologist

Fig. S6 FW increase of Arabidopsis WT, *ca2* and *ca1 ca2* cell cultures.

Fig. S7 Protein subunit identification of protein complexes of WT and *ca1 ca2* double mutant lines.

Fig. S8 Genotyping of complemented *ca1 ca2* lines.

Fig. S9 Reconstitution of complex I in complementation lines.

Fig. S10 Expression of *CA* and *CAL* genes in developing seeds.

Table S1 Reciprocal crossings of plants that were homozygous for the T-DNA integration in one *CA* locus, but hemizygous for

the T-DNA integration in the other *CA* locus (*CA1/ca1 ca2/ca2, ca1/ca1 CA2/ca2, ca2/ca2 CA1/ca1* and *CA2/ca2 ca1/ca1*) with WT plants

Table S2 Embryo development of azygous (az) plants, *ca1* mutants, *ca2* mutants, and descendants derived from selfing of the *CA1/ca1 ca2/ca2, ca1/ca1 CA2/ca2, ca2/ca2 CA1/ca1* and *CA2/ca2 ca1/ca1* genotypes and *ndufs4* mutant plants
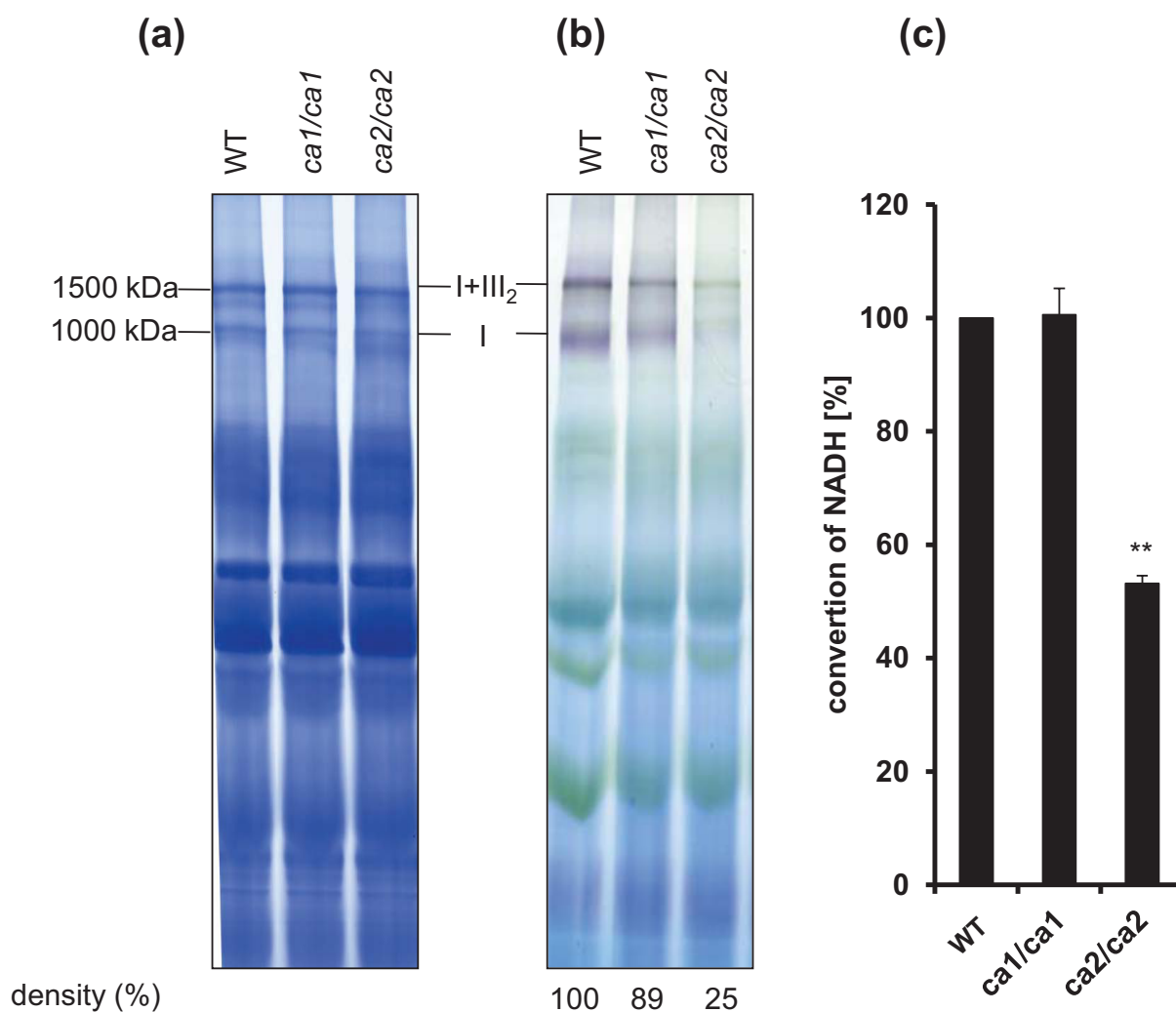
Please note: Wiley Blackwell are not responsible for the content or functionality of any supporting information supplied by the authors. Any queries (other than missing material) should be directed to the *New Phytologist* Central Office.

About *New Phytologist*

- *New Phytologist* is an electronic (online-only) journal owned by the New Phytologist Trust, a **not-for-profit organization** dedicated to the promotion of plant science, facilitating projects from symposia to free access for our Tansley reviews.

- Regular papers, Letters, Research reviews, Rapid reports and both Modelling/Theory and Methods papers are encouraged. We are committed to rapid processing, from online submission through to publication 'as ready' via *Early View* – our average time to decision is <27 days. There are **no page or colour charges** and a PDF version will be provided for each article.

- The journal is available online at Wiley Online Library. Visit **www.newphytologist.com** to search the articles and register for table of contents email alerts.

- If you have any questions, do get in touch with Central Office (np-centraloffice@lancaster.ac.uk) or, if it is more convenient, our USA Office (np-usaoffice@lancaster.ac.uk)

- For submission instructions, subscription and all the latest information visit **www.newphytologist.com**

New Phytologist

***New Phytologist* Supporting Information Figs S1–S10 and Tables S1 & S2**

Article title: Mitochondrial gamma carbonic anhydrases are required for complex I assembly and plant reproductive development

Authors: Steffanie Fromm, Hans-Peter Braun and Christoph Peterhansel

Article acceptance date: 4 January 2016

The following Supporting Information is available for this article:

Fig. S1 Complex I activity in Arabidopsis WT and *ca1* and *ca2* single mutants.

Fig. S2 Genotyping of pale developing seeds.

Fig. S3 *ca1 ca2* double mutant seeds were aborted in the silique.

Fig. S4 Analysis of male sterility of azygous, *ca1* and *ca2* single mutants and *ca1 ca2* double mutants.

Fig. S5 Embryo rescue of azygous and *ca1 ca2* lines.

Fig. S6 FW increase of Arabidopsis WT, *ca*2 and *ca1 ca2* cell cultures.

Fig. S7 Protein subunit identification of protein complexes of WT and *ca1 ca2* double mutant lines.

Fig. S8 Genotyping of complemented *ca1 ca2* lines.

Fig. S9 Reconstitution of complex I in complementation lines.

Fig. S10 Expression of *CA* and *CAL* genes in developing seeds.

Table S1 Reciprocal crossings of plants that were homozygous for the T-DNA integration in one *CA* locus, but hemizygous for the T-DNA integration in the other *CA* locus (*CA1/ca1 ca2/ca2, ca1/ca1 CA2/ca2, ca2/ca2 CA1/ca1* and *CA2/ca2 ca1/ca1*) with WT plants

Table S2 Embryo development of azygous (az) plants, *ca1* mutants, *ca2* mutants, and descendants derived from selfing of the *CA1/ca1 ca2/ca2*, *ca1/ca1 CA2/ca2*, *ca2/ca2 CA1/ca1* and *CA2/ca2 ca1/ca1* genotypes and *ndufs4* mutant plants

(a) **(b)** **(c)**

WT ca1/ca1 ca2/ca2

WT ca1/ca1 ca2/ca2

1500 kDa — — I+III$_2$

1000 kDa — — I

density (%)

100 89 25

Fig. S1 Complex I activity in Arabidopsis WT and *ca1* and *ca2* single mutants. (a) Protein complexes of mitochondria isolated from green tissue were resolved by BN-PAGE. Gels were stained with colloidal Coomassie. (b) Corresponding gels were used for complex I in gel activity assays using NBT as artificial electron acceptor (for details see the Material and Methods section). Molecular masses of the resolved protein complexes are given to the left of the figure (I, complex I; I+III$_2$, supercomplex formed of complex I and dimeric complex III). Identity of selected mitochondrial protein complexes are given in between the gels. (c) Photometric complex I activity assay of mitochondria isolated from cell culture was also carried out (*n* = 5, mean ± SE). **, *P* ≤ 0.01 according to Student's *t*-test mutants compared to WT.
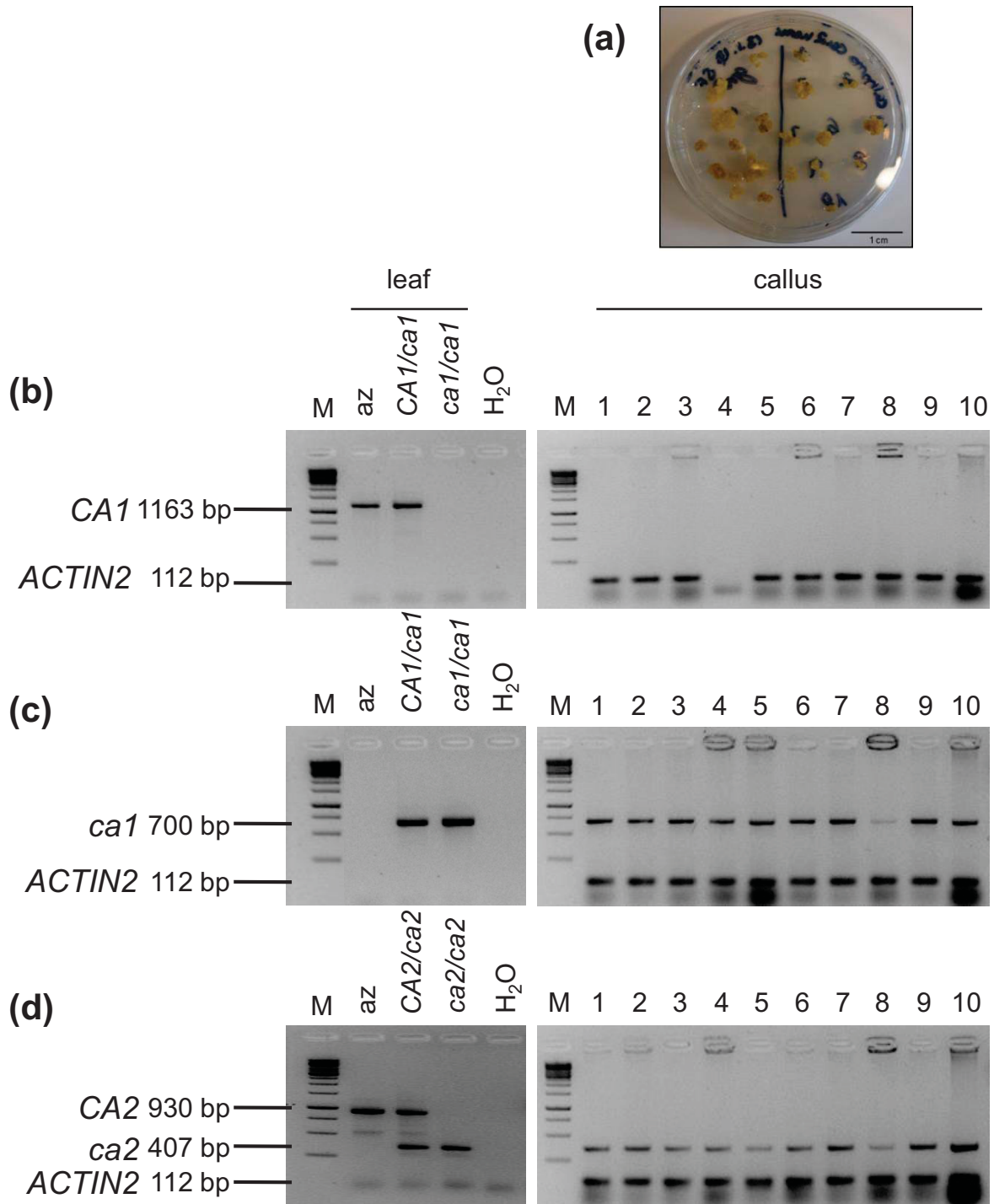
Fig. S2 Genotyping of pale developing seeds. (a) Callus cultures were established from embryos isolated form pale seeds. (b–d) Genotypes were determined by PCR. DNAs from leaves of azygous (az) plants, hemizygous and homozygous mutants were used as controls. A fragment of

New
Phytologist

the *Actin*2 gene (112 bp) was amplified form all callus samples as a control for successful DNA isolation. Specific oligonucleotides for genomic loci and T-DNA integrations are given in Materials and Methods section and sizes of expected amplification products are given in the figure. M = 1 kb GeneRuler (Thermo Scientific, Braunschweig, Germany).

(a)

(b)
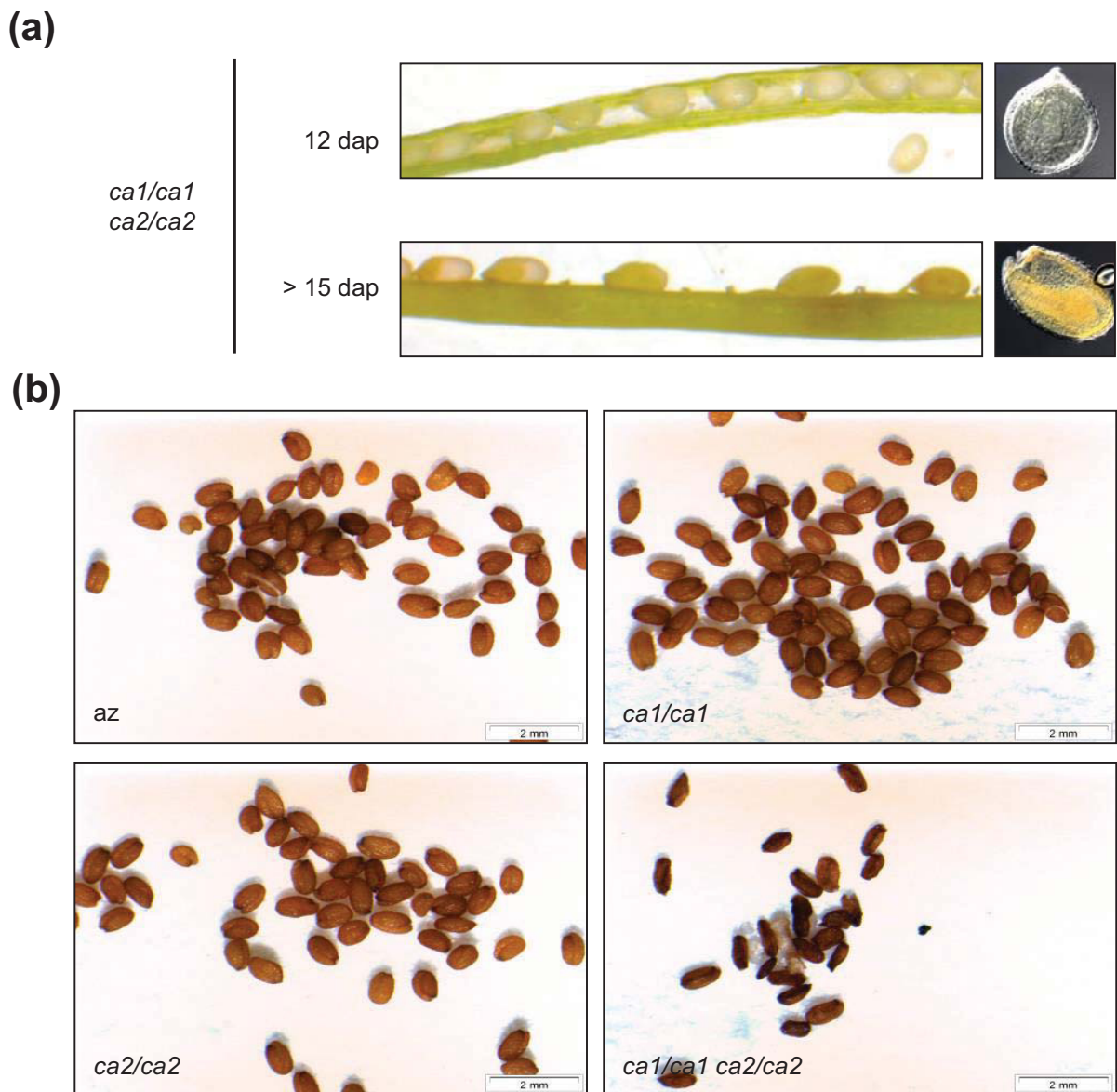
Fig. S3 *ca1 ca2* double mutant seeds were aborted in the silique. (a) Representative pictures of dissected siliques and corresponding embryos in seeds are shown for *ca1 ca2* double mutant at 12 d after pollination (dap) and >15 dap. (b) Mature seeds of azygous (az), *ca1* and *ca2* single mutants and the *ca1 ca2* double mutant are shown.
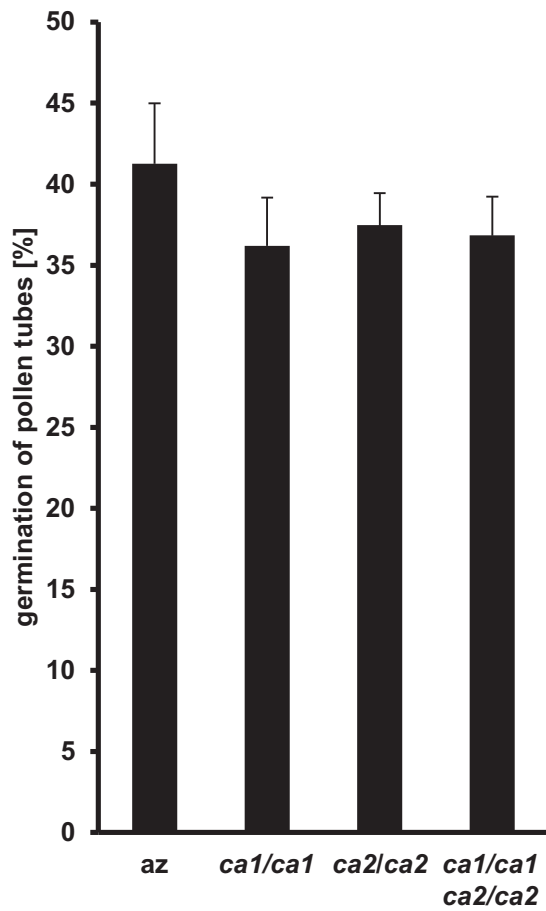
Fig. S4 Analysis of male sterility of azygous (az), *ca1* and *ca2* single mutants and *ca1 ca2* double mutants. *In vitro* pollen tube germination assay (*n* = 6 plants, mean ± SE).

(a)

(b)
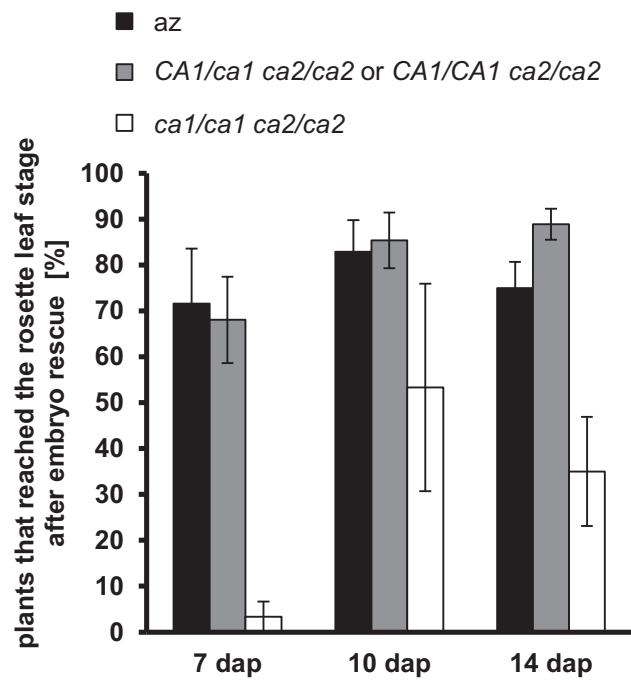
Fig. S5 Embryo rescue of azygous (az) and *ca1 ca2* lines. Seven days after pollination, 10 dap and 14 dap old siliques were dissected and seeds were transferred to 0.5 MS media containing 3% (w/v) sucrose. (a) Rescued azygous and *ca1 ca2* plants 20 d after the transfer. (b) Thirty-four days after the transfer the relative number of rescued plants that were able to form rosette leaves was analyzed (mean ± SE).
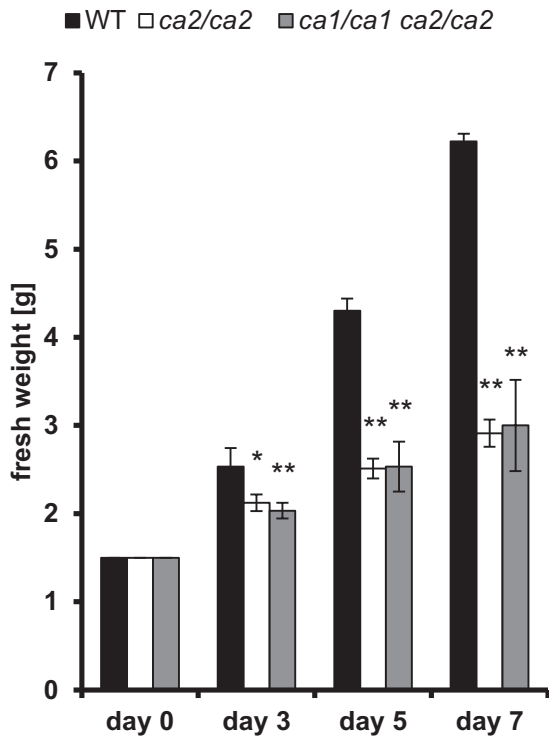
Fig. S6 FW increase of Arabidopsis WT, *ca*2 and *ca1 ca2* cell cultures. Starting material (day 0) for WT (black bars), *ca2* (white bars), and *ca1 ca2* (grey bars) cultures was always 1.5 g. FW (g) was recorded after 3, 5 and 7 d (n = 9, mean ± SE). *, $P \leq 0.05$; **, $P \leq 0.01$ according to Student's *t*-test mutants compared to WT.
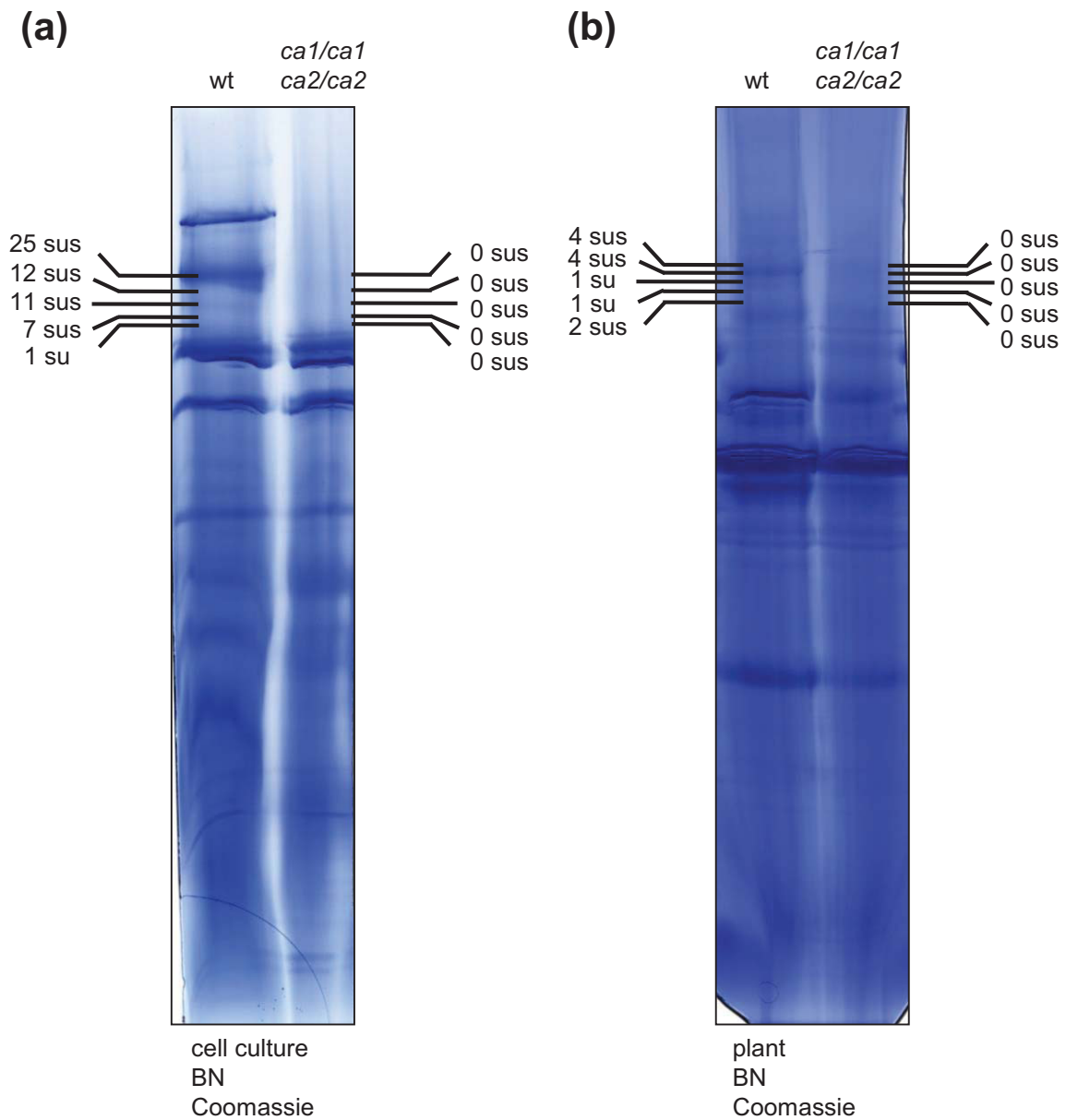
Fig. S7 Protein subunit identification of protein complexes of WT and *ca1 ca2* double mutant lines. (a, b) Protein complexes of isolated mitochondria of WT and *ca1 ca2* of cell culture and green tissue were separated by BN-PAGE and Coomassie stained afterwards. In the surrounding of complex I proteins were analyzed by LC-MS. The number of identified complex I subunits (su/ sus) for WT and *ca1 ca2* mutant is given beside the gels.
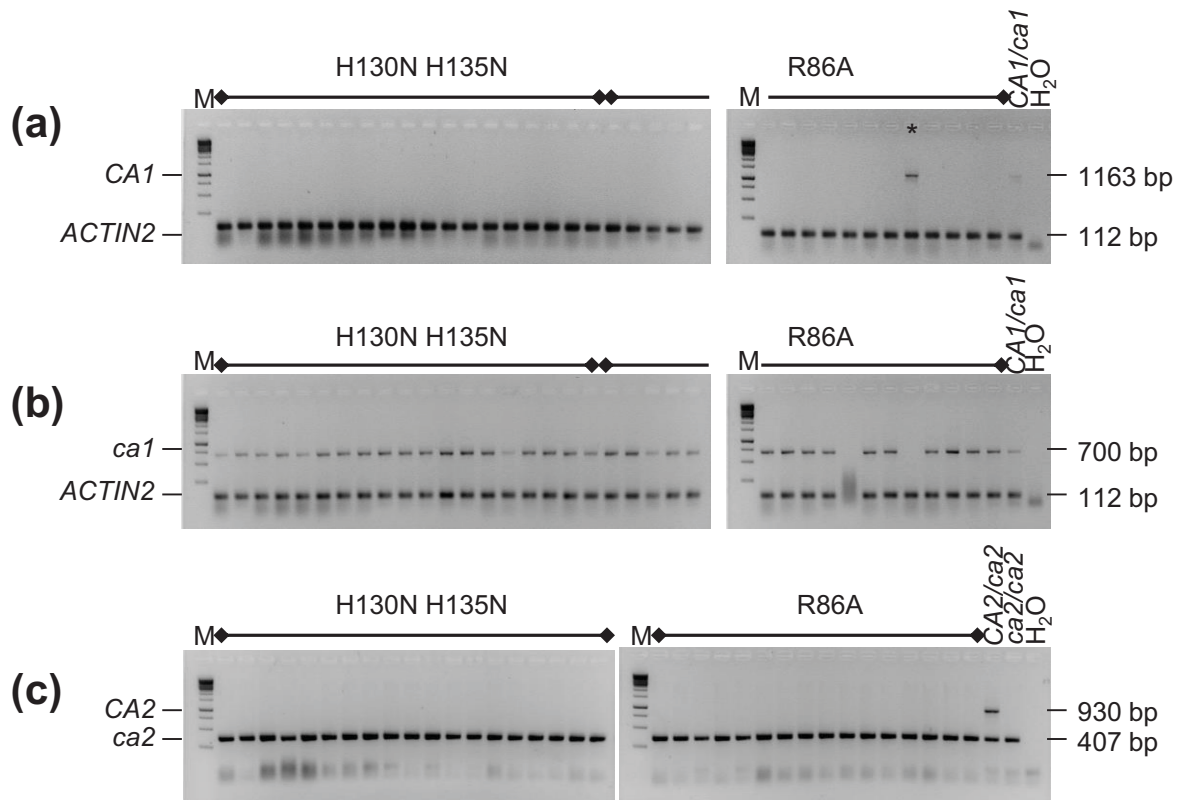
Fig. S8 Genotyping of complemented *ca1 ca2* lines. (a–c) Genotypes were determined by PCR. DNAs from leaves of hemizygous and homozygous mutants were used as controls. A fragment of the *ACTIN2* gene (112 bp) was amplified from all samples in combination with the *CA1* genomic and *ca1* T-DNA oligonucleotides as a control for successful DNA isolation. A multiplex PCR system was used for *CA2* and *ca2*. Specific oligonucleotides for genomic loci and T-DNA integrations are given in Materials and Methods and sizes of expected amplification products are given in the figure. M = 1 kb GeneRuler (Thermo Scientific, Braunschweig, Germany). *Plant was excluded from activity measurements.

Fig. S9 Reconstitution of complex I in complementation lines. Protein complexes of protein extracts from leaves were separated in a BN-PAGE and used for in gel complex I activity staining (I, complex I). Image sections are assembled from different parts of a gel that have been reorganized. az, azygous; CA2-WT, *ca1/ca1 ca2/ca2* mutant complemented with the *CA2* wildtype sequence; R86A, *ca1/ca1 ca2/ca2* mutant complemented with *CA2* R86A; H130N H135N, *ca1/ca1 ca2/ca2* mutant complemented with *CA2* H130N H135N.

Fig. S10 Expression of *CA* and *CAL* genes in developing seeds. Gene expression data were taken from Arabidopis eFP Browser (http://bar.utoronto.ca/~dev/eplant/). Low and high expression levels are indicated in yellow and red, respectively**.**

New
Phytologist

Table S1 Reciprocal crossings of plants that were homozygous for the T-DNA integration in one CA locus, but hemizygous for the T-DNA integration in the other CA locus (CA1/ca1 ca2/ca2, ca1/ca1 CA2/ca2, ca2/ca2 CA1/ca1 and CA2/ca2 ca1/ca1) with WT plants

		Observed/expected					
Mother	Father	*CA1/ca1 CA2/ca2*	*CA1/ca1 CA2/CA2*	*CA1/CA1 CA2/ca2*	Total	Chi²	*P*-value
CA1/ca1 ca2/ca2	WT	59/51	-	43/51	102	2.51	<0.1
WT	*CA1/ca1 ca2/ca2*	60/51	-	42/51	102	3.18	<0.1
ca1/ca1 CA2/ca2	WT	78/73.5	69/73.5	-	147	0.55	<0.5
WT	*ca1/ca1 CA2/ca2*	49/45.5	42/45.5	-	91	0.53	<0.5
ca2/ca2 CA1/ca1	WT	83/75	-	67/75	150	1.71	<0.25
WT	*ca2/ca2 CA1/ca1*	75/67.5	-	60/67.5	135	1.67	<0.25
CA2/ca2 ca1/ca1	WT	27/27	27/27	-	54	0	0.0
WT	*CA2/ca2 ca1/ca1*	65/76.5	88/76.5	-	153	3.45	<0.1

After crossing, the F_1 progeny was analyzed. Observed and expected numbers are given and Chi² test indicates if the observed values fit the expected 1 : 1 segregation (5% significance threshold = 3.81).

New Phytologist

Table S2 Embryo development of azygous (az) plants, ca1 mutants, ca2 mutants, and descendants derived from selfing of the CA1/ca1 ca2/ca2, ca1/ca1 CA2/ca2, ca2/ca2 CA1/ca1 and CA2/ca2 ca1/ca1 genotypes and *ndufs4* mutant plants

Parental genotype	Seed colour	Embryo stage					
		Transition	Heart	Early torpedo	Torpedo	Late torpedo	Mature
az		4.0 ± 0.1	5.4 ± 0.5	6.6 ± 0.3	7.5 ± 0.3	8.0 ± 0.6	11.8 ± 0.4
ca1/ca1		4.3 ± 0.6	6.0 ± 1.2	6.8 ± 0.3	7.5 ± 0.1	8.3 ± 0.1	12.4 ± 0.2
ca2/ca2		4.7 ± 0.2	5.6 ± 0.4	7.2 ± 0.1	7.9 ± 0.3	10.2* ± 0.1	11.9 ± 0.6
ca1/ca1	Green	6.3** ± 0.3	6.3 ± 0.1	7.8* ± 0.1	8.6* ± 0.2	10.0* ± 0.1	13.1 ± 0.3
CA2/ca2	Pale	6.8** ± 0.1	7.1* ± 0.2	9.8** ± 0.3	11.9** ± 0.5	14.2** ± 0.2	-
CA1/ca1	Green	6.4** ± 0.2	7.7 ± 0.8	7.6 ± 0.3	9.0* ± 0.2	10.4* ± 0.3	13.3* ± 0.1
ca2/ca2	Pale	7.2** ± 0.1	7.7** ± 0.2	10.7** ± 0.2	12.5** ± 0.3	13.8** ± 0.1	-
ca2/ca2	Green	6.3** ± 0.1	6.5 ± 0.1	7.8* ± 0.1	9.2** ± 0.1	10.7 ± 0.1	13.2* ± 0.1
CA1/ca1	Pale	7.5** ± 0.1	7.9** ± 0.1	11.1** ± 0.1	13.4** ± 0.2	14.4* ± 0.1	-
CA2/ca2	Green	6.1** ± 0.1	6.4 ± 0.1	7.5 ± 0.3	9.0* ± 0.3	10.7** ± 0.1	13.3* ± 0.1
ca1/ca1	Pale	7.3** ± 0.1	7.6* ± 0.1	10.6** ± 0.1	12.5** ± 0.1	14.4** ± 0.1	-
*ndufs*4		nd	nd	7.1 ± 0.1	8.1 ± 0.1	9.2 ± 0.1	13.0 ± 0.1

Embryo development was analyzed in three biological replicates from 4 dap to 15 dap by DIC microscopy. For segregating lines, green and pale ovules were separately analyzed ($n > 500$ seeds, mean dap ± SE). *, $P ≤ 0.05$; **, $P ≤ 0.01$ according to Student's *t*-test mutants compared with WT.

Publication 3

2.3.   The carbonic anhydrase domain of plant mitochondrial complex I

Steffanie Fromm[1,2], Jennifer Senkler[1], Eduardo Zabaleta[3], Christoph Peterhänsel[2], Hans-Peter Braun[1]

[1] Institut für Pflanzengenetik, Leibniz Universität Hannover, Herrenhäuser Str. 2, 30419 Hannover, Germany
[2] Institut für Botanik, Leibniz Universität Hannover, Herrenhäuser Str. 2, 30419 Hannover, Germany
[3] Instituto de Investigaciones Biológicas IIB-CONICET-National University of Mar del Plata, cc 1245 7600 Mar del Plata, Argentina

Type of authorship:	First author
Type of article:	Review article
Share of the work:	50 %
Contribution to the publication:	prepared some figures and assisted in writing the paper
Journal:	Physiologia Plantarum
5-year impact factor:	3.49
Date of publication:	(in press)
Number of citations (google scholar on May. 24th, 2016):	1
DOI:	10.1111/ppl.12424
PubMed-ID:	26829901

MINIREVIEW

The carbonic anhydrase domain of plant mitochondrial complex I

Steffanie Fromm[a,b], Jennifer Senkler[a], Eduardo Zabaleta[c], Christoph Peterhänsel[b] and Hans-Peter Braun[a,*]

[a]Institut für Pflanzengenetik, Leibniz Universität Hannover Hannover, 30419, Germany
[b]Institut für Botanik, Leibniz Universität Hannover, Hannover 30419, Germany
[c]Instituto de Investigaciones Biológicas IIB, CONICET, National University of Mar del Plata, Mar del Plata 7600, Argentina

Correspondence
*Corresponding author,
e-mail: braun@genetik.uni-hannover.de

The mitochondrial NADH dehydrogenase complex (complex I) consists of several functional domains which independently arose during evolution. In higher plants, it contains an additional domain which includes proteins resembling gamma-type carbonic anhydrases. The *Arabidopsis* genome codes for five complex I-integrated gamma-type carbonic anhydrases (γCA1, γCA2, γCA3, γCAL1, γCAL2), but only three copies of this group of proteins form an individual extra domain. Biochemical analyses revealed that the domain is composed of one copy of either γCAL1 or γCAL2 plus two copies of the γCA1/γCA2 proteins. Thus, the carbonic anhydrase domain can have six distinct subunit configurations. Single and double mutants with respect to the γCA/γCAL proteins were employed to genetically dissect the function of the domain. New insights into complex I biology in plants will be reviewed and discussed.

Introduction

The NADH dehydrogenase complex is the first protein complex of the mitochondrial oxidative phosphorylation (OXPHOS) system and the main site of electron insertion into the respiratory chain (Hirst 2013). It is composed of two large and longish domains called arms: the membrane arm, which mainly is inserted into the inner mitochondrial membrane, and the peripheral arm, which protrudes into the mitochondrial matrix. The domains are put together end-by-end, forming an L-like particle. The structure was first described using electron microscopy (EM) (Hofhaus et al. 1991, Weiss et al. 1991) and later by X-ray crystallography (Hunte et al. 2010, Zickermann et al. 2015). The most detailed structure has been resolved for complex I of the bacterium *Thermus thermophilus*, which is only composed of 16 subunits

(Baradaran et al. 2013). In contrast, mitochondrial complex I is larger and includes more than 40 subunits (Carroll et al. 2006, Balsa et al. 2012). The structure of *Bos taurus* complex I has been recently resolved using cryo-electron microscopy (Vinothkumar et al. 2014).

Over ten years ago the first EM images of complex I from plants were published (Dudkina et al. 2005). It also has an L-like shape but surprisingly turned out to have a second matrix-exposed domain which is attached to the membrane arm at a central position (Fig. 1). Besides complex I from the model plant *Arabidopsis thaliana*, this extra domain meanwhile also has been described for potato, maize and the alga *Polytomella* (Sunderhaus et al. 2006, Peters et al. 2008, Bultema et al. 2009) and is considered to represent a general feature of plant complex I (Braun et al. 2014). Since its discovery it was speculated that this extra domain is

---

Abbreviations – γCA, gamma-type carbonic anhydrase; γCAL, gamma-type carbonic anhydrase like; CCM, CO_2 concentrating mechanism; EM, electron microscopy; complex I, NADH dehydrogenase complex; NADH, nicotinamide adenine dinucleotide; OXPHOS, oxidative phosphorylation.
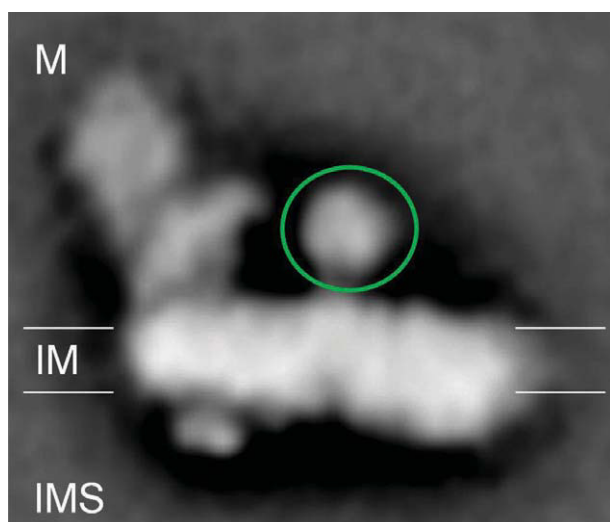
Fig. 1. Structure of mitochondrial complex I from *Arabidopsis thaliana* as revealed by single particle electron microscopy. The extra domain, which is absent in complex I from animals and fungi, is indicated by a green circle. From: Sunderhaus et al. 2006, modified.

composed of additional subunits which do not form part of complex I in animals and fungi. Indeed, proteomic analyses of complex I subunits of plants have revealed a number of plant-specific subunits (Heazlewood et al. 2003, Cardol et al. 2004, Sunderhaus et al. 2006). A total of 49 different types of subunits have meanwhile been described for *A. thaliana*, some of which occur in different isoforms (Peters et al. 2013, Braun et al. 2014). Of the extra-subunits in plants, most remarkable is a group of five structurally related proteins which resemble γ-type carbonic anhydrases (Parisi et al. 2004, Perales et al. 2004).

The carbonic anhydrase subunits of complex I in plants

Three of the five gamma-type carbonic anhydrase subunits of *A. thaliana* have a largely conserved active site with respect to the archaebacterial gamma-type carbonic anhydrases of *Methanosarcina thermophila* (Parisi et al. 2004, Ferry 2010) and are named γCA1 (AGI code: At1g19580), γCA2 (At1g47260) and γCA3 (At5g66510). The two remaining proteins lack two of the histidines essential for zinc binding and therefore are called γ-carbonic anhydrase-like proteins, γCAL1 (At5g63510) and γCAL2 (At3g48680). Amino acid sequence conservation is in the range of 70–75% for the γCAs and even 91% for the two γCALs (Wang et al. 2012). The latter proteins therefore most probably represent isoforms. All five proteins are nuclear encoded and post-translationally transported into mitochondria. The

γCA1/γCA2/γCA3 proteins lack cleavable mitochondrial presequences, whereas the γCAL1/γCAL2 proteins have short presequences of 12 (γCAL1) and 15 (γCAL2) amino acids (Braun et al. 2014). The mature γCA1 and γCA2 proteins have masses of 30 kDa, γCA3 has a mass of 28 kDa and the two γCAL proteins of 25 kDa, respectively. Despite extensive attempts, carbonic anhydrase activity to this day has not been proven for any of the γCA subunits of plant complex I. It has been speculated that carbonic anhydrase activity of the γCA proteins might depend on attachment to native complex I (Braun and Zabaleta 2007, Zabaleta et al. 2012). However, γCA2 overexpressed in *Escherichia coli* has been proven to bind CO_2/bicarbonate (Martin et al. 2009).

All genomes of higher plants code for complex I-integrated carbonic anhydrases. However, genomes of several plants such as rice, maize and poplar only comprise one gene encoding γCAL (Meyer 2012), further supporting that the *Arabidopsis* γCAL1 and γCAL2 proteins represent isoforms. Moreover, some plant genomes only code for two γCA subunits (maize, sorghum), while other code for three (*Arabidopsis*, rice, poplar) (Meyer 2012). As a consequence, a minimal set of complex I integrated γ-carbonic anhydrase subunits might consist of one γCAL and two γCA proteins.

The carbonic anhydrase domain of plant complex I

Extensive evidence has been presented that the extra matrix-exposed domain of plant complex I indeed is composed of the γCA/γCAL proteins. Looking at EM images of plant complex I, the extra domain has a spherical shape and a diameter of about 60 Å (Dudkina et al. 2005, Peters et al. 2008). This allows estimating a molecular mass of 75 kDa, plus some mass for anchoring the domain within the membrane arm of complex I. The prototype γ-carbonic anhydrase of *Methanosarcina thermophila*, which has been characterized by X-ray crystallography (Iverson et al. 2000), is a spherical homotrimer of very similar dimensions and shape (Peters et al. 2008). Localization of the γCA/γCAL subunits at the matrix-exposed side of the membrane arm was furthermore demonstrated by protease protection experiments (Sunderhaus et al. 2006). Finally, systematic dissection of the membrane arm of isolated complex I from *Arabidopsis* by treatment with low concentrations of SDS allowed separating an 85 kDa subcomplex from the membrane arm (Klodmann et al. 2010). It has been demonstrated using mass spectrometry that this domain includes the γCA1, γCA2, γCAL1 and γCAL2 proteins (γCA3 was not detected). A smaller version of the membrane arm is detectable upon detachment of the 85 kDa
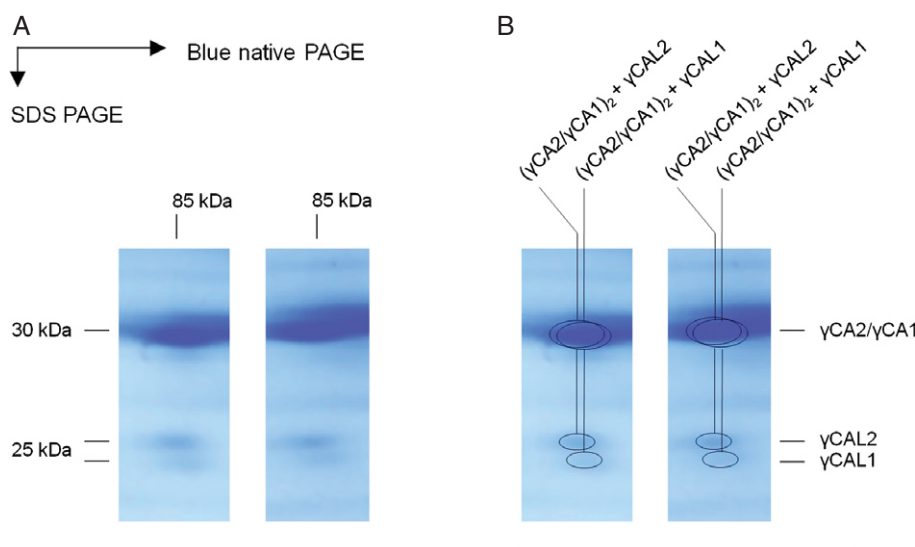
Fig. 2. Subunit composition of the carbonic anhydrase domain. Dissection products of complex I were analyzed by 2D Blue native/SDS PAGE (Klodmann et al. 2010; dissection by pre-treatment of isolated complex I with low concentrations of SDS). Only small areas of the 2D gels are shown [native (horizontal) gel dimension: ~75–100 kDa, SDS (vertical) gel dimension: ~ 20–40 kDa]. (A) Results of two different experiments (Coomassie-stained 2D gels). (B) Same gels including identified proteins (Klodmann et al. 2010; protein identifications using mass spectrometry). An interpretation with respect to the subunit composition of the carbonic anhydrase domain is given above the gels in B.

subcomplex which includes all known subunits of the membrane arm except for the γCA/γCAL proteins. It was concluded that detachment of the γCA/γCALs does not destabilize the membrane arm (Klodmann et al. 2010). In summary, experimental data indicate that the extra domain of plant complex I consists of three γCA/γCAL proteins and has a molecular mass of approximately 85 kDa.

Subunit composition of the carbonic anhydrase domain

The genome of *Arabidopsis* codes for five complex I integrated γCA/γCAL proteins but the carbonic anhydrase domain of complex I only includes three of these proteins. How can this be explained? Careful inspection of 2D Blue native/sodium dodecyl sulfate (SDS) gels separating complex I dissection products revealed that the 85 kDa complex includes the γCA1, γCA2, γCAL1 and γCAL2 subunits, but that the latter two proteins are not exactly aligned on a vertical line as required for subunits forming part of the same protein complex (Fig. 2). It therefore was concluded that two ~85 kDa complexes closely co-migrate on the 2D gels, both including two copies of the γCA1/γCA2 proteins and additionally *either γCAL1 or γCAL2*. These findings are nicely supported by yeast-two hybrid data: It has been found that γCA2 interacts with γCA2, γCAL1 and γCAL2 (Perales et al. 2004, Braun et al. 2011). Interaction of γCAL1

and γCAL2 has not been found by yeast-two-hybrid analyses. Again, no interaction data could be obtained for γCA3.

In summary, location of γCA3 within the γCA domain of complex I remains elusive. Several lines of evidence indicate that γCA3, although detectable using MS in total complex I fractions, is of very low abundance and unclear localization: (i) few γCA3-specific peptides were detected in the course of proteomic analyses of intact complex I (Peters et al. 2013), (ii) γCA3 was not detectable using MS in the 85 kDa domain (Klodmann et al. 2010), and (iii) interaction of γCA3 with any of the other γCA/γCAL proteins was not detected by yeast-two-hybrid screens. We conclude that γCA3 might not be included in the γCA domain (Fig. 3). Furthermore, γCAL1 and γCAL2 do not simultaneously form part of individual complex I particles, but alternatively occur within two distinct 85 kDa subcomplexes. Finally, two copies of the γCA proteins form part of the 85 kDa subcomplexes. Because yeast-two-hybrid data indicate that γCA2 also can interact with γCA2, we speculate that the γCA pair can be either homo- or heteromeric (γCA1 + γCA2, or γCA1 + γCA1, or γCA2 + γCA2). However, further experiments have to be carried out to prove that all three possible CA1/CA2 pairs indeed occur. Taken together, available data are compatible with occurrence of up to six subunit configurations for the gamma carbonic anhydrase domain as illustrated in Fig. 4.
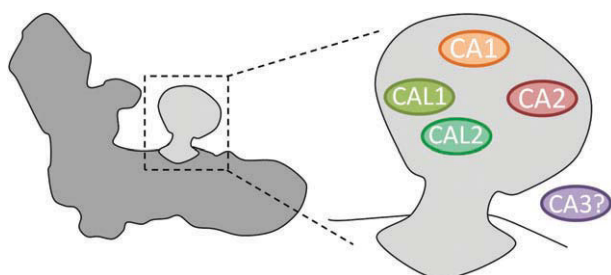
Fig. 3. Scheme of the subunit composition of the carbonic anhydrase domain of complex I in *Arabidopsis thaliana*. CAL subunits are given in light or dark green, CA subunits in orange red and purple. The CA3 protein was not found to be part of the carbonic anhydrase domain.

Function of the carbonic anhydrase domain

Single and double knock-out mutants with respect to the γCA/γCAL proteins were employed to genetically dissect the function of the γCA domain in *A. thaliana*. Plants deficient in γCA2 had no visible phenotype at the conditions tested (Perales et al. 2005). However, a suspension cell culture of γca2-deficient plants had reduced growth and oxygen-uptake rates. Analyses of the respiratory chain by 2D Blue native/SDS-polyacrylamide gel electrophoresis (SDS-PAGE) revealed drastic reduction in complex I amount and activity (Perales et al. 2005). However, single particle EM showed that complex I particles from mutant cells had a normal shape and included the characteristic γCA domain (Sunderhaus et al. 2006). It was concluded that γCA2 could be replaced by other γCA/γCAL proteins, most probably γCA1. In contrast to plants deficient in γCA2, deletion of γCA3 had less influence on complex I amount (Perales et al. 2005) further supporting a more cryptic role of this member of the γCA/γCAL protein family. Meanwhile, knock out mutants for all five γCA/γCAL genes have been analyzed in *Arabidopsis*. They all lack visible phenotypes (Wang et al. 2012). It was concluded that reciprocal substitutions can compensate depletion of single γCA/γCAL proteins. However, complex I amount and activity was reduced in the mutants indicating that the γCA/γCAL subunits are required for complex I assembly or stability. Nevertheless, they should not be considered representing

assembly factors because they clearly form part of mature complex I, constituting the very significant extra domain. A role of the γCA/γCAL subunits in early stages of complex I assembly has been demonstrated by analysis of complex I subcomplexes in *Arabidopsis* mutant lines (Meyer et al. 2011) and by ^{15}N-labeling experiments (Li et al. 2013). Interestingly, genomes of some protists also code for the complex I-integrated γCA/γCAL proteins (Gawryluk and Gray 2010), possibly indicating their involvement in ancient complex I assembly processes which became lost during evolution in animal and fungal lineages.

Beside their importance for complex I assembly, the structural significance of the γCA domain clearly points to another specific role of the γCA/γCAL protein family. Even though carbonic anhydrase activity could not be demonstrated up to date, active site conservation with respect to the prototype γCA from *Methanosarcina thermophila* much supports a role of these proteins in mitochondrial CO_2–bicarbonate conversion. Alternatively, because γCA proteins form part of a larger protein superfamily which also includes acetyltransferases (Parisi et al. 2004), a role in mitochondrial protein acetylation has been proposed but also could not be experimentally demonstrated (Wang et al. 2012). Finally, sequence similarity of the γCA/γCAL proteins to the M-subunit of the cyanobacterial 'carbon concentration mechanism' (CcmM) machinery has been recognized (Parisi et al. 2004). Some of the CcmM proteins exhibit carbonic anhydrase activity, but others do not (Peña et al. 2010). The CcmM protein is important for efficient carbon fixation in the carboxysomes of cyanobacteria (Rae et al. 2013).

In analogy to the cyanobacterial CcmM it has been proposed that complex I integrated γCAs in plants participate in an inner-cellular carbon transfer mechanism that allows recycling of mitochondrial CO_2 released by matrix-localized catabolic processes (including glycine–serine conversion during photorespiration) for carbon fixation in chloroplasts (Braun and Zabaleta 2007, Zabaleta et al. 2012). This hypothesis is supported by some experimental evidence (summarized in Fromm et al. 2016): (i) when photosynthetic rates were
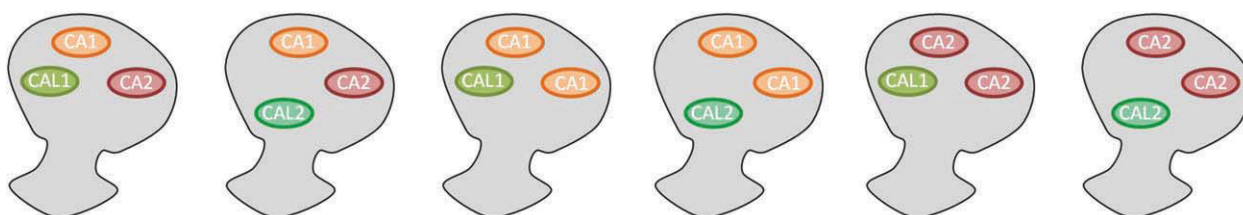

Fig. 4. The six subunit arrangements of the carbonic anhydrase domain.

Fig. 5. Consequences of mutations with respect to the γCA/γCAL proteins on the six possible subunit arrangements of the carbonic anhydrase domain (Fig. 4). The following mutants were generated: (A) RNAi-mediated depletion of γCAL2 in the background of a γcal1 knock-out (Δγcal1/γcal2i). (B) γca2/γcal1 and γca2/γcal2 knock outs (Soto et al. 2015). (C) A γca1/γca2 double knock out (Fromm, Braun and Peterhänsel, unpublished results). Red cross: complex I assembly not possible anymore; yellow arrow: complex I assembly depleted.

compared between protoplasts and isolated chloroplasts, the protoplasts performed better at low CO_2 suggesting that an internal CO_2 source was available in protoplasts, but not in isolated chloroplasts (Riazunnisa et al. 2006). Higher photosynthetic rates in protoplasts were not detectable in the presence of inhibitors of carbonic anhydrases. (ii) Transcription of genes encoding the γCA/γCAL proteins is reduced if plants are cultivated at high CO_2 (Perales et al. 2005). (iii) The tobacco 'CMSII' mutant, which has drastically reduced amounts of complex I, exhibits diminished steady-state photosynthesis. Inhibition of photosynthesis was reduced if plants were cultivated at conditions diminishing photorespiration (Dutilleul et al. 2003). However, the above listed experimental results also could be interpreted representing general effects of complex I dysfunction on photorespiration. Altered mitochondrial NAD^+/NADH ratios caused by complex I depletion might directly affect GDC function (Bykova et al. 2014).

Characterization of double mutants for investigating γCA/γCAL function

Until now, conclusive evidence for involvement of the γCA/γCAL proteins in recycling mitochondrial CO_2 for carbon fixation by photosynthesis so far has not been presented. Very recently, double mutants with respect to the γCA/γCAL proteins have been analyzed for investigating the function of the γCA domain in *Arabidopsis* (Wang et al. 2012, Soto et al. 2015, Fromm et al. 2016). Overall, four different double mutants have been characterized so far:

(i) Δγca1/Δγca3 (Wang et al. 2012). Genes encoding γCA1 and γCA3 are deleted in this *Arabidopsis* mutant line. Plants do not show a visible phenotype under the conditions tested and are not distinguishable form a γca1 single mutant. The biological role of γCA3 therefore has to be further studied.

(ii) Δγcal1/γcal2i (Wang et al. 2012). Because deletion of either γCAL1 or γCAL2 did not reveal

any phenotypic alterations, mutant lines were crossed to generate γcal double mutants. However, resulting seeds turned out to arrest in development. To obtain viable plants, the $\gamma CAL2$ gene was downregulated by RNAi in the background of a homozygous $\gamma CAL1$ knockout (Fig. 5). $\Delta\gamma cal1/\gamma cal2$i plants showed delayed germination and significantly postponed development. In the light, $\Delta\gamma cal1/\gamma cal2$i plants developed a short hypocotyl phenotype. The gene encoding chalcone synthase, a key enzyme of anthocyanin synthesis, was induced in the mutant lines. It was concluded that γCAL1 and γCAL2 play important roles in light-dependent growth and development in *Arabidopsis* (Wang et al. 2012). Meanwhile, $\Delta\gamma cal1/\gamma cal2$i plants have been characterized with respect to the mitochondrial compartment (Fromm et al. 2016). Complex I amount was reduced by 90–95% and oxygen consumption of isolated mitochondria is much diminished. Comparative proteome analyses revealed several changes in the mutant which not only refer to complex I subunits but also point to specific alterations of central mitochondrial metabolism, e.g. pyruvate, glutamate and stress metabolism. However, it still is difficult to dissect molecular consequences caused by complex I depletion on the one side and diminishment of γCAL proteins on the other.

(iii) $\Delta\gamma ca2/\Delta\gamma cal1$ and $\Delta\gamma ca2/\Delta\gamma cal2$ (Soto et al. 2015). These double mutants lack the $\gamma CA2$ gene and additionally either $\gamma CAL1$ or $\gamma CAL2$. This only allows for assembly of one out of six possible subunit configurations of the γCA domain (Fig. 5). Both mutant lines are clearly delayed in growth and development. Interestingly, this effect is reverted if plants are cultivated in the presence of high CO_2, indicating that γCA function might be especially relevant in the presence of photorespiration. Reduction of complex I (about 80%) is similar to the degree of complex I reduction in $\gamma ca2$ single mutants. However, the $\gamma ca2$ mutant did not exhibit a growth phenotype. The double mutants also exhibit altered glycine metabolism. It is concluded that γCA/γCAL function is important in the context of photorespiration, but the precise role of the γCA/γCAL proteins still remains elusive.

Outlook

For future research, precise differentiation between general complex I function and specific function of the γCA/γCAL subunits will be of great importance. Very recently, a $\Delta\gamma ca1/\Delta\gamma ca2$ mutant has been generated (Fromm, Braun and Peterhänsel, unpublished results and Córdoba, Soto and Zabaleta, unpublished data). This mutant, which lacks both main γCA proteins of the γCA domain (presence of γCA3 within this domain is questionable) is severely impaired in development. Plants can be rescued but development is extremely delayed. As predicted (Fig. 5), complex I is completely absent. This double mutant was genetically transformed with γCA genes encoding modified γCA proteins which allow reconstitution of complex I assembly, but lack their specific enzymatic function. Analysis of resulting plant lines might help to finally uncover the significance of the γCA domain of plant complex I.

References

Balsa E, Marco R, Perales-Clemente E, Szklarczyk R, Calvo E, Landázuri MO, Enríquez JA (2012) NDUFA4 is a subunit of complex IV of the mammalian electron transport chain. Cell Metab 16: 378–386

Baradaran R, Berrisford JM, Minhas GS, Sazanov LA (2013) Crystal structure of the entire respiratory complex I. Nature 494: 443–448

Braun HP, Zabaleta E (2007) Carbonic anhydrase subunits of the mitochondrial NADH dehydrogenase complex (complex I) in plants. Physiol Plant 129: 114–122

Braun P et al., The *Arabidopsis* Interactome Mapping Consortium (2011) Evidence for network evolution in an *Arabidopsis* interactome map. Science 333: 601–607

Braun HP, Binder S, Brennicke A, Eubel H, Fernie AR, Finkemeier I, Klodmann J, König AC, Kühn K, Meyer EH, Obata T, Schwarzländer M, Takenaka M, Zehrmann A (2014) The life of plant mitochondrial complex I. Mitochondrion 19(Pt B): 295–313

Bultema J, Braun HP, Boekema E, Kouril R (2009) Megacomplex organization of the oxidative phosphorylation system by structural analysis of respiratory supercomplexes from potato. Biochim Biophys Acta 1787: 60–67

Bykova NV, Møller IM, Gardeström P, Igamberdiev AU (2014) The function of glycine decarboxylase complex is optimized to maintain high photorespiratory flux via buffering of its reaction products. Mitochondrion 19(Pt B): 357–364

Cardol P, Vanrobaeys F, Devreese B, Van Beeumen J, Matagne RF, Remacle C (2004) Higher plant-like subunit composition of mitochondrial complex I from *Chlamydomonas reinhardtii*: 31 conserved components among eukaryotes. Biochim Biophys Acta 1658: 212–224

Carroll J, Fearnley IM, Skehel JM, Shannon RJ, Hirst J, Walker JE (2006) Bovine complex I is a complex of 45 different subunits. J Biol Chem 281: 32724−32727

Dudkina NV, Eubel H, Keegstra W, Boekema EJ, Braun HP (2005) Structure of a mitochondrial supercomplex formed by respiratory-chain complexes I and III. Proc Natl Acad Sci USA 102: 3225−3229

Dutilleul C, Driscoll S, Cornic G, De Paepe R, Foyer CH, Noctor G (2003) Functional mitochondrial complex I is required by tobacco leaves for optimal photosynthetic performance in photorespiratory conditions and during transients. Plant Physiol 131: 264−275

Ferry JG (2010) The gamma class of carbonic anhydrases. Biochim Biophys Acta 1804: 374−381

Fromm S, Göing J, Lorenz C, Peterhänsel C, Braun HP (2016) Depletion of the "gamma-type carbonic anhydrase-like" subunits of complex I affects central mitochondrial metabolism in *Arabidopsis thaliana*. Biochim Biophys Acta 1857: 60−71

Gawryluk RM, Gray MW (2010) Evidence for an early evolutionary emergence of gamma-type carbonic anhydrases as components of mitochondrial respiratory complex I. BMC Evol Biol 10: 176

Heazlewood JL, Howell KA, Millar AH (2003) Mitochondrial complex I from *Arabidopsis* and rice: orthologs of mammalian and fungal components coupled with plant-specific subunits. Biochim Biophys Acta 1604: 159−169

Hirst J (2013) Mitochondrial complex I. Annu Rev Biochem 82: 551−575

Hofhaus G, Weiss H, Leonard K (1991) Electron microscopic analysis of the peripheral and membrane parts of mitochondrial NADH dehydrogenase (complex I). J Mol Biol 221: 1027−1043

Hunte C, Zickermann V, Brandt U (2010) Functional modules and structural basis of conformational coupling in mitochondrial complex I. Science 329: 448−451

Iverson TM, Alber BE, Kisker C, Ferry JG, Rees DC (2000) A closer look at the active site of gamma-class carbonic anhydrases: high-resolution crystallographic studies of the carbonic anhydrase from *Methanosarcina thermophila*. Biochemistry 39: 9222−9231

Klodmann J, Sunderhaus S, Nimtz M, Jänsch L, Braun HP (2010) Internal architecture of mitochondrial complex I from *Arabidopsis thaliana*. Plant Cell 22: 797−810

Li L, Nelson CJ, Carrie C, Gawryluk RM, Solheim C, Gray MW, Whelan J, Millar AH (2013) Subcomplexes of ancestral respiratory complex I subunits rapidly turn over in vivo as productive assembly intermediates in *Arabidopsis*. J Biol Chem 288: 5707−5717

Martin V, Villarreal F, Miras I, Navaza A, Haouz A, González-Lebrero RM, Kaufman SB, Zabaleta E (2009) Recombinant plant gamma carbonic anhydrase homotrimers bind inorganic carbon. FEBS Lett 583: 3425−3430

Meyer EH (2012) Proteomic investigations of complex I composition: how to define a subunit? Front Plant Sci 3: 106

Meyer EH, Solheim C, Tanz SK, Bonnard G, Millar AH (2011) Insights into the composition and assembly of the membrane arm of plant complex I through analysis of subcomplexes in *Arabidopsis* mutant lines. J Biol Chem 286: 26081−26092

Parisi G, Perales M, Fornasari MS, Colaneri A, Gonzalez-Schain N, Gomez-Casati D, Zimmermann S, Brennicke A, Araya A, Ferry JG, Echave J, Zabaleta E (2004) Gamma carbonic anhydrases in plant mitochondria. Plant Mol Biol 55: 193−207

Peña KL, Castel SE, de Araujo C, Espie GS, Kimber MS (2010) Structural basis of the oxidative activation of the carboxysomal gamma-carbonic anhydrase, CcmM. Proc Natl Acad Sci USA 107: 2455−2460

Perales M, Parisi G, Fornasari MS, Colaneri A, Villarreal F, Gonzalez-Schain N, Echave J, Gomez-Casati D, Braun HP, Araya A, Zabaleta E (2004) Gamma carbonic anhydrase like complex interact with plant mitochondrial complex I. Plant Mol Biol 56: 947−957

Perales M, Eubel H, Heinemeyer J, Colaneri A, Zabaleta E, Braun HP (2005) Disruption of a nuclear gene encoding a mitochondrial gamma carbonic anhydrase reduces complex I and supercomplex I+III$_2$ levels and alters mitochondrial physiology in *Arabidopsis*. J Mol Biol 350: 263−277

Peters K, Dudkina NV, Jänsch L, Braun HP, Boekema EJ (2008) A structural investigation of complex I and I+III$_2$ supercomplex from *Zea mays* at 11−13 Å resolution: assignment of the carbonic anhydrase domain and evidence for structural heterogeneity within complex I. Biochim Biophys Acta 1777: 84−93

Peters K, Belt K, Braun HP (2013) 3D gel map of *Arabidopsis* complex I. Front Plant Sci 4: 153

Rae BD, Long BM, Whitehead LF, Förster B, Badger MR, Price GD (2013) Cyanobacterial carboxysomes: microcompartments that facilitate CO_2 fixation. J Mol Microbiol Biotechnol 23: 300−307

Riazunnisa K, Padmavathi L, Bauwe H, Raghavendra AS (2006) Markedly low requirement of added CO_2 for photosynthesis by mesophyll protoplasts of pea (*Pisum sativum*): possible roles of photorespiratory CO_2 and carbonic anhydrase. Physiol Plant 128: 763−772

Soto D, Córdoba JP, Villarreal F, Bartoli C, Schmitz J, Maurino V, Braun HP, Pagnussat GC, Zabaleta E (2015) Functional characterization of mutants affected in the carbonic anhydrase domain of the respiratory complex I in *Arabidopsis thaliana*. Plant J 83: 831−844

Sunderhaus S, Dudkina N, Jänsch L, Klodmann J, Heinemeyer J, Perales M, Zabaleta E, Boekema E, Braun HP (2006) Carbonic anhydrase subunits form a matrix exposed domain attached to the membrane arm of

mitochondrial complex I in plants. J Biol Chem 281: 6482–6488

Vinothkumar KR, Zhu J, Hirst J (2014) Architecture of mammalian respiratory complex I. Nature 515: 80–84

Wang Q, Fristedt R, Yu X, Chen Z, Liu H, Lee Y, Guo H, Merchant SS, Lin C (2012) The γ-carbonic anhydrase subcomplex of mitochondrial complex I is essential for development and important for photomorphogenesis of *Arabidopsis*. Plant Physiol 160: 1373–1383

Weiss H, Friedrich T, Hofhaus G, Preis D (1991) The respiratory-chain NADH dehydrogenase (complex I) of mitochondria. Eur J Biochem 197: 563–576

Zabaleta E, Martin MV, Braun HP (2012) A basal carbon concentrating mechanism in plants? Plant Sci 187: 97–104

Zickermann V, Wirth C, Nasiri H, Siegmund K, Schwalbe H, Hunte C, Brandt U (2015) Structural biology. Mechanistic insight from the crystal structure of mitochondrial complex I. Science 347: 44–49

Publication 4

2.4. Life without complex I: proteome analyses of an Arabidopsis mutant lacking the mitochondrial NADH dehydrogenase complex.

Steffanie Fromm[1,2], Jennifer Senkler[1,] Holger Eubel[1], Christoph Peterhänsel[2], Hans-Peter Braun[1]

[1] Institut für Pflanzengenetik, Leibniz Universität Hannover, Herrenhäuser Str. 2, 30419 Hannover, Germany
[2] Institut für Botanik, Leibniz Universität Hannover, Herrenhäuser Str. 2, 30419 Hannover, Germany

Type of authorship:	First author
Type of article:	Research article
Share of the work:	75 %
Contribution to the publication:	planned and performed experiments, analyzed data, prepared all figures and wrote the paper with assistance
Journal:	Journal of Experimental Botany
5-year impact factor:	6.31
Date of publication:	May, 2016
Number of citations (google scholar on May. 24th, 2016):	1
DOI:	10.1093/jxb/erw165
PubMed-ID:	27122571

*Note that the some excel lists of the supplementary material for chapter 2.4 are not printed but included in the compact disc attached to this work.

RESEARCH PAPER

Life without complex I: proteome analyses of an Arabidopsis mutant lacking the mitochondrial NADH dehydrogenase complex

Steffanie Fromm[1,2], Jennifer Senkler[1], Holger Eubel[1], Christoph Peterhänsel[2] and Hans-Peter Braun[1,*]

[1] Institut für Pflanzengenetik, Leibniz Universität Hannover, Herrenhäuser Str. 2, 30419 Hannover, Germany
[2] Institut für Botanik, Leibniz Universität Hannover, Herrenhäuser Str. 2, 30419 Hannover, Germany

* Correspondence: braun@genetik.uni-hannover.de

Abstract

The mitochondrial NADH dehydrogenase complex (complex I) is of particular importance for the respiratory chain in mitochondria. It is the major electron entry site for the mitochondrial electron transport chain (mETC) and therefore of great significance for mitochondrial ATP generation. We recently described an *Arabidopsis thaliana* double-mutant lacking the genes encoding the carbonic anhydrases *CA1* and *CA2*, which both form part of a plant-specific 'carbonic anhydrase domain' of mitochondrial complex I. The mutant lacks complex I completely. Here we report extended analyses for systematically characterizing the proteome of the *ca1ca2* mutant. Using various proteomic tools, we show that lack of complex I causes reorganization of the cellular respiration system. Reduced electron entry into the respiratory chain at the first segment of the mETC leads to induction of complexes II and IV as well as alternative oxidase. Increased electron entry at later segments of the mETC requires an increase in oxidation of organic substrates. This is reflected by higher abundance of proteins involved in glycolysis, the tricarboxylic acid cycle and branched-chain amino acid catabolism. Proteins involved in the light reaction of photosynthesis, the Calvin cycle, tetrapyrrole biosynthesis, and photorespiration are clearly reduced, contributing to the significant delay in growth and development of the double-mutant. Finally, enzymes involved in defense against reactive oxygen species and stress symptoms are much induced. These together with previously reported insights into the function of plant complex I, which were obtained by analysing other complex I mutants, are integrated in order to comprehensively describe 'life without complex I'.

Key words: *Arabidopsis thaliana*, carbonic anhydrase, complex I, mitochondrial metabolism, photosynthesis, proteomics, respiratory chain.

Introduction

Cellular respiration is the fundamental ATP generating process common to most eukaryotes. Mitochondria carry out the final steps of this process and efficiently generate ATP through oxidative phosphorylation (OXPHOS). The mitochondrial OXPHOS system consists of five inner mitochondrial membrane-embedded protein complexes – the four respiratory chain protein complexes (complexes I–IV) and the ATP synthase complex (complex V) – and two mobile electron transporters (ubiquinone and cytochrome *c*).

3080 | Fromm *et al.*

The OXPHOS complexes catalyse the electron transfer from NADH or FADH$_2$ to molecular oxygen as the terminal electron acceptor. Electrons are inserted into the mitochondrial electron transport chain (mETC) via NADH generated by glycolysis, the TCA cycle (additionally electrons come from FADH$_2$), and other catabolic processes such as the photorespiration pathway in plants. As first proposed by Peter Mitchell (1961), electron transport at the mETC is coupled to the translocation of protons from the mitochondrial matrix into the intermembrane space. This creates an electrochemical gradient across the inner mitochondrial membrane that results in a proton motive force. Complex V can use this proton gradient to generate ATP, which finally is exported and used for driving energy-demanding processes.

The NADH dehydrogenase complex (complex I) is of special importance for the OXPHOS system because it is the main site for electron insertion into the mETC and can provide up to 40% of the protons for mitochondrial ATP formation (Hunte *et al.*, 2010; Braun *et al.*, 2014). The structure of complex I has been investigated in *Escherichia coli*, *Thermus thermophilus*, *Bos taurus*, and *Yarrowia lipolytica* (Morgan and Sazanov, 2008; Baradaran *et al.*, 2013; Vinothkumar *et al.*, 2014; Zickermann *et al.*, 2015). Its L-like shape, which originates from two orthogonally arranged 'arms', is well conserved in these species. One arm is hydrophobic, embedded in the inner mitochondrial membrane, and termed the 'membrane arm'. The second arm, which is designated the 'peripheral arm', is hydrophilic and is attached to the end of the membrane arm. It protrudes into the mitochondrial matrix. In plants, complex I contains an additional spherical domain, which is attached to the membrane arm at a central position on its matrix-exposed side (Dudkina *et al.*, 2005; Sunderhaus *et al.*, 2006).

Despite overall similarity in shape, complex I from prokaryotes is comparatively small and has a simple subunit composition. The 14 subunits present in the 550 kDa complex I of *E. coli* constitute the 'minimal set' of subunits (Weidner *et al.*, 1993; Yagi and Matsuno-Yagi, 2003; Sazanov, 2007). Complex I of eukaryotes is nearly twice as large (1000 kDa) (Friedrich and Böttcher, 2004; Brandt, 2006). In addition to the conserved 'minimal set' of subunits, eukaryotic complex I includes several accessory subunits (Friedrich, 2001). However, due to the occurrence of some lineage-specific accessory subunits the overall number of complex I subunits varies between different eukaryotes (e.g. *Chlamydomonas reinhardtii*: 42; *Yarrowia lipolytica*: 42; *Bos taurus*: 45; *Arabidopsis thaliana*: 49) (Cardol *et al.*, 2004; Carroll *et al.*, 2006; Angerer *et al.*, 2011; Peters *et al.*, 2013).

Plant complex I includes nine lineage-specific subunits (Braun *et al.*, 2014), most notably a group of carbonic anhydrases located within the spherical extra domain attached to the membrane arm (Sunderhaus *et al.*, 2006). Within this domain, which is designated the 'carbonic anhydrase domain' of plant complex I, three gamma-type carbonic anhydrase (γCA) proteins (γCA1, γCA2, γCA3) and two gamma-type carbonic anhydrase-like (γCAL) proteins (γCAL1 and γCAL2) are located (Perales *et al.*, 2004; Klodmann *et al.*, 2010). Since the γCA domain has a molecular mass of 85 kDa

it can only include three out of the five γCA/γCAL proteins at the same time (Klodmann *et al.*, 2010). Based on investigations using γCA/γCAL mutants, six possible subunit arrangements have been suggested to occur (Fromm *et al.*, 2016a): each γCA domain contains either the γCAL1 or the γCAL2 protein and additionally two copies of the γCA proteins (γCA1 or γCA2, or both but not γCA3).

The γCA/γCAL subunits have been found to be essential for the early steps of complex I assembly (Meyer *et al.*, 2011; Li *et al.*, 2013). Deletion of the gene encoding Arabidopsis γCA2 causes reduction of complex I (Perales *et al.*, 2005). Deletion or downregulation of more than one gene encoding the γCA/γCAL subunits in Arabidopsis has drastic effects on the amount of complex I (Soto *et al.*, 2015; Fromm et al., 2016*b, c*). Similarly, deletion of other genes encoding complex I subunits has been reported to cause significant reduction of complex I levels (e.g. deletion of the *ndufs4*, *bir6*, and *slo3* genes; Kühn *et al.*, 2015; Koprivova *et al.*, 2010; Hsieh *et al.*, 2015). In contrast to vertebrates, plants can withstand complex I reduction and dysfunction because they possess alternative NADH dehydrogenases in the mitochondria, which are important for mitochondrial functioning, especially if plants are growing under unfavorable growth conditions (Rasmusson *et al.*, 2008).

A few Arabidopsis mutants have been described that completely lack mitochondrial complex I. In one mutant the NDUFV1 subunit (also called the 51-kDa subunit of complex I) is missing, causing complete absence of complex I. The mutant displayed increased fluxes through glycolysis and the TCA cycle (Kühn *et al.*, 2015). In a second complex I-deficient Arabidopsis mutant the genes encoding γCA1 and γCA2 are absent. Mutant seeds do not germinate but can be rescued in the presence of high sucrose by an embryo rescue method (Fromm *et al.*, 2016c). Growth of the resulting plants is extremely retarded. In the *ca1ca2* mutant the cytochrome *c* oxidase complex is much induced, probably compensating for the loss of complex I with respect to proton translocation across the inner mitochondrial membrane (Fromm *et al.*, 2016c).

Complex I-deficient mutants offer the unique opportunity to study 'plant life without complex I'. Here we report a systematic proteomic comparison between *ca1ca2* and wildtype Arabidopsis lines that is based on three distinct experimental strategies: 2D IEF/SDS PAGE, 2D BN/SDS PAGE, and a label-free quantitative shotgun proteome approach. MS analyses allowed in-depth insights into the molecular mechanisms compensating for the lack of complex I.

Material and Methods

Plant material and growth conditions

Arabidopsis (*Arabidopsis thaliana*) lines used for this study were of the Columbia ecotype. The SALK_109391 (AT1G19580, *ca1/ca1*) and SALK_010194 (AT1G47260, *ca2/ca2*) mutant lines were obtained from The European Arabidopsis Stock Centre (NASC; Loughborough, UK). *ca1* and *ca2* single mutants were crossed to generate *ca1ca2* double-mutants (Fromm *et al.*, 2016c). Plants were grown on 0.5 Murashige and Skoog medium in climate chambers under the following conditions: 8 h of light (120 µmol s^{-1} m^{-2})/16 h

of dark, 22 °C, 65% humidity, atmospheric CO_2 concentrations. Homozygous *ca1ca2* mutants were germinated and rescued by cultivation on 0.5 MS medium containing 3% (w/v) sucrose. After 6 weeks plants were transferred to soil and cultivation was continued under the same conditions without sucrose. Wildtype and double-mutant plants were harvested at the 10-rosette-leaf developmental stage, and leaves were used for proteomic analyses.

Cell cultures of Arabidopsis lines were established as described by May and Leaver (1993). Callus was maintained as suspension culture according to Sunderhaus *et al.* (2006).

Isolation of mitochondria

Mitochondria from cell culture were purified by differential centrifugation and Percoll density gradient centrifugation as described by Werhahn *et al.* (2001).

Protein gel electrophoresis procedures and staining procedures

One-dimensional Blue Native PAGE (1D BN PAGE) was performed according to Wittig *et al.* (2006). Mitochondrial membranes were solubilized by digitonin at a concentration of 5 g g^{-1} mitochondrial protein (Eubel *et al.*, 2003). For subsequent SDS PAGE, BN lanes with separated protein complexes were transferred horizontally onto SDS gels. Second-dimension PAGE was carried out as outlined previously (Wittig *et al.*, 2006). Differential gel electrophoresis (DIGE), which is based on labeling of proteins with CyDyes before 2D BN/SDS PAGE, was carried out according to Peters and Braun (2012).

Two-dimensional IEF/SDS PAGE was carried out as described by Mihr and Braun (2003). For the IEF gel dimension, Immobiline DryStrip gels (24 cm, non-linear gradient pH 3–11) were used. Focusing took place for 24 h at 30 to 8000 V using the Ettan IPGphor 3 system (GE Healthcare).

For the second gel dimension, IPG stripes were equilibrated for 15 min with DTT (0.4 g/40 ml) and then 15 min with iodoacetamide (1.0 g/40 ml). SDS PAGE was carried out using the High Performance Electrophoresis (HPE) FlatTop Tower-System (Serva Electrophoresis) using precast Tris-Glycine gels (12.5% polyacrylamide, 24 x 20 cm).

Gels were fixed for 2 h in 15% (v/v) ethanol, 10% (v/v) acetic acid and stained with Coomassie Brilliant Blue G250 (Neuhoff *et al.*, 1985, 1990).

Comparative proteome analyses were based on gel triplicates and data evaluation using the Delta 2D software 4.3 (Decodon, Greifswald, Germany) according to Berth *et al.* (2007) and Lorenz *et al.* (2014).

Protein identification by mass spectrometry

Tryptic digestion of proteins and their identification by mass spectrometry (MS) were performed as described by Klodmann *et al.* (2010). Peptide separation was carried out by using the EASY-nLC System (Proxeon, Thermo Scientific, Bremen, Germany) and coupled MS analyses by using the MicrOTOF-Q II mass spectrometer (Bruker Bremen, Germany). MS primary data were evaluated using the Proteinscape software package (version 2.1, Bruker, Bremen, Germany), the Mascot Search Engine (Matrix Science, London, UK), the Arabidopsis protein database (www.arabidopsis.org; release TAIR10), and an updated version of a complex I database (Klodmann *et al.*, 2010) that represents a subset of the Arabidopsis TAIR10 database. The threshold Mascot Score was set to 30 or 60 for proteins and 20 for peptides.

Label-free quantitative shotgun mass spectrometry

Sample preparation for ESI-MS/MS

Total proteins of five biological replicates of wt and *ca1ca2* leaves were extracted. Then 50 µg of protein were solubilized in 2× sample buffer [4% (w/v) SDS, 125 mM Tris-HCl (pH 6.8), 20% (v/v) glycerol,

and 0.5% (w/v) bromophenol blue (BPB)] and loaded on a glycine/SDS gel [10% (w/v) acrylamide in stacking gel, 14% (w/v) in separation phase]. To concentrate proteins in a single band the gel run was stopped when the BPB front reached the end of the stacking gel. Gels were then Coommassie-stained and the protein bands were extracted and transferred into low-binding Eppendorf caps (Eppendorf, Wesseling-Berzdorf, Germany). After drying in a vacuum centrifuge (Eppendorf, Wesseling-Berzdorf, Germany), gel pieces were rehydrated in 200 µl reduction solution [20 mM DTT, 0.1 M ammonium bicarbonate (AmBiC)] for 30 min at 56 °C. Afterwards, they were dehydrated again by addition of 200 µl acetonitrile (ACN) for 10 min. The supernatant was removed and alkylation of cysteine residues was achieved by incubation in 200 µl alkylating solution (55 mM iodoacteamide, 0.1 M AmBiC) for 30 min in the dark. After ACN-dehydration for 10 min the supernatant was removed and 200 µl of 0.1 M AmBiC were added. After 15 min of incubation the supernatant was removed and gel pieces were dehydrated by addition of ACN. After removal of residual ACN, gel pieces were dried by vacuum centrifugation for 20 min. The dried gel pieces were treated with trypsin (Promega, Mannheim, Germany) solution prepared according to the manufacturer's instruction. Eighty microliters were added to each sample, which were subsequently incubated overnight at 37 °C. Extraction of peptides was initiated by adding 40 µl of 50% (v/v) ACN, 5% (v/v) formic acid (FA) (30 min, 37 °C, 800 rpm). The tryptic peptide-containing supernatants were collected in new low-binding Eppendorf tubes. The procedure was repeated twice by first adding 40 µl of 50% (v/v) ACN, 1% (v/v) FA, and then 100% (v/v) ACN afterwards. The supernatants for each sample were pooled in the same Eppendorf tubes and subsequently dried using a vacuum centrifuge at 30 °C. For mass spectrometry peptides were absorbed in 20 µl 2% (v/v) ACN, 0.1% (v/v) FA.

ESI-MS/MS

Tandem mass spectrometry (MS/MS) analysis was performed by means of a Q-Exactive (Thermo Fisher Scientific, Dreieich, Germany) mass spectrometer coupled to an Ultimate 3000 (Thermo Fisher Scientific, Dreieich, Germany) UPLC.

Seven microliters of sample solution were drawn from 0.25-ml glass insert vials (Sun-SRI, Rockwood, TN, US) kept at 8 °C in the sample compartment and stored in a 20-µl sample loop before being injected into a 2 cm, C18, 5 µm, 100 Å reverse phase trapping column (Acclaim PepMap100, Thermo Fisher Scientific, Dreieich, Germany) at a rate of 4 µl min^{-1}. Peptide separation was achieved on a 50 cm, C18, 3 µm, 100 Å reverse phase analytical column (Acclaim PepMap100, Thermo Fisher Scientific, Dreieich, Germany). Peptides were eluted using a non-linear 2% to 30% (v/v) acetonitrile gradient in 0.1% (v/v) formic acid with a flow of 300 nl min^{-1} over a period of 60 mins and at a set column oven temperature of 35 °C. To clean the column, the ACN concentration was subsequently raised to 95% (v/v) within 10 min, where it was kept for another 15 min before column equilibration to 2% (v/v) ACN commenced.

Transfer of eluted peptides into the mass spectrometer was achieved by means of a NSI source (Thermo Fisher Scientific, Dreieich, Germany) using stainless steel nano-bore emitters (Thermo Fisher Scientific, Dreieich, Germany) connected to the column outlet by a 50-cm, 0.05 mm ID fused silica capillary. During MS analysis spray voltage was set to 2.2 kV, capillary temperature to 275 °C, and S-lens RF level to 50%. The MS was run in positive ion mode, MS/MS spectra (top 10) were recorded from 30 mins to 220 min. For full MS scans, the number of microscans was set to 1, resolution to 70 000, AGC target to 1e6, maximum injection time to 400 ms, number of scan ranges to 1, scan range to 400–1600 m/z, and spectrum data type to 'profile'. For dd-MS2, the number of microscans was set to 1, resolution to 17 500, AGC target to 1e5, maximum injection time to 250 ms, Loop count to 10, MSX count to 1, isolation window to 3.0 m/z, fixed first mass to 100.0 m/z, NCE to 27.0 (stepped NCE deactivated), and spectrum data type to 'profile'. Data dependent (dd) settings were as follows: underfill ratio, 0.5%; intensity threshold, 2.0e3; apex trigger, 10 to 40 s; charge exclusion,

unassigned, 1, 5, 5–8, >8; peptide match, preferred; exclude isotopes, on; dynamic exclusion, 45.0 s.

MS/MS data were queried against an in-house TAIR10 database, modified to also include common contaminants (keratin, trypsin), MS-standards (BSA, fibrinopeptide) and known modifications of mitochondrial encoded proteins based on RNA-editing (AGIs) using Proteome Discoverer (Thermo Fisher Scientific, Dreieich, Germany). Search runs employed the Mascot (Matrix Science, London, United Kingdom), peptide selector settings employed the following spectrum properties filter: Lower Rt limit, 0; upper RT limit, 0; first scan, 0; last scan, 0; lowest charge state, 1; highest charge state, 5; min. precursor mass, 350 Da; max. precursor mass, 5000 Da; total intensity threshold, 0; and minimum peak count, 1. The scan event filter was adjusted to the following settings: mass analyser, ftms; ms order, MS2; activation type, HCD; min. collision energy, 0; max. collision energy, 1000; scan type, full; ionization source, nanospray; polarity mode, +. The S/N threshold was set to 1.5. For Mascot, the number of maximum missed cleavage sites was limited to 1, precursor mass tolerance to 10 ppm, and fragment mass tolerance to 0.8 Da. Allowed variable modifications were oxidation of methionine residues and N-terminal acetylations. Carbamidomethylation of cysteine residues was selected as fixed modification. For the target decoy PSM validator, strict target FDR was set to 0.01, while 0.05 was selected for relaxed target FDR.

Identification and protein quantification

Q-Exactive raw-files were loaded into the MaxQuant software (Cox and Mann, 2008) and processed using the following group specific parameters: variable modifications, acetyl (N-term), oxidation (M); digestion mode, specific; enzyme, Trypsin/P; max. number of missed cleavages, 2; match type, match from and to; number of threads, 3; max. instrument type, Orbitrap; first search peptide tolerance, 20; main search tolerance, 4.5; peptide tolerance unit, ppm; individual peptide mass tolerance, chosen; isotope match tolerance, 2 (ppm); centroid match tolerance, 8 (ppm); centroid half width, 35 (ppm); time valley factor, 1.4; isotope time correlation, 0.6; theoretical isotope correlation, 0.6; recalibration unit, ppm; use MS1 centroids, not chosen; use MS2 centroids, not chosen; intensity dependent calibration, not chosen; min. peak length, 2; max. charge, 5; min. score for recalibration, 70, cut peaks, chosen; gap scans, 1; advanced peak splitting, not chosen; intensity threshold, 500; intensity determination, value at maximum, label-free quantitation (LFQ) min. ratio count, 2; Fast LFQ, chosen; LFQ min. number of neighbors, 3; LFQ average number of neighbors, 6; number of modifications per peptide, 5; min. time, NaN; max. time NaN; additional var mods for special proteins, not chosen; separate variable modifications for first search, not chosen; separate enzyme for first search, not chosen.

Global parameters were chosen as follows: a fasta file containing all Uni-Prot listed *Arabidopsis thaliana* protein sequences; fixed modifications, carbamidomethyl (C); re-quantify, not chosen; match between runs, chosen; match time window, 0.7 min; alignment time window, 20 min; match unidentified features, not chosen; decoy mode, revert; special AAs, KR; include contaminants, chosen; I=L, not chosen; max peptide mass, 4600 Da; min. peptide length for unspecific search, 8; max. peptide length for unspecific search, 25; PSM FDR, 0.01; protein fdr, 0.01; Site decoy fraction, 0.01; min. peptide length, 7; min. peptides, 1; min. razor + unique peptides, 1; min. unique peptides, 0; min. score for unmodified peptides, 0; min. score for modified peptides, 40; min. delta score for unmodified peptides, 0; min. delta score for modified peptides, 6; base FDR calculation of delta score, not chosen; razor protein FDR, chosen; split protein groups by taxonomy ID, not chosen; filter labelled amino acids, chosen; second peptides, chosen; dependent peptides, not chosen; min ratio count, 1.5; peptides for quantification, unique + razor; use only unmodified peptides and selected modifications, chosen; modifications used in protein quantification, acetyl (N-term), oxidation (M); discard unmodified counterpart peptide, chosen; separate LFQ in parameter groups, not chosen; stabilize large LFQ ratios,

chosen; require MS/MS for LFQ comparisons, chosen; iBAQ, chosen; Log fit, chosen; advanced site intensities, chosen.

LFQ intensities from the corresponding MaxQuant 'proteinGroups.txt' file were uploaded into the Perseus software (http://www.biochem.mpg.de/5111810/perseus) to build a quantitation matrix. Data were cleaned from the matrix by applying the following parameters: columns identified only by site, reverse, potential contaminant; mode, remove matching rows; filter mode, reduce matrix. Categorical annotation of rows was performed manually ('create') and invalid data were removed by filtering rows based on valid values: min. number of values, 3; mode, in at least one group; values should be greater than 0; filter mode, reduce matrix. Two-sample testing was achieved by means of a *t*-test using the following parameters: S0; side, both; permutation-based FDR, 0.05, number of randomizations, 250; preserve grouping in randomizations, none; –log10, chosen. The –log10 *P*-value was calculated and the cut-off for the following analysis was *P*-value >1.31. Localization of proteins was analysed with SUBAcon (Tanz *et al.*, 2013; Hooper *et al.*, 2014) and the functional context with MapMan (Thimm *et al.*, 2004).

Oxygen consumption measurements

Oxygen consumption of isolated mitochondria was measured using a Clark-type oxygen electrode (Hansatech Instruments, Norfolk, UK) according to Meyer *et al.* (2009). The reaction buffer included 100 µg mitochondrial protein in 3 ml respiration buffer (300 mM sucrose, 5 mM KH_2PO_4, 10 mM TES, 10 mM NaCl, 2 mM $MgSO_4$, 0.1% [w/v] BSA, pH 7.2) supplied with 5 mM succinate and 500 µM ATP. At stable oxygen consumption, 200 µM ADP was added for measuring ADP-dependent respiration. For estimation of AOX capacity, 500 µM of AOX inhibitor n-propyl gallate (nPG) was added and the O_2 consumption rate after adding nPG was subtracted from the ADP-dependent O_2 consumption rate.

Results

Comparison of the mitochondrial proteomes of wt and ca1ca2 *lines using 2D IEF/SDS PAGE*

To investigate the consequences of the absence of complex I on the mitochondrial compartment, comparative proteome analyses of wt and *ca1ca2* mitochondria isolated from cell culture lines were performed. Proteins were separated by 2D IEF/SDS PAGE and spot volumes were systematically compared using the Delta 2D software package (Decodon, Greifswald).

Volumes of 121 spots were significantly altered, with a fold change of >1.5 (*P*-value < 0.01) between wt and *ca1ca2* lines. Forty-four spots had higher volume in the *ca1ca2* mutant, whereas 77 spot volumes were increased in wt (reduced in *ca1ca2*) (Fig. 1). All 121 spots were analysed by mass spectrometry. After applying a MASCOT threshold score of 60, overall a total of 288 identified proteins were included in further analyses. More than one protein was identified for several spots. Changes in volume were only assigned to a specific protein if a spot only included one main protein. This further reduced the number of unambiguously changed proteins to 106. Sixty-six of these proteins were of decreased abundance in the mutant and 40 of increased abundance. These proteins were annotated according to their functional context (Supplementary Table S1 at *JXB* online).
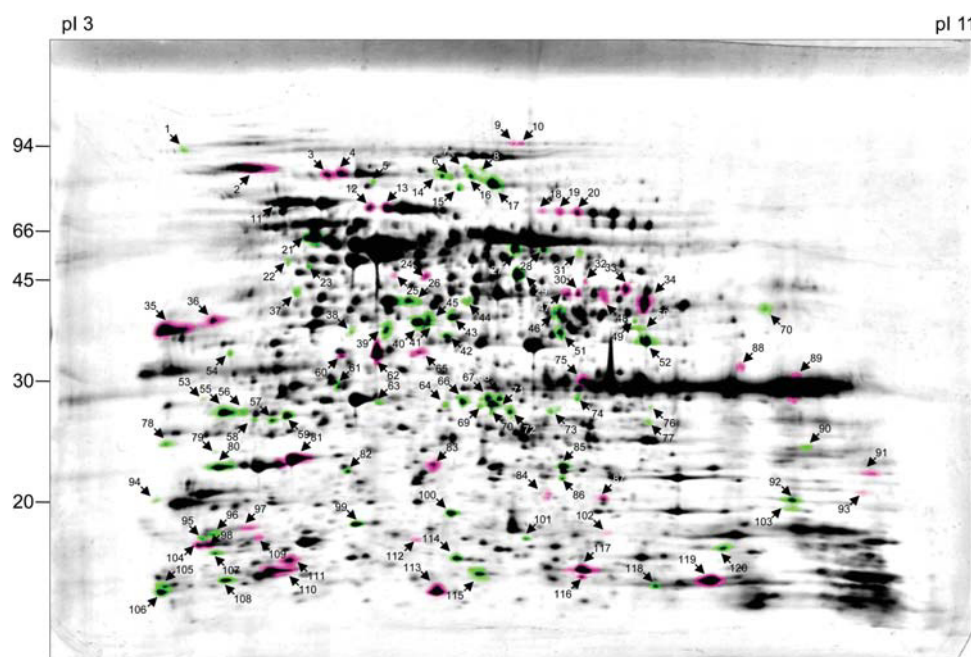
Fig. 1. Comparative analysis of the mitochondrial proteomes of Arabidopsis wt and *ca1ca2* lines. Mitochondria were isolated as described in the Materials and Methods. Total mitochondrial protein was separated by 2D IEF/SDS PAGE and proteins were stained by Coomassie blue. Three replicates were produced per line and used for the calculation of master gels (Delta 2D software package, Decodon, Germany). The molecular masses of standard proteins are given to the left of the 2-D gel (in kDa). Isoelectric focusing range is from pH 3 (left) to pH 11 (right). Proteins indicated in pink are more abundant in the mutant (>1.5-fold increase); proteins indicated in green are less abundant in the mutant (>1.5-fold decrease). Spots indicated by numbers were identified by mass spectrometry (for results see Supplementary Table S1).

As expected, many proteins of reduced abundance were complex I subunits (15 proteins). We did not find all the complex I proteins because 2D IEF/SDS PAGE does not allow separation of very hydrophobic proteins. Reduction of complex I subunits was on average 5-fold. It was shown previously by Fromm *et al.* (2016c) that complex I is completely absent in the mutant (Supplemantary Fig. S1); however, non-assembled subunits may be present in mitochondria. Furthermore, reduction of levels of complex I subunits can be expected to be even higher because nearly all spots included not only one main protein but also in addition some proteins of low abundance, which probably were of unchanged or not much changed abundance. As a consequence, fold-changes in general might be slightly higher than determined in the frame of our study. Other proteins of reduced abundance in the mutant are involved in the central mitochondrial metabolism whereas many proteins of increased abundance play roles in transport or stress response processes (Table 1).

Detailed evaluation of the dataset revealed the following. Changes in abundance of TCA cycle enzymes were not uniform. We found subunits of citrate synthase (AT2G44350), malate dehydrogenase (AT3G15020), and succinyl-CoA ligase (AT5G08300) of decreased abundance in the *ca1ca2* mutant, whereas a subunit of the oxoglutarate dehydrogenase complex (AT5G55070) was increased. Glutamate dehydrogenase (AT5G18170) was also increased in the mutant. Notably, several subunits of the TIM translocase were increased (TIM8, TIM9, TIM23). Several of the most induced proteins in the mutant are involved in plant stress responses.

Some of the proteins of changed abundance were subunits of the remaining OXPHOS complexes II–V. Again, not

Table 1. *Relative spot volumes of altered proteins involved in defined functional processes in* ca1ca2 *mutant lines. Proteins were separated by 2D IEF/SDS PAGE (Fig. 1), normalized spot volumes of differential OXPHOS subunits were summed up and relative spot volumes were calculated by the Delta 2D software package*

Functional context (number of proteins of changed abundance)	Relative spot volume with respect to wt plants (%)
Stress response (12)	186
Transport (7)	159
Processing of nucleic acids (5)	157
Protein folding and processing (6)	143
Oxidative phosphorylation without complex I (18)	133
Uncharacterized (4)	111
Miscellaneous proteins (6)	102
Amino acid metabolism (7)	75
Lipid metabolism (9)	68
TCA cycle (5)	45
Carbon fixation (4)	28

all of the subunits were identified because many of them are very hydrophobic and not resolvable by 2D IEF/SDS PAGE. It became apparent that several complex IV subunits are clearly induced. To get a more complete impression on how the mutant is altered with respect to the OXPHOS system, we next compared mitochondrial fractions of wt and *ca1ca2* lines using 2D BN/SDS PAGE, a gel electrophoresis system known to be particularly suitable for analysing membrane-bound proteins and protein complexes.
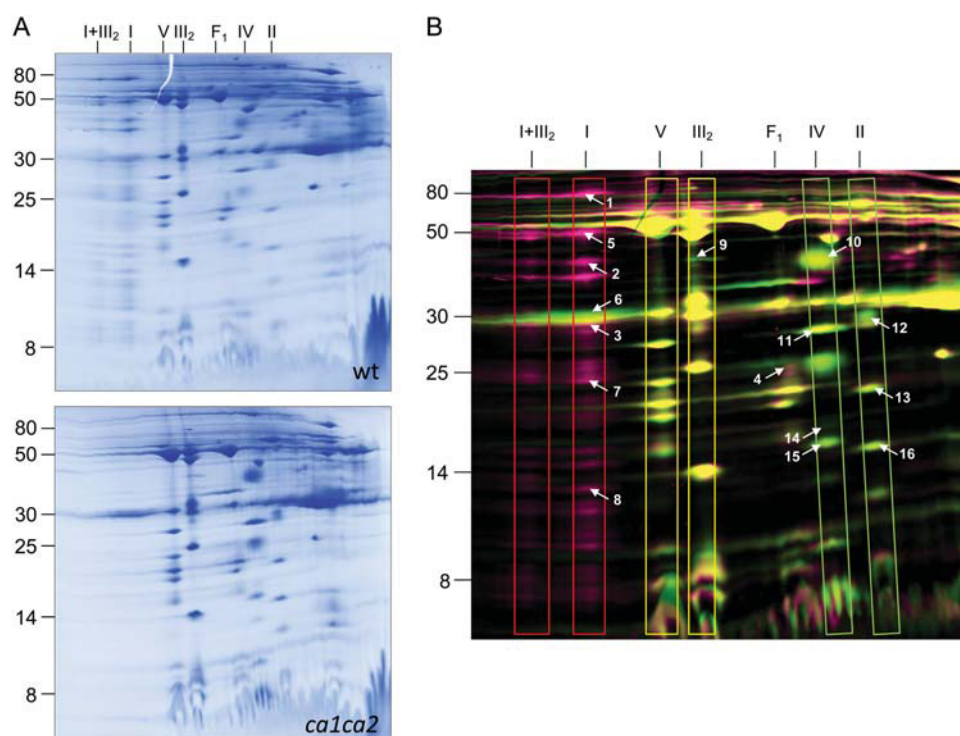
Fig. 2. Comparative analysis of the mitochondrial membrane proteomes of Arabidopsis wt and *ca1ca2* lines. Mitochondria were isolated as described in the Materials and methods. Mitochondrial membrane proteins were separated by 2D BN/SDS PAGE and proteins were stained by colloidal Coomassie (A). Three replicates were produced per fraction and used for the calculation of a master gel (Delta 2D software package, Decodon, Germany) (B). The molecular masses of standard proteins are given to the left of the 2-D gels (in kDa). OXPHOS complexes are boxed in (B); their identities are given above the gels (I, complex I; V, complex V; III$_2$, dimeric complex III; I+III$_2$, supercomplex formed of complex I and dimeric complex III; F$_1$, F$_1$ part of complex V; IV, complex IV; II, complex II). Proteins indicated in pink are less abundant in the mutant (>1.5-fold decrease); proteins indicated in green are more abundant in the mutant (>1.5-fold increase). Spots indicated by numbers were identified by mass spectrometry (for results see Supplementary Table S2).

Comparison of the mitochondrial proteomes of wt and ca1ca2 lines using 2D BN/SDS PAGE

As previously reported, the *ca1ca2* mutant shows changes in the activities of complex II and complex IV (Fromm *et al.*, 2016*c*). In order to evaluate changes in the amounts of the OXPHOS complexes II–V in the absence of complex I in more detail, comparative proteome experiments by 2D BN/SDS PAGE were performed with mitochondrial membrane fractions of wt and *ca1ca2* cell culture lines. The comparisons were based on two methods: (i) Delta 2D-mediated comparison of 2-D gels, and (ii) fluorophore based comparison (2D DIGE).

Visual inspection of the 2D BN/SDS gels used for Delta 2D comparison clearly revealed the absence of complex I and the I+III$_2$ supercomplex in the mutant (Fig. 2A). On the resulting overlay image (Fig. 2B) the complexes III$_2$ and V are more-or-less unchanged, while the complexes II and IV are clearly increased in the mutant. Average spot volumes were calculated for each complex in the two fractions using the Delta 2D software (Fig. 2B, Table 2). The following amounts of the OXPHOS complexes were found for the mutant (wt=100%): complex II, 133%; complex III, 108%; complex IV, 200%; and complex V, 107%. Proteins within 16 spots were analysed by MS (Supplementary Table S2) and all revealed the expected identifications (see the 2D BN/SDS GelMap of the Arabidopsis mitochondrial proteome for comparison, https://gelmap.de/1227).

Table 2. *Relative spot volumes of OXPHOS complexes in* ca1ca2 *lines. Proteins were separated by 2D BN/SDS PAGE (Fig. 2), normalized spot volumes of differential OXPHOS subunits were summed up and relative spot volumes were calculated by the Delta 2D software package*

OXPHOS complex	relative spot volume with respect to wt plants (%)
Complex I	- *
Complex II	133
Complex III	108
Complex IV	200
Complex V	107

* not detectable

A more extended comparison of the mitochondrial membrane proteomes of mutant and wt cell lines was carried out based on 2D BN/SDS DIGE (Fig. 3, Supplementary Table S3). Spots differing in volumes between the two fractions were analysed by MS. After applying a MASCOT threshold score of 60, overall 147 identified proteins were included in further analyses; however, a difference in spot volume only could be assigned to a specific protein if a spot included only one main protein. This further reduced the number of unambiguously changed proteins to 44. These were grouped according to functional context. Changes of individual

subunits of OXPHOS complexes were in accordance with the results of the Delta 2D analysis. In addition, several other membrane proteins were found to be of changed abundance in the mutant. Seven subunits of the TIM and TOM transport machineries and one ABC transporter were identified. All were more abundant in the *ca1ca2* mutant.

Comparison of total protein extracts of wt and ca1ca2 *lines by label-free quantitative shotgun proteomics*

In addition to effects on the mitochondrial compartment, the consequences of *ca1ca2* deletion at the whole-plant level were investigated. Wild type and *ca1ca2* mutant plants were harvested at a comparable growth stage and differential protein abundances were analysed by comparative quantitative shotgun MS (note that growth and development of *ca1ca2* plants is much delayed; see Fromm *et al.*, 2016c). The experiment was based on five biological replicates. In total, 2233 different proteins were identified. The quantitative analysis of identified proteins was carried out using MaxQuant. After application of a –log10 *P*-value (*P*>1.31), 318 proteins of changed amounts were confirmed (Supplemantary Table S4) and were included in further analyses.

The proteins were assigned into categories according to subcellular localization and functional context. Subcellular localization was assigned according to SUBAcon (Fig. 4). Most of the identified proteins are localized in the cytosol (30.4%), followed by plastids (29.4%), mitochondria (15.2%), and other compartments with minor contributions (Fig. 4A). Proteins of increased abundance in *ca1ca2* plants are mostly localized in the cytosol (44.1%) and mitochondria (19.8%) (Fig. 4B). In contrast, proteins of decreased abundance in *ca1ca2* plants are mostly localized in plastids (62.3%) (Fig. 4C).

Assignment of proteins differing in amount between wt and *ca1ca2* mutant plants to functional categories was carried out according to TAIR functional annotations (https://www. arabidopsis.org/, TAIR10 genome release) and evaluated by MapMan (Fig. 5, Table 3). Proteins especially induced in mutant plants are involved in glycolysis, fermentation, the TCA cycle, amino acid metabolism, redox regulation, protein folding, as well as stress responses (Supplemantary Table S4). Decreased protein abundances in *ca1ca2* plants were mainly found in the functional categories of photosynthesis (photosystem I, photosystem II, Calvin cycle, photorespiration) and tetrapyrrole synthesis (Fig. 5). As expected, complex I subunits were much decreased in the mutant. At the same time, AOX1A (AT3G22370) and alternative NADH dehydrogenase NDB2 (AT4G05020) were clearly induced.

Finally, we analysed the BIN coverage of the identified proteins in order to assess the influence of the absence of complex I on cellular processes (Table 4). We calculated the number of identified proteins in relation to the number of genes that code for proteins of the BINs. The following BINs were most significantly changed in the mutant: fermentation (28.6%), glycolysis (15.4%), nitrogen metabolism (15.4%), TCA cycle (13.8%), photosynthesis (12.6%), tetrapyrrole synthesis (11.1%), mitochondrial ETC (7.5%), and amino acid metabolism (6.8%). The BIN coverage indicates that these cellular process are particularly affected by absence of complex I.

Changes in protein levels in *ca1ca2* plants with respect to wildtype plants as obtained by label-free quantitative shotgun proteomics are summarized in Fig. 6 and in the discussion below.

Discussion

In previous studies, the *ca1ca2* mutant has been characterized with respect to development, mitochondrial metabolism, and features of the OXPHOS system (Fromm *et al.*, 2016c). In
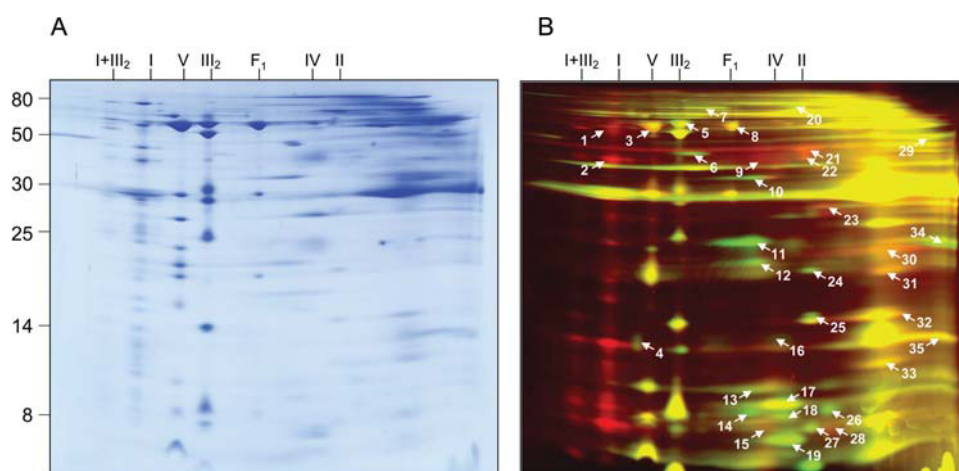

Fig. 3. Comparative analysis of the mitochondrial membrane proteomes of Arabidopsis wt and *ca1ca2* lines by differential gel electrophoresis (DIGE). Mitochondria were isolated as described in the Materials and Methods. Mitochondrial membrane proteins of wt and *ca1ca2* were labeled with different CyDyes and separated by 2D BN/SDS PAGE. Proteins were stained by colloidal Coomassie (A). The same gel was used for fluorescence detection of the two CyDyes (B). The molecular masses of standard proteins are given to the left of the 2-D gel (in kDa). The identities of selected mitochondrial protein complexes are given above the gels (I, complex I; V, complex V; III₂, dimeric complex III; I+III₂, supercomplex formed of complex I and dimeric complex III; F₁, F₁ part of complex V; IV, complex IV; II, complex II). Proteins indicated in red are less abundant in the *ca1ca2* mutant (>1.5-fold decrease) and proteins indicated in green are more abundant in the *ca1ca2* mutant (>1.5-fold increase). Proteins given in yellow are not changed in abundance. Spots indicated by numbers were identified by mass spectrometry (for results see Supplementary Table S3). Note: if compared to the comparative experiment shown in Fig. 2, several subunits of OXPHOS complexes appear to be absent in the DIGE approach. This is due to the fact that CyDye labeling takes place at native conditions. As a consequence, only proteins exposed to the surface of protein complexes are labeled. In contrast, image evaluation based on the Delta 2D approach (Fig. 2) allows visualization of all subunits of a protein complex.
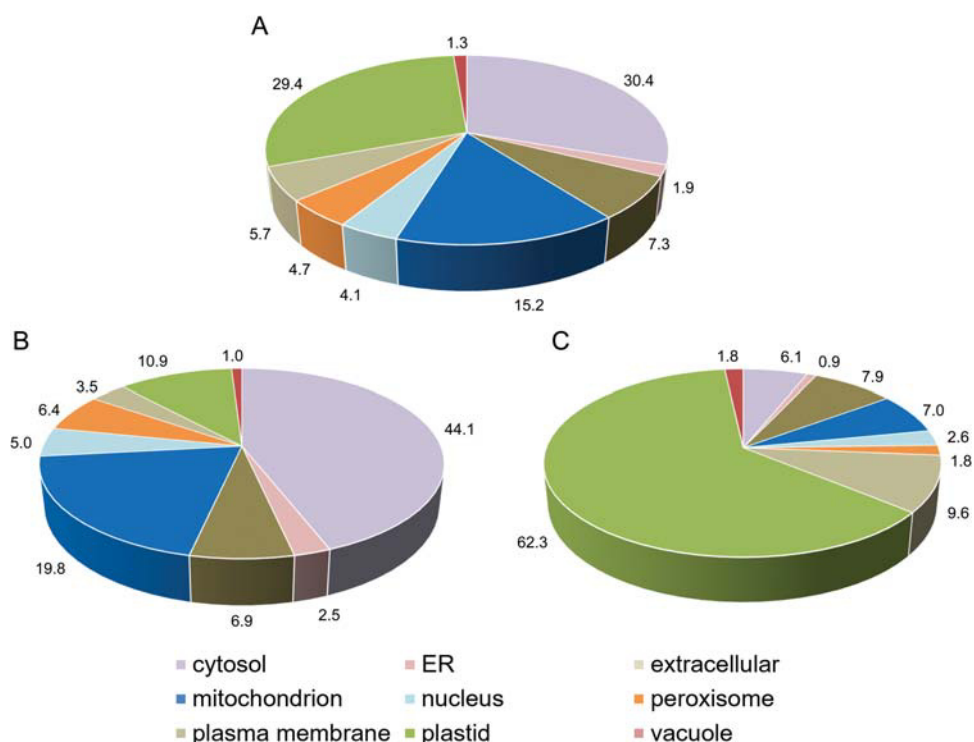
Fig. 4. Subcellular localization of proteins of altered abundances in the *ca1ca2* line as obtained by label free quantitative shotgun proteomics. Total protein was extracted from wt and *ca1ca2* mutant plants at a similar developmental stage. Proteins were identified and quantified by shotgun MS (for details see the Material and Methods). Predicted localizations of proteins of changed abundances between the two lines were obtained from the SUBA3 database (http://suba3.plantenergy.uwa.edu.au/). (A) Predicted localization of all proteins changed (*P*-value <0.05). (B) Predicted localization of proteins more abundant in *ca1ca2* compared to wt. (C) Predicted localization of proteins less abundant in *ca1ca2* mutant compared to wt. Numbers indicate amounts relative to the sum of altered protein species (%).
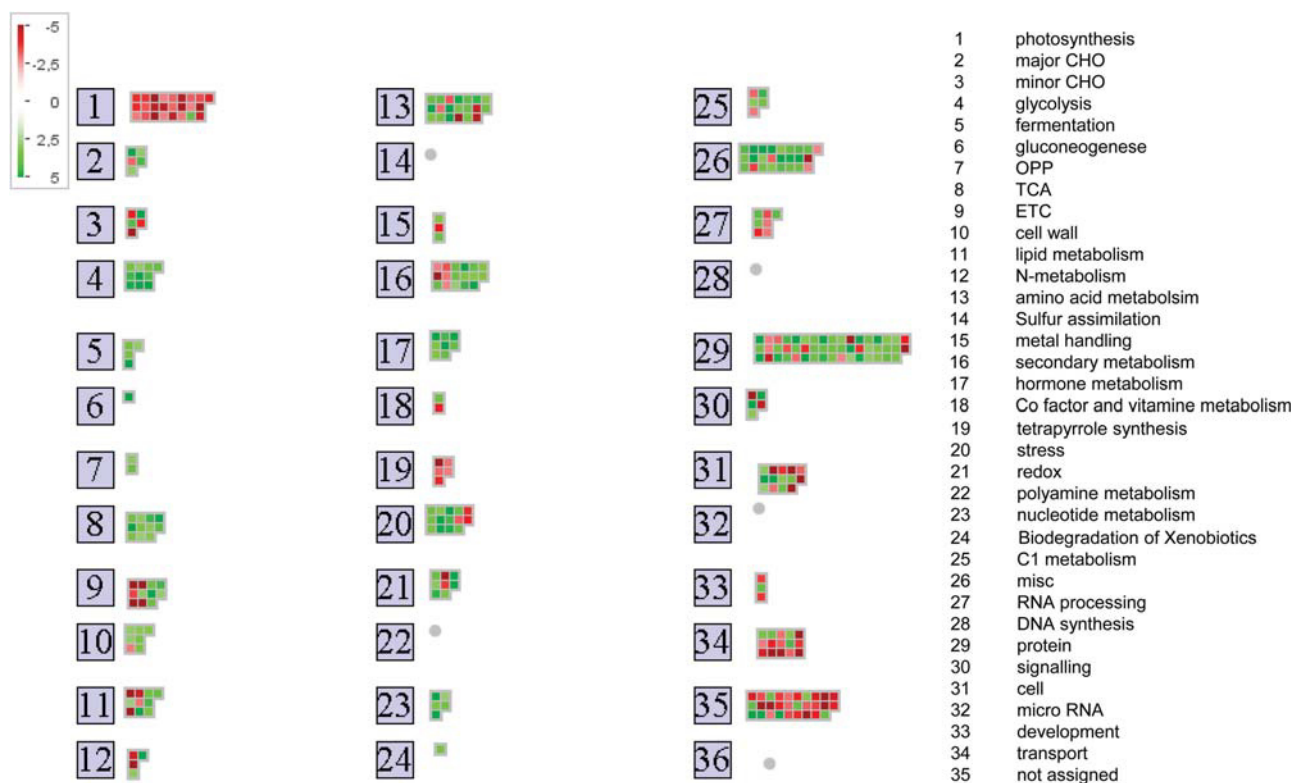
Fig. 5. Functional annotation of proteins identified by quantitative label-free shotgun MS. The 318 proteins of differential abundances between wt and *ca1ca2* mutant plants were grouped into functional BINs using MapMan. BINs are given to the right. Proteins more abundant in *ca1ca2* are indicated in green and proteins that are less abundant in red (*P*-value <0.05). Each square represents one protein. BINs without any identified protein are with a grey dot (for results see Supplementary Table S4).

order to systematically monitor the consequences of the double gene deletion on the mitochondrial proteome and the entire leaf proteome, we report here the results of three different experimental approaches, two of which were based on gel electrophoresis and one on gel-free shotgun proteomics. All three experimental systems have advantages and limitations. 2D IEF/SDS PAGE-based analyses excel in investigating prominent hydrophilic proteins. 2D BN/SDS PAGE is strong in analysing membrane proteins and membrane-bound protein complexes, which also are relatively abundant. Shotgun proteome analysis is a less systematic approach that allows the analysis of a very large number of proteins at the same time, and as such it better covers proteins of comparatively low abundance than the two gel-based approaches. Furthermore it should be noted that the 2D IEF/SDS and 2D BN/SDS PAGE approaches were carried out using cell cultures whereas shotgun proteomics was performed on total protein extracts from leaves. Cell suspension cultures are always well supplied with sucrose, whereas plants have to generate sugars by photosynthesis on their own. Therefore, the outcomes of the three experimental approaches need to be compared critically (Tables 1 and 3).

Although the three experimental systems and the sources of the analysed protein fractions differed, all the approaches gave similar results in respect to proteomic alterations taking place in the *ca1ca2* double-knock-out mutant. As expected, all the approaches indicated a dramatic reduction of complex I subunits. However, residual levels of non-assembled complex I proteins seem to be present in the mutant's mitochondria.

Levels of complex II and especially complex IV were much higher in the double-mutant, as were the levels of some of the alternative oxidoreductases of the plant mitochondrial OXPHOS system. This has been previously reported for other complex I mutants (Keren *et al.*, 2012; Hsu *et al.*, 2014). Upregulation of complex IV points to elevated proton translocation at the final segment of the mETC, which could partially compensate for the diminished proton translocation at the first segment of the mETC in the absence of complex I. Indeed, increased *in vitro* activity of complex IV in the *ca1ca2* mutant has been shown previously (Fromm *et al.*, 2016c). An increased oxygen consumption of *ca1ca2* mitochondria was observed if succinate was used as substrate (Supplemantary Fig. S2). This might indicate a higher complex II activity, but could also be the consequence of an elevated electron flux through the mETC caused by higher complex IV activity.

In contrast, levels of the complexes III and V were rather similar in the *ca1ca2* and wt lines, although relative abundances of some subunits of these complexes were altered (Supplemantary Tables S1 and S2). The overall upregulation of the OXPHOS complexes in mutant cells requires increased import rates of the corresponding nuclear encoded subunits by the TOM and TIM pre-protein import machineries (Murcha *et al.*, 2014). Indeed, levels of TIM and TOM subunits clearly went up in the double-mutant (Fig. 1, Supplemantary Table S3).

The alternative NADH dehydrogenase NDB2 (AT4G05020) and the alternative oxidase AOX1A (AT3G22370) were induced 4- and 8-fold higher in the mutant (Supplemantary Table S4). This corresponds to increased capacity for alternative oxidase in the *ca1ca2* mutants (Supplemantary Fig. S2). An increase of AOX has been previously reported for several plant complex I mutants, e.g. the *nmat1*, *opt43*, *cmsII*, *ndufv1*, and *mTerf15* lines (Gutierres *et al.*, 1999; de Longevialle *et al.*, 2007; Keren *et al.*, 2012; Hsu *et al.*, 2014; Kühn *et al.*, 2015; see Table 5 for information on complex I mutants discussed in this section). Indeed, increased oxygen consumption rates have been observed for some complex I mutants, e.g. the *ca1ca2* and *ndufv1* lines (Kühn *et al.*, 2015; Fromm *et al.*, 2016c).

Induction of the alternative oxidoreductases of the respiratory chain is known to be an integral part of the general plant stress response (Vanlerberghe, 2013). This, together with the induction of a large number of further stress related proteins [such as beta glucosidases (AT1G66270,

Table 3. *Relative protein intensities of altered proteins involved in defined functional processes in* ca1ca2 *mutant lines analysed by label-free quantitative shotgun MS approach. Proteins were identified and quantified using MaxQuant software*

Functional context (number of proteins of changed abundance)	Relative protein intensities with respect to wt plants (%)
Fermentation (4)	183
Glycolysis (10)	173
Protein folding (9)	172
Oxidative pentose phosphate (2)	166
Signalling (5)	162
Redox (8)	160
TCA cycle (11)	159
Stress response (14)	152
Amino acid metabolism (17)	149
Mitochondrial electron transport without complex I (5)	144
Cell wall (7)	140
Cell organisation (14)	132
Miscellaneous proteins (25)	121
Lipid metabolism (10)	120
Secondary metabolism (13)	114
Protein processing (6)	110
Protein degradation (18)	102
Protein synthesis (11)	95
Co-factor and vitamine metabolism (2)	89
Development (3)	89
Metal handling (2)	89
Protein targeting (7)	85
Uncharacterized (29)	81
Carbon metabolism (14)	79
Transport (15)	78
Photorespiration (4)	75
Calvin cycle (9)	66
Photosystem II (4)	66
Photosystem I (2)	66
Tetrapyrrole synthesis (5)	65
Light reaction others (3)	64
N-metabolism (4)	64
Processing of nucleic acids (11)	63
ATP synthase (plastid) (3)	61

3088 | Fromm *et al.*

Table 4. *BIN coverage of proteins of altered abundances in* ca1ca2 *plants as determined by label-free quantitative shotgun MS*

MapMan BIN	BIN name	Sum of genes	Number of differential proteins in wt and *ca1ca2*	Number of differential proteins / sum of genes per BIN (%)
5	Fermentation	14	4	28.6
4	Glycolysis	65	10	15.4
12	N-metabolism	26	4	15.4
8	TCA	80	11	13.8
1	Photosynthesis	199	25	12.6
19	Tetrapyrrole synthesis	45	5	11.1
25	C1 metabolism	39	4	10.3
6	Gluconeogenese	10	1	10.0
9	Mitochondrial electron transport	146	11	7.5
13	Amino acid metabolism	251	17	6.8
7	Oxidative pentose phosphate pathway	31	2	6.5
2	Major carbon metabolism	100	5	5.0
21	Redox	194	8	4.1
3	Minor carbon metabolism	124	5	4.0
24	Biodegradation of Xenobiotics	27	1	3.7
15	Metal handling	67	2	3.0
16	Secondary metabolism	438	13	3.0
23	Nucleotide metabolism	169	5	3.0
18	Co-factor and vitamine metabolism	79	2	2.5
11	Lipid metabolism	398	10	2.5
31	Cell organisation	746	14	1.9
26	Miscellaneous proteins	1397	25	1.8
20	Stress response	874	14	1.6
34	Transport	996	15	1.5
29	Protein folding and processing	3409	51	1.5
10	Cell wall	496	7	1.4
17	Hormone metabolism	495	5	1.0
33	Development	681	3	0.4
30	Signalling	1239	5	0.4
35	Not assigned	7748	29	0.4
27	RNA processing	2567	6	0.2
14	Sulfur assimilation	12	0	0.0
32	Micro RNA	4	0	0.0
28	DNA synthesis	1352	0	0.0
22	Polyamine metabolism	18	0	0.0

AT3G09260, AT3G09260, AT3G16420), catalase 3 (AT1G20620), ascorbate peroxidase 4 (AT4G09010) and glutathione syntethase 2 (AT5G27380)] in the double-mutant strongly indicates that the absence of complex I strongly affects the metabolic balance and the redox homeostasis of the plant cell.

High levels of complex II, complex IV, and alternative oxidoreductases of the mETC require increased provision of electrons to the mETC. Indeed, the enzymes involved in glycolysis were clearly induced in the double-mutants. It has been shown previously for the *ndufv1* mutant, which also completely lacks mitochondrial complex I, that complex I deficiency causes a metabolic switch and that flux through glycolysis significantly increases (Kühn *et al.*, 2015). Furthermore, our data point to an extended usage of fermentation to compensate for decreased ATP generation and decreased capacity of NADH oxidation by the complex I-deficient mETC. In contrast, the proteomic changes with respect to the citric acid cycle are more difficult to understand, as some enzymes are reduced

whereas others are increased in the *ca1ca2* double-mutant. This points to a scenario that the absence of complex I does not induce the entire citric acid cycle, but rather specific segments of the pathway. Indeed, it is known that plant mitochondria have, depending on the physiological state of the respective cell, quite a number of non-cyclic operation modi with respect to the citric acid cycle (Sweetlove *et al.*, 2010).

Electrons for the mETC can also originate from amino acid breakdown (Sweetlove *et al.*, 2010; Schertl and Braun 2014; Hildebrandt *et al.*, 2015). Several proteins involved in mitochondrial amino acid catabolism were identified by our shotgun proteome approach and found to be induced in the *ca1ca2* mutant, e.g. alanine, tyrosine, and branched-chain aminotransferases (AT1G17290, AT4G23600, AT3G19710), glutamate dehydrogenase (AT5G18170, AT5G07440), arginase (AT4G08870), and methylmalonate-semialdehyde dehydrogenase (AT2G14170). The latter enzyme is involved in a step of branched-chain amino acid oxidation. The number of electrons provided for the mETC from amino acid breakdown
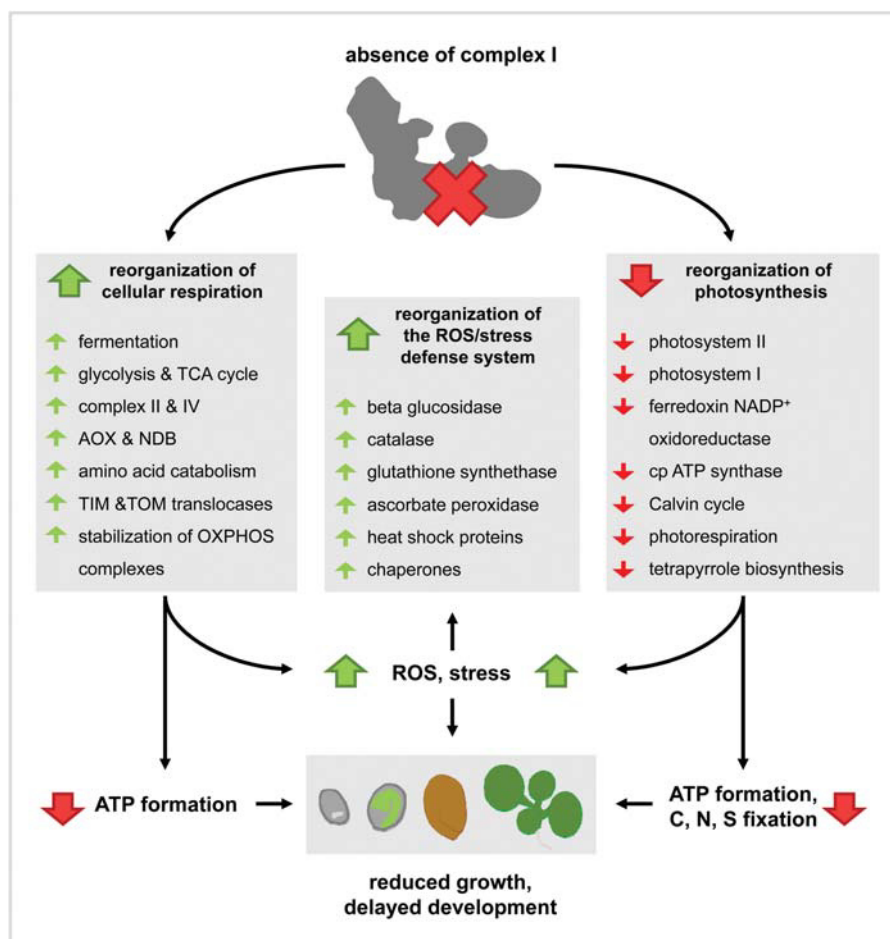
Fig. 6. Life without complex I. The figure is based on altered protein levels in *ca1ca2* plants relative to wildtype plants as obtained by label-free quantitative shotgun proteomics. Green arrows within the grey boxes indicate increased protein levels in the double-mutant, and red arrows indicate decreased levels. Absence of complex I causes reorganization of the cellular respiration system. Since electron insertion into the first segment of the mETC is not possible, increased electron insertion at later segments takes place (induction of complexes II, IV). This requires increased oxidation of organic substrates (induction of enzymes of glycolysis, the TCA cycle, and amino acid catabolism). Mitochondrial ATP formation most likely is still reduced, which requires increased fermentation. The growth rate of the double-mutant is drastically reduced. This is reflected by reduced amounts of the two photosystems, Calvin cycle enzymes, and enzymes of the tetrapyrrole biosynthesis pathway. Furthermore, altered metabolism and electron transport pathways in the mitochondria and chloroplasts cause increased ROS formation and stress symptoms. Several components of the ROS and stress defense system are induced in the double-mutant, as is the alternative oxidase, a well-known stress indicator in plants. Note: causal events indicated by black arrows do not necessarily indicate primary effects, but may well represent indirect consequences. For further details see the discussion section.

is especially high during oxidation of the branched chain amino acids (Hildebrandt *et al.*, 2015).

Prohibitins and stomatin-like proteins (SLP) were very much increased in the *ca1ca2* mutant, as revealed by all three proteome analyses. In animal cells respiratory supercomplexes are stabilized by cardiolipin and SLPs. SLPs can bind cardiolipin and interact with prohibitins (Mitsopoulos *et al.*, 2015). Similar interactions have also been reported for the mitochondria of plants (Gehl *et al.*, 2014; Gehl and Sweetlove, 2014). Knock-out mutants for *slp1* have reduced complex I levels and activity, and form lower amounts of supercomplexes, indicating that SLPs and prohibitins can affect the assembly and/or the stability of OXPHOS complexes (Gehl *et al.*, 2014). Complex I subunits that cannot be assembled might be stabilized to a certain degree by prohibitins and SLPs. Furthermore, prohibitins play a role in mitochondrial DNA organization, stress tolerance, and triggering

retrograde signals in response to stress and mitochondrial dysfunction (Van Aken *et al.*, 2010).

The phenotype of complex I mutant plants often includes curled leaves and a delayed vegetative and reproductive development (de Longevialle *et al.*, 2007; Meyer *et al.*, 2009; Wang *et al.*, 2012; Kühn *et al.*, 2015; Hsu *et al.*, 2014). The degree of the developmental delay and the curly leaf phenotype are dependent on the amount of residual complex I (Kühn *et al.*, 2015). For example, trace amounts of complex I are sufficient for plants to pass through embryogenesis, whereas mutants lacking complex I, such as *cal1cal2*, *opt43*, *indh*, *ndufv1*, and *ca1ca2*, cannot complete this developmental stage and hardly germinate (de Longevialle *et al.*, 2007; Wang *et al.*, 2012; Wydro *et al.*, 2013; Kühn *et al.*, 2015; Fromm *et al.*, 2016c). The growth rate of the *ca1ca2* mutant has been reported to be drastically reduced (Fromm *et al.*, 2016c). This is clearly reflected by our shotgun proteome data.

Table 5. *Summary of complex I mutants in plants*

Name of mutant	Mutation of ...	Complex I depletion (i) or absence of complex I (ii)	Plant species	Reference
ca2	Complex I subunit	i	*Arabidopsis thaliana*	Perales *et al.*, 2005 & Fromm *et al.*, 2016c
ca1ca2	Complex I subunit	ii	*Arabidopsis thaliana*	Fromm *et al.*, 2016c
cal1cal2i	Complex I subunits	i	*Arabidopsis thaliana*	Fromm *et al.*, 2016b
ca2cal1 or ca2cal2	Complex I subunits	i	*Arabidopsis thaliana*	Soto *et al.*, 2015
ndufs4	Complex I subunit	i	*Arabidopsis thaliana*	Kühn *et al.*, 2015
ndufv1	Complex I subunit	ii	*Arabidopsis thaliana*	Kühn *et al.*, 2015
gldh	Assembly factor	ii	*Arabidopsis thaliana*	Pineau *et al.*, 2008
indh	Assembly factor	ii	*Arabidopsis thaliana*	Wydro *et al.*, 2013
opt43	*NAD1* splicing factor	ii	*Arabidopsis thaliana*	de Longevialle *et al.*, 2007
nMat1	*NAD1* splicing factor	ii	*Arabidopsis thaliana*	Keren *et al.*, 2012
mTERF15	*NAD2* splicing factor	ii	*Arabidopsis thaliana*	Hsu *et al.*, 2014
nms1	*NAD4* splicing factor	i	*Nicotiana sylvestris*	Brangeon *et al.*, 2000
slo3	*NAD7* splicing factor	i	*Arabidopsis thaliana*	Hsieh *et al.*, 2015
bir6	*NAD7* splicing factor	i	*Arabidopsis thaliana*	Koprivova *et al.*, 2010
cmsII	Leads to NAD7 deletion	ii	*Nicotiana sylvestris*	Gutierres *et al.*, 1999
ncs2	Replacing the 3′-end of *NAD4* with sequences from *NAD7*	ii	*Zea mays*	Karpova *et al.*, 2002

Overall, proteins involved in developmental processes and photosynthesis were very much reduced in the *ca1ca2* mutant. More than 60% of the proteins of lower abundance in the *ca1ca2* mutant are localized in plastids (Fig. 4C). All detected subunits of the two photosystems (PS) were reduced, as were the ferredoxin-NADP$^+$ oxidoreductase (AT5G66190, AT1G20020) and the subunits of the chloroplast ATP synthase complex. The maize *ncsII* and *ncs6* mutants also have a decrease in PSI while other photosynthetic complexes are unaffected. The chloroplast ultrastructure is abnormal (Roussel *et al.*, 1991; Jiao *et al.*, 2005). Two recently described small twin cystein proteins, which are specifically induced in complex I-deficient plants, also specifically affect chloroplast metabolism (Wang *et al.*, 2016). Furthermore, enzymes involved in the Calvin cycle are of reduced abundance in *ca1ca2* plants. This indicates substantial consequences of the absence of complex I on photosynthesis. Additionally, tetrapyrrole synthesis is impaired. Tetrapyrroles are essential for chlorophyll biosynthesis. It has been suggested that reduction of photosynthetic proteins may be caused by impaired chlorophyll synthesis (Brzezowski *et al.*, 2015). Our results are in line with those obtained for the *cmsII* mutant of *Nicotiana sylvestris*, which also lacks complex I. In *cmsII* mutants photosynthetic efficiency is reduced (Sabar *et al.*, 2000; Dutilleul *et al.*, 2003). Defects in the photosystems may result in ROS formation (Schmitt *et al.*, 2014). Higher ROS levels have indeed been observed in the *ca1ca2* and other complex I mutants (Keren *et al.*, 2012; Córdoba *et al.*, 2016; Fromm *et al.*, 2016c).

ROS may cause cellular damage and programmed cell death (Li and Xing, 2010), and thus they negatively affect plant development. Our proteome data indicate that seed photosynthesis in *ca1ca2* mutant embryos may also be impaired by complex I dysfunction. A higher ROS content has been found in *ca1ca2* embryos (Córdoba *et al.*, 2016, Ostersetzer-Brian 2016). Defects in the photosynthetic apparatus should cause decreased synthesis and accumulation of seed storage compounds, which will be further impaired by mitochondrial dysfunction (Schwender *et al.*, 2006). Seed storage compounds such as fatty acids are essential to drive the germination process (Carrie *et al.*, 2013). *ca1ca2* mutant embryos depleted in energy-rich components are not able to develop normally during germination, which results in seed abortion (Córdoba *et al.*, 2016, Fromm *et al.*, 2016c).

Reduced photosynthesis affects photorespiration. Indeed, all the identified proteins of the photorespiration pathway were reduced in the *ca1ca2* mutant. This also applies for the T and the P subunits of the mitochondrial glycine decarboxylase complex (GDC) (AT1G11860; AT2G26080). Down-regulation of the GDC complex has been reported to be caused either by impaired photosynthesis or by feedback inhibition by an elevated NADH pool in the matrix (Oliver, 1994; Peterhänsel *et al.*, 2010), which may be caused by the absence of complex I.

Besides the absence of the electron transfer function of complex I, which is coupled to proton translocation across the inner mitochondrial membrane, complex I is assumed to include further enzymatic and transport functions (Braun *et al.*, 2014). In particular, the complex I-integrated carbonic anhydrase subunits have been suggested to play a role in recycling mitochondrial CO_2 for carbon fixation in the chloroplasts (Zabaleta *et al.*, 2012). Thus it may well be that the *ca1ca2* mutant lacks more than just the NADH-ubiquinone-oxidoreductase activity. However, the *ca1ca2* mutant very much behaves like other mutants that completely lack complex I, e.g. *ndufv1* (Kühn *et al.*, 2015). Furthermore, in mutants lacking complex I due to the absence of other complex I subunits the formation of the carbonic anhydrase domain is also prevented. This makes the *ca1ca2* mutant an excellent model for studying the role of mitochondrial

complex I in plants, the proteomic level of which has been addressed in this study.

Conclusions

'Life without complex I' is not so easy, even in plants that possess some alternative dehydrogenases in the mitochondrial compartment (which, however, do not contribute to the proton gradient across the inner mitochondrial membrane). The metabolic balance of the plant cell is deeply disturbed in the absence of complex I. Complex I dysfunction causes reorganization of cellular respiration and affects metabolic processes in mitochondria, plastids, peroxisomes, and other cellular compartments with drastic consequences for growth and development. Specifically, proteins involved in glycolysis and the TCA cycle are induced, as are subunits of other OXPHOS complexes, especially the complex IV. This requires an upregulation of the TIM and TOM translocases for mitochondrial protein import. Furthermore, alternate electron entry pathways into the mETC are induced, e.g. oxidation of amino acids. Increased flux of electrons through the mETC causes elevated ROS formation in *ca1ca2* plants. ATP formation in the chloroplasts is reduced by decreased photosynthesis, e.g. caused by defective chlorophyll biosynthesis in *ca1ca2* mutant plants. In summary, plant cells metabolically rearrange in the absence of complex I in order to maintain a minimum level of energy supply and to balance redox homeostasis. At the same time, *ca1ca2* mutants suffer from increased ROS production and reduced ATP generation by both, respiration and photosynthesis.

Supplementary data

Supplementary data are available at *JXB* online.

Figure S1. Growth phenotype of *ca1ca2* plants, in the absence of complex I.

Figure S2. Respiration through complex II and the AOX capacity of mitochondria derived from *Arabidopsis thaliana* wildtype (wt) and *ca1ca2* double-mutant lines.

Table S1. (a) Proteins of altered abundance in the *ca1ca2* mutant as revealed by 2D IEF/SDS PAGE (see Fig. 1). (b) Short version of (a).

Table S2. Identification of proteins from wt and *ca1ca2* mutant lines after separation by 2D BN/SDS PAGE and gel evaluation by Delta 2D software (see Fig. 2).

Table S3. Identification of proteins from wt and *ca1ca2* mutant lines after analysis by 2D BN/SDS DIGE (see Fig. 3).

Table S4. (a) Proteins of altered abundance in the *ca1ca2* mutant as obtained by label-free quantitative shotgun MS analysis. (b) Short version of (a).

Acknowledgements

References

Angerer H, Zwicker K, Wumaier Z, *et al.* 2011. A scaffold of accessory subunits links the peripheral arm and the distal proton-pumping module of mitochondrial complex I. The Biochemical Journal **437,** 279–288.

Baradaran R, Berrisford JM, Minhas GS, Sazanov LA. 2013. Crystal structure of the entire respiratory complex I. Nature **494,** 443–448.

Berth M, Moser F, Kolbe M, Bernhardt J. 2007. The state of the art in the analysis of two-dimensional gel electrophoresis images. Applied Microbiology and Biotechnology **76,** 1223–1243.

Brandt U. 2006. Energy converting NADH:quinone oxidoreductase (complex I). Annual Review of Biochemistry **75,** 69–92.

Brangeon J, Sabar M, Gutierres S, *et al.* 2000. Defective splicing of the first nad4 intron is associated with lack of several complex I subunits in the *Nicotiana sylvestris* NMS1 nuclear mutant. The Plant Journal **21,** 269–280.

Braun HP, Binder S, Brennicke A, *et al.* 2014. The life of plant mitochondrial complex I. Mitochondrion **19,** 295–313.

Brzezowski P, Richter AS, Grimm B. 2015. Regulation and function of tetrapyrrole biosynthesis in plants and algae. Biochimica et Biophysica Acta **1847,** 968–985.

Cardol P, Vanrobaeys F, Devreese B, van Beeumen J, Matagne RF, Remacle C. 2004. Higher plant-like subunit composition of mitochondrial complex I from *Chlamydomonas reinhardtii*: 31 conserved components among eukaryotes. Biochimica et Biophysica Acta **1658,** 212–224.

Carrie C, Murcha MW, Giraud E, Ng S, Zhang MF, Narsai R, Whelan J. 2013. How do plants make mitochondria? Planta **237,** 429–439.

Carroll J, Fearnley IM, Skehel JM, Shannon RJ, Hirst J, Walker JE. 2006. Bovine complex I is a complex of 45 different subunits. The Journal of Biological Chemistry **281,** 32724–32727.

Córdoba JP, Marchetti F, Soto D, Martin MV, Pagnussat GC, Zabaleta E. 2016. The CA domain of the respiratory complex I is required for normal embryogenesis in *Arabidopsis thaliana*. Journal of Experimental Botany **67,** 1589–1603.

Cox J, Mann M. 2008. MaxQuant enables high peptide identification rates, individualized p.p.b.-range mass accuracies and proteome-wide protein quantification. Nature Biotechnology **26,** 1367–1372.

de Longevialle AF, Meyer EH, Andrés C, Taylor NL, Lurin C, Millar AH, Small ID. 2007. The pentatricopeptide repeat gene OTP43 is required for trans-splicing of the mitochondrial nad1 Intron 1 in *Arabidopsis thaliana*. The Plant Cell **19,** 3256–3265.

Dudkina NV, Eubel H, Keegstra W, Boekema EJ, Braun HP. 2005. Structure of a mitochondrial supercomplex formed by respiratory-chain complexes I and III. Proceedings of the National Academy of Sciences, USA **102,** 3225–3229.

Dutilleul C, Driscoll S, Cornic G, Paepe R de, Foyer CH, Noctor G. 2003. Functional mitochondrial complex I is required by tobacco leaves for optimal photosynthetic performance in photorespiratory conditions and during transients. Plant Physiology **131,** 264–275.

Eubel H, Jänsch L, Braun HP. 2003. New insights into the respiratory chain of plant mitochondria. Supercomplexes and a unique composition of complex II. Plant Physiology **133,** 274–286.

Friedrich T. 2001. Complex I: a chimaera of a redox and conformation-driven proton pump? Journal of Bioenergetics and Biomembranes **33,** 169–177.

Friedrich T, Böttcher B. 2004. The gross structure of the respiratory complex I: a Lego System. Biochimica et Biophysica Acta **1608,** 1–9.

Fromm S, Senkler J, Zabaleta E, Peterhänsel C, Braun HP. 2016*a*. The carbonic anhydrase domain of plant mitochondrial complex I. Physiologia Plantarum : in press, doi: 10.1111/ppl.12424.

Fromm S, Göing J, Lorenz C, Peterhänsel C, Braun HP. 2016*b*. Depletion of the "gamma-type carbonic anhydrase-like" subunits of complex I affects central mitochondrial metabolism in *Arabidopsis thaliana*. Biochimica et Biophysica Acta **1857,** 60–71.

3092 | Fromm *et al.*

Fromm S, Braun HP, Peterhänsel C. 2016*c*. Mitochondrial gamma carbonic anhydrases are required for complex I assembly and plant reproductive development. New Phytologist : in press, doi: 10.1111/nph.13886.

Gehl B, Sweetlove LJ. 2014. Mitochondrial Band-7 family proteins: scaffolds for respiratory chain assembly? Frontiers in Plant Science **5,** 141.

Gehl B, Lee CP, Bota P, Blatt MR, Sweetlove LJ. 2014. An Arabidopsis stomatin-like protein affects mitochondrial respiratory supercomplex organization. Plant Physiology **164,** 1389–1400.

Gutierres S, Combettes B, de Paepe R, Mirande M, Lelandais C, Vedel F, Chétrit P. 1999. In the *Nicotiana sylvestris* CMSII mutant, a recombination-mediated change 5′ to the first exon of the mitochondrial nad1 gene is associated with lack of the NADH:ubiquinone oxidoreductase (complex I) NAD1 subunit. European Journal of Biochemistry **261,** 361–370.

Hildebrandt TM, Nunes Nesi A, Araujo WL, Braun HP. 2015. Amino acid catabolism in plants. Molecular Plant **8,** 1563–1579.

Hooper CM, Tanz SK, Castleden IR, Vacher MA, Small ID, Millar AH. 2014. SUBAcon: a consensus algorithm for unifying the subcellular localization data of the Arabidopsis proteome. Bioinformatics **30,** 3356–3364.

Hsieh W, Liao J, Chang C, Harrison T, Boucher C, Hsieh M. 2015. The SLOW GROWTH3 pentatricopeptide repeat protein is required for the splicing of mitochondrial NADH dehydrogenase subunit7 intron 2 in Arabidopsis. Plant Physiology **168,** 490–501.

Hsu YW, Wang HJ, Hsieh MH, Hsieh HL, Jauh GY. 2014. Arabidopsis mTERF15 is required for mitochondrial nad2 Intron 3 splicing and functional complex I activity. PLoS ONE **9,** e112360.

Hunte C, Zickermann V, Brandt U. 2010. Functional modules and structural basis of conformational coupling in mitochondrial complex I. Science **329,** 448–451.

Jiao S, Thornsberry JM, Elthon TE, Newton KJ. 2005. Biochemical and molecular characterization of photosystem I deficiency in the NCS6 mitochondrial mutant of maize. Plant Molecular Biology **57,** 303–313.

Karpova OV, Kuzmin EV, Elthon TE, Newton KJ. 2002. Differential expression of alternative oxidase genes in maize mitochondrial mutants. The Plant Cell **14,** 3271–3284.

Keren I, Tal L, des Francs-Small, CC, Araujo WL, Shevtsov S, Shaya F, Fernie AR, Small I, Ostersetzer-Biran O. 2012. nMAT1, a nuclear-encoded maturase involved in the trans-splicing of nad1 intron 1, is essential for mitochondrial complex I assembly and function. The Plant Journal **71,** 413–426.

Klodmann J, Sunderhaus S, Nimtz M, Jänsch L, Braun HP. 2010. Internal architecture of mitochondrial complex I from *Arabidopsis thaliana*. The Plant Cell **22,** 797–810.

Koprivova A, des Francs-Small CC, Calder G, Mugford ST, Tanz S, Lee B, Zechmann B, Small I, Kopriva S. 2010. Identification of a pentatricopeptide repeat protein implicated in splicing of intron 1 of mitochondrial nad7 transcripts. The Journal of Biological Chemistry **285,** 32192–32199.

Kühn K, Obata T, Feher K, Bock R, Fernie AR, Meyer EH. 2015. Complete mitochondrial complex I deficiency induces an upregulation of respiratory fluxes that is abolished by traces of functional complex I. Plant Physiology **168,** 1537–1549.

Li L, Nelson CJ, Carrie C, Gawryluk RM, Solheim C, Gray MW, Whelan J, Millar AH. 2013. Subcomplexes of ancestral respiratory complex I subunits rapidly turn over *in vivo* as productive assembly intermediates in Arabidopsis. Journal of Biological Chemistry **288,** 5707–5717.

Li Z, Xing D. 2010. Mitochondrial pathway leading to programmed cell death induced by aluminum phytotoxicity in *Arabidopsis*. Plant Signaling and Behavior **5,** 1660–1662.

Lorenz C, Rolletschek H, Sunderhaus S, Braun HP. 2014. *Brassica napus* seed endosperm — Metabolism and signaling in a dead end tissue. Journal of Proteomics **108,** 382–426.

May MJ, Leaver CJ. 1993. Oxidative stimulation of glutathione synthesis in *Arabidopsis thaliana* suspension cultures. Plant Physiology **103,** 621–627.

Meyer EH, Solheim C, Tanz SK, Bonnard G, Millar AH. 2011. Insights into the composition and assembly of the membrane arm of plant complex I through analysis of subcomplexes in Arabidopsis mutant lines. Journal of Biological Chemistry **286,** 26081–26092.

Meyer EH, Tomaz T, Carroll AJ, Estavillo G, Delannoy E, Tanz SK, Small ID, Pogson BJ, Millar AH. 2009. Remodeled respiration in *ndufs4* with low phosphorylation efficiency suppresses Arabidopsis germination and growth and alters control of metabolism at night. Plant Physiology **151,** 603–619.

Mihr C, Braun HP. 2003 Proteomics in plant biology. In: Michael P. ed. *Handbook of proteomics methods* . Totowa: Humana, 409–416.

Mitchell P. 1961. Coupling of phosphorylation to electron and hydrogen transfer by a chemi-osmotic type of mechanism. Nature **191,** 144–148.

Mitsopoulos P, Chang Y, Wai T, Konig T, Dunn SD, Langer T, Madrenas J. 2015. Stomatin-like protein 2 is required for *in vivo* mitochondrial respiratory chain supercomplex formation and optimal cell function. Molecular and Cellular Biology **35,** 1838–1847.

Morgan DJ, Sazanov LA. 2008. Three-dimensional structure of respiratory complex I from *Escherichia coli* in ice in the presence of nucleotides. Biochimica et Biophysica Acta **1777,** 711–718.

Murcha MW, Wang Y, Narsai R, Whelan J. 2014.The plant mitochondrial protein import apparatus — The differences make it interesting. Frontiers of Mitochondrial Research **1840,** 1233–1245.

Neuhoff V, Stamm R, Eibl H. 1985. Clear background and highly sensitive protein staining with coomassie blue dyes in polyacrylamide gels: a systematic analysis. Electrophoresis **6,** 427–448.

Neuhoff V, Stamm R, Pardowitz I, Arold N, Ehrhardt W, Taube D. 1990. Essential problems in quantification of proteins following colloidal staining with coomassie brilliant blue dyes in polyacrylamide gels, and their solution. Electrophoresis **11,** 101–117.

Oliver DJ. 1994. The glycine complex from plant-mitochondria. Annual Review of Plant Physiology and Plant Molecular Biology **45,** 323–337.

Ostersetzer-Biran O. 2016. Respiratory complex I and embryo development. Journal of Experimental Botany **67,** 1205–1207.

Perales M, Eubel H, Heinemeyer J, Colaneri A, Zabaleta E, Braun HP. 2005. Disruption of a nuclear gene encoding a mitochondrial gamma carbonic anhydrase reduces complex I and supercomplex I+III$_2$ levels and alters mitochondrial physiology in Arabidopsis. Journal of Molecular Biology **350,** 263–277.

Perales M, Parisi G, Fornasari MS, *et al*. 2004. Gamma carbonic anhydrase like complex interact with plant mitochondrial complex I. Plant Molecular Biology **56,** 947–957.

Peterhänsel C, Horst I, Niessen M, Blume C, Kebeish R, Kurkcuoglu S, Kreuzaler F. 2010. Photorespiration. The Arabidopsis book / American Society of Plant Biologists **8,** e0130.

Peters K, Braun HP. 2012. Comparative analyses of protein complexes by blue native DIGE. Methods in Molecular Biology (Clifton, N.J.) **854,** 145–154.

Peters K, Belt K, Braun HP. 2013. 3D gel map of Arabidopsis complex I. Frontiers in Plant Science **4,** 153.

Pineau B, Layoune O, Danon A, Paepe R de. 2008. L-galactono-1,4-lactone dehydrogenase is required for the accumulation of plant respiratory complex I. The Journal of Biological Chemistry **283,** 32500–32505.

Rasmusson AG, Geisler DA, Møller IM. 2008. The multiplicity of dehydrogenases in the electron transport chain of plant mitochondria. Mitochondrion **8,** 47–60.

Roussell DL, Thompson DL, Pallardy SG, Miles D, Newton KJ. 1991. Chloroplast structure and function is altered in the NCS2 maize mitochondrial mutant. Plant Physiology **96,** 232–238.

Sabar M, De Pape R, de Kouchkovsky Y. 2000. Complex I impairment, respiratory compensations, and photosynthetic decrease in nuclear and mitochondrial male sterile mutants of *Nicotiana sylvestris*. Plant Physiology **124,** 1239–1250.

Sazanov LA. 2007. Respiratory complex I: mechanistic and structural insights provided by the crystal structure of the hydrophilic domain. Biochemistry **46,** 2275–2288.

Schertl P, Braun HP. 2014. Respiratory electron transfer pathways in plant mitochondria. Frontiers in Plant Science **5,** 163.

Schmitt FJ, Renger G, Friedrich T, Kreslavski VD, Zharmukhamedov SK, Los DA, Kuznetsov VV, Allakhverdiev SI. 2014. Reactive oxygen species: re-evaluation of generation, monitoring and role in stress-signaling in phototrophic organisms. Biochimica et Biophysica Acta **1837,** 835–848.

Schwender J, Shachar-Hill Y, Ohlrogge JB. 2006. Mitochondrial metabolism in developing embryos of *Brassica napus*. The Journal of Biological Chemistry **281,** 34040–34047.

Soto D, Córdoba JP, Villarreal F, Bartoli C, Schmitz J, Maurino VG, Braun HP, Pagnussat GC, Zabaleta E. 2015. Functional characterization of mutants affected in the carbonic anhydrase domain of the respiratory complex I in *Arabidopsis thaliana*. The Plant Journal **85,** 831–844.

Sunderhaus S, Dudkina NV, Jänsch L, Klodmann J, Heinemeyer J, Perales M, Zabaleta E, Boekema EJ, Braun HP. 2006. Carbonic anhydrase subunits form a matrix-exposed domain attached to the membrane arm of mitochondrial complex I in plants. The Journal of Biological Chemistry **281,** 6482–6488.

Sweetlove LJ, Beard, KFM, Nunes-Nesi A, Fernie AR, Ratcliffe RG. 2010. Not just a circle: flux modes in the plant TCA cycle. Trends in Plant Science **15,** 462–470.

Tanz SK, Castleden I, Hooper CM, Vacher M, Small I, Millar HA. 2013. SUBA3: a database for integrating experimentation and prediction to define the SUBcellular location of proteins in Arabidopsis. Nucleic Acids Research **41,** 1185–1191.

Thimm O, Blasing O, Gibon Y, Nagel A, Meyer S, Kruger P, Selbig J, Muller LA, Rhee SY, Stitt M. 2004. MAPMAN: a user-driven tool to display genomics data sets onto diagrams of metabolic pathways and other biological processes. The Plant Journal **37,** 914–939.

Van Aken O, Whelan J, van Breusegem F. 2010. Prohibitins: mitochondrial partners in development and stress response. Trends in Plant Science **15,** 275–282.

Vanlerberghe GC. 2013. Alternative oxidase: a mitochondrial respiratory pathway to maintain metabolic and signaling homeostasis during abiotic and biotic stress in plants. International Journal of Molecular Sciences **14,** 6805–6847.

Vinothkumar KR, Zhu J, Hirst J. 2014. Architecture of mammalian respiratory complex I. Nature **515,** 80–84.

Wang Q, Fristedt R, Yu X, Chen Z, Liu H, Lee Y, Guo H, Merchant SS, Lin C. 2012. The gamma-carbonic anhydrase subcomplex of mitochondrial complex I is essential for development and important for photomorphogenesis of Arabidopsis. Plant Physiology **160,** 1373–1383.

Wang Y, Lyu W, Berkowitz O, *et al*. 2016. Inactivation of mitochondrial complex I induces the expression of a twin-cysteine protein that targets and affects cytosolic, chloroplastidic and mitochondrial function. Molecular Plant : in press, doi: 10.1016/j.molp.2016.01.009.

Weidner U, Geier S, Ptock A, Friedrich T, Leif H, Weiss H. 1993. The gene locus of the proton-translocating NADH: ubiquinone oxidoreductase in *Escherichia coli*. Organization of the 14 genes and relationship between the derived proteins and subunits of mitochondrial complex I. Journal of Molecular Biology **233,** 109–122.

Werhahn W, Niemeyer A, Jänsch L, Kruft V, Schmitz UK, Braun HP. 2001. Purification and characterization of the preprotein translocase of the outer mitochondrial membrane from Arabidopsis. Identification of multiple forms of TOM20. Plant Physiology **125,** 943–954.

Wittig I, Carrozzo R, Santorelli FM, Schägger H. 2006. Supercomplexes and subcomplexes of mitochondrial oxidative phosphorylation. Biochimica et Biophysica Acta **1757,** 1066–1072.

Wydro MM, Sharma P, Foster JM, Bych K, Meyer EH, Balk J. 2013. The evolutionarily conserved iron-sulfur protein INDH is required for complex I assembly and mitochondrial translation in Arabidopsis. The Plant Cell **25,** 4014–4027.

Yagi T, Matsuno-Yagi A. 2003. The proton-translocating NADH-quinone oxidoreductase in the respiratory chain: the secret unlocked. Biochemistry **42,** 2266–2274.

Zabaleta E, Martin MV, Braun HP. 2012. A basal carbon concentrating mechanism in plants? Plant Science **187,** 97–104.

Zickermann V, Wirth C, Nasiri H, Siegmund K, Schwalbe H, Hunte C, Brandt U. 2015. Structural biology. Mechanistic insight from the crystal structure of mitochondrial complex I. Science **347,** 44–49.

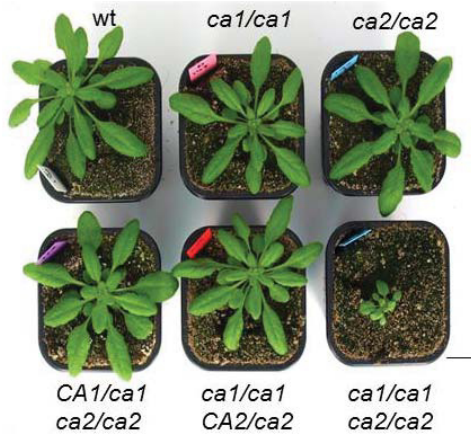***Journal of Experimental Botany*** **Supporting Information**

Article title: Life without complex I:
Proteome analyses of an Arabidopsis mutant lacking the mitochondrial NADH dehydrogenase complex
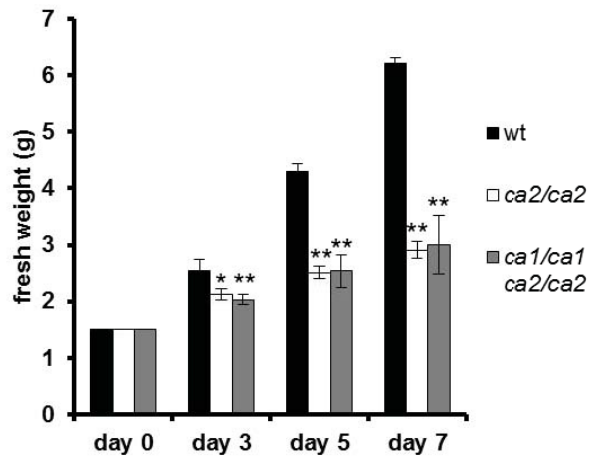Authors: Steffanie Fromm, Jennifer Senkler, Holger Eubel, Christoph Peterhänsel, Hans-Peter Braun
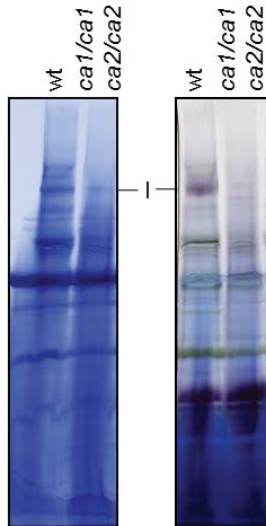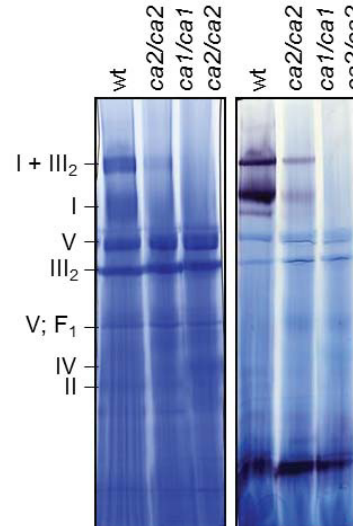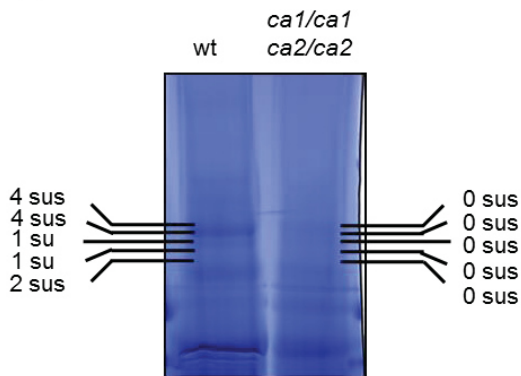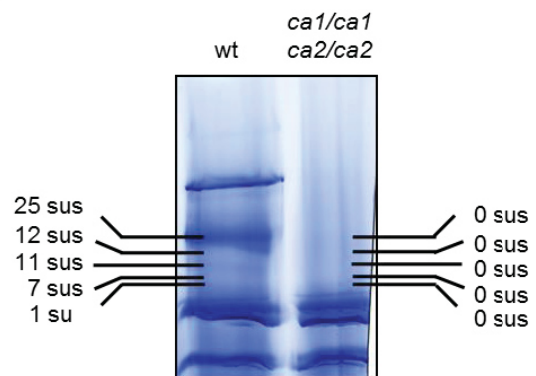Article acceptance date: 21 March 2016

Fig. S1 Growth phenotype of *ca1ca2* plants, absence of complex I. A: Rosettes of ten weeks old plants grown under short-day (10 h : 14 h, light : dark) conditions. Scale bar is 2 cm. *ca1/ca1*: plant line homozygous for knock-out of *CA1*; *ca2/ca2*: plant line homozygous for knock-out of *CA2*; *CA1/ca1 ca2/ca2*: plant line homozygous for knock-out of *CA2* but hemizygous for knock-out of *CA1*; *ca1/ca1 CA2/ca2*: plant line homozygous for knock out of *CA1* but hemizygous for knock out in *CA2*; *ca1/ca1 ca2/ca2*: plant line homozygous for knock-outs of *CA1* and *CA2*. B Fresh weight increase of Arabidopsis wt, *ca2* and *ca1ca2* cell cultures. Starting material (day 0) for wt (black bars), *ca2* (white bars), and *ca1ca2* (grey bars) cell cultures was always 1.5 g. Fresh weight (g) was recorded after three, five and seven days (n = 9, mean ± SE). * = p ≤ 0.05; ** = p ≤ 0.01 according to Student's t-test mutants compared to wt. C and D: Protein complexes of mitochondria isolated from leaves (C) and cell culture (D) were resolved by BN-PAGE. Gels were stained with colloidal Coomassie. Corresponding gels were used for *in gel* activity assays of complex I. Identities of selected mitochondrial protein complexes are indicated beside the gels (I: complex I; II: complex II; III$_2$: dimeric complex III; I+III$_2$: supercomplex formed of complex I and dimeric complex III; IV: complex IV; V: complex V; F1: F1 part of complex V). Note: the faint band at the position of complex I in the mitochondria from leaves of the double mutant does not represent complex I as determined by mass spectrometry (data not shown and data shown in the following figure parts) E and F: Protein complexes of isolated mitochondria of wt and *ca1ca2* of leaves (E) and cell culture (F) were separated by BN-PAGE and Coomassie stained afterwards. In the surrounding of complex I proteins were analyzed by LC-MS. The number of identified complex I subunits (su/sus) for wt and *ca1ca2* mutant is given beside the gels. Some parts of this figure represent modified versions of figures published previously in Fromm *et al.* 2016c.
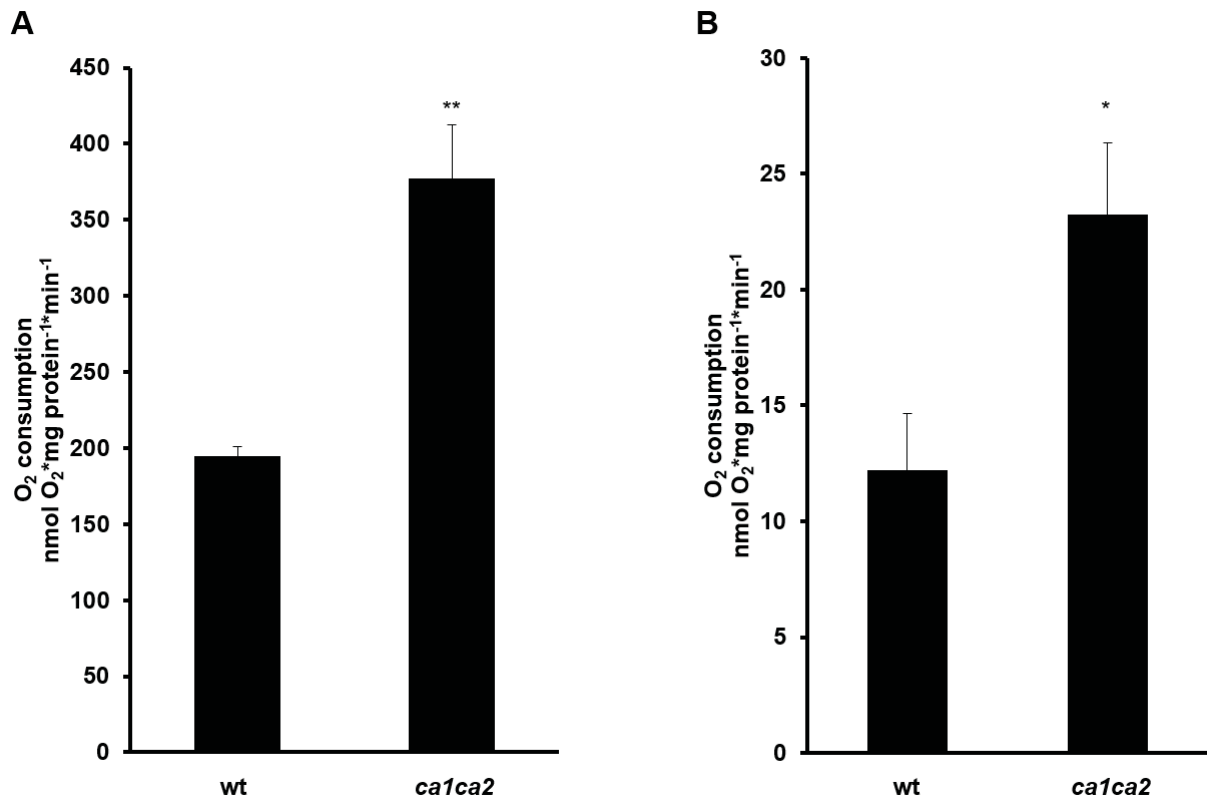
Fig. S2 Respiration through complex II and AOX capacity of mitochondria derived from *Arabidopsis thaliana* wildtype (wt) and *ca1ca2* double mutant lines. Oxygen consumption of isolated mitochondria was measured to estimate the respiration through complex II by adding succinate as substrate (A) and the capacity of AOX by adding AOX inhibitor n-propyl gallate (nPG) (B) using a Clark-type oxygen electrode (n = 5, mean ± SE). * = $p \leq 0.05$; ** = $p \leq 0.01$ according to Student's t-test mutants compared to wt.

Appendix

Curriculum Vitae

Name:	Steffanie Fromm
Date of Birth:	July 2nd, 1987
Place of Birth:	Burgwedel, Germany
Citizenship:	Citizen of Germany

SCHOOL EDUCATION

1994 - 1998	Primary School in Uetze
1998 - 2000	"Orientierungsschule" in Uetze
2000 - 2007	Secondary school "Gymnasium Uetze" in Uetze
	Qualification A-level

ACADEMIC EDUCATION

Oct. 2007 – Sept. 2010	Student at the Leibniz Universität Hannover, B. Sc. Plant Biotechnology (grade: "good") Thesis: "Proteomic characterization of Succinate dehydrogenase in homozygous *Arabidopsis thaliana* knock out plants"
Oct. 2010 – Sept. 2012	Student at the Leibniz Universität Hannover, M. Sc. Plant Biotechnology (grade: "very good") Thesis: "Functional characterization of gamma carbonic anhydrases associated with mitochondrial complex I of the respiratory chain"
Since Nov. 2012	PhD student at the Leibniz Universität Hannover, Institute of Plant Genetics, Department of Plant Proteomics, Prof. Dr. Hans-Peter Braun and Institute of Botany, Prof. Dr. Christoph Peterhänsel

---

List of publications

Fromm S, Senkler J, Eubel H, Peterhänsel C, Braun HP (2016)

Life without complex I: Proteome analyses of an *Arabidopsis* mutant lacking the mitochondrial NADH dehydrogenase complex.

Journal of Experimental Botany, **67**: 3079-3093.

Fromm S, Braun HP, Peterhänsel C (2016)

Mitochondrial gamma carbonic anhydrases are required for complex I assembly and plant reproductive development.

The New Phytologist, **211**: 194-207.

Fromm S, Senkler J, Zabaleta E, Peterhänsel C, Braun HP (2016)

The carbonic anhydrase domain of plant mitochondrial complex I.

Physiologia Plantarum, *in press* (doi: 10.1111/ppl.12424).

Fromm S, Göing J, Lorenz C, Peterhänsel C, Braun HP (2016)

Depletion of the "gamma-type carbonic anhydrase-like" subunits of complex I affects central mitochondrial metabolism in *Arabidopsis thaliana*.

Biochimica et Biophysica Acta **1857**: 60–71.

Conference contributions

2nd International Conference on Photorespiration – Key to Better Crops, Germany (June 2015)

Lecture: "Complete loss of complex I in mitochondria of *Arabidopsis ca1ca2* double mutants results in embryo lethality and an upregulation of the mitochondrial electron transport chain."

9th International Conference for Plant Mitochondrial Biology" in Wrocław, Poland (May 2015)

Poster: "Depletion of the „gamma-type carbonic anhydrase-like" subunits of complex I affects central mitochondrial metabolism in *Arabidopsis thaliana*"

"Promics" meeting in Postdam, Germany (September 2014)

Lecture: "Gamma carbonic anhydrases are required for early plant development"

"Promics" meeting in Düsseldorf, Germany (October2013)

Lecture: "A role of mitochondrial gamma carbonic anhydrase in photorespiration?!"

"Botanikertagung 2013" in Tübingen, Germany (September 2013)

Poster: "Mitochondrial gamma carbonic anhydrase are required for early plant development"